# THE USE OF INTEGRATED GEOPHYSICAL METHODS FOR GROUNDWATER EXPLORATION IN GHANA

## M.Sc. THESIS

### Hafiz MOHAMMED NAZIFI

Department            :  GEOPHYSICAL  ENGINEERING

Supervisor           :  Prof. Dr. Levent  GÜLEN

**June 2015**

**SAKARYA UNIVERSITY**
**INSTITUTE OF SCIENCE AND TECHNOLOGY**

# THE USE OF INTEGRATED GEOPHYSICAL METHODS FOR GROUNDWATER EXPLORATION IN GHANA
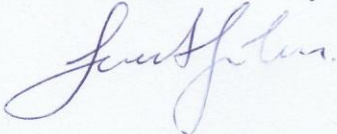
**M.Sc. THESIS**

**Hafiz MOHAMMED NAZIFI**

| | | |
|---|---|---|
| Department | : | GEOPHYSICAL ENGINEERING |
| Supervisor | : | Prof. Dr. Levent GÜLEN |

This thesis has been accepted unanimously by the examination committee on 24.06.2015
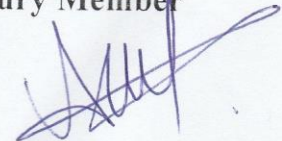
Prof. Dr. Levent GÜLEN
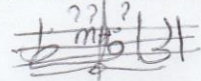Head of Jury

Yrd. Doç. Dr. Ertan PEKŞEN
Jury Member

Yrd. Doç. Dr. Asude ATEŞ
Jury Member

# DECLARATION

I hereby declare that the submission is my own work towards the MSc and that to the best of my knowledge, it contains no material previously published by another person nor material which has been accepted for award of any other degree of this university or any other university, except where due acknowledgement has been made in the text.

Hafiz MOHAMMED NAZIFI

24.06.2015

# ACKNOWLEDGEMENTS

# TABLE OF CONTENTS

CHAPTER 6.

# LIST OF SYMBOLS AND ABBREVIATIONS

A : Cross – sectional area

a, b and c : Empirical constants

B : Magnetic Induction, or Flux Density (Wb/m$^2$ or tesla)

B : Thickness of the aquifer

C : Shape factor which depend upon the shape, particle size and packing of the porous media

D : Electric Displacement (C/m$^2$)

d : Distance (radius of hemisphere)

$d_m$ : Mean particle size (d50) (L,m)

E : Electric Field Intensity (V/m)

EM : Electromagnetic

f : Frequency (Hz)

f : Fraction of pores containing water

FDEM : Frequency – Domain Electromagnetic

g : Acceleration due to gravity (L/T$^2$, m/s$^2$)

GCM : Ground Conductivity Meters

GPR : Ground Penetrating Radar

GPS : Global Positioning System

H : Magnetizing Field Intensity (A/m)

HD : Horizontal Dipole

HLEM : Horizontal Loop Electromagnetic systems

HMD : Horizontal Magnetic Dipole

$H_s$ : Secondary Magnetic field at the receiver coil

$H_p$ : primary magnetic field at the receiver coil

| | |
|---|---|
| i | : Current |
| $J_x$ | : Current density |
| K | : Hydraulic conductivity |
| K | : Geometrical factor |
| L | : Length of the bar |
| MRS | : Magnetic Resonance Sounding Method |
| n | : Porosity (percentage) |
| PHC | : Population and Housing Census |
| r | : Resistance of a resistor |
| s | : Intercoil spacing (m) |
| $S_y$ | : Specific yield |
| $S_r$ | : Specific retention |
| T | : Transmissivity |
| TDEM | : Time – Domain electromagnetic |
| THLDD | : Twifo – Hemang Lower Denkyira District |
| V | : Charge in potential |
| $V_v$ | : Volume of void or pore space in a unit of earth material ($L^3$, $cm^3$, or $m^3$) |
| V | : Unit of the earth material, including both voids and solid ($L^3$, $cm^3$, or $m^3$) |
| $V_w$ | : Volume of water in a unit volume of earth materials ($L^3$, $cm^3$, or $m^3$) |
| $V_o$ | : Electric Potential at source |
| $V_d$ | : Electric Potential at sink |
| $V_c$ | : Potential at an internal electrode |
| $V_A$ | : Potential from the current source at A |

| | |
|---|---|
| $V_B$ | : Potential from the current sink at B |
| VD | : Vertical Dipole |
| VES | : Vertical Electrical Sounding |
| VLF | : Very Low Frequency |
| VMD | : Vertical Magnetic Dipole |
| | |
| w | : Angular Freqency |
| $\rho$ | : Mass density (M/L$^3$, Kg/m$^3$) |
| $\mu$ | : Viscosity (M/T.L, Kg/s.m) |
| $\phi$ | : Porosity |
| $\rho w$ | : Resistivity of water |
| $2\pi d^2$ | : Area of hemisphere |
| $\Delta V$ | : Potential difference |
| $\rho_a$ | : Apparent Resistivity |
| $\sigma$ | : Conductivity and measured in unit of milliSiemens per meter (mS/m) |
| $\varepsilon$ | : Dielectric Permittivity (F/m) |
| $\mu$ | : Magnetic Permeability (H/m) |
| $\sigma$ | : Permeability of free space |
| $\mu_o$ | : Permeabilite (geçirgenlik) katsayısı |

# LIST OF FIGURES

**xvii**

# LIST OF TABLES

# SUMMARY

Keywords: Groundwater Exploration, Electromagnetic Profiling, Schlumberger, Vertical Electrical Sounding, Ghana, and weathering / weathered zone.

Integrated geophysical methods were used for groundwater exploration in the Twifo – Hemang Lower Denkyira District of the Central Region of Ghana. Electromagnetic and Vertical Electrical Sounding (VES) data were acquired using Geonics EM 34-3 Ground Conducting Meter and ABEM Terrameter SAS 1000C, respectively. The geophysical explorations were carried out in ten communities within the district for the purpose of determining zones of high groundwater potentials and recommending suitable sites for location of boreholes for community water supply. First the electromagnetic measurements were carried out; the data were qualitatively interpreted and weathered zones identified. A total of 29 electromagnetic profiles were obtained throughout the 10 communities considered in this work. Profile lengths of traverses range between 410 m and 100 m. The apparent or terrain conductivity values also range between 67 m mhos/m and -20 m mhos/m. The EM readings on 13.79% of the traverse lines were taken using 10 m coil spacing at 5 m intervals. The remaining 86.21% of the traverse lines, 20 m coil spacing and 10 m interval were used in the EM readings. Generally, the EM measurements in most communities show significant variations in both Horizontal Dipole (HD) mode and Vertical Dipole (VD) mode, respectively. The variable nature of the EM values is interpreted to be caused by the complexity of the subsurface. The vertical electrical sounding (VES) using Schlumberger array was conducted at points on the electromagnetic profiles that displayed weathering. Zondip1d software was used to compute geological layered model of the subsurface beneath the sounding points. A total of 52 vertical electrical soundings surveys were conducted throughout the 10 communities. The sounding curves revealed 3 - layer (51.9% occurrence), 4 - layer (44.2%) and 5 - layer (3.8%) earth models, respectively. In most communities the $2^{nd}$ and or the $3^{rd}$ layer is expected to be the water-bearing layers. Only two curve types were displayed by the 3-layered sounding curves; the type H which was the dominant and then type A curve. For the 4 - layered geological subsurface, the sounding curve types were KH, QH, KA and HA. The 5 - layered curve types were QHA and HKH. Interpretations of the one-dimensional inversion of the VES data provided information on the resistivity and thicknesses of the layers and hence the structure of the subsurface. The Surfer 9 software was then used to plot stacked contour maps of the VES data with the GPS coordinates. The maps displayed the resistivity response of the rocks beneath the overburden at specific depths. Some of the communities like Esukese Ekyir, Mbaa Mpe Hia No. 2 and Nyameyeadom are shown to be underlain by great amount of groundwater while others like Aboso, Kwanyarko and Nyamebekyere have less groundwater. On the basis of resistivity values and thicknesses of the layers in both the one-dimensional sounding curve model and the contour map model, sites were recommended for drilling wells for community water supply.

# GANA BÖLGESİNDE YERALTI SUYU ARAŞTIRMALARI İÇİN ENTEGRE JEOFİZİK YÖNTEMLERİN KULLANILMASI

## ÖZET

Anahtar kelimeler: Ayrışma / yıpranmış bölge, Dikey Elektrik Sondajı, Elektromanyetik profil, Gana, Kontur haritası modeli, Schlumberger, ve Yeraltısuyu Arama.

Gana bölgesinde yer olan Twifo-Hemang Lower Denkyira İlçesinin mevcut yeraltı suyu varlığının incelenmesi için entegre jeofizik yöntemler kullanılmıştır. Bu ilçede yaşamını sürdüren bazı topluluklar su sorunları ile karşı karşıya kalmaktadırlar. Bu problem bölgesel olarak su taşıyan boru sistemine yörenin bağlanması ile çözülebilir. Fakat olumsuz ekonomik etkenler ve bölgede yaşayan halkın yöreye konum olarak dağılımı bu çözümü mümkün kılmamaktadır. İçme ve evlerde ihtiyaç duyulan su için sadece birkaç el kazılmış kuyu, dere ve nehirler kaynak olarak kullanılmaktadır. Bu kaynaklar bölgede bulunan çiftçilik ve küçük ölçekli madencilik faaliyetleri nedeniyle kirlenme eğilimindedir. Kirlenmiş suların kullanılması ile cyclosporiasis, amebiazisli, hepatit A, kolera, ishal, bilharziasis gibi ciddi hastalıklar gün yüzüne çıkabilmektedir. Bu hastalılardan kaynak sularını arındırmak maliyet açısından oldukça fazla bir götürüsü olacağından bölgenin acil bir şekilde maliyeti düşük bir şekilde ortaya çıkarılacak ve işlenebilecek su kaynaklarına ihtiyacı bulunmaktadır. Su kaynağının ortaya çıkarılmasının bir başka önemli nedeni ise nüfusun hızla artmasıdır. Nüfus arttıkça su tüketimi artmakta buda mevcut olan sınırlı sayıda kaynakların tükenmesine yola açacaktır. Bu sorunun çözümü ise daha fazla sondaj kuyusu açıp su temin etmektir. Su temin etmekteki bir başka sorun ise dere, nehir ve kuyulardan insan gücüyle su getirmek için harcanan vakittir. Suyu taşıyanların kadın ve çocuklar olduğu dikkate alınırsa özellikle çocukların bu zaman kaybı nedeniyle eğitimi olumsuz etkilenmektedir. Bu çalışma yukarıda bahsi geçen tüm bu olumsuzuklara ışık tutabilmek amacıyla yapılmıştır.Bölgede çeşitli jeofizik yöntemler uygulanarak veriler elde edilmiştir. Elektromanyetik (EM) veriler ve Düşey Elektrik Sondaj (DES) verileri sırasıyla Geonik EM 34-3 ground conducting meter ve ABEM Terrameter SAS 1000C aletleri kullanılarak elde edilmiştir. Jeofizik araştırmaları, topluluk su temini için yüksek yeraltı suyu potansiyeline sahip bölgeleri belirlemek ve uygun sondaj yerini önermek amacıyla ilçenin içindeki on (10) topluluğun bulunduğu alanlarda yürütülmüştür.

Tüm bu çalışmalarda uygun içme sularının temin edebilmenin yanında aynı zamanda akademik anlamda rezistivite yöntemi kullanılarak özdirenç değerleriyle birlikte

suyun derinlik bilgisinin de tartışılıyor olmasıdır. GPS ile belirlenmiş DES noktalarında yapılan çalışmalarda elde edilen özdirenç değerleri ile yeraltı içi yığılmış kontur haritası modeli oluşturulmuştur. Bu sayede bozuşmuş veya kırık bölgeler ortaya çıkarılmakta çalışma alanının altındaki su taşyan akiferler tespit edilip kalınlıkları hakkında bilgiler edinilmiştir.

Kullanılan her iki elektromanyetik ve düşey elektrik sondaj yöntemi teorileri ve saha prosedürleri, Telford vd 1990 Applied Geophysics, Keary vd 2002 An Introduction to Geophysical Exploration, Reynolds 1997 An Introduction to Applied and Environmental Geophysics, Sharma 1997 Environmental and Engineering Geophysics, Robinson and Çoruh 1988 Basic Exploration Geophysics ve Reinhard 2006 Groundwater Geophysics standart esaslarına dayanmaktadır.

Çalışma alanı Twifo – Hemang Lower Denkyira İlçe içinde on toplulukların oluşmaktadır. Toplulukların adları Ablaso Topluluğu, Aboso Topluluğu, Achiase Topluluğu, Beseadze Topluluğu, Esukese Ekyir Topluluğu, Kwanyarko Topluluğu, Mbaa Mpe Hia No 2 Topluluğu, Moseaso Topluluğu, Nyamebekyere No 2 Topluluğu ve Nyameyeadom Topluluğudur. İlçe toplam 1.199 km² alana ve 1.510 kişi nüfusa sahiptir. Üç bölge meclisi bölünmüştür ve sırasıyla bunlar Hemang, Wawase ve Jukwa'dır. Ayrıca, iki kraliyet Hemang ve Denkyira oluşur. Bölge 5 ° 50', N ve 5 ° 51'N enlemleri ve 1 ° 50' W ve 1 ° 10'W boylamları arasında yer almaktadır. İlçenin kuzeyi Upper Denkyira East Belediyesi tarafından sınırlanmıştır. Abura Asebu Kwamankese İlçesi, Cape Coast Başkent ve Komenda-Edina-Eguafo-Abirem Belediyesi güney sınırını oluşturmaktadır. Wassa Mpohor East İlçesi batı sınırını, Assin North Belediye ve Assin South ilçesi doğu sınırınıoluşturmaktadır.

Çalışma alanı, yarı ekvator kuşağında yer almaktadır ve Haziran ve Ekim aylarında 1750 mm yıllık ortalama yağış almaktadır. Bölgede 26° C (Mart'ta) ila 30° C (Ağustos'ta) arasında değişen oldukça yüksek sıcaklık değerleri vardır. Bağıl Nem yıl boyunca yüksektir. Kuru sezonunda % 80 - % 75 ve Islak sezon % 80 - % 70 arasında değişen değerlere ulaşmaktadır.

Çalışma alanının kaya jeolojisi Granit Formasyonudur. Ana kaya türleri granit ve granodiyorit ile gnays bulunmaktadır. Bu kayaçlar katlanmış, yapraklanmış ve eklemli türdedirler. Kırıklar ve damarlar boyunca yoğun ayrışma nedeniyle su sızıntıları yeraltı suyu rezervuarını oluşturmaktadır. İkincil gözeneklilik akiferleri oluşturmaktadır. İki ana akifer tipleri bozunmuş bölgeleri ve kırıkmış bölgeleri vardır. Bozunmuş bölgeleri kristalin temel kayalar üzerinde gelişir ve Kırık bölgeler taş yataklarında üzerinde gelişir.

Bölge genellikle baskın olarak yağmurla beslenen tarıma bağlı bir ekonomik yapıya sahiptir. Nüfusun % 69.9 dan fazlası tarıma bağlı olarak mevsimsel işçi olarak çalışmaktadır. Bu nedenle yağmurların olmaması tarımı etkilemekte bu da dolaylı yoldan çalışan sayısını etkileyerek yoksulluğa yol açmaktadır. Ancak, zengin doğal orman kaynakları tarımsal faaliyetlerini genişletmeye stratejik programların kabulü ile % 3 ilçe işsizlik oranını azaltma potansiyeline sahiptir. Çiftçiler ağırlıklı olarak

gıda bitkileri yetiştirirler. Yetiştirilen bitkiler arasında dikkat çeken kakao, yağ palmiyesi, muz, manyok, mısır, pirinç ve sebzelerdir. Tarımın yanı sıra gelişmiş olmasa da, ilçesinde ekonomik faaliyetler ve finansal hizmetler bir dizi de mevcuttur. Onlar periyodik ve günlük pazarlar, tarımsal işleme işletmeleri, bankacılık, konuk evleri ve zâviye ve montaj ve ve yakıt benzin istasyonları dahili olarak üretilen gelirin önemli ölçüde katkıda bulunmaktadır. İlçe de canlı turizm potansiyelleri ile donatılmıştır ve aralarında en önemli Kakum Milli Parkıdır. Bu park her yıl önemli sayıda yerli ve yabancı turistlerin dikkatini çekmektedir. Bu durum önemli ölçüde görevli istihdam yaratma ve gelir düzeyi yüksek ile ittifak geliştirilmesi ve tamamlayıcı hizmet ve sanayi açısından yerel ekonomiyi canlandırmak için bir potansiyele sahiptir.

Çizgisellik desenleri, kırıklar, uygun akiferlerin varlığı ve bunların kalınlıkları, yeraltı suyu kalitesi hakkında güncel bilgi kurmak için akifer ve su tablası derinlikleri ve beklenen litolojik dizileri geçmiş verileri derlenmiştir. Bu verilerin içerdiği topografik ve jeolojik haritalar, mevcut sondaj bilgi ve çalışma alanında gerçekleştirilen önceki hidrojeolojik çalışmalar raporlarda yer almaktadır. Böyle bitki örtüsü, mostralarda, akarsular desenleri, yaylar ve önceki sondajlardan ve kuyuların yerini, maruz kırıkları ve yüzey akış veya arazinin eğimi yönünü gibi araştırma alanında yüzey fizyografik ve jeolojik özellikleri dikkatle incelenmiştir. Aynı zamanda çok bilgiler eski çöplük, mezarlıklar, tuvalet tesisleri ve çevresel yasak yerle ilgili toplulukların ikamet aranmıştır. Bütün bu düşünceler sonra jeofizik yapılmıştır.

Elektromanyetik tekniği çalışma alanında yeraltı suyu oluşum hakkında iki önemli kontroller hem dar hem de geniş kırık bölgeleri yanı sıra kalın bozunmuş bölgelerin tespiti amaçlanmıştır. DES ölçümleri ana kayaya derinlik, yeraltı katmanlarının sayısını ve bunlara karşılık gelen özdirençlerin belirlemek için alınmıştır. Birden dörde kadar elektromanyetik profil hatları bu çalışmada tüm on toplulukları içinde oluşturulmuştur. Elektromanyetik ölçümler Geonics EM 34 – 3 ground conducting meter kullanarak erişir üzerinde gerçekleştirilmiştir. Ekipman, ölçüm bobin bölgede belirgin iletkenlik doğrudan okuma sağlar. Bu bir verici bobini bir birincil elektromanyetik alan üretilmesi ile elde edilmiştir ve daha sonra yeraltında bir ikinci manyetik alan indükler. Bir alıcı bobin hem birincil hem de ikincil alanında sonuçtaki elektromanyetik alan algılar. Bazı travers hatlar EM ölçümleri 5 meterlik aralıklarda 10 meter bobin boşluğu bırakılarak elde edilmiştir. Geri kalan travers hatlar EM ölçümleri 10 meterlik aralıklarda 20 meterlik bobin boşluğu bırakılarak elde edilmiştir. 10 meterlik bobin boşluk sırasıyla Yatay Dipol (HD) modu ve Dikey Dipol (VD) modu için 7.5 m ve 15 m bir keşif derinliğe sahiptir. Öte yandan 20 meterlik bobin boşluk sırasıyla Yatay Dipol (HD) modu ve Dikey Dipol (VD) modu için 15 m ve 30 m bir keşif derinliğe sahiptir. Elektromanyetik tepkiler dikey eksende (mohm / m) belirgin iletkenlik karşı yatay eksende (metre cinsinden) istasyonu aralıklarla grafikleri çizerek niteliksel olarak yorumlanmıştır. Daha ileri araştırmalar için seçilen Puan çapraz noktalarını (HD modu eğrileri ve VD modu eğrileri haçlar puan) ve genellikle daha yüksek belirgin iletkenlikleri değerlerle puan idi. Binalar çatı,

elektrik direkleri ve atık dökümlerini etkisi nedeniyle, yanlış anomalilerden kaçınılmıştır.

Düşey Elektrik Sondajı (DES) için Schlumberger elektrot dizilimi kullanılmıştır ve EM profillerde bozunmuş görüntülenen noktalarda yapılmıştır. Arazi verileri analizi hem kalitatif hem de kantitatif olarak yorumlanmıştır. İki adet jeofizik yazılımı işleme, modelleme ve direnç verilerinin yorumlanmasında kullanılmıştır. Bunların ismi Zondip1d ve surfer 9 programlarıdır. Arazide veriler kopyalanır daha sonra Zondip1d ve VES notepad penceresine yapıştırılır ve logaritmik eğrileri oluşturulmuştur. Oluşturulan eğriler üzerinde çalışılarak ve ters çözüm için başlangıç modeli elde edilmiştir. Bu veriler daha sonra ter çözüme sokulmuştur. Ölçülen değerler ile hesaplanan değerler arasındaki hata miktarı en az seviyeye düşünce çözüm kabul edilir. Zondip1d çıkışı dikey eksende görünür özdirenç ve yatay eksende akım elektrot ayrımları yarısından karşı logaritmik grafikler oluşur. 1D sondaj eğrilerinin 2D pseudosections da üretildi. Surfer 9 yazılımı, GPS (Global Konumlandırma Sistemi) ile belirlenmiş noktalarda alınmış DES ölçüleri sonucu elde edilen özdirenç değerlerinin haritalarının çiziminde kullanılmış ve su varlığının derinliği hakkında bilgiler edinilmeye çalışılmıştır. Surfer programından çıkmış kontur haritaları ve VES istasyon pozisyonları oluşur. Surfer modellerinde kullanılan renk bandı beş gruba ayrılmıştır. Birinci grup yeraltı sularının yüksek miktarda bölgelere (0 – 150 Ωm) atanmıştır. İkinci gruptaki renk bandı yeraltı sularının orta miktarda bölgelere (150 – 350 Ωm) atanmıştır. Üçüncü grup yeraltı sularının küçük miktarda bölgelere (350 – 700 Ωm), dördüncü grup çok az yeraltı suyu (700 – 1400 Ωm) içeren bölgelere atanmıştır. Son olarak, beşinci grup hiçbir yeraltı suyu (1400 - ∞ Ωm) ile bölgelere atanmıştır. Modelde sondaj için tavsiye edilen yer, kuru ve ıslak mevsim boyunca su içerebilir düşüncesiyle oluşturulmuştur.

Çalışma alanı içerisinde toplam 29 Elektromanyetik profillerinde veri toplanmıştır. Bunlar; Ablaso Topluluğunda 1 profil, Aboso Topluluğunda 4 profil, Achiase Topluluğunda 3 profil, Beseadze Topluluğunda 2 profil, Esukese Ekyir Topluluğunda 1 profil, Kwanyarko Topluluğunda 4 profil, Mbaa Mpe Hia No 2 Topluluğunda 4 profil, başka bir 4 profil Moseaso Topluluğunda, Nyamebekyere No 2 Topluluğunda 3 profil ve Nyameyeadom Topluluğunda son 3 profil olarak dağılmıştır. Traverslerinin profili uzunlukları 100 m - 410 m arasında değişmektedir. Nyamebekere No. 2 Topluluğunda en kısa travers hattı vardır ve Beseadze Topluluğunda en uzun travers hattı vardır. Belirgin veya arazi iletkenlik değerleri -20 mohm / m ve 64 mohm / m arasında değişmektedir. Esukese Ekyire Topluluğunda hem en yüksek hem de en düşük arazi iletkenlik değerlerini kaydedilmiştir. Ablaso Topluluğunda, Esukese Ekyire Topluluğunda ve Nyamebekyere No 2 Topluluğunda 2 profillerindeki elektromanyetik ölçümleri 10 metre bobin boşluğu bırakılarak elde edilmiştir. Bu EM travers hatlarının toplam 13.79% tamamlanır. Geri kalan travers hatlarının %86, 21'nin EM ölçümleri 10 meterlik aralıklarda 20 meterlik bobin boşluğu bırakılarak elde edilmiştir. Profil hatları eğer VD modundaki iletkenlik HD modundan daha yüksek değerleri görüntülese de derin yeraltı kırılmış olduğu yorumlamıştır. Eğer HD modundaki iletkenlik daha yüksekse sığ yeraltında kırılmış olduğu yorumlamıştır. EM grafiklerinde puanlar hem VD modları hem de HD

modları yüksek iletkenlik değerleri sahipleri sığ yeraltından derin yeraltıya kadar yeraltı suyu kaynaklarının yüksek miktarda bulma olasılığı yüksektir şeklimnde yorumlanır. Her iki eğri modları profilleri boyunca düzensiz hareketleri göstermek hangi grafikler karmaşık jeolojik alt yüzeyi önermektedir. VD ve HD modu için genel yüksek iletkenlik değerlerine sahip noktalar ve / veya çapraz noktaları VES kullanılarak başka deneyler için seçilmiştir.

Toplam olarak 52 düşey elektrik sondaj araştırmaları 10 topluluklar içinde yürütülmüştür. Bunlar aşağıdaki gibidir; Ablaso Topluluğunda 3 profil, Aboso Topluluğunda 6 profil, Achiase Topluluğunda 5 profil, Beseadze Topluluğunda 6 profil, Esukese Ekyir Topluluğunda 4 profil, 6 profil Kwanyarko Topluluğunda, Mbaa Mpe Hia No 2. Topluluğunda 6 profil, Moseaso Topluluğu'nda 5 profil, Nyamebekyere No 2. Topluluğunda 5 profil ve en son Nyameyeadom Topluluğunda 6 profil. Sondaj eğrileri sırasıyla 3 – katmanlı (% 51, 9 oluşum), 4 – katmanlı (% 44, 2) ve 5 – katmanlı (% 3,8) toprak modeli göstermiştir. Birçok toplulukta 2. ve / veya 3. katmanın su taşıyan katmanlar olduğu düşünülmektedir. Toplam 8 farklı eğri türleri sondaj eğrileri ile sergilenmiştir. 3 – katmanlı sondaj eğrilerinde egemen olan H eğri tipi ve A eğri tipi olmak üzere iki eğri tipi gösterilmiştir. 4 – katmanlı jelojik yeraltı sondaj eğri tipleri KH, QH, KA ve HA'dır. 5 – katmanlı eğri tipi ise QHA ve HKH'dır. Çalışma alanındaki baskın eğri tipleri, H tipi ve KH tipidir ve bu eğri türleri genellikle yeraltısuyu olanakları ile ilişkilidir.

Kontur haritası modeli bozunmuş ve / veya kırık zonlarının çalışma alanının altındaki davranışını gösterir. Kontur haritası modeli delinmiş zaman DES puan olması nasıl üretken belirlemek için bize yardımcı olur. Ayrıca bize bir toplulukta yapılan çeşitli DES noktasını karşılaştırmak için yardımcı olur. Bu haritalar ve diğer faktörlere bağlı olarak DES puan sıralamasında yardımcı olur. Kontur haritalar başarıyla derinlemesine aralıklarında çalışma alanının alt yüzeyi modellenmiştir. Bu yeraltı iyi gözlemler izin verir ve mümkün yeraltı suyu kaynağının düzeyinin belirlenmesinde yardımcı olur. Bir kuyu delinmiş olur ne ölçüde belirlemede yardımcı. Esukese Ekyir, Mbaa Mpe Hia No. 2 ve Nyameyeadom gibi bazı topluluklarda yeraltısularının büyük miktarda altta olduğu gosterilmiştir. Aboso, Kwanyarko ve Nyamebekyere gibi diğer topluluklarda ise az yeraltı suyunun olduğu gösterilmiştir.

Çalışma başarıyla yeraltı suyu aramalarında özdirenç verilerinin kullanımını maksimize. EM grafikler yüksek iletkenliği gösteren tüm bölgeleri de sondaj eğrileri üzerinde gelen düşük dirençliliğe göstermektedir. Bu iletkenlik ve direnç arasındaki ilişkiyi güçlendirmek temel fiziktir. Ayrıca bize bu veriler ve bunların analizi ve yorumlanması sondaj kararlarında güvenilir bir kanıt sağlamaktadır. Toplumsal su temini için gerekli olan sondaj kuyuları siteleri hem 1 – D sondaj eğrisi modeli hem de kontur haritası modelindeki özdirenç değerleri ve yeraltı katmanları kalınlıklarına göre tavsiye edilmiştir.

# CHAPTER 1. INTRODUCTION

## 1.1. General Introduction

Water is a transparent fluid which forms the world's streams, lakes, oceans and rain, and it's the major constituent of the fluids of living things (Wikipedia 2009).

Dramani, 2013; stated that water is an essential natural resource that sustains the life of man and all living things on earth. It is central to many human activities such as industrial, domestic, animal watering, hydro power generation, transport services, tourism and recreation.

Water covers 71% of the Earth's surface and is vital for all known forms of life. On Earth, 96.5% of the planet's water is found in seas and oceans (except mantle), 1.7% in groundwater, 1.7% in glaciers and the ice caps of Antarctica and Greenland, a small fraction in other layer water bodies, and 0.001% in air as vapour, clouds (formed of solid and liquid water particles suspended in air), and precipitation. Freshwater is 2.5 % of the Earth's water and 98.8% of that water is in ice and groundwater. Less than 0.3% of all freshwater is in rivers, lakes and the atmosphere. And even small amount of the Earth's freshwater (0.003%) is contained within biological bodies and manufactured products (Wikipedia 2009).

Groundwater can be defined as the water that saturates the tiny spaces between alluvial materials (sand, gravel, silt, clay) or crevices of fractures in rocks. According to Badrinarayanan n.d.; groundwater is the most widely distributed precious resources of the Earth. Among the natural water resources, groundwater forms an invisible component of the system.

Kumar 2011, reported that; groundwater is about 20% of the world's freshwater supply. Of the 0.62% of total water that is available as fresh water; about half is

below a depth of 800 m and not practically accessible on the surface. The earth's fresh water that is obtainable for man's use is about $4 \times 10^6 km^3$ and is mainly in the ground (Wilson, cited by Andorful 2013).

Over half of the world's population depend on groundwater for drinking water supplies. In the UK about 30% of the public water supplies are derived from groundwater, in the USA about 50%, and in Denmark 99% and in Germany 70% (Ewusi, 2006). In 2007, 55% of Turkey's groundwater was allocated to irrigation and the remainder to drinking water and industry (Apaydin, 2011). 52% of rural inhabitants have access to potable water mainly from groundwater source in Ghana (Ewusi, 2006).

According to Odada, in Obuobie & Barry 2010; in many world regions, particularly in the developing regions like Africa, availability and access of freshwater largely determines patters of economic growth and social development. Africa as a continent has an immense supply of rainfall, with an annual average of 744 mm and relatively low withdrawals of water for its three major water sectors, namely agriculture, community water supply and industry (Obuobie & Barry 2010).

In 2004, World Health Organization (WHO) estimated that 1.1 billion people (17% of the global population) lacked access to improved water sources. Every day 3900 children under the age of five die from water related diseases (Dramani, 2013).

In Ghana many people in the urban and rural communities are battling with the problem of inadequate availability of potable water for their daily activities. Often times, this problems greatly felt mostly by those living in the rural communities (Dramani, 2013).

Freshwater is very important for the survival of people and nations. Nature has distributed freshwater resources across the length and breadth of the earth, but not equally. The surface water like lakes and rivers are not safe due to the fact that they are easily polluted. The safest freshwater resource is the groundwater. Concerning groundwater, there are some fundamental questions about it, which are; where is it,

how much of it is there, and what is its quality? At what rate can the resource be used without adverse effect? These are exploration and productions questions for which geophysical techniques can help to answer (Fitterman & Stewartj, 1986) .

Electromagnetic (EM) Method and Vertical Electrical Sounding (VES) are the two complementary, widely used geophysical techniques or methods in groundwater exploration. They are use in the delineation of basement layers and locating fissured media and associated aquifer zones such as fractures, faults and joints in sedimentary formations (Anechana, 2013). These electromagnetic and electrical methods have proved particularly effective to groundwater studies, because many of the geological formation properties that are critical to hydrogeology such as porosity and permeability of rocks can be correlated with electrical conductivity signatures (Somiah, 2013).

## 1.2.   Statement of Problem

The ministry of food and agriculture of Republic of Ghana, reported that, according to the Ghana Statistical Services; the current population of Twifo – Hemang Lower Denkyira District (THLDD) of Central Region of Ghana is 166,224. The current population growth rate of THDD is 4.1% which is higher than the corresponding regional growth rate of 1.8% and even higher than the national growth rate of 2.7%. With this increasing population growth, it is an undeniable fact that there would be a corresponding pressure on the current water resources in the district.

Due to the dispersed and the scattered nature of most communities within these districts, they are not connected to piped systems and the current source of water for most household in this district is from surface water in forms of streams and rivers. This surface water are prone to environmental pollutions due to the activities of farmers and small scale mining operations. The continued use of water directly from surface water sources may lead to water borne diseases like cyclosporiasis, amoebiasis, hepatitis A, cholera, diarrhoea, bilharzias among others.

Furthermore, women and children spend a lot of time and effort everyday going to the streams and rivers sites to fetch water. These practises affect the productivity of these women and children and the district at large. Sometimes children waste precious school hours outside classrooms in search of water at the expense of their education.

## 1.3. Justification of the Study

A lot of time, money and other resources have been wasted in drilling and hand – dug of unproductive boreholes or wells. This waste of resources could have been reduced or totally avoided by the use of integrated geophysical studies. Interpretation of geophysical studies with detailed geological information could help in selecting borehole drilling or hand – dug sites.

## 1.4. Significance of the Study

In a Sub – Saharan African country like Ghana, there are a lot of water problems and water shortages. Residence of big cities and towns face problem of water shortages, although these cities have a well-organized water pipe system. Due to these situations one would not wonder why the people in districts should not face such problems looking at the lower level of developments in those districts. Still many communities in districts depend on surface water for their water supply and these water bodies are not safe and healthy for drinking. Regarding the health related problems of drinking from surface water, the shortages of surface water during the dry seasons and long distance women and children within these communities go to during the dry season before they could get water, and the advantages of groundwater resource over the surface water, one should not underestimate the importance of geophysical investigations of groundwater in the Twifo – Hemang Lower Denkyira District of the Central Region of Ghana.

## 1.5. Purposes and Objectives of the Study

The main aim of this study is to carry out Electromagnetic measurements using the Geonics EM 34-3 Ground Conducting Meter and Vertical Electrical Sounding (VES) using a ABEM Terrameter SAS 1000C equipment to identify zones of high groundwater potential and to select suitable sites for borehole drilling and / or hand dug in ten (10) communities in the Twifo – Hemang Lower Denkyira District of the Central Region of Ghana.

## 1.6. Scope of Work

The study involves an integrated geophysical survey using the electromagnetic method for investigating ground conductivity and vertical electrical sounding to measure apparent resistivity with change in vertical variation to delineate groundwater potential zones with ten (10) communities in the Twifo – Hemang Lower Denkyira District of the Central Region of Ghana. The data for this work were obtained from a project of the Community Water and Sanitation Agency (CWSA) – Central Region. This project was awarded to the Water Research Institute (WRI) of the Council for Scientific and Industrial Research (CSIR), Ghana to carry out groundwater investigations in ten communities within THLDD. This work is made up of geophysical field survey work, analysis and interpretation of the results and recommendations.

# CHAPTER 2. LITERATURE REVIEW AND STUDY AREA

## 2.1. Groundwater

The Oxford online dictionary (Oxford dictionary n.d.), defined groundwater as " the water held underground in soil or in pores and crevices in rock. In hydrology, groundwater is defined as the water that occurs as a saturated zone of variable thickness and depth below the earth's surface. One could also define groundwater as the water that exist in pore spaces and fractures of rocks and sediments beneath the earth surface. The groundwater scientists restrict the use of the term "groundwater" to underground water that can flows freely into well, springs, tunnels etc. This definition excludes underground water in the unsaturated zone.

### 2.1.1. The Sources and origin of groundwater

Groundwater is group into four bases on its origin. These are; Meteoric Water, Connate Water, Juvenile Water and Metamorphic Water. The meteoric water is the water found in circulatory system of hydrologic cycle. It is groundwater derived from rainfall and infiltration with the normal hydrological cycle. It name implies recent contact with the atmosphere. The connate water is the fossil interstitial water out of contact with the atmosphere for appreciable length of time. This water is mostly in sedimentary rocks and is normally saline. The juvenile water is the groundwater that originated from volcanic emanations and lastly metamorphic water are groundwater that are associated with heat, pressure and re-crystallization which created metamorphic rocks.

Groundwater accounts for about two − thirds of the freshwater resources of the world (table 2.1). Groundwater is an important component of the earth's water circulatory system. This circulatory system is termed hydrologic cycle or water cycle (figure 2.1) and is the most basic principle of groundwater hydrology. It involves the exchange of

energy which leads to temperature changes. The radiant energy received from the sun is the driving force of the circulation. Considering the freshwater part of the circulatory system; the inflow of freshwater is from precipitation in the form of rainfall and from melting snow and ice, and out flow occurs basically as stream flows or runoff and as well as evapotranspiration ( a combination of evaporation from water surface and the soil and transpiration from soil moisture by plant). Part of the precipitation infiltrates deeply into the ground. This may accumulate above the impermeable bed and saturated the pore spaces to form an underground body of water (Chilton & P. Seiler, n.d. p. 1).

Table 2.1. Estimated water Balance of the World (obtained from Occurrence of Groundwater (Anon n.d. p. 4) )

| Parameter | Surface area (Km²)*10⁶ | Volume (Km²)*10⁶ | Volume (%) | Equivalent depth (m)* | Resident time |
|---|---|---|---|---|---|
| Oceans and seas | 361 | 1370 | 94 | 2500 | ~ 4,000 years |
| Lakes and reservoirs | 1.55 | 0.13 | < 0.01 | 0.25 | ~ 10 years |
| Swamps | < 0.1 | < 0.01 | < 0.01 | 0.007 | 1-10 years |
| River channels | < 0.1 | < 0.01 | < 0.01 | 0.003 | ~ 2 weeks |
| Soil moisture | 130 | 0.07 | < 0.01 | 0.13 | 2 weeks – 1 year |
| Groundwater | 130 | 60 | 4 | 120 | ~ 2 weeks – 10,000 years |
| Icecaps and glaciers | 17.8 | 30 | 2 | 60 | |
| Atmospheric water | 504 | 0.01 | < 0.01 | 0.025 | 10-1000 years |
| Biospheric water | < 0.1 | < 0.01 | < 0.01 | 0.001 | ~ 10 days |
| | | | | | ~ 1 week |

* Computed as though storage were uniformly distributed over the entire surface of the earth.
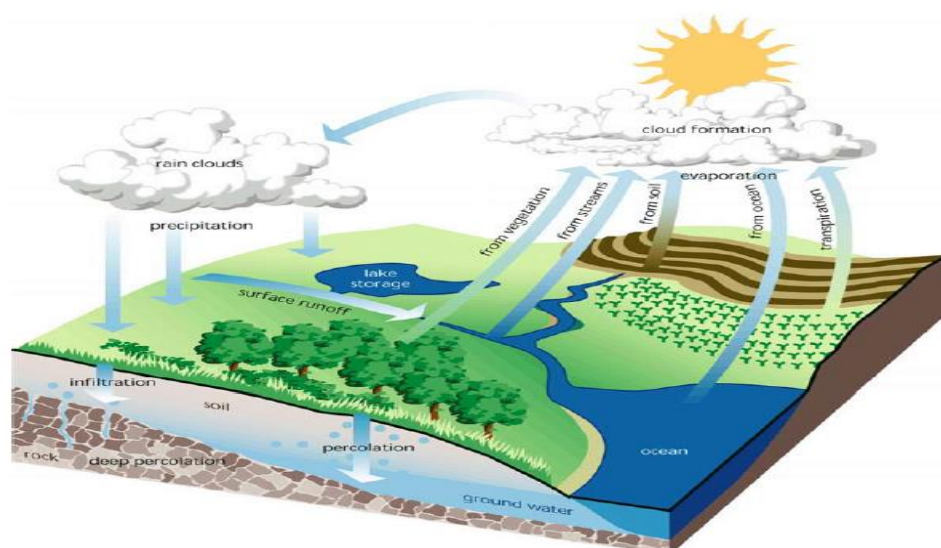


Figure 2.1. Schematic Representation of the Hydrologic Cycle (obtained from Occurrence of Groundwater (Anon n.d. p. 4))

The movement of water through the water cycle is being control by the physical processes of evaporation, condensation, precipitation, infiltration, runoff and subsurface flow. Water goes through different phases: liquid, solid (ice) and gas (vapour) as it move through the above mention physical processes (Wikipedia n.d.)

### 2.1.2. Groundwater occurrence and distribution

Rocks of the upper part of the earth's crust possess pores and voids, and these pores or voids are in almost all types of rocks of all origins and ages. It is in these pores that groundwater occupied (Anechana 2013 p. 31). The volume of water that rocks contain depends on the proportion of pores within the rock and this is termed porosity.

Surface water is grouped into different zones depending on the physical occurrence of the surface water in the soil. As seen from figure 2.2 below, the classification are; saturated zone and unsaturated zone.
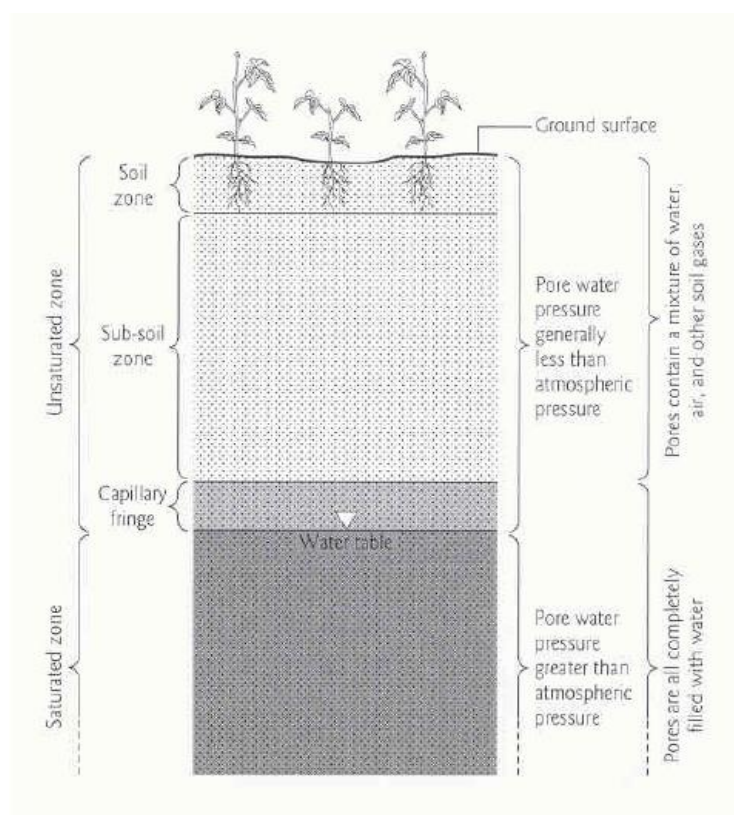


Figure 2.2. A schematic cross – section showing a typical distribution of subsurface water (obtained from Occurrence of Groundwater (Anon n.d. p. 8)

The saturated zone is a zone where voids are completely filled with water. This zone extend from the upper surface of saturation down to underlying impermeable rocks (Anon n.d. p. 7). The unsaturated zone is where the voids contain a mixture of water, moisture and air. This zone is further divided into the soil moisture zone, the intermediate zone and the capillarity zone. The soil moisture zone is essentially for plant and it differs in thickness depending on soil type and climate in the top layer. The movement of water in this zone can be either upward or downward depending on suction or gravity. The intermediate zone is where water is held due to intermolecular forces against the pull of gravity. And lastly the capillarity zone; it is located above the water table and the water here is held by capillarity force acting against gravity (Nils & Lennart, 2005 p.12).

The mode of occurrence of groundwater depends largely upon the type of formation, and hence upon the geology of the area (Tsikudo Kwasi, 2009 p. 11). Some of the geological formations have higher ability of retaining and distributing water than others. Table 2.2 below shows some of the usual mode of water occurrence.

Table 2.2. Usual mode of water occurrence (Tsikudo Kwasi, 2009)

| Ground Type | Quality Water occurring in: |
|---|---|
| Sand and Gravel | Pores |
| Sandstone | Pores and fissures |
| Limestone | Fissures often expanding into caves |
| Chalk | Pores and fissures |
| Clay | Very small pores |
| Massive Igneous | Fissures with pores in weathered zones |
| Lava | Fissures with pores in igneous zones |
| Metamorphic | Fissures with spores in weathered zones |

The flow of water through the ground is being assisted by the differences in pressure within the subsurface. The pressure is highly influence by the effect of gravity. Generally water moves through the subsurface from high land area to low land areas

just like the surface water flows from uphill towards downhill (Andorful, 2013 p. 6). This kind of movement of subsurface water leads to the distribution of groundwater resource.

### 2.1.3. Water table and aquifer

### 2.1.3.1. Water table

Water table is simply defined as the saturated level of groundwater. It is said to be the surface below which all openings in the rock are filled with water (Somiah 2013 p. 9). The water table actually marks the boundary between the unsaturated zones and the saturated zone and it is the surface at which fluid pressure is exactly equal to atmospheric pressure (Chilton & Seiler, n.d. p. 3). The water table is found everywhere below the earth surface but depending on the season, location and the long term climate variations; the depth of the water table varies. It either rises or falls and normally follows the topography of the surface (Somiah, 2013 p. 10). The depth of the water table of several places in Ghana and other part of the world normally increases during the dry seasons and decreases in the wet seasons.

### 2.1.3.2. Aquifer

The word aquifer was derived from two Latin words; "aqui (aqua)" meaning "water" and "fer (ferre)" meaning " to bear". In this regard aquifer literary means "to bear water". Geologically speaking; an aquifer is a geologic formation, or group of formations, which contain water and permit significant amount of water to move through it under ordinary field conditions (Awomeso n.d.). Groundwater reservoir (or basin) and water bearing zone (formation) are some of the terms that are used in place of aquifer. Aquifers provide two important functions and these are; (1) they transmit groundwater from area of recharge to the area of discharge, and (2) they provide a storage medium for useable quantities of groundwater (in Occurrence of Groundwater (Anon n.d. p. 8).

Aquifers are generally extensive and may overlie or underlain by a confining bed, which may be an aquiclude, aquifuge or aquitard. An aquiclude is a relatively

impermeable material that does not yield appreciable quantities of water to wells. It may contain water but is incapable of transmitting significant quantities of water under ordinary field condition and a typical example of aquiclude are clay and shale. An aquifuge is a geological formation neither containing nor transmitting water. And examples are fresh granite and basalt. Lastly an aquitard is a poorly permeable geologic formation that transmits water at a very low rate compared to an aquifer and an example is sandy clay. It may also transmit appreciable water to or from adjacent aquifers when sufficiently thick and may constitute an important groundwater storage zone. Aquifers are classified as confined, unconfined and leaky.
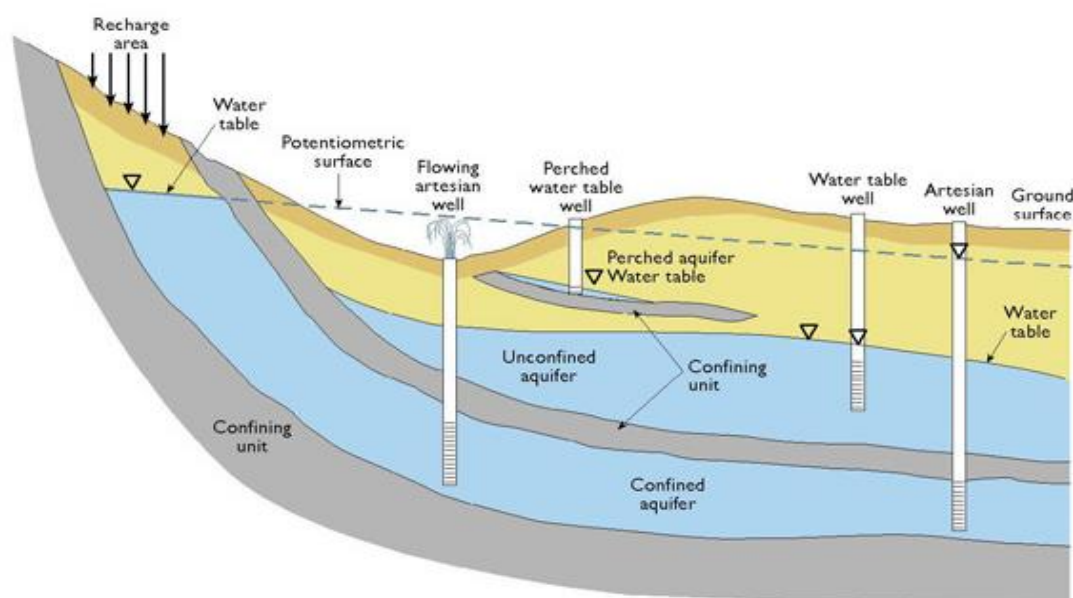


Figure 2.3. Schematic Cross section of Aquifer types (obtained from Occurrence of Groundwater(Anon n.d. p. 9)

The confined aquifer is also known as pressure or piezometric aquifer; is an aquifer that is confined above and below by an imperious (may contain water but cannot transmit) layer under pressure greater than the atmospheric. The water in this kind of aquifer flow freely without pumping and that the water in this aquifer is called artesian or confined water.

The unconfined aquifer (phreatic aquifer) is an aquifer that is opened to receive water from the surface, and whose water table surface is free to fluctuate up or down, depending on the recharge and discharge rate as it can be seen from figure 2.4.

Figure 2.4. Schematic cross-section of unconfined aquifer ( obtained from Groundwater Storage (Anon n.d.))

Figure 2.5 below show a special type of an unconfined aquifer called the perched aquifer which occurs whenever a semi-pervious layer of limited extend is located between the water table of the unconfined aquifer and the ground surface, thereby making a groundwater body, separated from the main groundwater body, to be formed (Awomeso n.d.p.3).
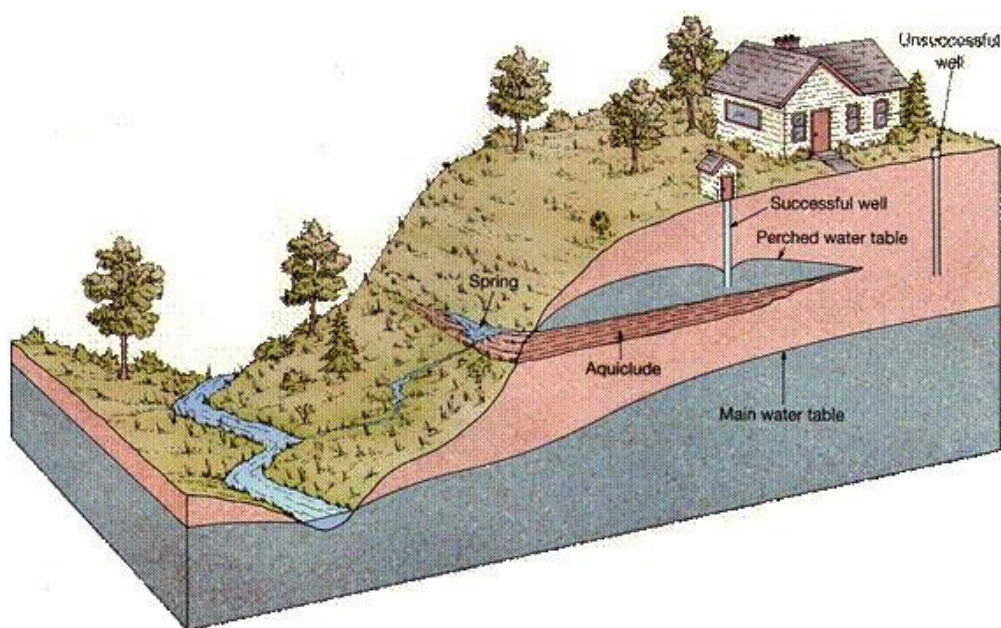


Figure 2.5 Schematic of perched aquifer (Nkhoma n.d.)

The leaky aquifer is semi – confined aquifer that is overlain or underlain by semi-pervious strata. This type of aquifer is a common feature in plains, alluvial valleys or former lake basins. Water is removed from this aquifer by horizontal flow within the aquifer and by vertical flow through the aquitard into the aquifer.

### 2.1.4.  Hydraulic properties of rocks

The hydraulic properties of rocks are the physical properties of rocks that affect the accumulation, retention, and removal of groundwater. In some books these hydraulic properties are also referred to as aquifer properties. In this thesis the hydraulic properties that would be discussed are; porosity, specific yield and specific retention, recharge and discharge, coefficient of permeability, transmissivity, and storativity.

### 2.1.4.1.  Porosity

Porosity is defined as the percentage of rock or soil that is void of material. The higher the porosity of a rock or formation is, the higher the water holding capacity of that rock or formation will be. Mathematically, porosity can be expressed as

$$n = \frac{v_v}{v} \times 100\% \qquad\qquad\qquad (2.1)$$

Where
 n is the porosity (percentage),
$V_v$ is the volume of void or pore space in a unit of earth material ($L^3$, $cm^3$, or $m^3$) and
V is the unit of the earth material, including both voids and solid ($L^3$, $cm^3$, or $m^3$).

The importance of porosity in groundwater hydrology is that; it tells us the maximum amount of the water that a rock can contain when it is saturated (Ralph, 1982 p. 8). Porosity can be a primary or secondary porosity. The primary porosity is that which is created at the time of origin of the rock in which they occur. And secondary porosity is the porosity that result from the actions of subsequent geological, climatic and biotic factors upon the original rock, example include faults, fracture and opening cause by plants and animals. Various geological materials have their typical porosity ranges and table 2.3 below, show the ranges of porosity of some of the common geologic materials.

Table 2.3. Ranges of porosity and specific yield of geologic materials (Anechana 2013)

| Material | Porosity | Specific yield |
|---|---|---|
| **Unconsolidated sediments** | | |
| Gravel | 0.25 − 0.35 | 0.16 − 0.23 |
| Coarse sand | 0.30 − 0.45 | 0.1 − 0.22 |
| Fine sand | 0.26 − 0.5 | 0.1 − 0.25 |
| Silt | 0.35 − 0.5 | 0.05 − 0.1 |
| Clay | 0.45 − 0.55 | 0.01 − 0.03 |
| Sand and gravel | 0.2 − 0.3 | 0.1 − 0.2 |
| Glacial till | 0.2 − 0.3 | 0.05 − 0.15 |
| **Consolidated sediments** | | |
| Sandstone | 0.05 − 0.3 | 0.03 − 0.15 |
| Siltstone | 0.2 − 0.4 | 0.05 − 0.1 |
| Limestone and dolomite | 0.01 − 0.25 | 0.005 − 0.1 |
| Karstic limestone | 0.05 − 0.35 | 0.02 − 0.15 |
| Shale | 0.01 − 0.1 | 0.005 − 0.05 |
| **Igneous and metamorphic rocks** | | |
| Vesicular basalt | 0.1 − 0.4 | 0.05 − 0.15 |
| Fractured basalt | 0.05 − 0.3 | 0.02 − 0.1 |
| Tuff | 0.1 − 0.55 | 0.05 − 0.2 |
| Fresh granite and gneiss | 0.0001 − 0.03 | <0.001 |
| Weathered granite and gneiss | 0.05 − 0.25 | 0.005 − 0.05 |

### 2.1.4.2. Specific yield ($S_y$) and Specific retention ($S_r$)

Specific yield ($S_y$) is the ratio of the volume of water drains from a saturated rock owing to the attraction of gravity (or by pumping from wells) to the total volume of saturated aquifer. Mathematically, this definition can be expressed as

$$s_y = \frac{v_w}{v} \times 100\% \qquad (2.2)$$

Where $V_w$ is the volume of water in a unit volume of earth materials ($L^3$, $cm^3$, or $m^3$), V is the unit volume of earth material, including solid and voids ($L^3$, $cm^3$, or $m^3$).

Specific retention ($S_r$) is the ratio of the volume of water that cannot be drained out to the total volume of the saturated aquifer. The sum of specific yield and specific retention equals porosity (Anon n.d.) And we can express it as

$$n = s_r + s_y \qquad (2.3)$$

n= porosity

$s_y$ = specific yield

$s_r$ = specific retention

In the table 2.3 above, typical ranges of specific yield of some geologic material are shown. A basic explanation of the specific yield and specific retention is that; specific yield tells how much water is available for man's use and specific retention tells us how much water remain in the rock after it is drained by gravity (Ralph 1982 p. 9). The table 2.4 below show selected value of porosity, specific yield and specific retention of geological materials.

Table 2.4. Selected value of porosity, specific yield and specific retention of geological materials. Values in percent by volume (Ralph 1982)

| Material | Porosity | Specific yield | Specific retention |
|---|---|---|---|
| Soil | 55 | 40 | 15 |
| Clay | 50 | 2 | 48 |
| Sand | 25 | 22 | 3 |
| Gravel | 20 | 19 | 1 |
| Limestone | 20 | 18 | 2 |
| Sandstone (semiconsolidated) | 11 | 6 | 5 |
| Granite | .1 | .09 | .01 |
| Basalt (young) | 11 | 8 | 3 |

### 2.1.4.3. Recharge and discharge

Recharge of groundwater is the injection of water into an aquifer. It represents the portion of surface water or rainfall which reaches an aquifer. Recharge includes stream bed percolation, deep percolation of rainfall, leakage from ponds, lakes and reservoir.

Discharge on the other hand is emerging of water from the underground. Most discharge occurs as flows into surface water bodies such as, streams, lakes or oceans. Evaporation from within the soil and transpiration from vegetation that has access to the water table are other ways that discharge occurs. These can be refers to as natural discharge and the artificial discharge of groundwater occurs by pumping of water from wells.

### 2.1.4.4. Coefficient of permeability (hydraulic conductivity (K))

The coefficient of permeability is equal to the discharge ($m^3$/s) per unit area ($m^2$) of soil mass under unit hydraulic gradient. Permeability is the ease with which water can flow in a soil or rock ( Occurrence of Groundwater (Anon n.d. p 26)). Mathematically hydraulic conductivity is expressed as;

$$K = \frac{\left[ Cd_m^2 \right] \rho g}{\mu}$$

(2.4)

Where

C = the shape factor which depend upon the shape, particle size and packing of the porous media,

$d_m$ = the mean particle size (d50) (L,m)

$\rho$ = the mass density ($M/L^3$, $Kg/m^3$)

g = the acceleration due to gravity ($L/T^2$, $m/s^2$)

$\mu$ = the viscosity (M/T.L, Kg/s.m)

It is possible to have a highly porous rock with little or no interconnection between the pores and because of this reason, high porosity does not necessarily imply high permeability but low porosity usually result in low permeability (Anon n.d.). Typical values of hydraulic conductivity for some geologic materials are given in the table 2.5 below.

### 2.1.4.5. Transmissivity (T)

Transmissivity is defined as the rate at which water is transmitted through a unit width of an aquifer under a unit hydraulic gradient.

$$T = Kb$$

(2.5)

Where

T = transmissivity

K= hydraulic conductivity

b= the thickness of the aquifer

Transmissivity is usually expressed as $m^2/s$, or $m^3/day/m$. The value of transmissivity differs in different aquifers and from place to place in the same aquifer because it depends on both the hydraulic conductivity and the thickness of the aquifer (Ralph ,1982).

Table 2.5. Hydraulic conductivity of some common geological materials. (obtained from Occurrence of Groundwater(Anon n.d. p. 27).

| Medium | K (m/day) |
| --- | --- |
| **Unconsolidated deposits** | |
| Clay | $10^{-8} - 10^{-2}$ |
| Fine sand | 1 - 5 |
| Medium sand | 5 - 20 |
| Coarse sand | $20 - 10^2$ |
| Gravel | $10^2 - 10^3$ |
| Sand and gravel mixes | $5 - 10^2$ |
| Clay, sand, gravel mixes (e.g. till) | $10^{-3} - 10^{-1}$ |
| **Hard Rocks** | |
| Chalk (very variable according to fissures if not soft) | 30.0 |
| Sandstone | 3.1 |
| Limestone | 0.94 |
| Dolomite | 0.001 |
| Granite, weathered | 1.4 |
| Schist | 0.2 |

### 2.1.4.6. Storativity

Storativity is the volume of water release from storage, or taken into storage, per unit of aquifer storage area per unit change in head. It is also known as Storage Coefficient. The water yielding ability of an aquifer is expressed in terms of its storage coefficient. Ralph (1982) stated that; the size of storage coefficient depends on the type of the aquifer (either confined or unconfined).

### 2.1.5. Groundwater quality

The quality of water depends both on the substance dissolves in the water and on certain properties and characteristic that these substances impart to the water. Water is known to be a universal solvent because of its ability to dissolve at least small amount of almost all substance that it contacts (Ralph 1982 p. 64).

Water moves through several zones before it finally settle in pores of rocks and soil as groundwater. And by so doing it might have dissolved substance which might affect the health of people who would use it for drinking and other activities.

According to Ralph (1982 p. 64); the composition and concentration of substances dissolved in unpolluted groundwater depend on the chemical composition of precipitation, on biological and chemical reaction occurring on the land surface and in the soil zone, and on the mineral composition of the aquifers and confining beds through which the water moves. Table 2.6 and 2.7 show natural inorganic constituents commonly dissolved in water that are likely to affect use of water and table 2.8 below show the summary of the major types and the extent of deterioration in freshwater quality.

Table 2.6. Dissolved inorganic major constituents in groundwater by abundance (after David and De Wiest, 1966 as cited in (Anon n.d.)

| Major constituents (> 5 mg/L) | |
|---|---|
| Cations | Anions |
| Magnesium | Bicarbonate |
| Calcium | Chloride |
| Sodium | Sulfate |
| Minor constituents (0.01 to 10.0 mg/L) | |
| Boron | Carbonate |
| Iron | Fluoride |
| Potassium | Nitrate |
| Strontium | |

Table 2.7.  Dissolved inorganic trace constituents in groundwater by abundance (after David and De Wiest, 1966 as cited in(Anon n.d.)

| Trace constituents (< 0.1 mg/L) | | | |
|---|---|---|---|
| Aluminum | Antimony | Arsenic | Barium |
| Beryllium | Bismuth | Bromide | Cadmium |
| Cerium | Cesium | Chromium | Cobalt |
| Copper | Gallium | Germanium | Gold |
| Indium | Iodide | Lanthanum | Lead |
| Lithium | Manganese | Molybdenum | Nickel |
| Niobium | Phosphate | Platinum | Radium |
| Rubidium | Ruthenium | Scandium | Selenium |
| Silver | Thallium | Thorium | Tin |
| Titanium | Tungsten | Uranium | Vanadium |
| Yttrium | Zinc | Zirconium | |

Table 2.8 Freshwater quality deterioration at global level (obtained from (Bartram & Richard 1996)

| | Rivers | Lakes | Reservoirs | Groundwaters |
|---|---|---|---|---|
| Pathogens | xxx | $x^2$ | $x^2$ | x |
| Suspended solids | xx | oo | X | oo |
| Decomposable organic matter[3] | xxx | x | xx | x |
| Eutrophication[4] | x | xx | xxx | oo |
| Nitrate as a pollutant | x | o | o | xxx |
| Salinisation | x | o | o | xxx |
| Heavy metals | xx | xx | xx | xx[5] |
| Organic micro-pollutants | xx | x | xx | xxx[5] |
| Acidification | x | xx | x | o |
| Changes to hydrological regimes[6] | xx | xx | xx | x |

Radioactive and thermal wastes are not considered here.

xxx Globally occurring, or locally severe deterioration
xx   Important deterioration
x    Occasional or regional deterioration
o    Rare deterioration
oo  Not relevant

The use of synthetic chemical such as herbicides and insecticides, and fertilizers on farmlands and as well as industrial chemical discharges greatly affect the safety of groundwater use for drinking and domestic activities.

## 2.2. Literature Review

### 2.2.1. Geophysical methods used in groundwater prospecting

Geophysics is a branch of geosciences that applied the principles of physics to the study of the Earth. According to Telford et al. (1990) geophysics deals with all aspects of the physics of the earth, its atmosphere and space. For search of minerals, oil and gas, applied geophysical methods are used and these methods are divided into; gravity, magnetic, seismic, electrical, electromagnetic, radioactivity, well logging methods (Telford et al. 1990 p.2).

Certain geophysical conditions are generally associated with each and every mineral, others with gas and oil, for this matter a general or deep knowledge of the geological setting of geophysical research sites is very important to geophysical investigations and interpretations.

The choice of techniques to locate a certain mineral depends on the nature of the mineral and of the surrounding rocks. Sometimes a geophysical method may give a direct indication of the presence of the mineral being sought, at other times the method may give just indicated only whether or not conditions are favourable to the occurrence of the minerals sought (Telford et al. 1990 p. 3-4). The type of physical property to which a geophysical method responds clearly indicated its range of application (Kearey et al., 2002 p. 2).

The primary interest of many geophysical investigations is the local variation in measured parameter, relative to some normal background value. This local variation which is also known as geophysical anomaly is attributed to a localized subsurface zone of distinctive physical property and possible geophysical importance (Kearey et al., 2002). A large share of all geophysical explorations and of course all groundwater prospecting, is for the purpose of determining the conditions beneath the earth's surface. To achieve this purpose, geophysical methods are used both for surface surveys and for subsurface survey (Carl & Stewart, 1943 p. 1) Because of the scope of this work only the surface geophysical survey would be discussed.

According to Carl & Stewart (1943); almost all the geophysical methods and techniques have been tried and many of them have been found successful in groundwater exploration, but the electrical methods receive the widest application in both surface and subsurface surveying at the present time.

For groundwater explorations it is not the groundwater its self that is the target of the geophysical investigations rather it is the geological situation in which the water exists (Anon 1997). These include mapping depth and thickness of aquifers, mapping aquitards or confining units, locating preferential fluid migration paths such as

fractures and fault zones and mapping contamination of the groundwater such as that from saltwater intrusion (Anon 1997).

The main reasons for using geophysical methods in groundwater studies are to reduce the risks of drilling dry holes and reduce the cost associated with poor groundwater production.

The main geophysical methods used mostly in groundwater exploration is discussed below. These discuss include; the main reasons of using those methods, the physical parameters that they measure and extend of usage.

### 2.2.1.1. Magnetic method

The magnetic method or geomagnetic method measure the remnant magnetic field associated with a geological structure or man-made object. The use of geomagnetic for direct groundwater investigation is little because groundwater does not have a magnetic signature.

According to Babu et al., 1991; the role of magnetic method in groundwater exploration is to locate structures such as dikes, faults, fractures etc. that control the accumulation and the movement of groundwater. It was also stated in the same article that; in mapping bedrock topography from magnetic anomalies, the information about the thickness of the weathered layer would help in assessing the groundwater potential of the region.

Currently, magnetic resonance method permits a direct detection of groundwater from surface measurements. The method excites the H protons of the water molecules with a magnetic field produced by a loop of current at a specific frequency. The amplitude of the magnetic field produced in return by these protons in the same loop is proportional to the water content, while the time constant of decay is linked to the mean pore size of the formation, thus to the permeability (Bernard 2003).

According to Bernard & Legchenko (2003); the Magnetic Resonance Sounding Method (MRS) has been used in the past years with success in various geological and geographical contexts for groundwater surveys. The intensity of excitation in this method determines the depth of investigation. The primary application of this method concerns the determination of the water level and the total quantity of water available down to 100 to 150 m depths. MRS can also help in selecting the best site for drilling, predicting a yield using a calibration, and in determining the geometry of an aquifer layer for hydrogelogical modelling (Bernard & Legchenko 2003)

### 2.2.1.2. Electric and Electromagnetic methods

According to several publications as stated in (Anon 1997), electrical and electromagnetic techniques have been extensively used in groundwater geophysical investigation because of the correlation that often exist between electrical properties, geologic formations and their fluid content.

Electrical methods are still the most widely geophysical method use for groundwater exploration; both for sounding and electrical profiling. Electrical techniques can be divided into a number of types based on the configuration of electrodes that are used to impart the electrical current into the ground and the nature of the electrical signatures in the groundwater recorded and interpreted.

The direct current resistivity method and the electromagnetic profiling method will be discussed in details in the next chapter. Other electromagnetic methods that are used for groundwater exploration such as Very Low Frequency (VLF) technique, Frequency – Domain Electromagnetic (FDEM) profiling and Time – Domain electromagnetic (TDEM) techniques are briefly discuss below.

VLF survey method is an electromagnetic method that relies on transmitted current inducing secondary response in conducting geologic unit. A VLF anomaly represents a change in the attitude of the electromagnetic vector overlying conductive materials in the subsurface (GEM 1990). VLF is used to detect conductive bodies containing water in bedrock or in the vicinity of fractures. Ariyo et al., 2009, mention that; the

application of VLF in groundwater investigation is to prospect for basement terrain and mostly VLF is used as a reconnaissance tool.

Frequency – Domain Electromagnetic (FDEM) and Time – Domain electromagnetic (TDEM) are other types of electromagnetic techniques that are also used for groundwater investigations. FDEM surveys are used for mapping lateral geological changes in conductivity, water bearing faults and fractures. TDEM surveys are mainly used for depth sounding and for mapping freshwater saline water boundaries (Anon 1997).

In practise, mostly geophysical methods are used in combination. Mostly one method is used for reconnaissance survey and another for detail survey. The use of combine geophysical methods in an investigation is helpful in that should in case at the interpretation stage, ambiguity arises from the results of one survey method, this ambiguity may be removed by the consideration of the results from the second survey method (Kearey et al., 2002).

### 2.2.1.3. Ground penetrating radar

Ground Penetrating Radar is an electromagnetic technique for measuring the displacement current in the ground. Displacement currents are defined by the movement of charge within the ground by polarization and can be relating to applied electromagnetic by the electrical permittivity of the ground or the dielectric constant ( Annan as cited in (Anon 1997)). GPR has been a significant increase in use through the 1990's in near surface investigation with a number of case histories now recorded for groundwater (Anon 1997). It has been successfully applied to large – scales groundwater prospecting (Blindow et al. cited in (Zhu et al. 2009)).

GPR technique help in obtaining quantitative information about water table changes and the hydraulic properties could be estimated by combining GPR data and hydrogeologic data. GPR is very good in estimating the hydraulic properties of an aquifer (Zhu et al., 2009).

### 2.2.2. Some previous groundwater exploration projects in Ghana

### 2.2.2.1. Main methods use in groundwater investigation in Ghana

The use of geophysical techniques are not much popular in Ghana but there have being some improvement in the current years. The important roles in the use of geophysical methods for groundwater investigations is being realized in the current decade and it is the duties of the geophysicists educate and encourage the groundwater drilling and production companies, government agencies and other people involve in groundwater investigation on the need of the usage of geophysical methods in groundwater prospecting.

The main methods use for groundwater investigations in Ghana include;
A. The review of archival reports,
B. Interpretations of topographical, geological and structural maps,
C. Survey of existing boreholes and other water sources and
D. Discussions with residents of the communities.

These methods would not be the best but that are some of the methods widely used in Ghana (Gyau-Boakye & Dapaah-Siakwan 2000).

Traditionally, there are factors or indicators that help in locating aquifers. These ecological and physical indicators include;
A. Ant hills in the Accra Plains,
B. Valleys and low lying areas,
C. The presence of baobab trees in the north part of the country
D. Alignment of big trees or cluster of trees in the forest areas may indicate either a fracture or localized aquifer (Gyau-Boakye & Dapaah-Siakwan 2000).

### 2.2.2.2. Some groundwater geophysical investigation projects

There are no published reports or papers on any groundwater geophysical investigation in the research site but there are some published thesis, reports and articles on the use of geophysical methods in groundwater investigations in the Central Region and other regions of Ghana. And that some of them would be

discusses below to give us a broad review of the limit and applications of geophysical methods to groundwater investigations in Ghana.

According Bosu (2004), electrical resistivity profiling and sounding were used in 20 communities within the Assin District of the Central Region of Ghana to delineate regions of fractured zones, faults and the thickness of layers that might give clues to the presence of groundwater. The sounding data were modelled using Sondel software to obtain the layer structures of each sounding point together with the resistivity values. In communities within Assin district where this study was conducted, resistivity profile length of 160 – 190 m were chosen, the apparent resistivity values of the profiling ranges between 292 – 2099 Ωm. The VES indicate subsurface layers ranging from 3 to 4. The first layer generally has thickness between 1.3 – 3.5 m and apparent resistivity values ranging from 30 – 517 Ωm, the second layer has thickness of 3 – 44 m and generally classified as weathered granic zones, or weathered material with apparent resistivity between 15 – 1858 Ωm. The third layer which in some communities happen to be the basement rock have apparent resistivity values between 95 – 4961 Ωm. In communities with a 4 – layer model the third layer has averages thickness between 10.5 – 12 m. finally the fourth layers, the basement rock in some communities has apparent resistivity between 216 – 4606 Ωm. Generally the results of the geophysical works show possibilities of groundwater within most of the sounding points.

Electrical Resistivity Method was used to prospect for groundwater in Fanteakwa District of the Eastern Region of Ghana by Afoh. In Afoh 2000, lateral (profiling) and vertical (sounding ) of resistivity method using ABEM Terrameter SAS 300C meter in Dipole – Dipole configuration were conducted. Suitable sites for drilling were successful selected from the interpretation of the both the profiling and sounding and the drilling confirmed the presence of considerable freshwater. In all 98 boreholes were drilled within communities in the district based on the results of the work and 65% success was recorded. The predicted depths of water table from the interpretations of sounding data were correlated with the drilling results of the boreholes and a positive linear correlation was found.

In Adansi North District of the Ashanti Region of Ghana, vertical electrical sounding and resistivity profiling measurement were carried out in Dipole – Dipole array using Mc Ohm Resistivity Meter in seventeen communities within the district. VES at points on the profiling that show considerably low resistivity values. From the results of the VES, it was deducted that; most communities were underlain by an overburden of thickness between 12 and 16 m. Base on the geophysical interpretations of the data 36 sites were recommended for drilling and out of the 36 holes drilled 23 were successful whiles 13 were dry wells giving a success rate of 64% (Andorful 2013). Generally the uses of the resistivity methods yield an appreciable result.

Anechana, 2013 reported in his thesis work that; electromagnetic profiling using Geonics EM 34 – 3 and vertical electrical sounding using the Schlumberger electrode configuration were deployed along traverses within the Kintampo North Municipality of the Brong Ahafo Region of the Republic of Ghana. The qualitative analysis of the electromagnetic data indicated relatively high conductive zones which may possibly be fracture zones or weathered layers along the traverses. The interpretations of the VES delineate between three to five subsurface layers at different communities. The results of the study confirm that interpretation of EM and VES methods are very suitable for sitting boreholes in those communities with complex Voltaian sedimentary formation.

Asare & Menyeh, 2013 reported the used of geo-electrical resistivity profiling and vertical electrical sounding for groundwater recourses and aquifer characteristics investigations in two communities within the Gushiegu and Karaga District of the Northern Ghana. ABEM Terrameter SAS300C was used in this work to acquire the apparent resistivity data. VES were conducted to delineate the different subsurface geo-electric layers (resistivity and thickness of geological materials) and profiling was to map out any lateral variations in the subsurface resistivity that might exist in the survey area along the transverses. 1X1D Interpex software was used for the quantitative interpretations of the electrical sounding data. From the VES data the variation of apparent resistivity with depth were derived and they provided the geophysical signatures of the subsurface groundwater potential zones. On the bases

of the perceived aquifer properties, sites were recommended for drilling water supply boreholes for the communities.

In Menyeh et al., 2005, electromagnetic method of geophysical prospecting was used for identifying suitable groundwater potential sites for location of boreholes in an attempt to solve the chronic water supply problem and to increase the access of potable water for the residents of Gushigu –Karaga District, the third largest of the thirteen districts of the Northern Region of Ghana. In the project Geonics EM 34 -3 equipment was used for taking field measurements. Horizontal Dipole (HD) mode and Vertical Dipole mode readings were taken at each station. The field data were then plotted as apparent conductivity versus station profiles and from the results and interpretations of the data, it was inferred that; the study areas have good groundwater potentials and that water – bearing zones were between 30.0 to 60.0 m depth. It was concluded that, the electromagnetic technique is fast, efficient and effective in locating water – bearing zones. Electromagnetic method was recommended for use in investigation to locate suitable borehole sites in programmes aimed at accelerating rural water supply to rural communities.

Electromagnetic terrain conductivity and vertical electrical sounding methods were applied in investigation of groundwater potential in some communities in the Jirapa – Lambussie and Lawra Districts of the Upper West Region of Ghana. The electromagnetic method was used for reconnaissance survey and VES was used for detailed survey. After careful deductions in various communities, it was stated that there were possibilities of finding groundwater within 30 to 50 m depth. Six communities out of the ten communities investigated have high groundwater potentials at all sounding points (Adomako 1996).

### 2.2.3. Study area

### 2.2.3.1. Brief introduction

The study area comprise of ten Communities within The Twifo – Hemang Lower Denkyira District (THLDD) are the study areas. These communities include: Ablaso, Aboso, Achiase, Beseadze, Esukese Ekyir, Kwanyarko, Mbaa Mpe Hia No 2,

Moseaso, Nyameyeadom and Nyamebekyere No. 2 (figure 2.6). THLDD is one of the Twenty (20) Metropolitan, Municipalities, and Districts in the Central Region of Ghana. It was established in 2012 by Legislative Instrument (LI) 2022 with its administrative capital at Twifo Hemang. The district was inaugurated on the 28th June, 2012. The District has total area of 1,199 km$^2$ and 1,510 settlements. The district is subdivided into three (3) Area Councils viz. Hemang, Wawase and Jukwa. It consists of two (2) paramouncies, namely: Hemang and Denkyira and are coterminous with the Twifo Hemang - Lower Denkyira constituency with over 90 settlements.

According to the 2010 Population and Housing Census (PHC) of Ghana, the district (together with Twifo Atti-Morkwa) has population of 116,874 made up of 57,624 males representing 49.4% and 59,250 females representing 50.6%. However, the Twifo Hemang Lower Denkyira district as a new district is yet to access its demographic details of the 2010 PHC from the statistical service.
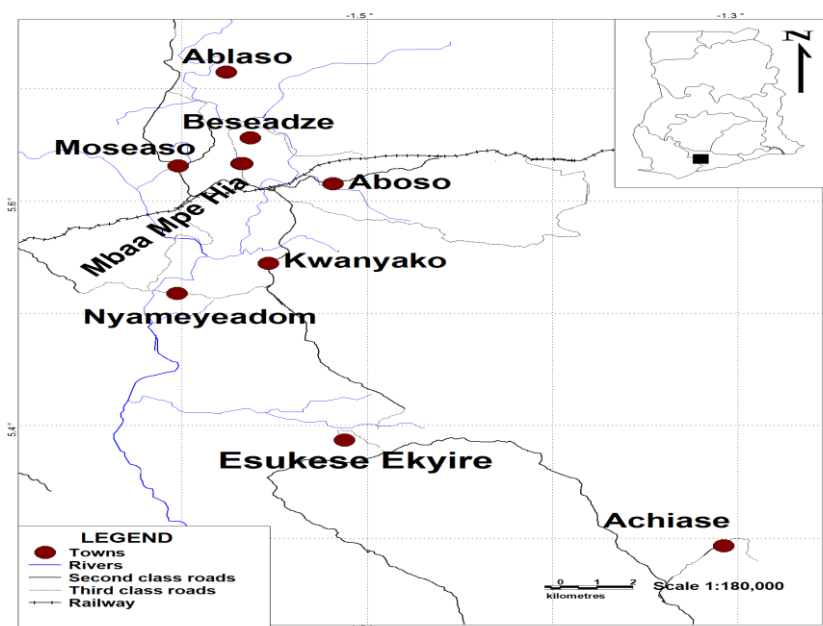


Figure 2.6. Map showing the study areas within the District.

## 2.2.3.2. Location, topography and drainage pattern of the study area

The District is located between latitudes 5°50'N and 5°51'N and longitudes 1°50'W and 1°10'W. The district is located at the north-western part of the central region and it is bounded on the north by the Upper Denkyira East Municipality, to the south by the Abura Asebu Kwamankese district, Cape Coast Metropolis and Komenda-Edina-Eguafo-Abirem Municipality, to the west by the Wassa Mpohor East District and to the East by Assin North Municipal and Assin South District (figure 2.7 and 2.8 below).
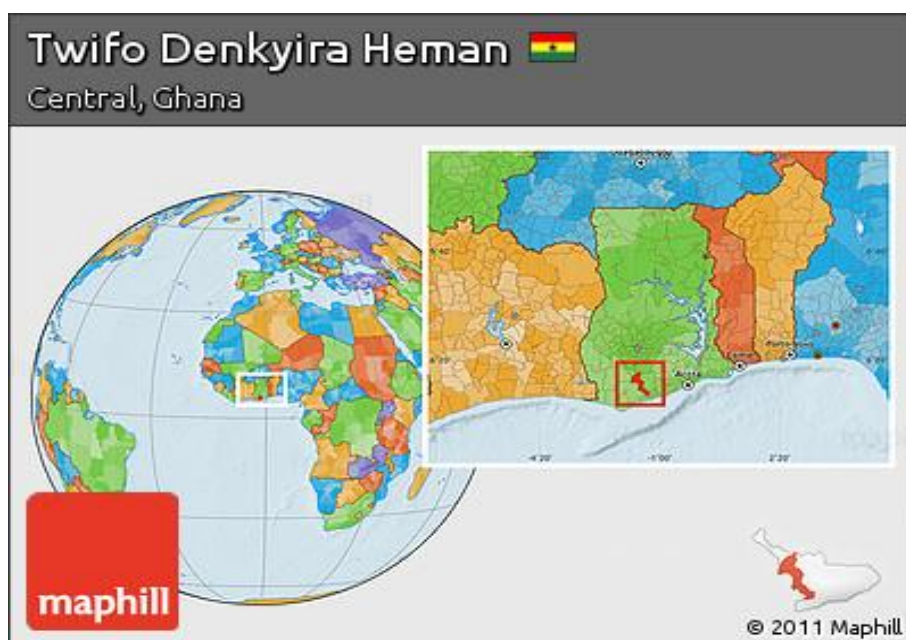


Figure 2.7. Map of Twifo Hemang Lower Denkyira District by Maphill on line map creator (Anon 2013)
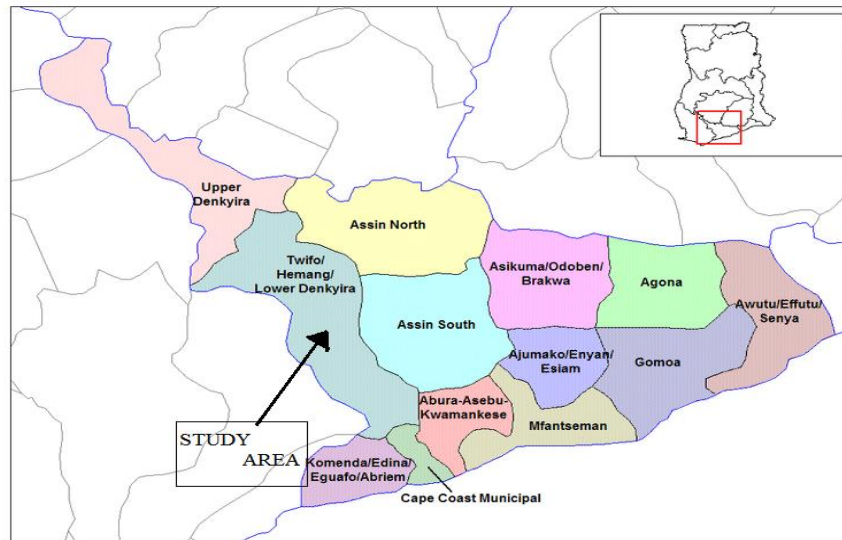
Figure 2.8. District Map of Central Region of Ghana by Wikimedia Commons (Anon 2014a)

The general altitude within the district is between 60 – 200 meters above sea level. The highest point in the district is Bepotsin (212 meters), west of Mfuom. The Pra River and its tributaries including Obuo, Bimpong and Ongwa drain the district. The Kakum River also takes its source from the Kakum forest reserve. The District has a rolling landscape.

### 2.2.3.3. Climate and vegetation of the study area

The district lies within the semi-equatorial zone marked by double maximal rainfall which peaks in June and October, and with a mean annual rainfall of 1750 mm. It has fairly high uniform temperature ranging between 26°C (in August) and 30°C (in March). Relative Humidity is generally high throughout the year, ranging between 70 – 80 percent in the dry season and 75 – 80 percent in the wet season.

The District's vegetation consists basically of semi-deciduous forest. Portions of which have been largely disturbed by the activities of man through farming, logging and mining among others. There are however, large areas of forest reserves including the Kakum National Park, Bimpong Forest Reserve, Pra Suhyen Forest Reserve, Minta Forest Reserve, and Bonsaben Forest Reserve. These forest reserves and the Kakum National Park altogether cover an area of 288 km$^2$ that is 24.0 percent of the entire surface area of the district.

### 2.2.3.4.  Regional geological and hydro-geological settings

There are two major formations that dominate the geology of Ghana. These include: the basement crystalline rocks associated with the West African Craton which covers 54% of the country and the Palaeozoic consolidated sedimentary formation formed in a depression of the West African Craton which covers 45% of the country. Minor geological formations underlie the remaining 1% of the country which includes the Cenozoic, Mesozoic and Palaeozoic sedimentary strata lying along narrow belts on the coast and Quaternary alluvium lying along the major stream courses (Obuobie & Barry, 2010 cited in (Somiah 2013)). Figure 2.9 below shows the geological map of Ghana. The basement crystalline rocks are of Precambrian age and consist of granite-gneiss- green stone rocks, phyllite, schist, quartzite, strongly deformed metamorphic rocks and amorogenic intrusions (Key in (Somiah 2013)). The principal tectonics stress orientation generally influences the structural trend in these basement rocks and they therefore follow a northeast-southwest axis. This formation is normally subdivided into the Birimian group (with associated granatoid intrusions), Granite, Tarkwaian group, Dahomeyan formation, Togo formation and Buem formation. The Birimian group covers densely populated areas including most of western, south-central, northeast and northwest of the country and can be as thick as 15,000 m and therefore is said to be the dominant group of the basement crystalline formation (Key in (Somiah 2013)).

On the other hand, the Palaeozoic consolidated sedimentary formation usually known as the Voltaian formation comprises principally of sandstone, shale, arkose, mudstone, sandy and pebbly beds and limestone. On the basis of lithology and field relationships, the Voltaian is further grouped into the upper, middle and lower Voltaian. The first subgroup being the upper Voltaian comprises masses and thin-bedded quartzite sandstones interbeded with shale and mudstone in some areas. The middle Voltaian (usually the Obusum and Oti Beds) consists of shales, sandstones, arkose, mudstones and siltstones whereas the lower Voltaian mainly comprises massive quartzite sandstone and grit (WARM in (Somiah 2013)).

The minor geological formations which include the Cenozoic, Mesozoic and Palaeozoic sedimentary strata are made up of two coastal formations namely, the coastal Block-Fault and the coastal Plain. The coastal Block-Fault comprises a narrow discontinuous belt of Devonian and Jurassic sedimentary rocks that have been parted into numerous fault blocks and are cut across by minor intrusives. Semi-consolidated to unconsolidated sediments underlie the coastal plain formation. These sediments range from Cretaceous to Holocene in age in south-eastern Ghana and in a relatively small isolated area in the extreme southwestern part of the country. One other minor formation, the Alluvia, consists of narrow bands of alluvium of Quarternary age, which occurs mainly adjacent to the Volta River and its major tributaries and in the Volta delta (Dapaah- Siakwan and Gyau-Boakye, in (Somiah 2013)).
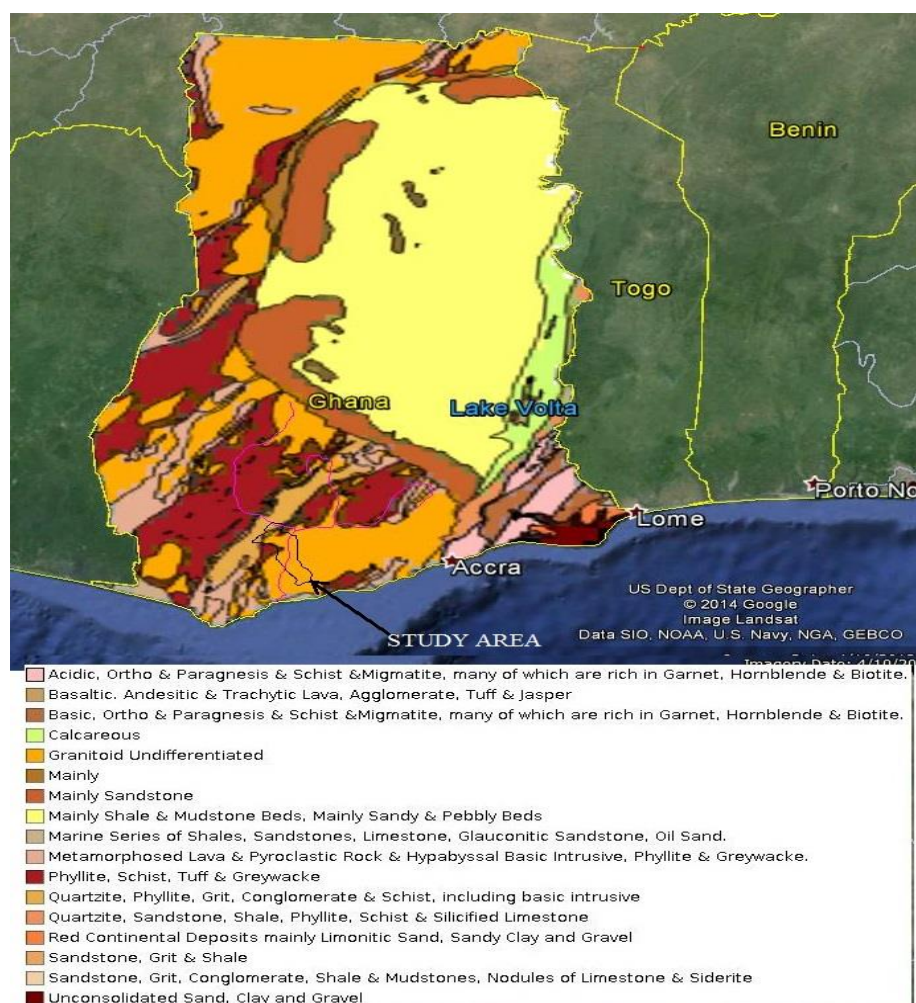


Figure 2.9. The Geological Formation Map of Ghana modified from Geological formation of Ghana (Anon n.d.)

The major geological formations in the country are overlain by the regolith. This regolith is a weathered layer that varies in thickness and lithology. The topography, structural characteristics, vegetation cover, lithology, erosion, climate, aquifer characteristics are all factors that influence the thickness of this regolith. Unlike in the extreme northwest part of the country where the thickness of the regolith can be up to 140 m, its thickness in the Precambian formation varies widely ranging from 2.7 to 40 m. The thickness of the regolith is generally thicker in the Precambian formation than in the Voltaian formation (Acheampong in (Somiah 2013)).

### 2.2.3.5. Local geology and hydrology of the study area

The bedrock geology of the study area is the Granite formation. The main rock types include granite and granodiorite with gneiss (Kesse 1985). These rocks are strongly folded, foliated and jointed. Intense weathering along fractures and veins had permitted water percolation to form groundwater reservoirs. Aquifers are therefore located where secondary porosity has developed. The two main aquifer types are (i) the weathered zone or 'regolith', which develops on the crystalline basement rocks, and (ii) fracture zones within the bedrock.
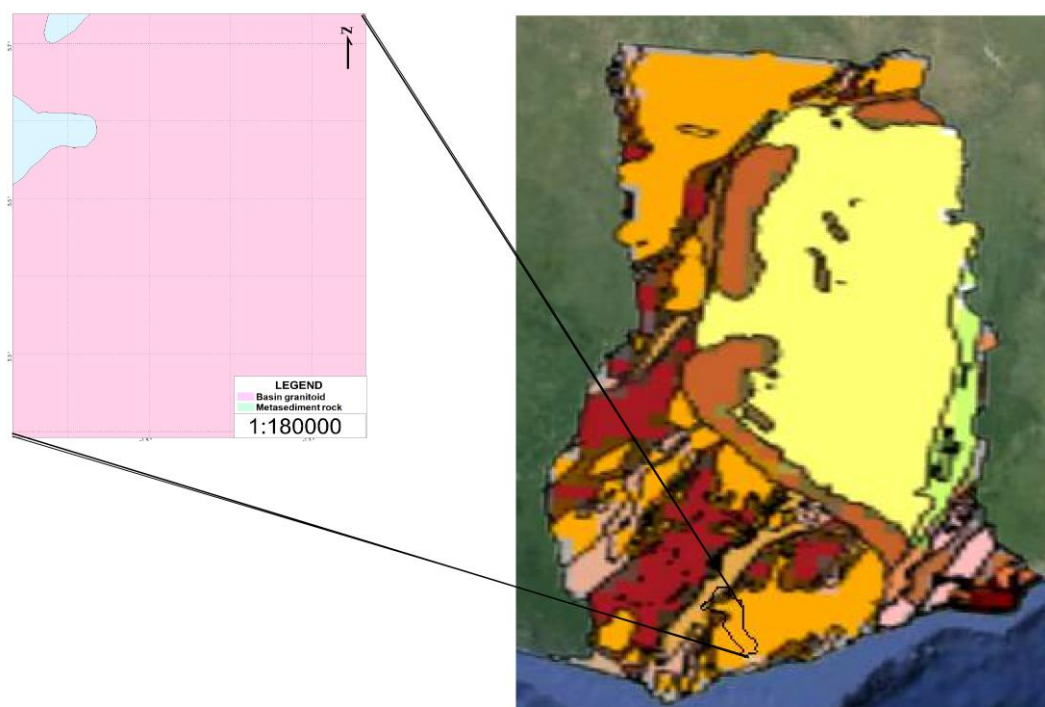


Figure 2.10. Section of the geological map of the study area. (modified from Geological formation of Ghana (Anon n.d.)

According to Gyamera & Kuma (2014), Basic granitic intrusives and granites underlie almost all the study area. Major rock types comprise well - foliated, medium - grained, potash-rich muscovite-biotite granites, grano-diorites and pegmatites (figure 2.10). Granites found in the study area are post Tarkwaian and can be divided into three groups: Bongo Granites, Dixcove Granite Complex and Cape Coast Granite complex. The Cape Coast granites are often associated with schists and gneisses, and intrude the lower Birimian meta-sediments. One characteristic of the granite is that it is not inherently permeable, but secondary permeability and porosity have developed as a result of fracturing and weathering. Groundwater occurs mainly in fractured portions of the bedrock. However, some amount of water may be obtained from the overburden and at the interface between the overburden and the bedrock.

### 2.2.3.6. Socio – economic activities of the study area

According to the composite budget of the THLDD Assembly document for the 2014 fiscal year (Anon 2014c); the district typically has a rural economy depending on rain fed agriculture, as the dominant employer. According to the 2010 PHC, 69.9% of the population is employed by agriculture implying that most the people are seasonal income earners and a failure of the rains is most likely to render them impoverished. However, the rich natural forest resources holds the potential to reduce the district's unemployment rate of 3% with the adoption of strategic programmes to expand agricultural activities The farmers mainly grow both cash and food crops. Notable among the crops grown are cocoa, oil palm, plantain, cassava, maize, rice and vegetables. Besides agriculture, there exist also a number of economic activities and financial services in the District, albeit not highly developed. They include periodic and daily markets, agro processing enterprises, banking, guest houses and lodges and fuel and gas stations which contribute significantly to the internally generated revenue of the assembly. The district is also endowed with viable tourism potentials and notable among them is the Kakum National Park, which attracts significant numbers of local and foreign tourists annually, with the potential to significantly boost the local economy in terms of the development of allied and complementary services and industry with the attendant employment generation and high income levels.

The district is composed of over 104 communities and hamlets in the district but only 43 (47.7%) currently connected to the national grid. This implies that over 50% of the district, although some of the communities are only farmsteads and hamlets, is yet to be connected, thus, limiting the opportunities of expanded business enterprises and accessibility to essential services and modern technology and thus worsening the poverty situation in these parts of the district.

The district is dominated by feeder roads. The district has 205.1 km of feeder road out of which 35.7km is bitumen surfaced and this includes the Hemang - Baakondidi (7.8 km), Jukwa township (3.5 km), Hemang – Bukusu (9.4 km) and Gyankobo – Abaka Nkwanta (2.0 km). The district is also traversed by an all year motorable 41 km highway from Jukwa – Twifo which forms part of the Cape Coast – Twifo Praso highway. Greater portions of the untarred roads especially the hilly areas of the district are difficult to travel on during the rainy season. This situation seriously makes transportation of goods, especially farm produce and service delivery very expensive, thereby affecting negatively the earning capacities of traders and other relevant service providers.

# CHAPTER 3. THEORETICAL BACKGROUND

## 3.1. Resistivity Method

### 3.1.1. Introduction

The resistivity method is an electrical method used in the study of horizontal and vertical discontinuities in the electrical properties of the ground, and also in the detection of three – dimensional bodies of anomalous electrical conductivity (Kearey et al., 2002 p. 183).

It is used extensively in the search for suitable groundwater sources and also to monitor types of groundwater pollution. It is used in engineering surveys to locate subsurface cavities, faults and fissures, permafrost, mine shafts etc. and in archaeology for mapping out the real extent of remnants of buried foundations of ancient buildings, amongst many other applications (Reynolds, 1997 p. 418).

General speaking, groundwater dissolves some salts and other elements and through the various dissolved salts it contains, it is ionically conductive and enables electric currents to flow into the ground. Consequently, measuring the ground resistivity gives the possibility to identify the presence of water, taking in consideration the following properties:

    A. A hard rock without pores or fracture and a dry sand without water or clay are very resistive; several tens thousands $\Omega$.m

    B. A porous or fractured rock bearing free water has a resistivity which depends on the resistivity of the water and on the porosity of the rock; several tens to several thousand $\Omega$.m

    C. An impermeable clay layer, which has bound water, has a low resistivity; several units to several tens $\Omega$.m

D. Mineral ore bodies (iron, sulphides, …) have very low resistivity due to their electronic conduction; usually lower or much lower than 1 $\Omega$.m (Bernard, 2003).

In the resistivity method, artificially generated electrical currents are introduced into the ground and the resulting potential differences are measured at the surface from these measurements the true resistivity of the subsurface can be estimated.

### 3.1.2. Brief historical background of resistivity method

According to some authors like Reynolds and Sharma; the electrical resistivity methods were developed in the early 1900s but become widely used since the 1970s due primary to the availability of computers to process and analyse the data. Sharma, 1997 stated that the technique of resistivity survey was developed by Conrad Schlumberger who conducted the first experiments (in 1912) in the field of Normandy. Löfgren n.d., explain the historical and theoretical background of resistivity method starting with the Einstein's (1905) equation that related diffusivity and ionic mobility of ions in liquid, then to the work of Archie (1942) which was titled 'The electrical resistivity log as an aid to determining some reservoir characteristics'. This work of Archie plays a great role in the development of theory of the resistivity method. There have been several contributions from several physicists and geoscientists particularly geophysicists to the development and improvement of the theories, instrumentations and the interpretation of the resistivity method as a geophysical technique.

According to Breusse in Zohdy et al., (1990 p. 8), the real progress in applying electrical methods to groundwater exploration began during World War II. French, Russian and German geophysicists are mainly responsible for the development of the theory and practise of direct current electrical prospecting methods.

### 3.1.3. Electrical resistivity in Earth materials

In resistivity exploration, the electrical current is carried through the earth material either

(a) Motion of free electrons or ions in the soil or

(b) Motion of ions in connate water.

The item (a) may be occasionally important when dealing with certain kinds of minerals such as graphite, magnetite, or pyrite. For most applications in engineering and hydrogeology, item (b) is overwhelmingly dominant.

The ions in connate water come from the dissociation of salts such as sodium chloride, magnesium chloride etc. Generally in water-bearing rocks and earth materials, the resistivity decreases with increasing;

    A. Fractional volume of the rock occupied by water,

    B. Salinity or free-ion content of the connate water,

    C. Interconnection of pores (permeability) and

    D. Temperature.

There are many factors that can conspire to distort the true value of an apparent resistivity reading. These may include; buried conductors like metallic pipelines, phone cables, oil and water tanks; metal fences; overhead high voltage lines and high voltage transformers on poles; water moving downslope or percolating just after a rain; etc. (Anon n.d.)

Resistivity is an extremely variable parameter; it changes from formation to formation and even within a particular formation. There are no general correlation of lithology with resistivity, nevertheless, a broad classification is possible according to which clays and shale, sand and gravel, compact sandstone and limestone, and unaltered crystalline rocks stand in order of increasing resistivity (Sharma, 1997). Figure 3.1 shows the approximate resistivity ranges in earth materials. No other physical property of natural occurring rocks or soils displays such a wide ranges of different values (Zohdy et al. 1990).
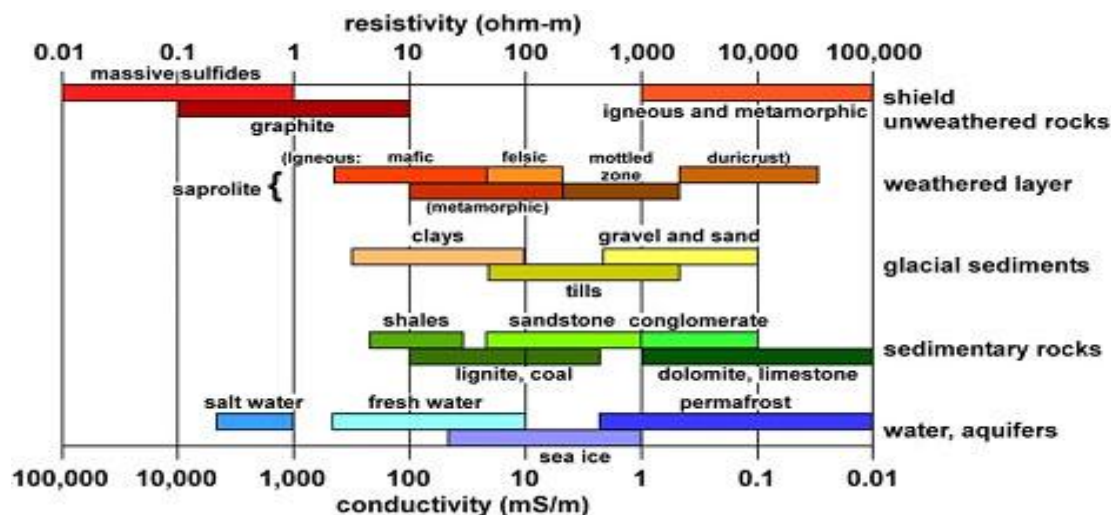
Figure 3.1. The approximate resistivity and conductivity ranges in earth materials (Crain n.d.)

The bases of the resistivity classification of the earth materials is that, the electrical condition in most rocks is essentially electrolytic because most mineral grains (except metallic ores and clay minerals) are insulators, electric conduction being through interstitial water in pores and fissures. Porosity is the major control of the resistivity of rocks, and that resistivity generally increases as porosity decreases. Porosity is related to resistivity in an empirical formula generated by Archie in 1942. The effective resistivity is expressed in terms of the resistivity and volume of the pore water present. This relationship is mathematically expressed as follows:

$$\rho = a\phi^{-b} f^{-c} \rho_w \tag{3.1}$$

Where $\phi$ is the porosity, f is the fraction of pores containing water of resistivity $\rho_w$ and a, b and c are empirical constants. $\rho_w$ can vary considerably according to the quantities and conductivities of dissolved materials.

### 3.1.4. Theory of Electrical resistivity method

### 3.1.4.1. Basic theory

In 1827 Georg Simon Ohm reported the following relationship between resistance (r) of a resistor, current (i), and corresponding charge in potential V:

$$V = ir \tag{3.2}$$

The empirical relationship is now known as Ohm's law. Consider rectangular resistor of length L and square cross – sectional area A. The resistance r of this resistor is described in terms of the length L of the path followed by a charge, the cross – sectional area A over which the charge are uniformly distributed and the resistivity $\rho$, which is a physical property of the substance used to make the resistor (fig 3.2). The current (i) flowing through the circuit is directly proportional to the resistance of the bar, which is inversely proportional to the cross – sectional area (A) and directly proportional to the length (L) of the bar.

$$r = \frac{\rho L}{A} \tag{3.3}$$

Equation 3.3 can be rearrange so that resistivity become the subject of the equation as below

$$\rho = \frac{rA}{L} \tag{3.4}$$
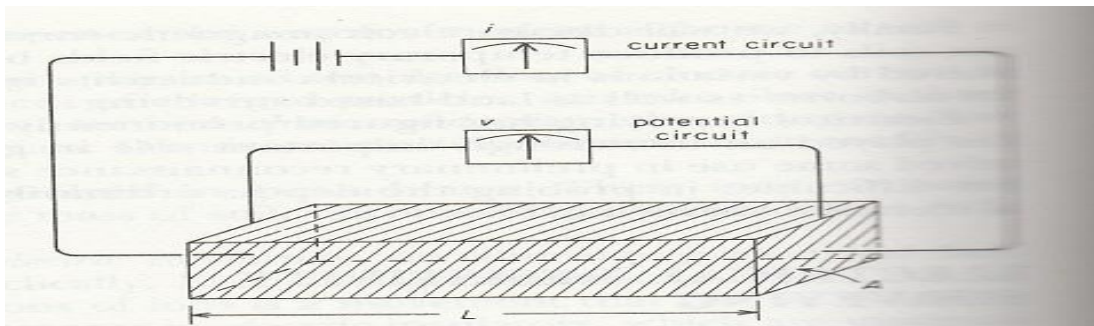


Figure 3.2. Electric circuit consist of resistor (consisting of a rectangular bar (Robinson S. & Çoruh, 1988))

The concentration of charge passing through a cross-sectional area of a resistor is called current density ($J_x$) and it is expressed as

$$J_x = \frac{i}{A} \tag{3.5}$$

From equations 3.2 and 3.3, one can write equation 3.5 as:

$$J_x = \frac{V}{\rho L} \tag{3.6}$$

### 3.1.4.2. Current flow in ground

Suppose that an electric circuit is constructed with the earth as the resistor. Two metal stakes serving as electrodes are driven into the ground at two different locations. One serving as source and another as sink and connected to battery terminals. Current is compelled to flow along paths leading from the source to the sink (Figure 3.3).

To determine the pattern of three dimensional current flows in the earth, the direction of current flow in each electrode is considered separately and then the combined effect is considered later. The source electrode is positively charged and that it repels positively charges, pushing them outward into the ground. The hemispherical zone is assumed to be an equipotential surface and resistivity in that surface is uniform. Current moves uniformly in all direction away from the source, radiating outward as shown by the paths in Figure 3.3.

The resistance of a current flow from the source through distance d (radius of the hemisphere) across the area $2\pi d^2$ of the hemisphere can be expressed from equation 3.3 as:

$$r = \frac{\rho \mathrm{d}}{2\pi d^2} = \frac{\rho}{2\pi}\left(\frac{1}{d}\right) \qquad\qquad (3.7)$$
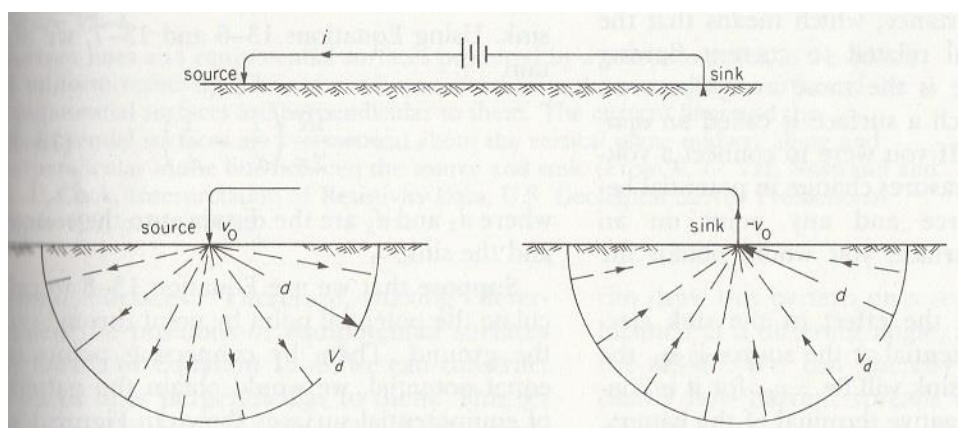


Figure 3.3. Schematic diagram of current flow through the earth (Robinson S. & Çoruh 1988)

The difference between the electric potential $V_o$ at the source and the electric potential $V_d$ at any point in the ground of the a distance d from the source is given as

$$V = \mathrm{i}r = \frac{\mathrm{i}\rho}{2\pi}\left(\frac{1}{d}\right) = V_0 - V_d \qquad (3.8)$$

The sink electrode is connected to the negative terminal of the battery and that the negative charged sink attracts positive charge and so current flow toward the sink. The difference between the electric potential - $V_o$ of the sink and the potential $V_d$ at all points a distance d away from it is express as:

$$-V = \mathrm{i}r = \frac{-1^{\rho}}{2\pi}\left(\frac{1}{d}\right) = V_d - V_0 \qquad (3.9)$$

The electric potential V at a point in the ground may be expressed as a combined contribution of the source and sink:

$$V = \frac{\mathrm{i}\rho}{2\pi}\left(\frac{1}{d_1} - \frac{1}{d_2}\right) \qquad (3.10)$$

Where $d_1$ and $d_2$ are the distances to the source and sink.

Suppose that equation 3.10 is used to calculate the potential point by point throughout the ground, and then by connecting points of equal potentials, a pattern of equipotential surface as shown in Figure 3.4 would be obtained. Figure 3.4 is the effect created by the combination of lines of equal potential of the source and sink in Figure 3.3
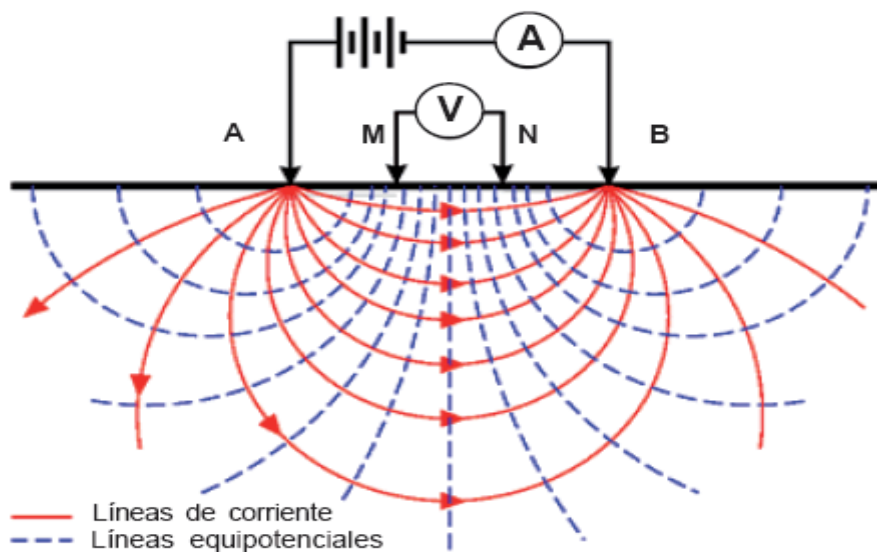
Figure 3.4. Schematic of current flow through the earth (Enrique et al., 2013)

In practise, it is difficult to monitor absolute potential (exact potential at a point), so potential difference between electrodes is measured. We now consider a generalized form of electrode configuration used in resistivity measurements (Figure 3.5).
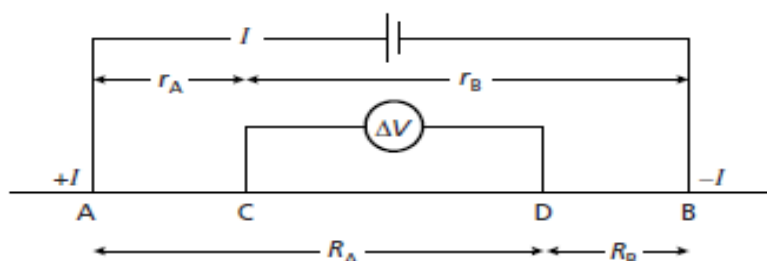


Figure 3.5. Generalized form of electrode configuration used in resistivity measurements (Kearey et al. 2002)

The potential $V_c$ at an internal electrode C is the sum of the potential contribution $V_A$ and $V_B$ from the current source at A and the sink at B.

$$V_C = V_A + V_B \qquad (3.11)$$

From equation 3.10, we can write $V_C$ as

$$V_C = \frac{i\rho}{2\pi}\left(\frac{1}{r_A} - \frac{1}{r_B}\right) \qquad (3.12)$$

Similarly

$$V_D = \frac{i\rho}{2\pi}\left(\frac{1}{R_A} - \frac{1}{R_B}\right) \tag{3.13}$$

The potential difference $\Delta V$ between electrodes C and D is measured:

$$\Delta V = V_C - V_D = \frac{ip}{2\pi}\left\{\left(\frac{1}{r_A} - \frac{1}{r_B}\right) - \left(\frac{1}{R_A} - \frac{1}{R_B}\right)\right\} \tag{3.14}$$

Therefore

$$\rho = \frac{2\pi\Delta V}{i\left\{\left(\frac{1}{r_A} - \frac{1}{r_B}\right) - \left(\frac{1}{R_A} - \frac{1}{R_B}\right)\right\}} \tag{3.15}$$

The ground in reality is not uniform as assumed in the derivation of the resistivity equation and that due to inhomogeneity of the subsurface; the resistivity will vary with relative position of the electrodes. Any computed value is then known as the apparent resistivity $\rho_a$ and will be a function of the form of the inhomogeneity.

$$\rho_a = 2\pi \frac{\Delta V}{i} \frac{1}{k} \tag{3.16}$$

Where K is geometrical factor and is expressed as;

$$K = \left(\frac{1}{r_A} - \frac{1}{r_B}\right) - \left(\frac{1}{R_A} - \frac{1}{R_B}\right) \tag{3.17}$$

### 3.1.4.3. Depth of penetration in resistivity method

Consider a current flowing in a homogenous medium between two point electrodes $C_1$ and $C_2$ as in Figure 3.6 below.
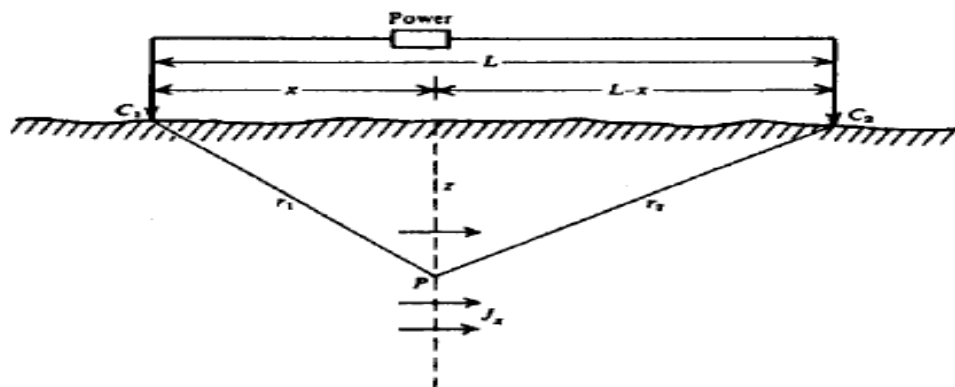


Figure 3.6. Diagram for determining the current density a uniform ground below two surface electrodes (Telford et al. 1990 p. 526)

The horizontal current density at point P is

$$J_x = \frac{i}{2\pi}\left(\frac{x}{r_1^3} - \frac{(x-L)}{r_2^3}\right)$$
(3.18)

And if point P is on the vertical plane midway between $C_1$ and $C_2$, then $r_1 = r_2 = r$ and

$$J_x = \frac{i}{2\pi}\left(\frac{L}{\left(z^2 + \frac{L^2}{4}\right)^{3/2}}\right)$$
(3.19)

From the equation 3.19 above, it could be seen that the depth of penetration of resistivity method largely depends on the current that flows in the ground and the distance of separation of current electrodes. Much current is needed into the ground for deeper penetration to be achieved. Figure 3.7 shows the variation in current density with depth across this plane (plane in Figure 3.6) when electrode separation is maintain constant. If on the other hand, the electrode spacing is varied, it is found

that $J_x$ is a maximum when L √2Z. For good penetration we must use large enough spacing that sufficient current reaches that target.
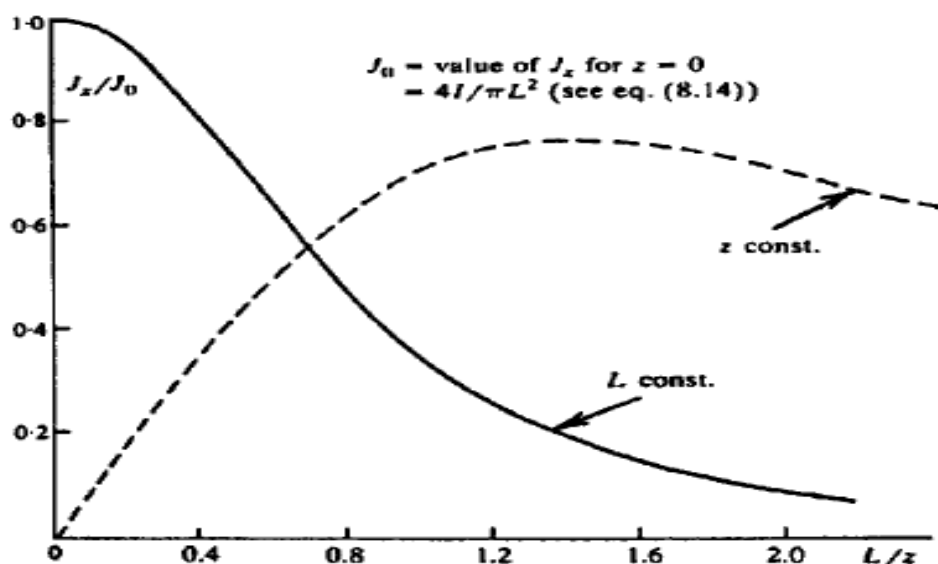


Figure 3.7. Graph showing current density versus depth (solid line) and electrode spacing (dashed lines)(Telford et al. 1990 p. 526)

### 3.1.5. Electrode arrays (spread)

Electrode array is also term electrode configuration or electrode spread. A number of electrode spread have been designed for field practice. Several commonly used linear array type arrangement are shown in Figure 3.7 for each arrangement the apparent resistivity equation can be obtained by using the approximate geometrical factor in equation 3.16 (Sharma 1997 p. 212).

### 3.1.5.1. Wenner array

In the Wenner array (Figure 3.7) four electrodes are equally spaced along a straight line, the distance between adjacent electrode is called the array spacing, a. The apparent resistivity of this array type can be calculated using the equation below;

$$\rho_a = 2\pi a \frac{\Delta V}{i} \qquad\qquad (3.20)$$

Wenner array has a simple geometry but often this arrangement is quite inconvenient for field work. For depth exploration using the Wenner spread; the electrodes are expanded about a fixed centre, increasing the spacing a in steps. For lateral exploration the spacing remain constant and all four electrodes are moved along the line, then along another line and so on.
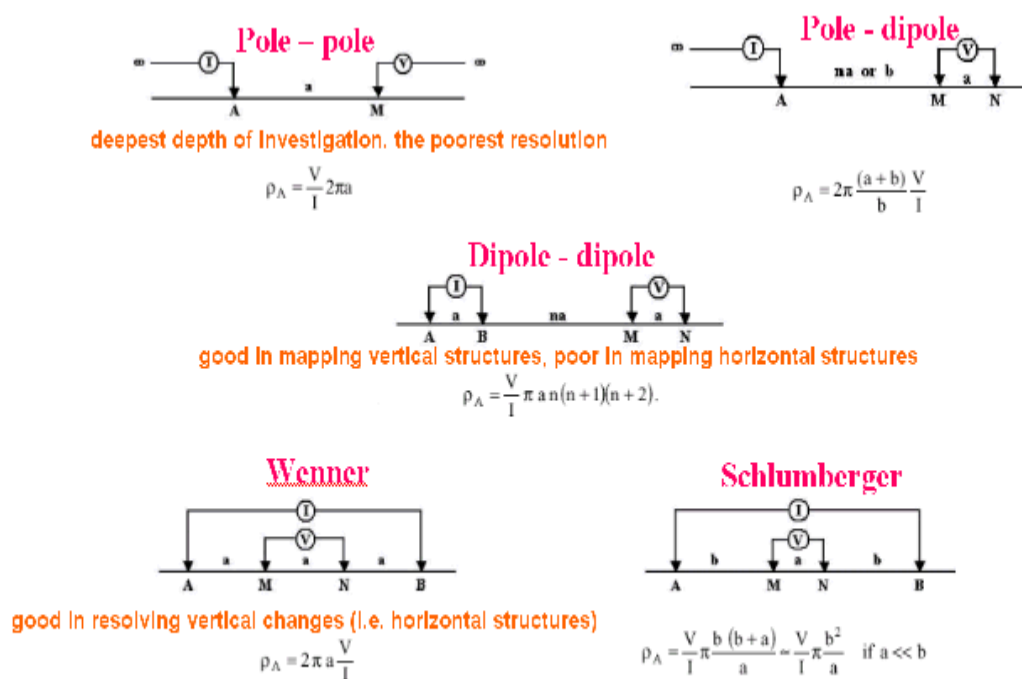


Figure 3.8. Different types of linear electrode arrays (Anon n.d.)

### 3.1.5.2. Schlumberger array

In the Schlumberger (symmetrical) array we can write a simplified formula for the apparent resistivity if we make b + a + b = 2L and a = 2l then the formula would be

$$\rho_a = \frac{\pi L^2}{2l} \frac{\Delta V}{i} \qquad\qquad (3.21)$$

In vertical sounding the potential electrodes remain fixed while the current electrodes spacing is expanded symmetrically about the centre of the spread. For a large value of L it may be necessary to increase the l also in order to maintain a measurable potential. This procedure is better than Wenner because only two electrodes need to

move. In lateral profiling several lateral movements of the potential electrodes may be accommodated without necessity of moving the current electrodes.

### 3.1.5.3.  Dipole - Dipole array

This array has been widely used in resistivity and IP surveys, because of the low EM coupling between the current and potential circuits. The arrangement of the electrodes is shown in Figure 3.7. The spacing between the current electrode pair A-B, is given as "a" which is the same as the distance between the potential electrodes pair M-N. This array has another factor marked as "n" in Figure 3.7. This is the ratio of the distance between the B and M electrodes to the A-B (or M-N) dipole length "a". For surveys with this array, the "a" spacing is initially kept fixed at the smallest unit electrode spacing and the "n" factor is increased from 1 to 2 to 3 until up to about 6 in order to increase the depth of investigation. The apparent resistivity of this array type can be calculated using

$$\rho_a = \pi a n (n+1)(n+2) \frac{\Delta V}{i} \tag{3.22}$$

### 3.1.5.4.  Pole –Dipole array

The pole-dipole array also has relatively good horizontal coverage, but it has a significantly higher signal strength compared with the dipole-dipole array and it is not as sensitive to telluric noise as the pole-pole array. Unlike the other common arrays, the pole-dipole array is an asymmetrical array (Figure 3.7). In pole-dipole array one of the current electrodes is fixed at a great distance from the other three. The spacing, a, between the potential electrodes is small compare to the distance na, to the current electrode (na >>a). The apparent resistivity equation for the observation point (midpoint between M and N) is

$$\rho_a = 2\pi a n (n+1) \frac{\Delta V}{i} \tag{3.23}$$

The effect of the current electrode B is approximately proportional to the square of ratio of the A-M distance to the B-M distance. Thus the pole-dipole array is less affected by the B remote electrode compared to the pole-pole array. If the distance of the B electrode is more than 5 times the largest A-M distance used, the error caused by neglecting the effect of the B electrode is less than 5% (the exact error also depends on the location of the N electrode for the particular measurement and the subsurface resistivity distribution).

### 3.1.5.5. Pole – Pole array

This array is not as commonly used as the Wenner, dipole-dipole and Schlumberger arrays. In practice the ideal pole-pole array, with only one current and one potential electrode (Figure 3.7), does not exist. To approximate the pole-pole array, the second current and potential electrodes (B and N) must be placed at a distance that is more than 20 times the maximum separation between A and M electrodes used in the survey. The effect of the B (and similarly for the N) electrode is approximately proportional to the ratio of the A-M distance to the B-M distance. If the effects of the B and N electrodes are not taken into account, the distance of these electrodes from the survey line must be at least 20 times the largest A-M spacing used to ensure that the error is less than 5%. In surveys where the inter electrode spacing along the survey line is more than a few meters, there might be practical problems in finding suitable locations for the B and N electrodes to satisfy this requirement. Another disadvantage of this array is that because of the large distance between the M and N electrodes, it is can pick up a large amount of telluric noise that can severely degrade the quality of the measurements. Thus this array is mainly used in surveys where relatively small electrode spacing (less than a few meters) is used. It is popular in some applications such as archaeological surveys where small electrode spacing are used. The apparent resistivity of this array type can be calculated using

$$\rho_a = 2\pi a \frac{\Delta V}{i} \tag{3.24}$$

### 3.1.6. Limitations of the resistivity method

Resistivity surveying is an efficient method for groundwater exploration and for delineating shallow layered sequences or vertical discontinuity involving changes in or contrast in resistivity. However, it has some limitations and because of these limitations using resistivity method with other geophysical methods are always recommended. Those limitations are: interpretations are ambiguous. The use of other geophysical methods as mentioned earlier, together with geological controls are necessary to discriminate between valid alternative interpretations of the resistivity data; interpretation is limited to simple structural configurations; topography and the effects of near surface resistivity variations can mask the effects of deeper variation and the depth of penetration of the methods is limited by the maximum electrical power that can be introduced into the ground and by the physical difficulties of laying out long lengths of cables.

### 3.1.7. The use of resistivity method in groundwater explorations

The purpose of electrical resistivity surveys is to determine the subsurface resistivity distribution by making measurements on the ground surface. From these measurements, the true resistivity of the subsurface can be estimated. The ground resistivity is related to various geological parameters such as the mineral and fluid content, porosity, and degree of water saturated in the rocks (Loke, 2001). The resistivity method have been found to be most useful not as an isolated measuring system but when used in connection with knowledge of geology (Anon n.d.). The resistivity methods have been widely used in hydrogelological, mining and geotechnical investigations and also in environmental surveys.

The direct current electrical resistivity methods for conducting VES has proved very popular with groundwater studies due to the simplicity of the technique and ruggedness of the instrumentation (Anon 1997). In groundwater studies, where the desired targets are thick aquifers saturated with fresh water overlying a high resistivity base, electrical surveys are ideal for determining thickness and even a measure of water quality ( Zohdy; Stoller and Roux; van Dam; Rogers and Kean; Urish; as cited in Dobecki (1985 p. 7). Resistivity method is also used in mapping

fracture zones in hardrock terrain, because high resistivity contrasts usually occur between fresh water and saturated fractured zones (Nascimento Da Silva et al. 2004); mapping boundary conditions in an aquifer systems; for siting wells and boreholes in crystalline basement aquifers and to access the directional variation in hydraulic conductivity of glacial sediments (Anon 1997) and among other uses or applications.

## 3.2. Electromagnetic Method

### 3.2.1. Introduction

The electromagnetic method is a geophysical prospecting method that involves the measurement of one or more electric or magnetic field component induced in the subsurface by a primary field produced from a natural (transient) or an artificial alternating current source.

Reynolds, 1997 p. 554, stated in his book that, among all the geophysical methods, the electromagnetic techniques must have the broadest range of different instrumental systems of any, matched by the remarkable range of applications to which these methods are applied. Although the EM method is mostly used in the mineral explorations; it also has a great role in the groundwater exploration. According to Nils & Lennart (2005); one big advantage with the EM method is that it does not need direct contact with the ground which eliminates problems associated with rocky surface or bad contact due to dry conditions. If there is an electric conductor body in the ground and an alternating magnetic flux in the surrounding, it produces a current in the body, which will produce a secondary magnetic flux in the opposite direction of the primary field. The speed with which EM surveys can be made is much greater than an equivalent survey using contacting electrical resistivity and also the induction process allows the method to be used from aircraft and in ships as well as down boreholes (Reynolds 1997).

### 3.2.2. Brief historical background of EM method

Probably the first electromagnetic method to be used for ore exploration was developed by Karl Sundberg in Sweden over two decades following the First World War (Sundberg in Reynolds (1997)). What is now known as the Sundberg Method

was developed in 1925 and was also used in structural mapping in hydrocarbon exploration (Sundberg and Hedström in Reynolds (1997). Other pioneering work was done in the early 1930s by a Russian geophysicist V. R. Bursian, whose work is little known in the West. Other electromagnetic methods have been available commercially only since the Second World War and particularly since the mid-1960s.

### 3.2.3. Electrical conductivity in Earth materials

Electrical conductivity of a substance is a measure of the ease at which an electrical current passes or flows through the substance. Conductivity is represented by a Greek symbol sigma ($\sigma$) and measured in unit of milliSiemens per meter (mS/m).

McNeil as cited by Tsikudo Kwasi (2009), explained that; most rock and soil minerals are electrical insulators of very high resistivity, however on rare cases conductive minerals such as magnetite, speculum's hematite, carbon, graphite, pyrite and pyrrhotite occur insufficient quantities in rocks and sils and thereby increasing their overall conductivity.

Conductivity and resistivity has an inverse relationship and that they are both affected by the same factors. Among some of the factors that may affect the conductivity of earth materials are; Porosity: shape and size of pores, number, size and shape of interconnecting passages; the extent to which pores are filled by water that is, the moisture content; the concentration of dissolved electrolytes in the contained moisture; temperature and phase state of the pore water and; amount and composition of colloids. Figure 3.1 shows the approximate resistivity and conductivity ranges in earth materials.

### 3.2.4. Theory of the electromagnetic method

### 3.2.4.1. Basic theory of electromagnetic method

Electromagnetic (EM) surveying methods make use of the response of the ground to the propagation of electromagnetic fields, which are composed of an alternating electric intensity and magnetizing force. Primary electromagnetic fields may be generated by passing alternating current through a small coil made up of many turns

of wire or through a large loop of wire. The response of the ground is the generation of secondary electromagnetic fields and the resultant fields may be detected by the alternating currents that they induce to flow in a receiver coil by the process of electromagnetic induction. The primary electromagnetic field travels from the transmitter coil to the receiver coil via paths both above and below the surface (Figure 3.9). Where the subsurface is homogeneous, there is no difference between the fields propagated above the surface and through the ground other than a slight reduction in amplitude of the latter with respect to the former. However, in the presence of a conducting body the magnetic component of the electromagnetic field penetrating the ground induces alternating
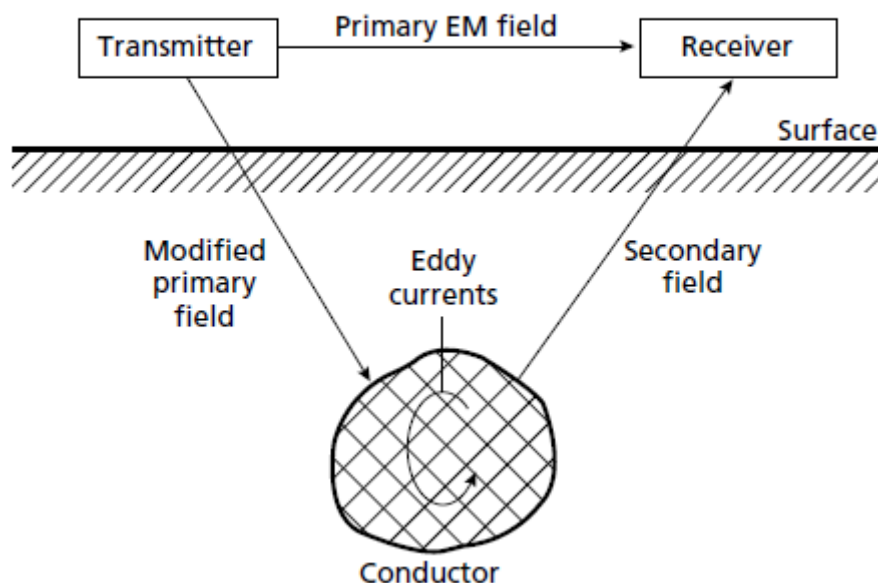
Figure 3.9. Generalized schematic diagram of EM survey (Kearey et al. 2002)

currents, or eddy currents, to flow in the conductor. The eddy currents generate their own secondary electromagnetic field which travels to the receiver. The receiver then responds to the resultant of the arriving primary and secondary fields so that the response differs in both phase and amplitude from the response to the primary field alone. These differences between the transmitted and received electromagnetic fields reveal the presence of the conductor and provide information on its geometry and electrical properties.

### 3.2.4.2. Fundamental quantities and field equation

An electromagnetic field is mostly described by four field vectors. The equation that relate the field vectors to their sources, a distribution of electric charge density $\rho_c$ (C/m$^3$) and of the electric current density i (A/m$^2$) is called the Maxwell equations. These equations are as follows:

$$CurlE = -\frac{\partial B}{\partial t} \tag{3.25}$$

$$CurlH = i + \frac{\partial D}{\partial t} \tag{2.26}$$

$$divB = 0 \tag{2.27}$$

$$divD = \rho_C \tag{2.28}$$

Where

E – The elecric field intensity (V/m)

H – The magnetizing field intensity (A/m)

B – The magnetic induction, or flux density (Wb/m$^2$ or tesla)

D – The electric displacement (C/m$^2$).

Other three relationships connecting the field vectors are

$$D = \varepsilon E \; ; \; B = \mu H \; ; \; i = \sigma E \tag{2.29}$$

Where $\varepsilon$, $\mu$ and $\sigma$ are, respectively the dielectric permittivity (F/m), magnetic permeability (H/m), and electric conductivity (S/m) of the medium. By using these relationships one can reduce Maxwell's equations in terms of only two vectors, E and H. And also by assuming for E and H a time-dependence of the form $E(t) = E_0 e^{iwt}$, where w (=$2\pi$f) is the angular frequency of the filed, the vectorial equations for the E and H take the below form:

$$\nabla^2 E = \mathrm{i}w\mu\sigma E - \varepsilon\mu w^2 E \tag{2.30}$$

$$\nabla^2 H = \mathrm{i}w\mu\sigma H - \varepsilon\mu w^2 H \tag{2.31}$$

Where $i = \sqrt{(-1)}$

These are the basic equations for the propagation of electric and magnetic field vectors in an isotropic, homogenous medium with physical properties ε, μ and σ. In equation 2.30 and 2.31, the terms involving $\mathrm{i}w\mu\sigma$ are related to the conduction currents, whereas the terms involving $\varepsilon\mu w^2$ are related to displacement currents. The rock properties (ε, μ and σ) and angular frequency w can be grouped into one term, $k^2$, which is given by

$$k^2 = \mathrm{i}w\mu\left(\sigma + \mathrm{i}w\varepsilon\right) = \mu\varepsilon w^2 - \mathrm{i}w\mu\sigma \tag{2.32}$$

The field equation 2.30 and 2.31 can then be written as

$$\nabla^2 E + k^2 E = 0 \,; \nabla^2 H + k^2 H = 0 \tag{2.33}$$

The quantity k is called the complex wave number or the propagation parameter. The behaviour of the propagation parameter with change in frequency is important to an understanding of EM wave propagation and attenuation.

Two important extreme cases can be distinguished,

Firstly, at low frequencies ( $f < 10^5$ Hz) the displacement currents are much smaller than the conduction currents ( $\varepsilon\mu w^2 \ll \mathrm{i}w\mu\sigma$ ), because ε for most rocks is small and the conductivity, σ, for favourable targets in EM surveys is usually greater than $10^{-2}$ S/m. This regime is known as the 'inductive' regime, the propagation parameter is approximately given by

$$k^z = -\mathrm{i}w\mu\sigma \tag{2.34}$$

In the second case, which is the other extreme, that is at high frequencies of the order of 10 MHz or higher, displacement currents dominate over conductive currents ($\varepsilon \mu w^2 \gg \mathrm{i} w \mu \sigma$) in the earth materials of low conductivity ($\sigma < 1$ S/m). For this case, the propagation parameter is given by

$$k^z = \mu \varepsilon w^2 \tag{2.35}$$

Thus, in the regime of high frequency and low conductivity, the propagation of the EM field depends mainly on the dielectric permittivity of the rock.

### 3.2.4.3. Attenuation of EM fields, and depth of penetration

According Sherrif in Tsikudo Kwasi (2009 p. 35), attenuation is the reduction in amplitude or energy caused by the physical characteristics of the transmitting media or system, including geometric effects such as the decrease in amplitude of a wave with increasing distance from the source and that attenuation is due to the interaction of the electromagnetic waves with matter as they are propagated through it. In effect, there is a decrease in amplitude or energy of the waves.

In trying to explaining the concept of attenuation and the depth of penetration of electromagnetic field, Sharma (1997) considers the case of a plane wave, propagating in the z – direction (vertically downwards) in a half-space of conductivity, σ, with an electric field having only x- component and the magnetic field only a y-component, and the amplitudes of the two fields varying sinusoidally with z (Figure 3.10). For this case, the field equations 2.33 have a simple solution, given by

$$E_x = E_0 \mathrm{e}^{-\mathrm{i}kz} = E_0 \mathrm{e}^{-\mathrm{i}\left(\beta + \mathrm{i}\alpha\right)z} \tag{2.36}$$

Where $E_o$ is the amplitude of the electric field component, $E_x$ at the reference point in the medium where z = 0, and k is the propagation parameter (or the wave propagation number). The solution of the magnetic field can be written likewise by replacing E with H.
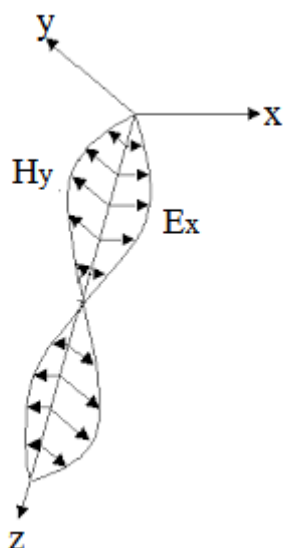
Figure 3.10. The sinusoidal behaviour of electromagnetic wave, modified from (Anon n.d.)

The real part of k is associated with the phase factor, and the imaginary part is associated with the attenuation factor. When the conduction currents dominate over displacement current, as is usual in EM prospecting for conducting bodies, the expressions for phase factor β and attenuation factor α is written as

$$\alpha = \beta \sqrt{\left(^{w\mu\sigma}\!/_2\right)} \tag{2.37}$$

The depth, δ, at which the amplitude of the field is reduced to 1/e (i.e., 37%) of its surface value is known as the skin depth. The depth is also referred to as the depth of penetration of EM wave. The skin depth is related to the attenuation factor in the below equation.

$$\delta = 1f \ \ \alpha = \left[2f \ \ \mu_0 \rho \omega\right]^{1f\ 2} = 504 \left(\rho f \ \ f\right)^{1f\ 2} \tag{2.37}$$

Where ρ is the resistivity in Ωm, f the frequency of EM wave in Hz, and μ ≈ μo (= 4π X 10$^{-7}$) for non-magnetic media.
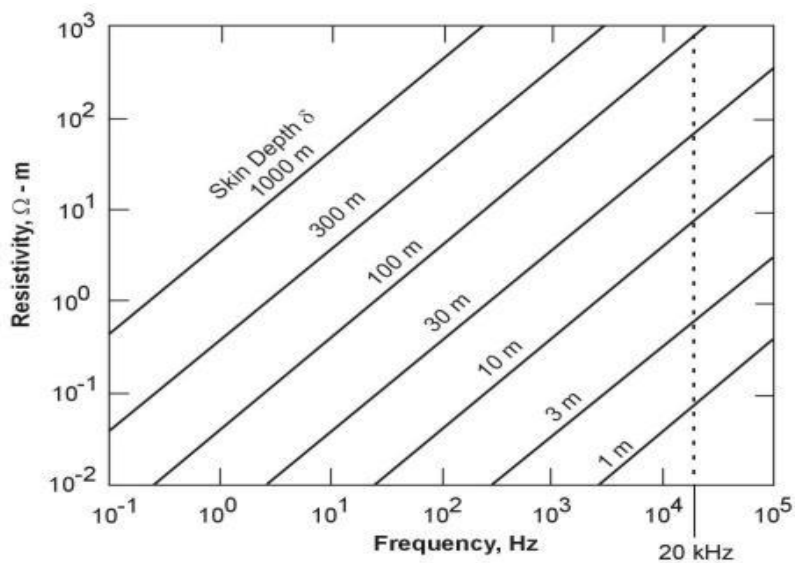
Figure 3.11. Skin depth as a function of resistivity and frequency (Anon n.d.)

Aside the above factor that affect the skin depth, it is also influenced by other factors such as instrument noise, relative magnitude of stray anomalies caused by near-surface conductivity variations, and the geometry of the deep conductor.

Table 3.1. Skin depth for some common materials as in (Anon n.d.)

| Material | $f = 60\,Hz$ | $f = 10^3\,Hz$ | $f = 10^6\,Hz$ | $f = 10^9\,Hz$ |
|---|---|---|---|---|
| Copper | 8.61 mm | 2.1 mm | 0.067 mm | 2.11 $\mu$m |
| Iron | 0.65 mm | 0.16 mm | 5.03 $\mu$m | 0.016 $\mu$m |
| Seawater | 32.5 m | 7.96 m | 0.25 m | 7.96 mm |
| Wet soil | 650 m | 159 m | 5.03 m | 0.16 m |

The usefulness of the skin depth concept is that it represents the maximum penetration of an EM method operating at frequency f in a medium of conductivity. The actual exploration depth may well be much less than a skin depth owing to other factors, notably the geometry of the prospecting system(Anon n.d.).

### 3.2.4.4. Slingram and Ground Conductivity Meters (GCM)

Horizontal Loop Electromagnetic (HLEM) systems or the Swedish name slingram is an electromagnetic system in which transmitter and receiver coils are horizontally oriented for exploration purposes (Reinhard, 2006). Ground Conductivity Meters

(GCM) are being classified as a frequency domain, active, near-field and small loop EM system. In this EM system, there are two coils, one being a transmitter which produces primary fields and the other is a receiver, separated by a constant distance of between 4 m to 100 m. This system is moved along in a survey transect. The point of reference for the measurement is usually the mid-coil position. Typical, dual-coil systems measure the quadrature component only or both the quadrature and in- phase components. The primary field is nulled so that in-phase and quadrature components of the secondary field can be measured (Reynolds, 1997).

Normally, the magnetic component of the superposition of primary and secondary field is measured. The measured field is split into the in-phase and out-phase component with respect to the primary field. Both components are recorded. A typical response of the in-phase and quadrature signal to a steeply dipping and highly conducting fracture zone is shown in Fig. 3.13.

According Reynolds (1997), GCM provides a direct reading of the quadrature component as the apparent conductivity of the ground in units of milliohms per meter. The in-phase is measured in parts per thousand.
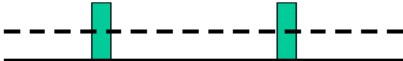
- HCP (horizontal co-planer)
- VCP (vertical co-planer)
- VCA (vertical Coaxial)

Figure 3.12. Orientation of ground conductivity meter (Anon n.d.)
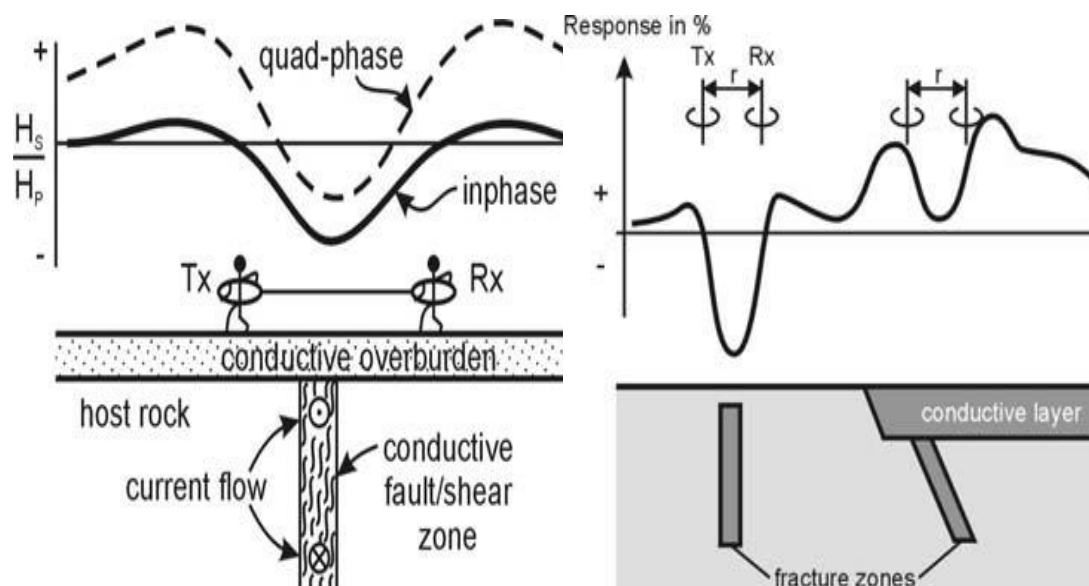
Figure 3.13. left: Slingram response over a highly conductive fracture zone. The offset at the quadrature response is due to the conductivity of overburden (after McNeill, 1990 in (Reinhard, 2006)), right: influence of a good conductive layer on the Sligram response (after Grissemann and Ludwig 1986 in (Reinhard, 2006)).

Induction number is the ratio of the inter–coil spacing divided by the skin depth. In a situation where the induction number is less than one, then the ratio of the secondary to the primary magnetic field at the receiver is directly proportional to apparent conductivity. Reynolds continue to explain that, if the ground is entirely homogenous and isotropic, the instrument should give a measure of true conductivity of the ground. However, real geological materials comprise of a mixture of constituents, most notably a solid matrix with pore spaces that may be partially or fully saturated with pore fluids which, in some cases, can make up of layers.

A ground conductivity meter responds to the conductivity composition of the ground, depending upon the orientation of the coils. There are two typical modes of orientation of the coils: horizontal coil with a vertical magnetic dipole (VMD), and a vertical coil with a horizontal magnetic dipole (HMD) (see Figure 3.12).

Sharma (1997) stated that; GCMs are operated in both vertical and horizontal dipole modes and each gives a significantly different response. When used in the vertical dipole mode (horizontal coil system) the device is responsive to the presence of relatively low-conductivity steeply dipping structures such as water-bearing fracture zones, whereas in the horizontal dipole mode (vertical coil system) the device is

quite insensitive to such structures and give fairly accurate measurements of ground conductivity in close proximity to them.

### 3.2.5. Limitation of EM methods

The electromagnetic method is a versatile and efficient survey technique, but it suffers from several drawbacks. They are as follows:

Electromagnetic methods do not work well for high resistive region. It is susceptible to interference from nearby metal pipes, cables, fences, vehicles and induced noise from power lines. Superficial layers with a high conductivity such as wet clays and graphite-bearing rocks may screen the effects of deeper conductors. Penetration is not very great, being limited by the frequency range that can be generated and detected. The quantitative interpretation of electromagnetic anomalies are complex, it may need more sophisticated interpretation skill. Most of the EM systems are not effective for very shallow measurements. And finally EM systems have fixed depth of investigation depending on frequency used and Tx-Rx separation (Kearey et al. 2002; Methods n.d.).

### 3.2.6. The slingram and GCM in groundwater prospecting

There are many type of electromagnetic methods used in groundwater prospecting and these methods have been demonstrated to provide a powerful suite of tools in hydrogeological investigations since the late 1970s (Reynolds, 1997). The use of EM methods is for general investigations of a groundwater regime (where the groundwater is prevalent within aquifers) and for searching within a local bedrock for fractures which may contain small but usable reservoirs of potable water (Reynolds (1997 p. 611)).

The GCM system as used in groundwater explorations is for detection of faults and fracture zones. These geological features are favourable for locating groundwater. As discussed earlier, in igneous rock areas where there are fractures, faults or other forms of cracks, water get the opportunity of passing through it and then finally settle within the rock and because of that most fracture zones have high conductivity. In

sedimentary rocks, mostly dry sedimentary formations have low conductivity and those formations that have their pores filled with water become highly conductive and these kind of conductivity is what the GCM measures.

# CHAPTER 4. INSTRUMENTATION AND METHODOLOGY

The Electromagnetic and Electrical Resistivity Methods were used in this research work. The electromagnetic method was used for reconnaissance survey. Points on the electromagnetic profiles that show adequate conductivity were considered for electrical resistivity sounding. Geonics EM34-3 Ground Conducting meter and ABEM Terrameter SAS 1000C equipment were used for electromagnetic profiling and vertical electrical sounding, respectively. In this chapter, the description, operation, and handling of the above mentioned equipment will be presented. Field procedures, data acquisition and data processing of both electromagnetic and resistivity methods will also be explained.

## 4.1. Instrumentation

### 4.1.1. Instrumentation of the Resistivity method

The equipment used for the resistivity surveying is the ABEM Terrameter SAS 1000C. This system was developed and marketed by ABEM. ABEM is a part of the Guideline Geo Group, global leader in geophysics and geo-technology. Figure 4.1 below is an image of the ABEM SAS 1000C.



Figure 4.1. Image of ABEM Terrameter SAS 1000C (Anon 2011)

### 4.1.1.1. Description of ABEM Terrameter SAS 1000C

According to the instrumentation manual for Terrameter SAS 4000/1000 (Anon 1999), the Terrameter SAS 1000 system consist of the following components:


- A. SAS 1000 instrument with one input channel
- B. SAS EBA External Battery Adapter
- C. DC Input cable for SAS EBA
- D. RS 232 Cable


ABEM Terrameter SAS 1000 is a highly competent Resistivity / IP system suitable for many different types of applications. By measuring both resistivity and IP simultaneously it minimizes expensive field time and it is expandable with a variety of accessories. ABEM Terrameter SAS 1000 is designed for demanding field work in tough conditions and has been well proven during years of field work in all parts of the world. Its cast aluminium casing is rugged and robust, yet light and easy to carry. It comprises a powerful built-in constant current transmitter that runs on either a clip-on battery pack or an external power source. The input channel is galvanically isolated and combined with a high resolution receiver which provides an excellent dynamic range. An intuitive user interface makes the ABEM Terrameter SAS 1000 easy to operate and measured data is exported and handled with the SAS Utility Software which also manages protocols and export of data to the most common interpretation software formats. A variety of accessories makes the Terrameter SAS 1000 capable to perform VES, 2D and 3D imaging as well as borehole logging surveys.

### 4.1.1.2. Principle of operation of ABEM Terrameter SAS 1000C

The Terrameter SAS 1000 operate in three modes; resistivity mode, induced polarization mode and voltage measuring mode. Due to the scope of this work only the principle of the resistivity mode will be discussed.


In the resistivity surveying mode, it comprises a battery powered, deep-penetrating resistivity meter with an output sufficient for a current electrode separation of 2000

meters under good surveying conditions. Discrimination circuitry and programming separates DC voltages, Self-Potentials and noise from the incoming signals.

The receiver measures the response voltage signals at discrete intervals when the eddy currents, the induced polarization and the cable transients have decayed to low levels.

The Terrameter SAS 1000 measures voltage responses created by the transmitter current while rejecting both DC (SP) voltage and noise. The ratio of voltage over current V/I is automatically calculated and displayed digitally in Kilo ohms, ohms or milliohms. The relevant receiver resistance range is automatically selected and the result is displayed to 3 or 4 digits. When the transmitter is operating at 500 mA, the Terrameter SAS 1000 has a resolution of 0.02 m$\Omega$ for a single reading. To take full advantage of the outstanding capacities of the Terrameter, care must be observed in the arrangement of cables and electrodes used in the field. Current leakage and creep can substantially reduce the attainable accuracy and sensibility and thus the depth of penetration.

### 4.1.1.3. ABEM Terrameter SAS 1000C handling and operation

As with all geophysical equipment the Terrameter must be handled with care to prevent damage. The operation of the Terrameter is not complex but rather easy. In taking a resistivity measurement on a field, the Terrameter is positioned half way between the potential electrode (M and N). And then terminals P1 and P2 are connected to terminals M and N respectively. The ABEM sounding cable set is used with conductors separated at the electrode end.

Current electrodes (A and B) are connected to terminals CI and C2, respectively. These cables are run in parallel adjacent to the Terrameter and they are arranged symmetrically with respect to the potential electrodes. The power is switched on after the arrangement is finished. The mode is now set on Resistivity and then the Measure Knob is activated so that resistivity measurement can be taken. After resistivity measurement is taken and recorded another reading is then taken or the set is moved

to another position to continue the resistivity measurement till the end of the survey (see Figure 4.2).
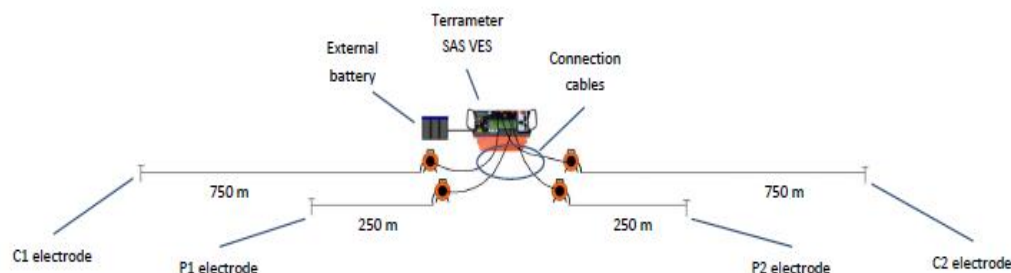


Figure 4.2. Schematic of field work using ABEM Terrameter SAS for VES (Anon 2014b)

## 4.1.2. Instrumentation of the electromagnetic method

Geonics EM34-3 was used for the Electromagnetic profiling surveys. This system was made by the Geonics limited located in Ontario, Canada. The Geonics EM34-3 is shown in Figure 4.3.



Figure 4.3. Image of Geonics EM34-3 system (Xia et al. 2001)

## 4.1.2.1. Description of the Geonics EM 34-3

The EM34-3 is a simple-to-operate, cost-effective instrument for the geologist and hydro geologist a like; applications have been particularly successful for the mapping of deeper groundwater contaminant plumes and for the exploration of potable

groundwater resources. The EM34-3 includes connectors for an analogue signal output, as well as an input which can be used with a rechargeable battery option. Digital signal output, required for data collection with the DL600/DAS70 system, is available as an option for all models of the EM34-3.

### 4.1.2.2. Principle of operation of Geonics EM 34-3

Consider Figure 4.4 in which a transmitter coil Tx energized with an alternating current at an audio frequency, is placed on the earth (assumed uniform) and a receiver coil Rx is located a short distance away. The time-varying magnetic field arising from the alternating current in
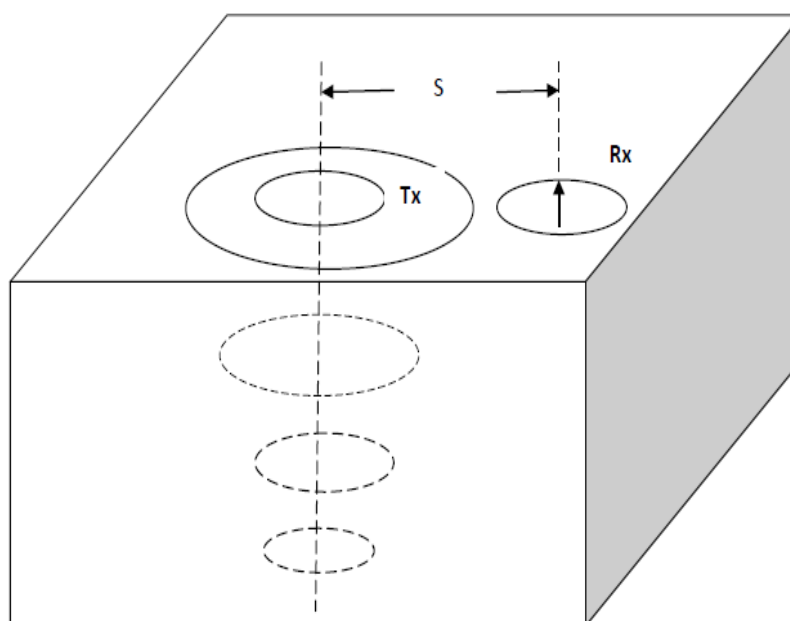


Figure 4.4. Induced current flow (homogenous half space) obtained from (Tsikudo Kwasi 2009)

the transmitter coil induces very small currents in the earth. These currents generate a secondary magnetic field $H_s$ which is sensed together with the primary field, $H_p$, by the receiver coil.

The secondary magnetic field is generally a complicated function of the intercoil spacing s, the operating frequency, f, and the ground conductivity σ. Under certain constraints, the secondary magnetic field is a very simple function of these variables.

These constraints are incorporated in the design of EM34-3 whence the secondary magnetic field is shown to be:

$$\frac{H_s}{H_p} \cong \frac{iw\mu_0\sigma s^2}{4}$$  (4.1)

Where $H_s$ = secondary magnetic field at the receiver coil

$H_p$ = primary magnetic field at the receiver coil

$W = 2\pi f$

$\mu_o$ = permeability of free space

$f$ = frequency (Hz)

$\sigma$ = ground conductivity (mho / m)

$s$ = intercoil spacing (m)

$i = \sqrt{(-1)}$

The ratio of the secondary to the primary magnetic field is now linearly proportional to the terrain conductivity, a fact which makes it possible to construct a direct-reading, linear terrain conductivity meter by simply measuring this ratio. Given $H_s$ / $H_p$ the apparent conductivity indicated by the instrument is defined from equation 4.1 as

$$\sigma_a = \frac{4}{w\mu_0 s^2}\left(\frac{H_s}{H_p}\right)$$  (4.2)

The units of conductivity are the mho (Siemens) per meter or, more conveniently, the millimho per meter (McNeill 1980).

### 4.1.2.3.  Handling and operation of Geonics EM 34-3

The Geonics EM34-3 is a two man portable system that has two coils flexibly connected. The intercoil spacing is measured electronically so that the receiver operator simply reads a meter to accurately set the coil to correct spacing, which can be 10, 20, or 40 meters so as to directly vary the effective depth of exploration as shown in table 4.1.

Table 4.1. Exploration depths of Geonics EM 34-3 at various intercoil spacing (Tsikudo Kwasi 2009; McNeill 1980)

| Intercoil Spacing (meters) | Exploration Depths (meters) | |
|:---:|:---:|:---:|
| | Horizontal Dipoles | Vertical Dipoles |
| 10 | 7.5 | 15 |
| 20 | 15 | 30 |
| 30 | 30 | 60 |

When measuring terrain conductivity, the transmitter operator stops at the measurement station; the receiver operator moves the receiver coil backwards or forward until his or her meter indicated correct inter coil spacing and he or she reads the terrain conductivity from a second meter. The coils are normally carried with their planes vertical (horizontal dipole mode) since in this configuration the measurement is relatively insensitive to misalignment of the coils. In the event that the greater depth of penetration resulting when the two coils are in the vertical dipole mode is desired, more care must be taken with intercoil alignment, this is because of the relatively short intercoil spacing correct alignment is usually not difficult to achieve (McNeill 1980).

## 4.2. Methodology

### 4.2.1. Introduction

Generally, before the geophysical surveys were conducted in the study area, desk studies, interpretation of available aerial photos and terrain evaluation studies were conducted in a way to make geophysical studies more easily and effectively. In this section reconnaissance surveys, geophysical surveys and the processing of results from the geophysical surveys will be discussed.

### 4.2.2.  Aerial photo interpretation

Aerial photos of the study area could not be obtained at the Survey Department for this project. Notwithstanding, traverse selection was guided by the drainage patterns delineated from topographic maps and terrain evaluation on the field. Generally, drainage schemes are highly responsive to types of rocks and bedding. Geologically, weak zones such as fractures and faults are favourable for surface water and groundwater development. Traverses were selected to intercept lineaments orthogonally as much as possible.

### 4.2.3.  Desk study and data compilation

The desk study involved compiling and assessing the following data sets: Topographic and geological maps, existing borehole information and reports on previous hydrogeological studies undertaken in the study area where they are available. The purposes of these were to establish the current knowledge about lineament patterns and fractures, the presence of suitable aquifers and their thickness, groundwater quality, the mean aquifer and water table depths and the expected lithological sequences.

### 4.2.4.  Reconnaissance survey and terrain evaluation

The main purpose of the reconnaissance survey was to locate target areas for geophysical investigations. It comprised of an assessment of topography, geology, hydrogeology, structural features, water points and soil surveys to detect sufficiently permeable strata that by virtue of their relative elevation or depression, geological history and hydrology could be water bearing. Furthermore, social, logistical and accessibility considerations were also taken into account. It also included setting out traverse lines in the selected target areas. Careful observation of the surface physiographic and geologic features in the survey area such as vegetation, outcrops, stream patterns, springs, and the location of any previous boreholes or wells, exposed fractures and the direction of runoffs or the slope of the terrain. Much information is also sought from members of the community, on environmentally prohibitive

locations such as rubbish dumps, cemeteries and toilets facilities. After collecting all these information, suitable locations are then earmarked for geophysical surveys.

### 4.2.5. Background data

Before the field data were collected and during the interpretation of the geophysical data, background data were considered. The background data for this work are available data on existing boreholes and / or hand-dug well within 5 km radius of study areas. What made this data important was that it contained information on lithology, depths yield and water quality of the already existing wells. These help to know what to expect to encounter on the study sites, although results can vary widely in some areas. It helped in planning of the field surveys and in interpreting the obtained geophysical data.

In some communities there were no data, while in some other communities there were available data on existing wells within a 5 km radius of the study sites.

### 4.2.6. Geophysical survey

The geophysical techniques employed included Electromagnetic (EM) profiling and Vertical Electrical Sounding (VES). The electromagnetic technique was aimed at detecting both narrow and large fracture zones as well as thick weathered zones (regolith), which are the two key controls on groundwater occurrence in the study area. The VES method was used to estimate the depth to bedrock, the number of subsurface geological layers, and their corresponding resistivities.

### 4.2.6.1. Electromagnetic profiling

Profile lines ranging from one to four were created within all the ten communities included in the research work. Place of noticeable ground water contamination such as areas around waste dumps, toilets facilities and grave yards among others were avoided. The electromagnetic measurements were carried out on traverses using the Geonics EM 34-3 ground conductivity meter. The equipment provides a direct reading of the apparent subsurface conductivity in the region of the measuring coil. This is achieved by generating a primary electromagnetic field from a transmitting

coil, which subsequently induces a secondary magnetic field in the subsurface. A receiving coil detects the resultant electromagnetic field from both the primary and secondary fields. A 20-m coil separation with EM readings taken at 10 m intervals was used for the profiling in some communities and in other communities a 10-m coil separation with EM reading taken at 5 m intervals was used. 10 m intercoil separation has an exploration depth of 7.5 m and 15 m for the HD mode and VD mode, respectively. The 20 m intercoil separation has also an exploration depth of 15 m and 30 m for the HD mode and VD mode, respectively. Generally, the standard 10 m separation coil is good enough to detect fractured zones as narrow as 5m (Beeson and Jones, 1988). Measurements were taken in horizontal dipole (HD) and vertical dipole (VD) modes.

Graphs of apparent conductivities (in mmhos/m) on vertical axes versus station intervals (in meters) on horizontal axes were plotted. Points where the vertical dipole (VD) conductivities exceeded the horizontal dipole (HD) conductivities were noted for VES investigation. Other points were also selected for VES investigation based on experience. Points near waste dumps and toilet facilities or under a roofing of buildings were avoided although these points might have high conductivities or crossover points. Those points were avoided due to possible contamination of the groundwater and dispute in the case where high conductivity points are very near to a buildings.

### 4.2.6.2. Vertical Electrical Sounding (VES)

VES measurements were confined to selected locations along the EM profiles and they were carried out using an ABEM Terrameter SAS 1000C and the Schlumberger (symmetrical) electrode array. The ABEM Terrameter SAS 1000C equipment was setup, ensuring that the batteries were fully charged and that, electrodes were well hammered into the ground. Cables were connected to both current and potential electrode terminals. The Schlumberger protocol was chosen. Direct current was applied into the ground through the current electrodes and the resulting potential difference measured by another pair of potential electrodes in the region of the current flow. Expanding the electrode system varied the depth of investigation. The resistivity values of each of the VES sites were read directly from the Terrameter. To

ensure reliable and consistent readings, measured results were plotted in the field during the measurements and inconsistent values were repeated to ensure uniformity in the readings.

The field data were analysed and interpreted using two geophysical programs namely; Zondip1d (Zond Geophysical Software) and Surfer 9 (a product of Golden Software). For the Zondip1d, the data were copied and pasted on VES notepad window (similar to excel window) and logarithmic curves of the data were automatically generated. The generated curves were studied and starting models were derived from them. The data were inverted using inversion button starting with the user models. The calculated and the measured resistivity values were adjusted to reduce the error to the possible minimum value. The inverted data were saved as Bitmap Image format. The first output is made of log-log of apparent resistivity versus current electrode separation which is referred to as the sounding curve and the other output is a pseudo section of the sounding curve which is made up of apparent resistivity and depths. The sounding curves and the pseudo section were edited using Microsoft Paint to remove unwanted images and to add additional information to the outputs.

Surfer 9 software was used to model the measured apparent resistivity values. GPS coordinates of VES stations were used together with resistivity values and the depth (at which the resistivity values were measured) to create contour maps. For the Surfer programme, the resistivity values for all VES stations in a community were considered collectively and these resistivity values were classified according to the depths they were measured at. The depths (in meters) are 1.5, 2.1, 3, 4.4, 6.3, 9.1, 13.2, 19, 27.5, 40, 58, and 83. Contour maps were created from the BLN data. The maps were stacked together and the locations of the VES stations were shown on the map on top of the stacked maps. The maps were exported from Surfer in BITMAP Image format. The images were further edited and some information added to them by using Microsoft Paint programme.
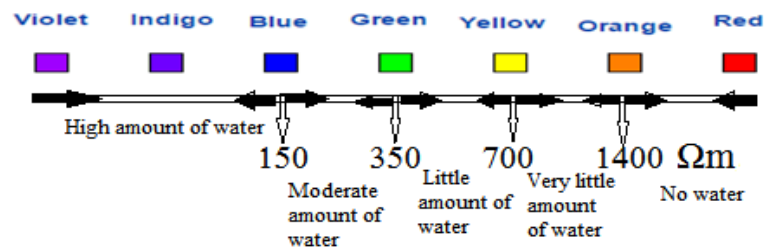
Figure 4.5. Colour spectrum model use in the surfer programme to represent apparent resistivity values

In the surfer program, the apparent resistivity models were created using the rainbow colour spectrum to represent the apparent resistivity values (Figure 4.5). The spectrum was divided into five groups and each group was assigned to some colours and resistivity values. The first group whose apparent resistivity values starts from 0 – 150 Ωm are assigned to colour between violets to blue (including the intermediate colours between them). The apparent resistivity values of the second group start from 150 – 350 Ωm and colours between blue to green were assigned to this group. The third group start from 350 Ωm (green) to 700 Ωm (yellow) and all the intermediate colours between green and yellow. The fourth group used in this model start from 700 Ωm to 1400 Ωm with colours from yellow to orange assigned to the group. Finally, the last group consists of any resistivity value from 1400 Ωm upward. This group has colours from orange to red representing it. This models is based on the fact that the resistivity values for weathered granite is in the range of 30 – 500 Ωm (Reynolds ,1997 p. 422).

The presence of groundwater within an aquifer in the study areas within this project is divided into five classes namely; high amount of groundwater (0 – 150 Ωm); moderate amount of groundwater (150 – 350 Ωm); little amount of groundwater (350 – 700 Ωm); very little amount of groundwater (700 – 1400 Ωm) and lastly zones with no water ground (1400 - ∞ Ωm). With this model recommendation for drilling a well at a point is given when the point falls within the first three classes or groups. Unless the community has generally low level of groundwater, points within the fourth class never get recommended. The main aim for using this kind of model is to recommend points where well could run throughout the year. Also since this project aimed at finding points to drill or hand dug wells for public use, the demand for

water from those wells would be high and for that reason zones which are capable of supplying adequate water should be recommended for construction of wells.

# CHAPTER 5. DATA INTERPRETATIONS AND DISCUSSIONS

## 5.1. Introduction

In this study as in any other groundwater exploration, it is not the groundwater itself that is the target of the geophysical investigations, but rather it is the geological situations in which the groundwater exists.

The electromagnetic method determines the ground conductivity, while the resistivity method determines the resistivity of the ground. From Physics, it is known that resistivity is inversely proportional to conductivity. The results from electromagnetic profiling give us the apparent or terrain conductivity of the site and this information are used to choose where to conduct VES measurements.

The resistivity values of freshwater are between 10 to 100 Ωm and usually resistivity of the aquifer can be between 50 to 2000 Ωm depending on the geology of the aquifer. As understood from the work of Anechana (2013), mostly when investigating for groundwater; in a hard rock (resistant) environment, a low resistivity anomaly will be the target while in a clayey or salty (conductive) environment, it is a high conductive anomaly which will most probably correspond to a fresh water aquifer. In sedimentary layers, the product of the aquifer resistivity by its thickness can be considered as representative of interest of the aquifer ( Bernard, 2003 cited in (Anechana, 2013).

The geological information shows that, the bedrock geology of the study areas is granite formation. These granites are Post Tarkwanian and consist of mainly of Cape Coast Granit Complex. The main rock types include granite and granodiorite with gneiss. Granite and granodiorite are both intrusive igneous rocks and igneous rocks are generally resistive in nature. There are records of strong folding, foliations and joints in the rocks of this formation. There are also intense weathering along fractures

and veins. Areas within the study sites that would show high conductivity in the case of the EM method and low resistivity (resistivity values between 30 – 500 Ωm (Reynolds, 1997 p. 422)) in the case of the VES would be of interest to this work because of the records of fractures, faults and other geological structures within this area that usually permit water to percolate forming groundwater reservoirs (Kesse 1985; Gyamera & Kuma 2014; Wikipedia 2015; Wikipedia 2014).

## 5.2.  Data presentation and interpretations

The EM data consist of EM profiling response for both HD and VD along traverse in all the communities where the data were collected. The EM profiles were not conducted evenly in the communities, in some communities only a single EM profile was conducted while in others more than one profile. In all 29 EM profiles were conducted in the study area.

The measured conductivity values in both dipole modes were plotted against the station interval (on the same Microsoft Excel sheet of the Microsoft 2007 package) to give dipole response curves. Both dipole responses were analysed qualitatively to select points of high conductivity and also free from potential groundwater pollution sources for further investigations. Emphasis was placed at points along the profiles where crossover were occurring and preferable where the VD response exceeds the HD. These points may indicate possible presence of weathered or fractured or faulted subsurface zone with possible groundwater potentials.

VES surveys were conducted at selected points along the EM profiles where relatively conductive layers have been detected. In all 52 VES surveys were conducted in study area. Modelled sounding curves and their pseudo section outputs consist of number of geological layers in subsurface and their corresponding resistivity, thicknesses and depths. The results of the sounding curves displayed 7 different curve types. The 3 – layered curve model revealed H and A curve types respectively. The 4 – layered curve model displayed 3 curve types; namely KH, QH and HA. Finally the 5 – layered curve model revealed 2 curve types. They are QHA and HKH. The sounding curves in all the communities will be presented base on the curve types. When particular curve type appear more than one in the results of a

particular community only one will be presented. Contour maps of apparent resistivity at different depth below the earth surface were created. These maps were stacked together to give a view of changing apparent resistivity values with depth. The modelled contour maps are divided into two zones the first zone is labelled A; it comprises of hot (red, orange, yellow and light green) colours and the second zone with cool (violet, indigo, blue and dark green) colours is labelled B. Any VES point in the B zone contain high amount of groundwater and points on zone A contain very little or no groundwater. These maps together with sounding curves were used in discussing the presence or absence of groundwater within the study areas.

## 5.3. Selection of drilling sites

According to a unpublished report of Water Research Institute of Ghana ((Mainoo et al. 2007a), generally, a thick regolith (overburden) with moderate resistivity values can produce an appreciable quantity of groundwater. Significant yield may also be obtained from the transitional zone between the regolith and fresh rock, a slightly weathered zone known as 'saprock'. Where the regolith is thin, deeper fracture zones may be able to yield groundwater to well. Selection of VES points for test drilling was based on

**A.** The thickness of the regolith and depth to bedrock,

B. The resistivity of the various layers within the regolith, bedrock and corresponding thicknesses.

## 5.4. Interpretation and Discussions of Terrain Conductivity Profiles and VES Models

### 5.4.1. Ablaso Community

In Ablaso Community only one EM traverse was conducted and 3VES measurements. The sounding curves reveal 4 – layered and 5 –layered subsurface structures respectively. There are 2 curve types displayed by VES results from this community. They are QH and QHA types respectively.

### 5.4.1.1. EM traverse

The only EM traverse was carried out in Ablaso Community was on a profile length of 200 m; and on a bearing of 275° from the True North. The EM readings were taking using 10 m coil spacing at 5 m intervals. The schematic layout of Ablaso community is shown in Figure 5.1.

The terrain conductivity of the community ranges between 3 to 39 m mhos / m with an average value of 20.60 m mhos / m. The erratic nature of the VD mode curves suggests a complex subsurface geology. Most parts of the profile show higher apparent conductivity values for HD mode than the VD mode from the beginning of the profile to station 175 m. Between station 175 m to 195 m the apparent conductivity values for VD mode are higher than HD mode, but between these two points apparent conductivity is generally low. At station 65 m the HD mode curve and VD mode curve meet at apparent conductivity of 27 m mhos / m and this point was chosen for VES investigation. Stations A20 and A80 were also chosen for VES investigation because of their higher apparent conductivity value than any other points aside station A65 (Figure 5.2). There might be slight fractured zones beneath these stations and that they were selected for further investigations.
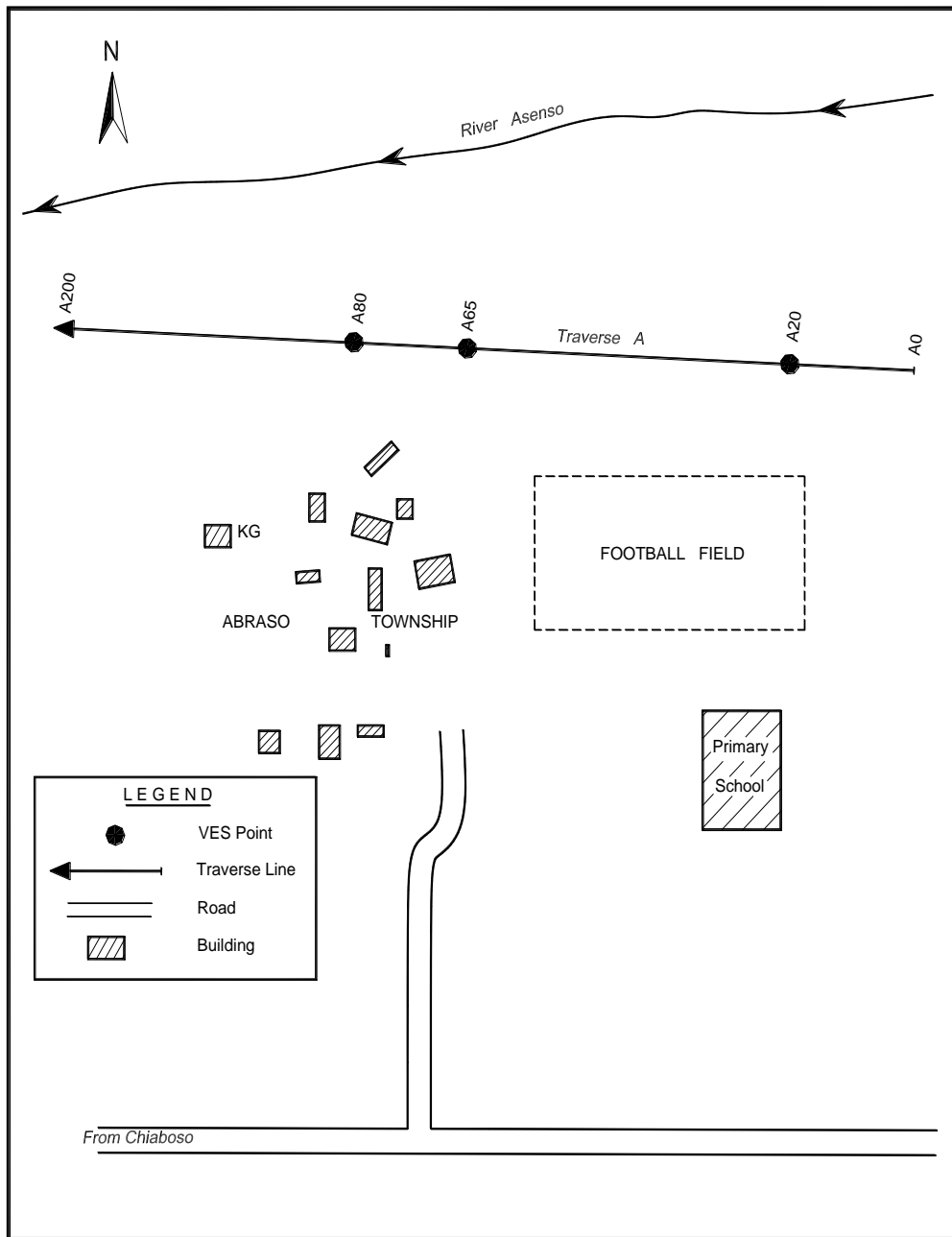
Figure 5.1. Schematic Layout of Ablaso Community (not to scale)
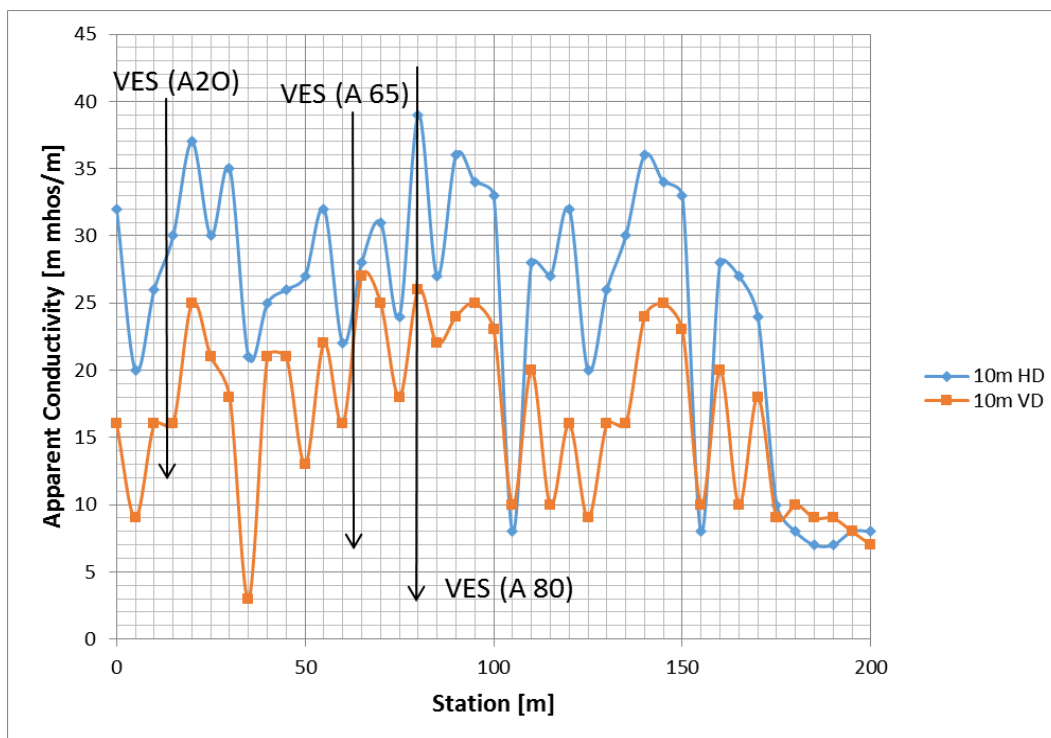
Figure 5.2. EM terrain conductivity measurements along a profile at Ablaso Community

## 5.4.1.2. Sounding curves

VES A65

The subsurface structures at station VES A65 is made up of four layers of apparent resistivity values ranging between 64.2 Ωm to about 4856 Ωm. The curve is a QH types which indicates a possibilities of locating a weathered zones third layer. The results from both modelled sounding curve and its pseudo section (Figures 5.3) indicate that, the top soil has an apparent resistivity value of 4856 Ωm and a thickness of 1.0 m. The second layer with apparent resistivity of 422.50 Ωm, has a thickness of 0.6 m. Third layer has a thickness of 13.7 m with apparent resistivity value of 64.20 Ωm. This layer is underlain by a fourth layer with apparent resistivity of 5042 Ωm
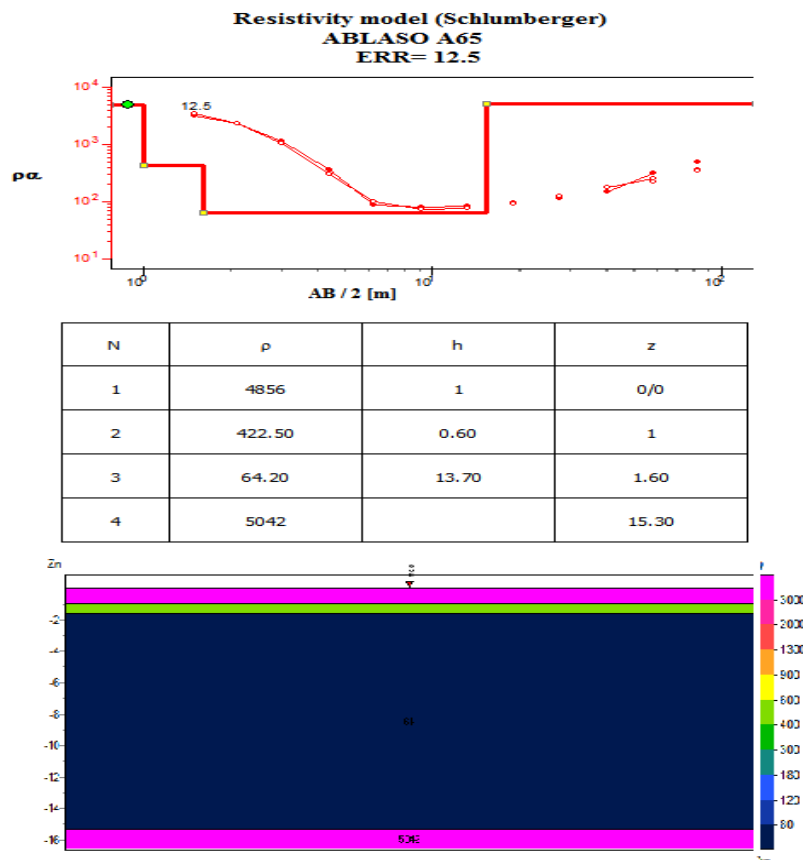
Figure 5.3. VES model curve at station A65 m, Ablaso Community

There is a great decrease in the apparent resistivity value from top layer to second layer and a sharp decrease from the second layer to third layer. There is a sharp increase of apparent resistivity values between the third layer and fourth layer indicating a fracture within the third layer. By considering the apparent resistivity value and the thickness of the third layer, this layer would be a good zone for groundwater accumulation and hence it was recommended for drilling a well.

VES A80

The curve in figure 5.4 is a QHA type. And it indicates a possibility of locating aquifer between layer 2 and 4 with layer 3 having the greatest potential. From the modelled sounding curve and pseudo section in Figures 5.4, it could be seen that; the station A80 has a five layered subsurface structures. The apparent resistivity values of layers of this station ranges from 19.70 Ωm to 18679 Ωm. First layer with thickness of 0.60 m, has the highest apparent resistivity value of 18679 Ωm and it is

underlain by second layer of apparent resistivity of 829.80 Ωm and a thickness of 1.80 m.



**Resistivity model (Schlumberger)**
**ABLASO A80**
**ERR = 39.1**

| N | ρ | h | z |
|---|---|---|---|
| 1 | 18679 | 0.60 | 0/0 |
| 2 | 829.80 | 1.80 | 0.60 |
| 3 | 19.70 | 4.90 | 2.40 |
| 4 | 238.50 | 5.70 | 7.30 |
| 5 | 4410 |  | 13 |
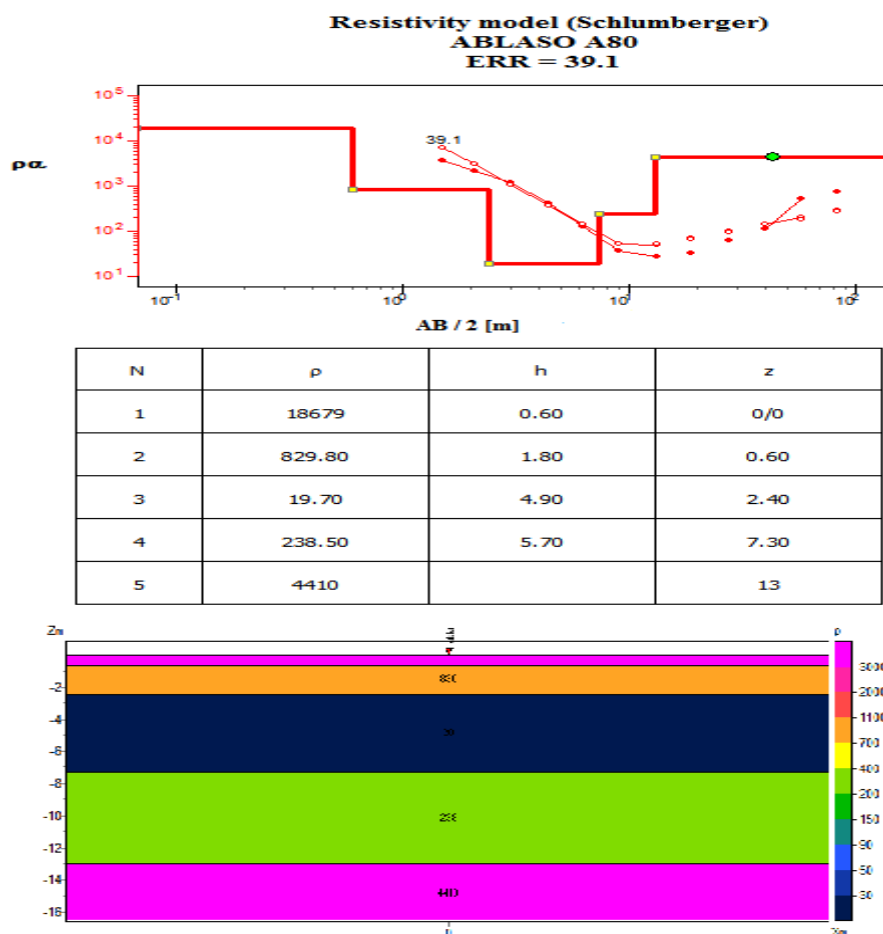
Figure 5.4. VES model curve at station A80 m, Ablaso Community

There is a drastic decrease of apparent resistivity from 829.80 Ωm of the second layer to 19.70 Ωm of third layer. This third layer has a thickness about 5 m. From this layer the apparent resistivity begins to increase to about 238 Ωm in the fourth layer and about 4410 Ωm in the fifth layer. This station is recommended for drilling wells, because of the very low apparent resistivity value of the third layer sandwich between two high resistive layers. This layer is believed to be highly fractured and contain sufficient groundwater for public usage.

### 5.4.1.3. Discussions of results from Ablaso Community

From all the three VES stations which were investigated, two of the stations i.e. station A20 and A65 indicated a four-layered geological structure while station A80 shows a five layered subsurface structure. The fifth layer in station A80 may be a

continuation of the layer four. Generally the analysis of the VES curves suggested that the Ablaso Community is underlain by four geological substrata. First layer has resistivity values ranging from 4,856.0 to 18,679.3 Ωm. and can be intercepted at a mean depth of 0.8m. The second layer, which has a thickness range of 0.6 – 2.2 m, has a mean apparent resistivity value of 473.4 Ωm. The third layer has apparent resistivity a value ranging 7.9 - 64.2 Ωm, whiles the fourth layer is has an apparent resistivity values ranging 480.3 – 5,042.0 Ωm. Groundwater within Ablaso Community may be located within the third layer and fourth layer.

The Figures 5.5a, 5.5b and 5.5c below, show groundwater (in high quantity) starting from depth 4.4 m down to 83.0 m at VES A20. For VES station A65, there is no sign of high quantity groundwater from depth 1.5 to 4.4 m. From depth 6.3 to 40 m, the subsurface show of high quantity groundwater. The VES A80 shows signs of high quantity of groundwater accumulation below the depth of 6.3 m to 58.0 m.

From this study of Ablaso Community, it is observed that areas towards North-western part of the community near River Asenso have their water table around a depth of 4.4 m and areas towards the North-eastern part of the community have their water table below the depth of 6.3 m. This difference may be due to the fact that areas towards West are closer to the river than those towards the East. The River Asenso may serve as a source of recharge for the groundwater beneath the area surrounding it. VES station A20 is ranked first in terms of availability and quantity of water, followed by A65 and then A80. These points are recommended for drilling. Table 5.1 provides a summary of the VES results including a rank-list of the selected points for drilling.
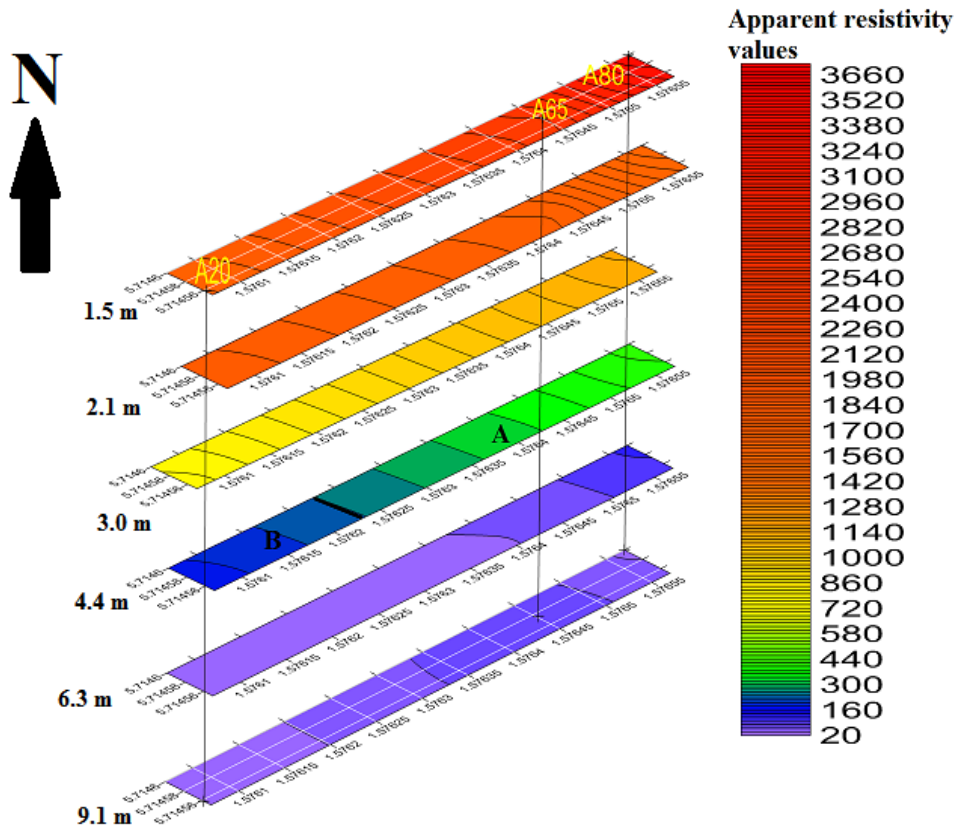
Figure 5.5a. Apparent resistivity contour maps from depth 1.5 to 9.1m at Ablaso Community
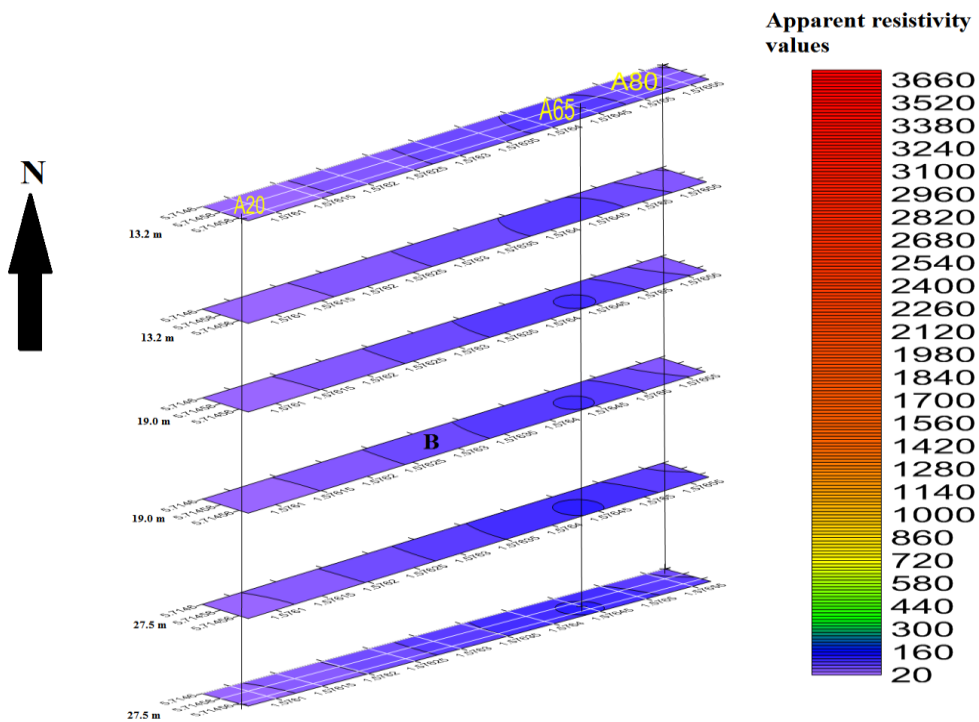


Figure 5.5b. Apparent resistivity contour maps in the depth range of 13.2 to 27.5 m at Ablaso Community
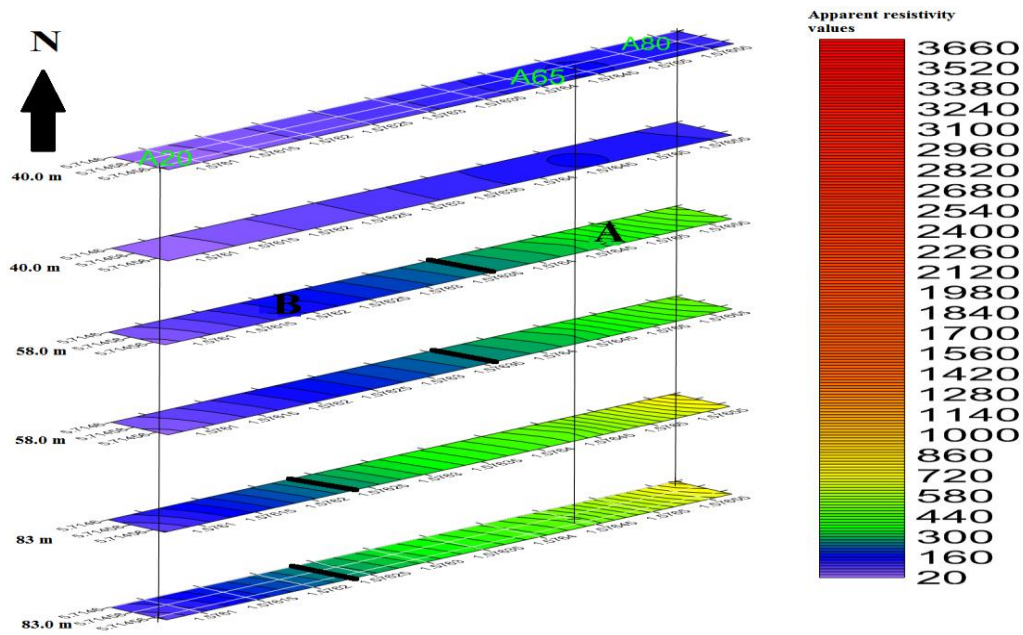
Figure 5.5c. Apparent resistivity contour maps in the depth range of 40 to 83 m at Ablaso Community

Table 5.1. Ranked VES points for hand-dug well development at Ablaso Community

| VES Point | Layer | ρ (Ω−μ) | Depth (m) | Thickness (m) | Rank | Location (GPS) |
|---|---|---|---|---|---|---|
| | 1 | 8146.7 | 0.9 | 0.9 | | 5.71455N |
| | 2 | 167.8 | 3.1 | 2.2 | | 1.57607W |
| | 3 | 7.9 | 13.3 | 10.2 | | |
| A20 | 4 | 480.3 | - | - | 1st | |
| | 1 | 4856 | 1 | 1 | | 5.71457N |
| | 2 | 422.5 | 1.6 | 0.6 | | 1.57645W |
| | 3 | 64.2 | 15.3 | 13.7 | | |
| A65 | 4 | 5042 | - | - | 2nd | |
| | 1 | 18679.3 | 0.6 | 0.6 | | 5.71460N |
| | 2 | 829.8 | 2.4 | 1.8 | | 1.57657W |
| | 3 | 19.7 | 7.3 | 4.9 | | |
| | 4 | 238.5 | 13 | 5.7 | | |
| A80 | 5 | 4410.2 | - | - | 3rd | |

## 5.4.2. Aboso Community

### 5.4.2.1. Introduction

Electromagnetic profiling was conducted along four (4) profiles across the Aboso Community and a total of six VES stations investigated. The VES stations

investigated displayed 3 different curve types and they are A, KH and HKH types respectively. The four traverse lines on which the electromagnetic readings were taken together with the VES stations are shown in Figure 5.7.

There are data on existing boreholes in and around 5 Km radius of the Aboso Community. It was used as an aid to the interpretation of geophysical data. Table 5.2 shows the existing boreholes within 5 Km of radius of the study area. The depths of available wells were used as a guide for interpretation of geophysical data. It gives an overview of the depth at which one could expect groundwater.
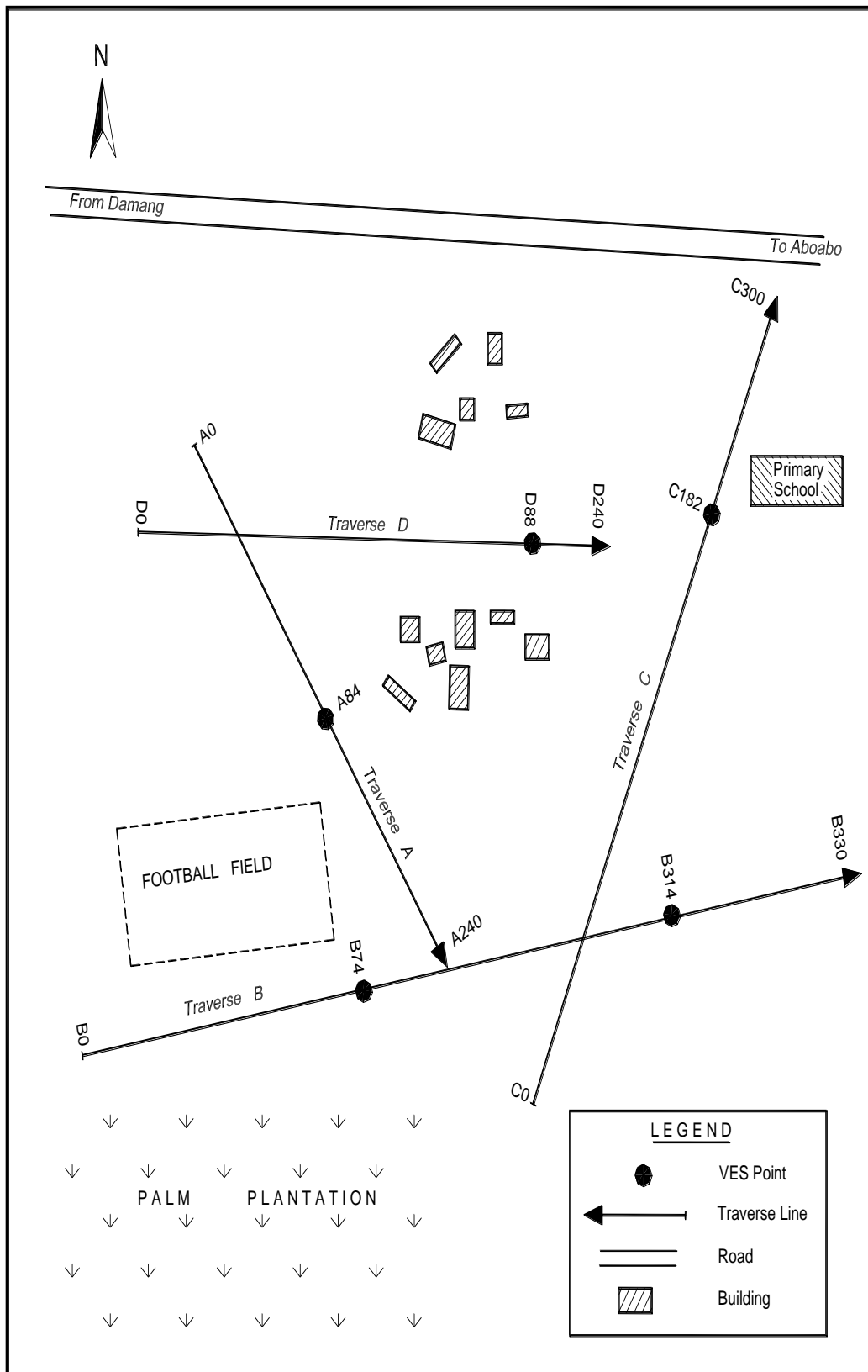
Figure 5.6. Schematic Layout of Aboso Community (not to scale)

Table 5.2. Existing Boreholes within 5 Km radius around Study Area ((Mainoo et al. 2007a)

| Community | BH No. | Depth (m) | Yield (m³/h) | SWL (m) | Water Quality | Lithology |
|---|---|---|---|---|---|---|
| MPEASEM | 084I214BU2 | 57 | 5.27 | 7.02 | | Phyllite / Mica schist |
| MPEASEM | 082C203BU2 | 63 | 2.81 | 14.77 | | Phyllite / Mica schist |
| TWIFO PRASO | 48/F/74-1 | 27 | | 4.76 | N/A | |
| TWIFO PRASO | 48/F/74-2 | 28 | | 1.29 | N/A | |
| TWIFO PRASO | 48/F/74-3 | 31 | | | N/A | |
| TWIFO PRASO | 48/F/74-4 | 28 | | 7.3 | N/A | |
| TWIFO PRASO | 48/F/74-5 | 37 | | | N/A | |
| TWIFO PRASO | 48/F/74-6 | 28 | | 6.84 | N/A | |
| TWIFO PRASO | 48/F/74-7 | 25 | | 0.95 | N/A | |

### 5.4.2.2. EM traverses

Traverse A was carried out on a profile length of 240 m on a bearing of 170° from the True North. The EM readings were taken using 20 m coil separation at 10 m interval.

The results of the EM profile on the traverse A, display higher values of apparent conductivity for VD mode more than that of HD mode which means that at deeper depth the subsurface is likely fractured. The average apparent or terrain conductivity value of the profile line A is 7.34 m mhos / m with the maximum apparent conductivity of 12 m mhos / m and the minimum of 4 m mhos / m. Station 90 m has the highest apparent conductivity value for both VD mode and HD mode. Station A84 m was chosen for VES investigation. Figure 5.7 shows a graph for the EM profiling on traverse A. Observing the characteristics of the curves between station 60 m and 115 m, it is noticed that, the curves sharply move from low terrain conductivity region to high conductivity zone, then to a lower terrain conductivity zone, indicating a possible fracture in the zone.
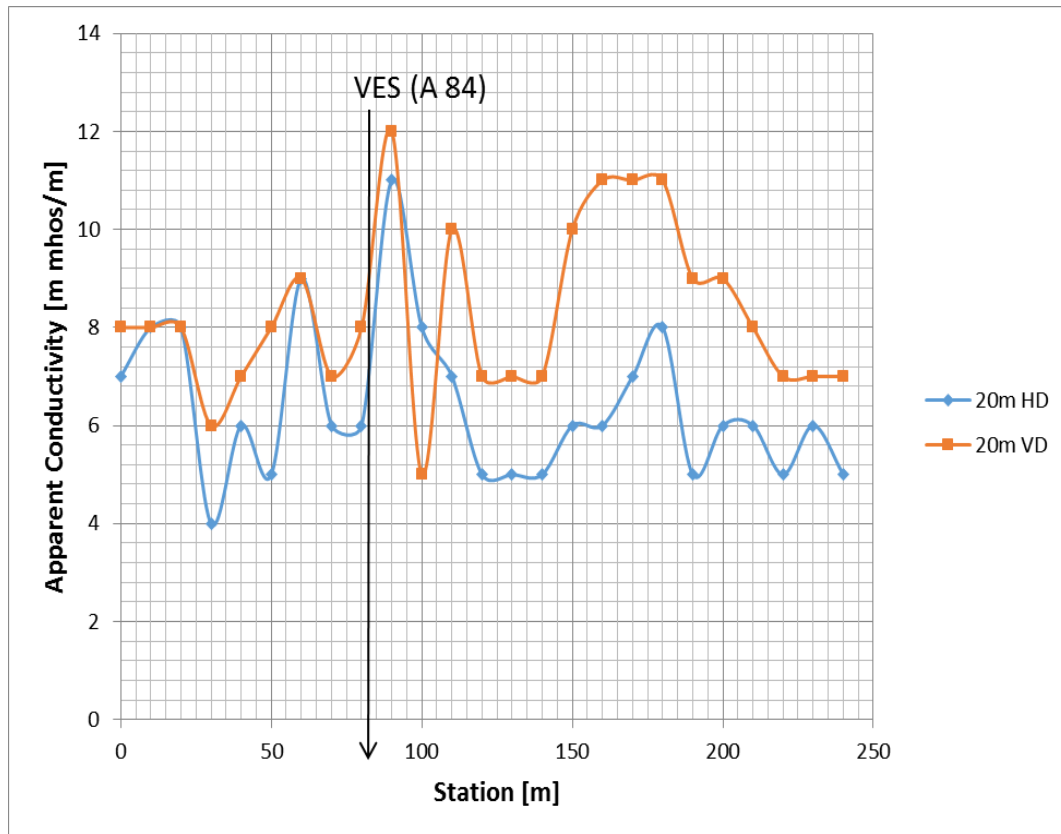
Figure 5.7. EM terrain conductivity measurements along a profile A at Aboso Community

Traverse B has a total length of 330 m long. The traverse B is on a bearing 075° from the True North. 20 m coil separation was used and EM reading was taken at 10 m interval.

The apparent conductivity values range on this profile line is between 4 – 11 m mhos / m with an average of 7.78 m mhos / m. Generally, the profile has a low terrain conductivity values and that the HD mode curve has a high terrain conductivity values compare with the VD mode (see Figure 5.8). It means that at deeper depth there are no much fractures and finding groundwater within that zone would be difficult. There are two peaks on the graph for VD mode, one at station 160 m and the other at station 320 m. The peak at station 320 m is near the crossover point and that the crossover point is selected for further VES investigation. The peak at station 160 m is not selected for VES because it is located very near to an abandoned toilet which may be a source of groundwater pollution should groundwater be present at that point. Point 74 m is also selected for VES investigation. This station is near the

highest terrain conductivity value for HD mode and has a high terrain conductivity value for VD mode.
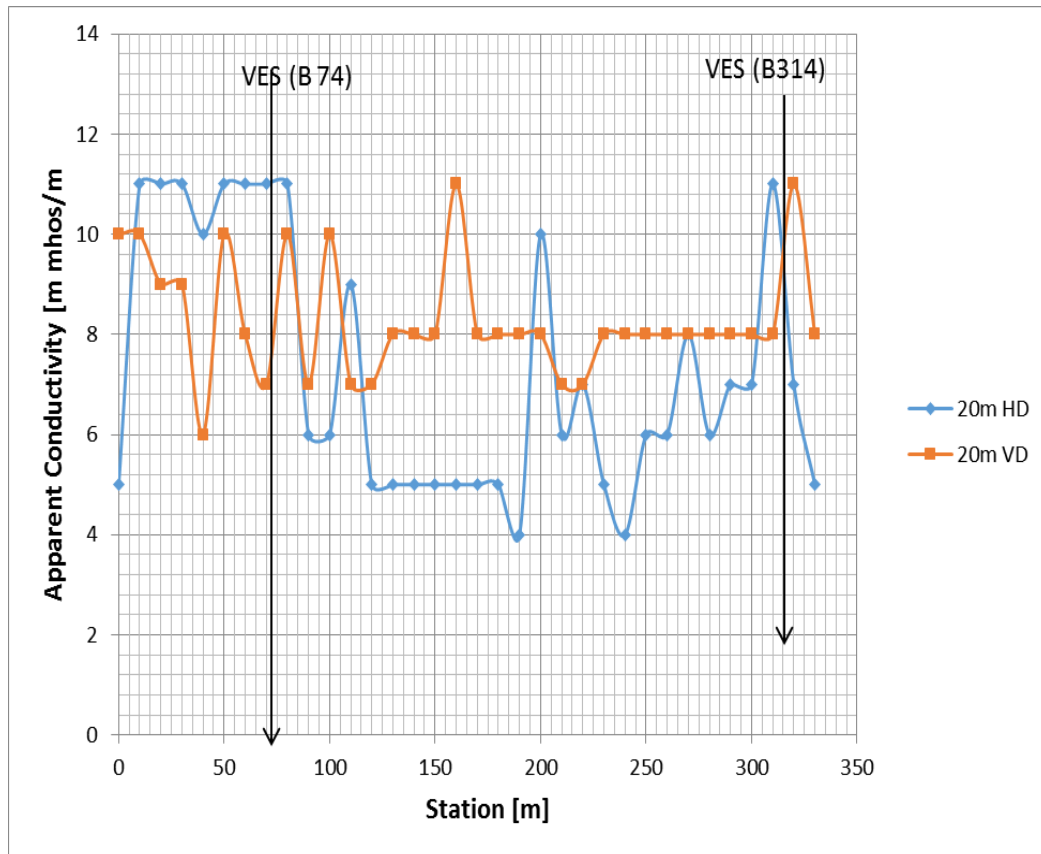


Figure 5.8. EM terrain conductivity measurements along a profile B at Aboso Community

Traverse C runs from south towards North behind the primary school of the community and across traverse B. The traverse has a length of 300 m and the EM readings were taken using 20 m coil spacing and 10 m interval. The profile was run on a bearing 050° from the True North.
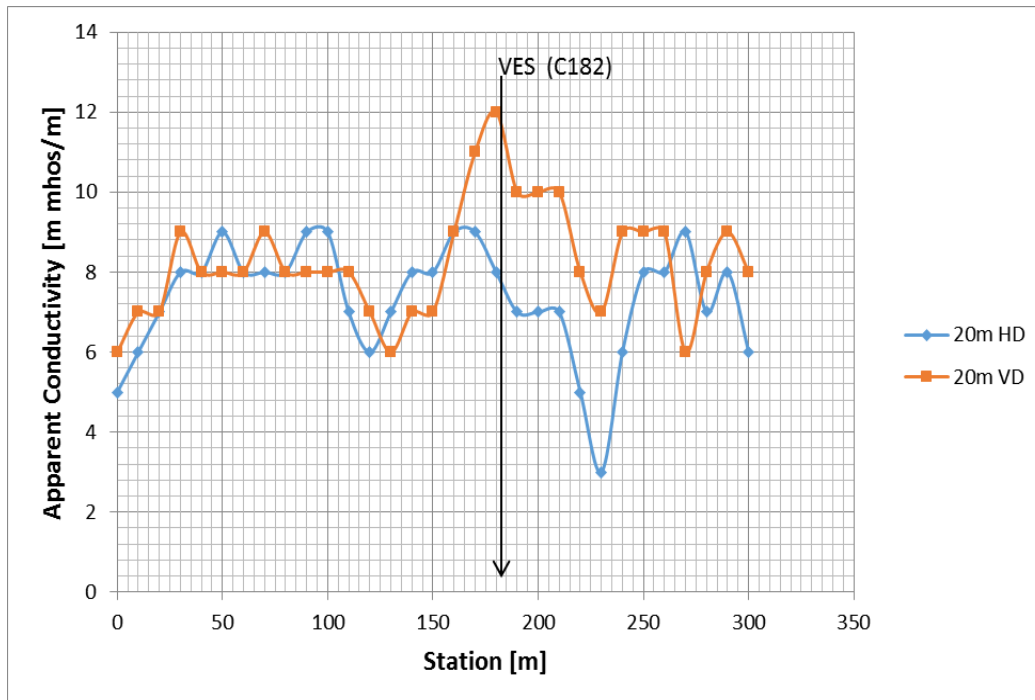
Figure 5.9. EM terrain conductivity measurements along a profile C at Aboso Community

Both HD mode and VD mode curves move erratically along the profile. From the graph in Figure 5.9; it can be observed that, the terrain conductivity of the VD mode is generally higher than that of HD mode and it is concluded that beneath this profile the subsurface is highly fractured and may accumulate groundwater. The peak value of terrain conductivity on the graph is that of VD mode (12 m mhos / m) and the minimum value is that of HD mode. The average terrain conductivity for this traverse is about 7.81 m mhos / m. There are five crossover points on the graph, but they were not selected for VES investigation because of their general low terrain conductivity values. Station 182 m was chosen for further investigation because the results indicate a possible fractured zone at a deeper level due to high terrain conductivity for VD mode.

Traverse D is the last of the four traverse run in Aboso Community. EM profiling was carried out along this traverse of length 240 m using 20 m coil spacing and EM readings were taken at 10 m intervals. The schematic layout of Aboso Community as shown in Figure 5.6 shows the location of this traverse line as conducted within the community.

The EM profiling was run on bearing of 130° from the True North. The average terrain conductivity value on this traverse D is 8.64 m mhos / m with 16 m mhos / m and 5 m mhos / m as the maximum and the minimum terrain conductivity values respectively.

The results for both HD and VD mode curves indicate that there are increases in terrain conductivity from station 0 m to station 90 m. Station 90 m recorded the highest terrain conductivity value on the graph (see Figure 5.10). From station 90 m there is a decrease in the terrain conductivity until a peak showed out at station 150 m. This peak was not considered for VES investigation because of location of a public toilet within its 20 m radius. The toilet facility may be a source of groundwater pollution beneath station 150 m. For health purposes this station wasn't investigated further. From the EM curves it could be observed that, there is a high probability of finding groundwater at station 88 m and hence it was selected for further VES investigation.
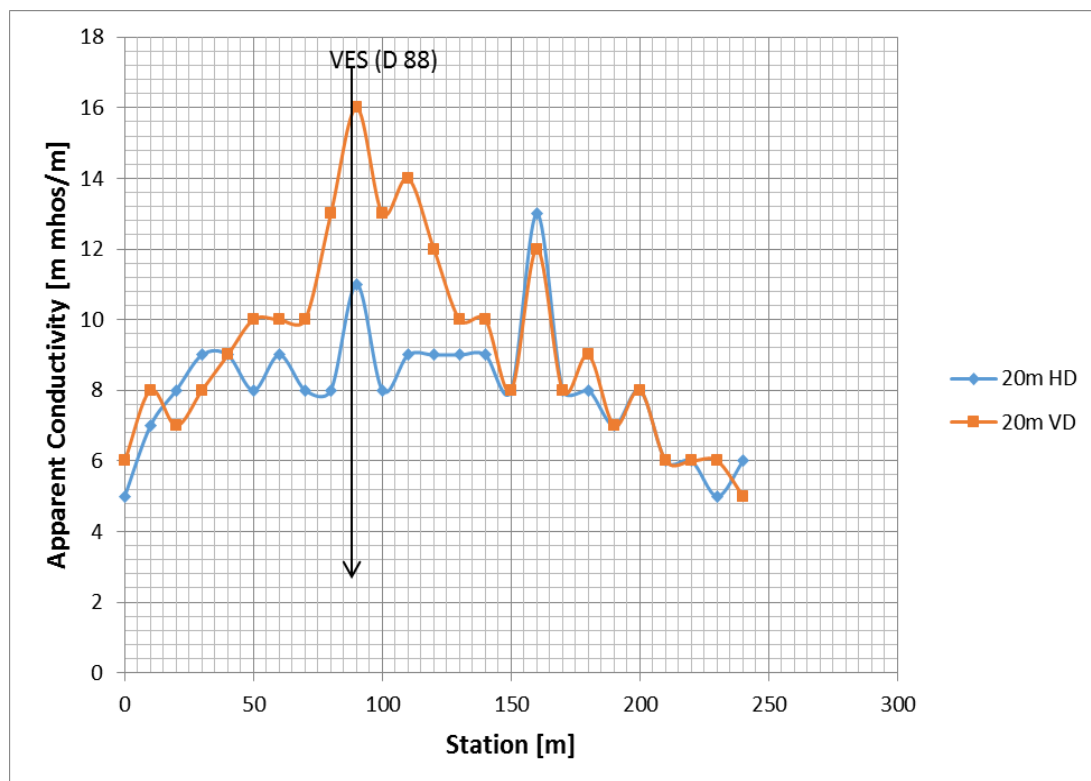


Figure 5.10. EM terrain conductivity measurements along a profile D at Aboso Community

### 5.4.2.3. Sounding curves

VES A84

The modelled sounding curve shows three layers for this station while pseudosection shows only two layers. The sounding curve displayed by VES is A – type which mean that the first layer is more weathered than the other two layers. This may be due to the thickness of the second layer which is about 26.93 m and that pseudosection couldn't display the third layer (see Figures 5.11). First layer has an apparent resistivity value of 114.13 Ωm and a thickness of 0.97 m, second and third layer have apparent resistivity values of 719.71 Ωm and 6824.65 Ωm, respectively.



| N | ρ | h | z |
|---|---|---|---|
| 1 | 114.13 | 0.97 | 0/0 |
| 2 | 719.71 | 26.93 | 0.97 |
| 3 | 6824.65 | | 27.89 |
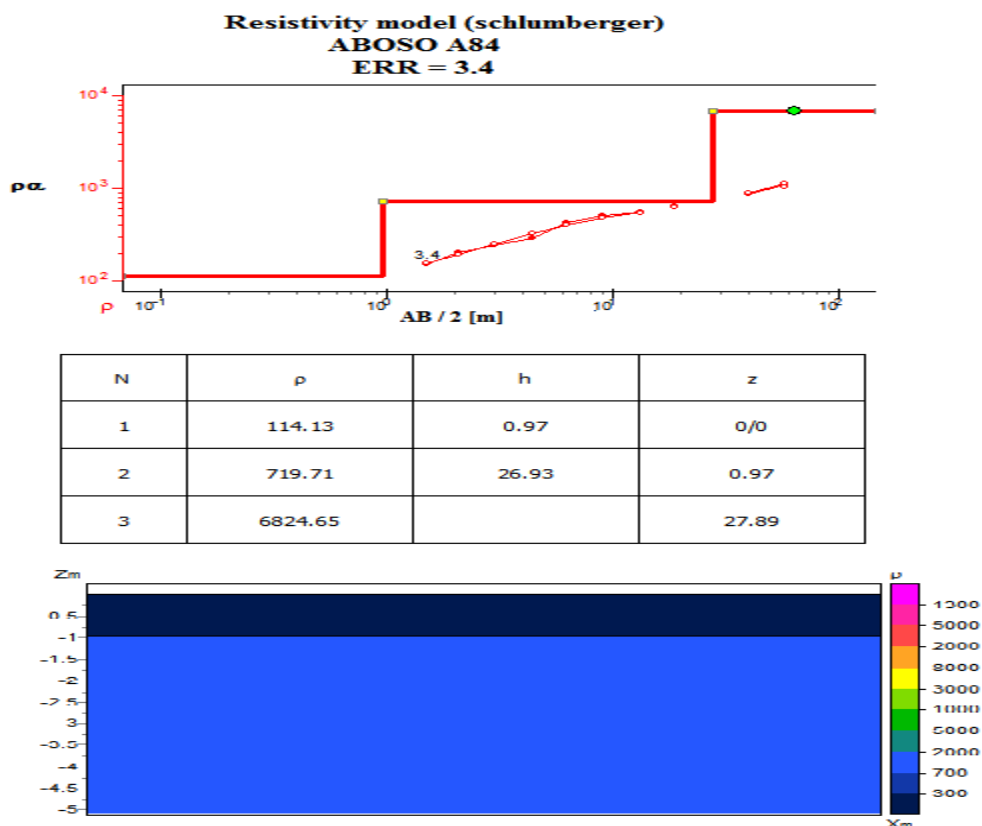
Figure 5.11. VES model curve at station A84 m, Aboso Community

The apparent resistivity values for layers beneath this station indicate a possibility of groundwater within them. Their apparent resistivity values are within the 50 – 2000 Ωm which is the usual ranges of aquifer. Also considering the geology of the community fall within high resistive granite formation, the value of the apparent resistivity show a little to moderate fracture within the zone and that the groundwater in the subsurface may be not be of high quantity. This station is recommended for drilling a well.

VES B74
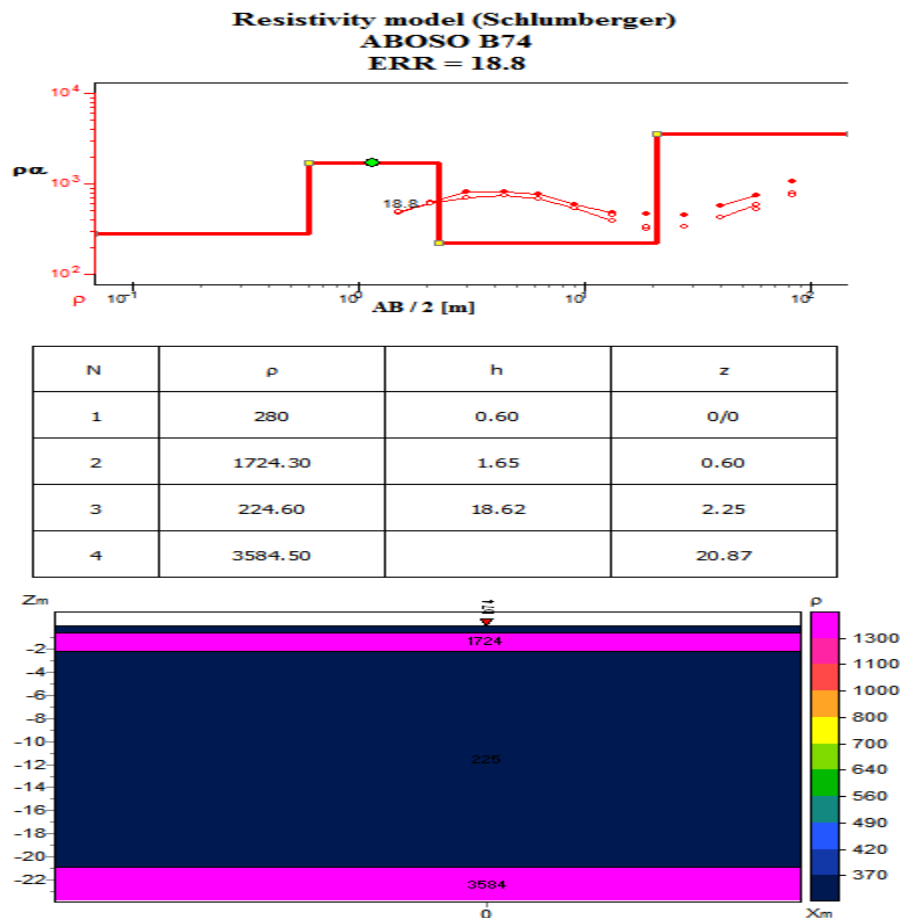


Figure 5.12. VES model curve at station B74 m, Aboso Community

The VES modelled curve and pseudosection of the subsurface at station B74 depicted a four layered modelled (Figure 5.12). The sounding curve is a KH – type. It means that the first and third layer has the minimum resistivity values and that are capable of containing water. Topsoil has an apparent resistivity of 280 $\Omega$m and a thickness of 0.60 m, second layer has an apparent resistivity of 1724.30 $\Omega$m and 1.65 m has its thickness. Third layer has thickness of 18.62 m and an apparent resistivity of 224.60 $\Omega$m and lastly layer four has an apparent resistivity of 3584.50 $\Omega$m. There is a very sharp increase of apparent resistivity from first layer to second layer, and a massive decrease in apparent resistivity from second layer (1724.30 $\Omega$m) to third layer (224.60 $\Omega$m). There is more than 3000 $\Omega$m difference between the apparent resistivity values of third and fourth layer. The characteristics of the model indicate a massive crack or fracture within the third layer. This station is recommended for drilling a well.

VES C182



**Resistivity model (Schlumberger)**
**ABOSO C182**
**ERR = 9.8**

| N | ρ | h | z |
|---|---|---|---|
| 1 | 222.13 | 1.04 | 0/0 |
| 2 | 145.99 | 7.08 | 1.04 |
| 3 | 8152.26 | | 8.12 |
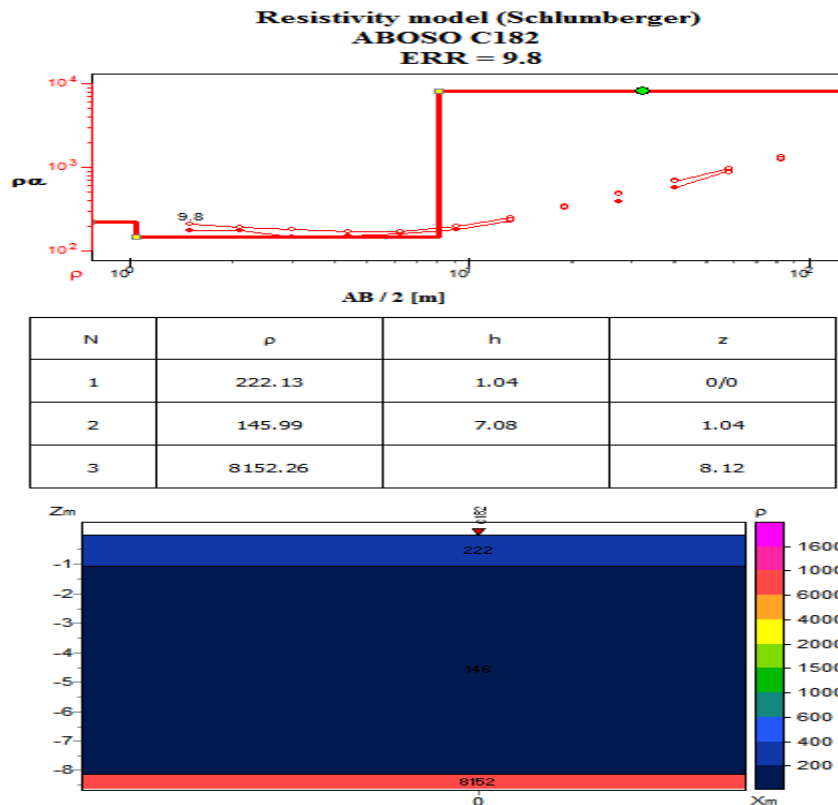
Figure 5.13. VES model curve at station C182 m, Aboso Community

The sounding curve displayed by VES C182 is H – type and that the aquifer is possible to be located in the second layer. The geological section at station C182 reveals that the subsurface structure consists of three layers with apparent resistivity values ranging between 145.99 Ωm and 8152.26 Ωm as shown in Figures 5.13 above. Top layer has a thickness and apparent resistivity value of 1.04 m and 222.13 Ωm, respectively. Second layer has a thickness of 7.08 m and an apparent resistivity value of 145.99 Ωm. Third layer has an apparent resistivity value of 8152.26 Ωm. Analysis of these results reveal the top layer to be probably fairly weathered and underlain by second layer which is most likely highly weathered than the first layer in view of their low apparent resistivity values. The second layer could contain an appreciable quantity of groundwater and hence it is recommended for borehole drilling.

VES D88

Station D88 revealed five-layered subsurface geological structures as shown in Figure 5.14. The sounding curve is HKH – type with the possiblilties of locating

weathered or fractured zones between layers 2 to 4. Comparing the VES results of this station with other VES stations within this community, this station is the only one that reveal five layered structure. The apparent resistivity value at this station range between 157.3 Ωm and 5452.50 Ωm. First layer has apparent resistivity of 379.44 Ωm and thickness of 0.5 m, second layer has an apparent resistivity of 157.30 Ωm and 0.93 m thickness. Third layer has a thickness of 1.99 m with an apparent resistivity of 399.45 Ωm. Fourth layer has an apparent resistivity value of 187.41 Ωm and thickness of 8.83 m. Fifth layer has apparent resistivity value of 5452.50 Ωm. The results of this station indicate a weathered or fractured formation in the first four layers and that these layers could host high quantity of groundwater for public water supply. Hence this station is recommended for borehole drilling.



| N | ρ | h | z |
|---|---|---|---|
| 1 | 379.44 | 0.50 | 0/0 |
| 2 | 157.30 | 0.93 | 0.50 |
| 3 | 399.45 | 1.97 | 1.43 |
| 4 | 187.41 | 8.83 | 3.40 |
| 5 | 5452.50 | | 12.23 |
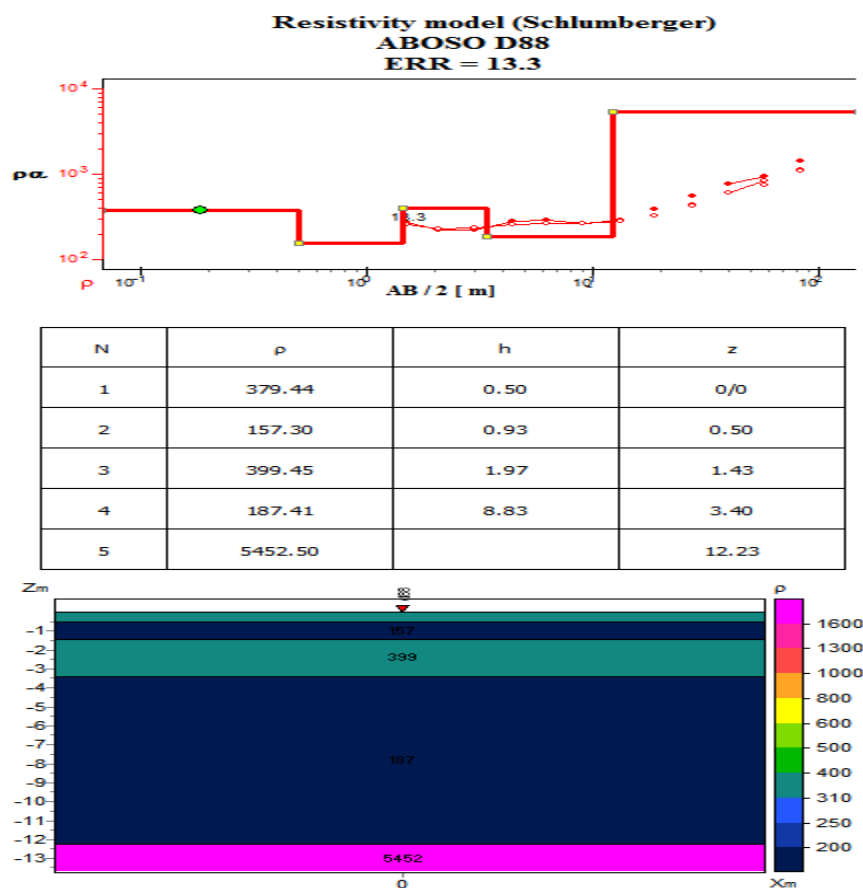
Figure 5.14. VES model curve at station D88 m, Aboso Community

### 5.4.2.4. Discussions of results from Aboso Community

Table 5.3 provides a summary of the VES results including a rank-list of selected points for drilling. Analysis of VES curves suggested that Aboso Community is underlain by three-four geological substrata. Out of the six VES stations investigated,

two stations revealed three layer structure for the subsurface, three stations indicated a four layered subsurface, while one station suggested a five layered structure. Generally the first layer has apparent resistivity values ranging from 114.13 – 505.72 $\Omega$m and it can be intercepted at a mean depth of 0.80 m. The second layer which has a thickness ranging from 0.97 – 1.70 m has a mean apparent resistivity value of 1080.38 $\Omega$m. The third layer has apparent resistivity value ranging from 224.50 – 8152.26 $\Omega$m and thickness ranging between 8.83 m and 21.40 m. The fourth layer generally has apparent resistivity values ranging between 187.41 and 29268.80 $\Omega$m.

From the sounding curves and the contour maps, the VES station C182 has the highest groundwater potential compare to the other VES stations. This station is followed in rank of groundwater potential by VES D88, A84 and S1. The maximum depth below the earth surface which was reach by this study is 83.0 m.

From the contour maps in Figures 5.15a – 5.15c below, it could be observed that, beneath VES station C182 high amount the groundwater (area labelled B) starts from 1.5 to 13.2 m and that it ceases to show up from depth 19.0 to 83.0 m. Drilling borehole at this point would yield high quantity of water. The station D88 which is the second in rank also shows sign of availability of high quantities of groundwater from depth of 1.5 to 13.2 m and from 19.0 to 83.0 m the water ceases. VES station A84 shows sign of presence high quantity of groundwater from 1.5 to 4.4 m and from depth 6.3 to 83.0 m.

Table 5.3. Ranked VES points for borehole drilling at Aboso Community

| VES Point | Layer | ρ (Ω–μ) | Depth (m) | Thickness (m) | Rank | Location (GPS) | Remarks |
|---|---|---|---|---|---|---|---|
| | 1 | 222.13 | 1.04 | 1.04 | | 5.61625N | |
| | 2 | 145.99 | 8.12 | 7.08 | | 1.51749W | |
| C182 | 3 | 8152.26 | - | - | 1st | | |
| | 1 | 379.44 | 0.5 | 0.5 | | 5.61647N | |
| | 2 | 157.3 | 1.43 | 0.93 | | 1.51773W | |
| | 3 | 399.45 | 3.4 | 1.97 | | | |
| | 4 | 187.41 | 12.23 | 8.83 | | | |
| D88 | 5 | 5452.5 | - | - | 2nd | | |
| | 1 | 114.13 | 0.97 | 0.97 | | 5.61619N | |
| | 2 | 719.71 | 27.9 | 26.93 | | 1.51813W | |
| A84 | 3 | 6824.65 | - | - | 3rd | | |
| | 1 | 334.6 | 1.28 | 1.28 | | 5.61691N | |
| | 2 | 246.62 | 2.84 | 1.56 | | 1.5733W | |
| | 3 | 373.27 | 22.1 | 19.26 | 4th | | |
| S1 | 4 | 29268.8 | - | - | | | |
| | | 280 | 0.6 | 0.6 | | | little signs of groundwater |
| | 1 | | | | | 5.61514N | |
| | 2 | 1724.3 | 2.25 | 1.65 | | 1.51837W | |
| | 3 | 224.6 | 20.87 | 18.62 | | | |
| B74 | 4 | 2584.5 | - | - | 5th | | |
| | | 505.72 | 0.6 | 0.6 | | | Little signs of groundwater |
| | 1 | | | | | 5.61543N | |
| | 2 | 1731.5 | 2.3 | 1.7 | | 1.51685W | |
| | 3 | 404.81 | 23.7 | 21.4 | | | |
| B314 | 4 | 5033.2 | - | - | 5th | | |

Figure 5.15a. Contour maps showing the apparent resistivity values from depth 1.5- 9.1 m beneath the Aboso Community
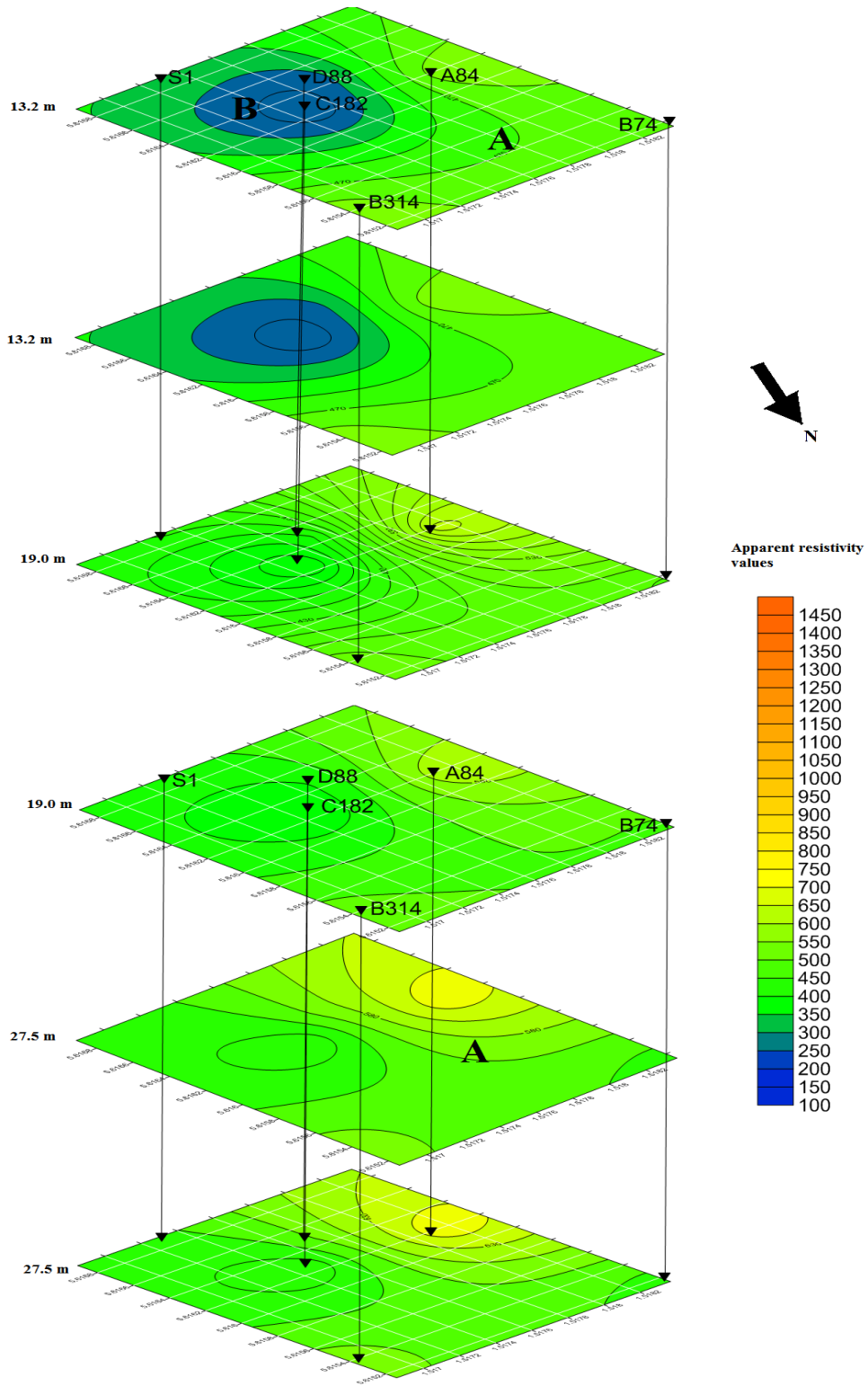
Figure 5.15b. Contour maps showing the apparent resistivity values from depth 13.2- 27.5 m beneath the Aboso
Community
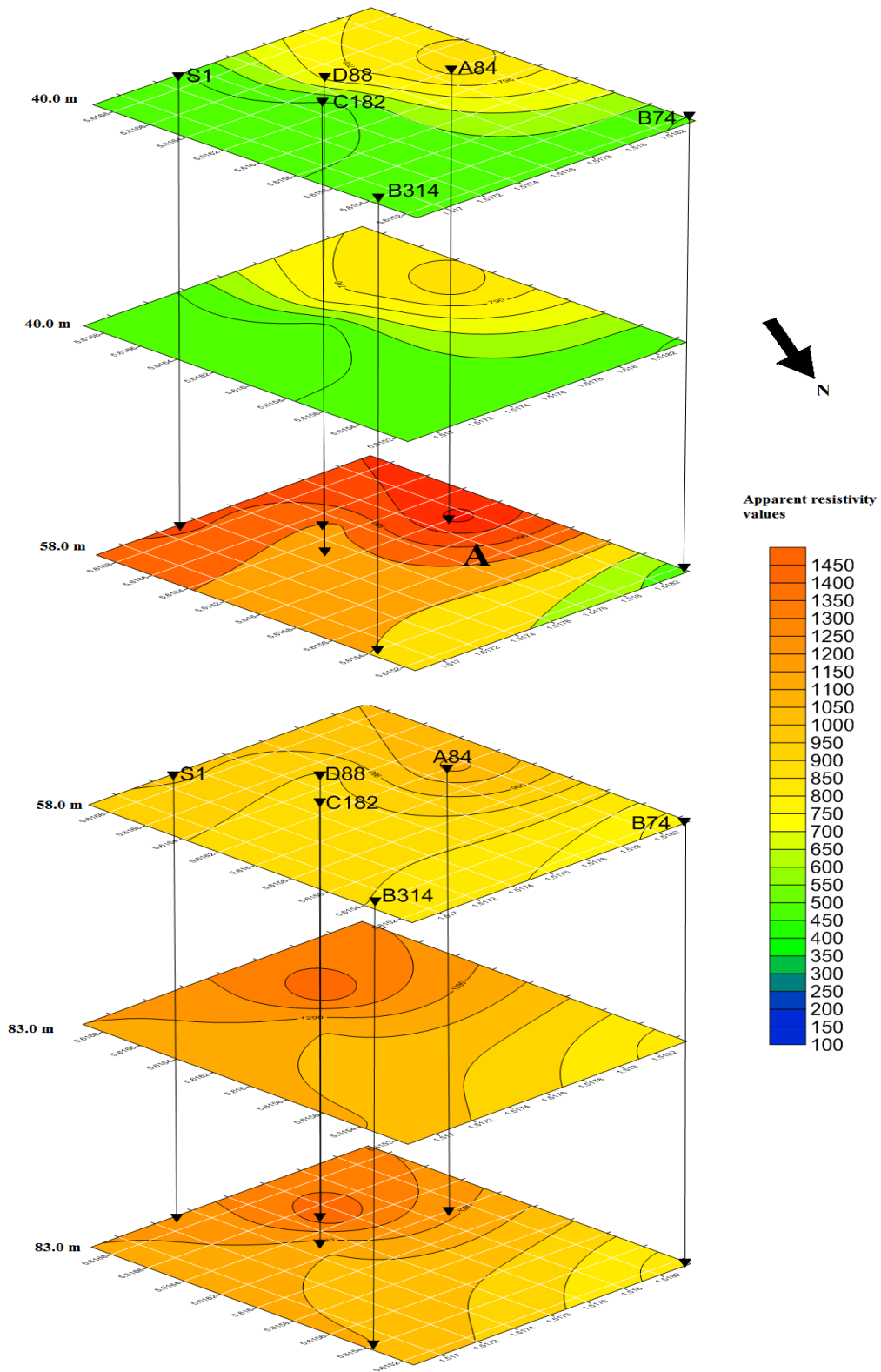
Figure 5.15c. Contour maps showing the apparent resistivity values from depth 40.0- 83.0 m beneath the Aboso Community

Observing the maps carefully, it is inferred that the groundwater beneath these three stations may be present even before the depth of 1.5 m. It is possible that it starts from a depth little before or below 0.60 m as suggested by the sounding curves. At VES station S1 there is no sign of high amount of groundwater present from 1.5 to 3.0 m. It is at depth 4.4 m that the contour maps show the presence high amount groundwater. From depths 6.3 m going downwards no further sign of enough groundwater are displayed at this station. The remaining two VES stations on EM profile B show little signs of groundwater present beneath them and that they are not recommended for drilling. If additional boreholes are required, they could be drilled at any point in the South-western part of the community, preferably within one or two hundred meters radius of VES stations C182, D88 and A84 in the South West direction. The South-western part of this community is interpreted to be a potential groundwater source from the contour maps.

### 5.4.3. Achiase Community

### 5.4.3.1. Introduction

Three EM traverses and five VES were conducted within this community. All the 5 VES station's results suggest 3 – layered modelled structure. The sounding curve types are A and H type respectively. Two of the EM traverses had a length of 250 m and one had a length of 350 m. They were run with the inter-coil spacing of 20 m in this community. The schematic layout of the traverse lines and the VES points in this community is shown in Figure 5.16 below.

About 5 km radius of the surroundings of Achiase, data of existing boreholes were collected and tabulated. This is used as an aid to both geophysical data collection and interpretation. The data is presented in Table 5.4.
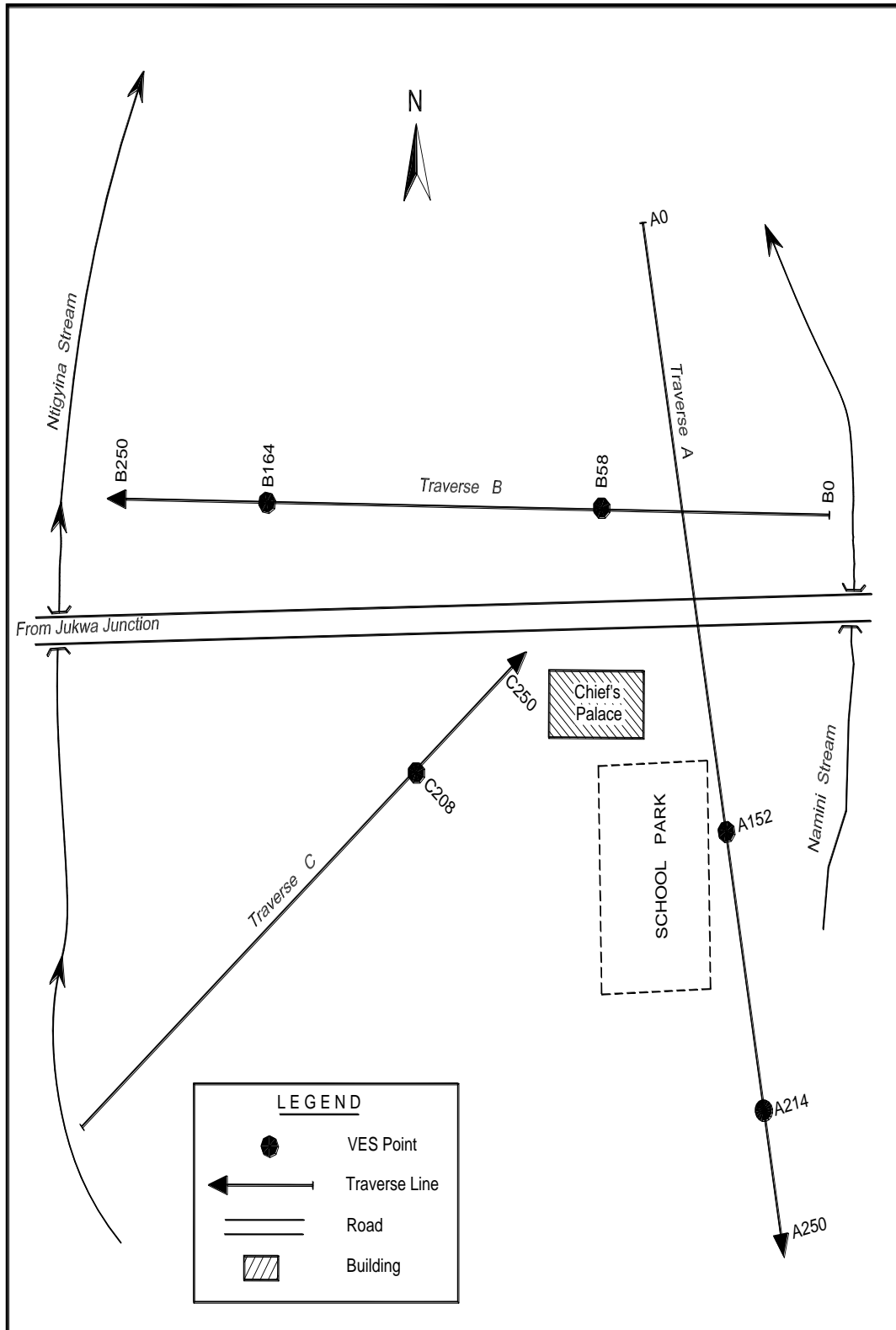
Figure 5.16. Schematic Layout of Achiase Community (not to scale)

Table 5.4. Existing Boreholes within 5Km radius around Achiase Community ( (Mainoo et al. 2007b)

| Community | BH No. | Depth (m) | Yield (m³/h) | SWL (m) | Water Quality | Lithology | Calibration |
|---|---|---|---|---|---|---|---|
| WATRESO | 27/I/51-1 | 26 | | 1.5 | N/A | Gneiss | |
| WATRESO | 27/I/51-2 | | | | N/A | | |
| NYAMEBEKYERE | 27/H/68-1 | 28 | | 0 | N/A | Quartz Diorite | |
| NYAMEBEKYERE | 27/H/68-2 | 34 | | | N/A | | |
| NYAMEBEKYERE | 27/H/68-3 | 40 | | | N/A | | |
| NYAMEBEKYERE | 27/H/68-4 | 37 | | 2.13 | N/A | Granite | |
| NYAMIENI | 27/H/59-1 | 40 | | | N/A | | |
| NYAMIENI | 27/H/59-2 | 40 | | | N/A | | |

### 5.4.3.2. EM traverses

The EM traverse on profile A of length 250 m was run on the bearing of 155° from the True North. The graph of HD mode and VD mode curves are shown in Figure 5.17. The Figure 5.17 shows a general higher value of the conductivity for HD values than VD values along most part of the profile indicating a general decrease in weathering with depth along the profile.

This traverse recorded a maximum conductivity value of 13 m mhos/m and a minimum of 8 m mhos/m with average terrain conductivity of 9.94 m mhos/m. The graph shows higher values of conductivity for HD from the station 10 m to about 57 m, where the first crossover point occurred, then from station 80 m to the station 140 m. Within station 140 m to station 215 m the VD curve dominate the HD curve and then from there to the end of the profile HD mode terrain conductivity values retain its high position. Stations 152 m and 214 m were chosen for vertical electrical sounding because of the high values of terrain conductivity for the VD mode they display. These high VD mode terrain conductivity values may be due to fracture at the deep subsurface which may be a reservoir for groundwater.
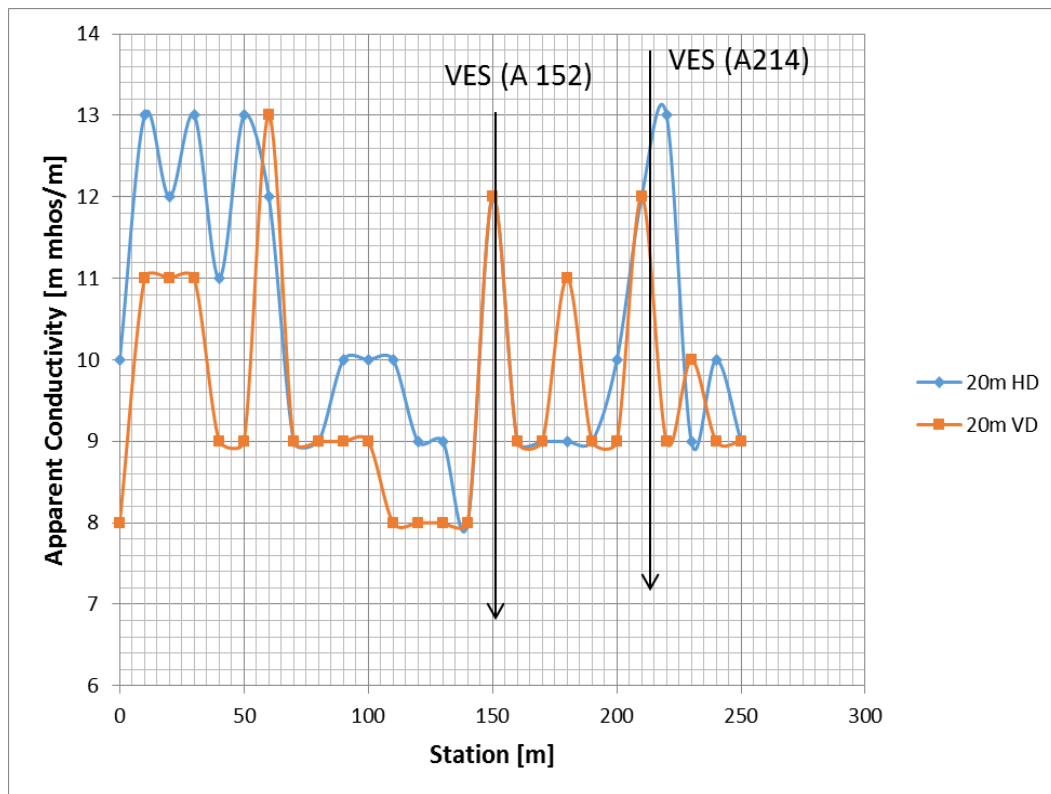


Figure 5.17. EM terrain conductivity measurements along a profile A at Achiase Community

The EM traverse on Profile B of the length 250 m was run on a bearing of 242˚ from the True North. Figure 5.18 the graph of apparent conductivity against station of the EM readings. It displays general higher terrain conductivities for HD values than VD values along most part of the profile. Something interesting with this profile is that, from Station 60 m to 110 m both HD mode curve and VD mode curve have almost the same values of terrain conductivities and that they cross each other. This profile

generally has high values of terrain conductivities with maximum of 20 m mhos/m and a minimum of 9 m mhos/m. The average terrain conductivity is 9 m mhos/m. The curves for both VD mode and HD mode are erratic in nature which shows the subsurface is a complex one. Two points (Stations B58 and B164) were chosen as VES points for further investigation.
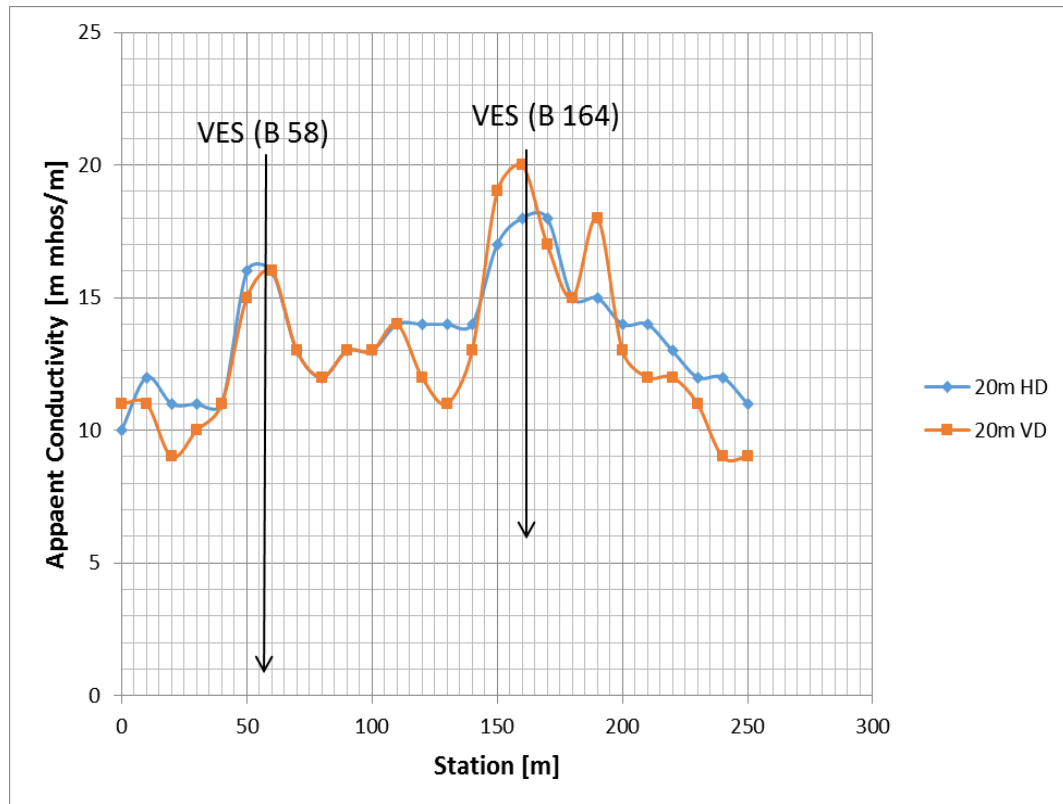


Figure 5.18. EM terrain conductivity measurements along a profile B at Achiase Community
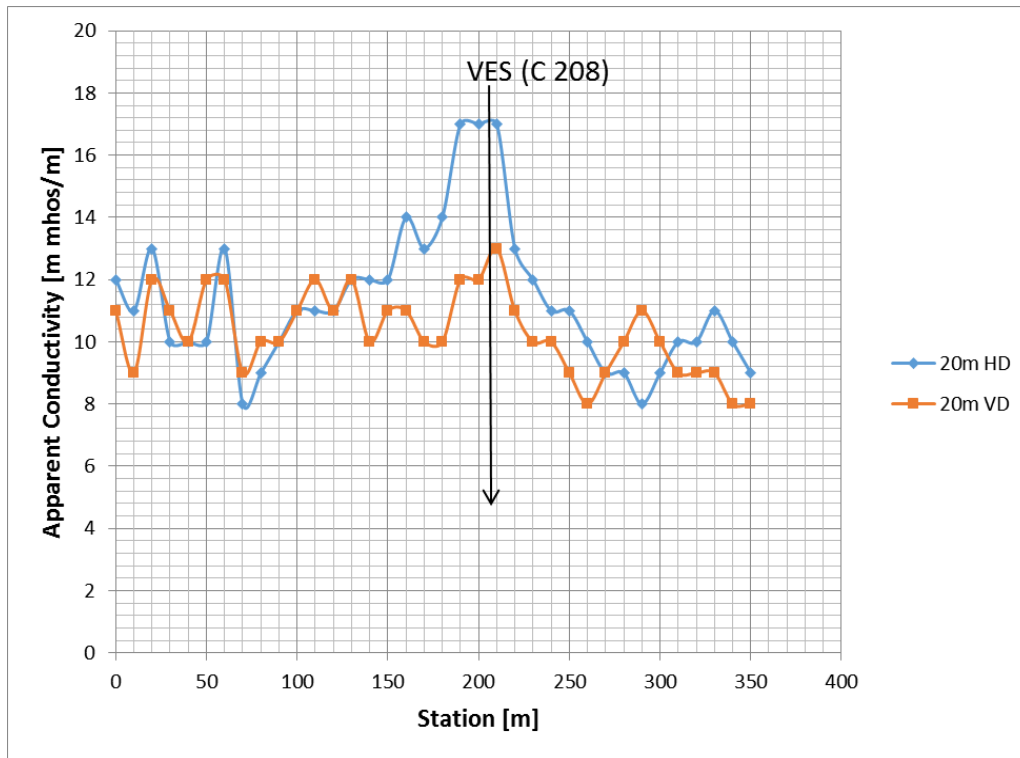
Figure 5.19. EM terrain conductivity measurements along a profile C at Achiase Community

EM traverse on profile line C is 350 m long. The EM profiling was run on bearing 060˚ from the True North. The average terrain conductivity value on this profile is 10.85 m mhos/m, the highest and the lowest terrain conductivity values are 17.0 m mhos/m and 8.0 m mhos/m respectively. It is observed from the graph in Figure 5.19 above that, the both HD mode and the VD mode curves are erratic and that the HD mode curve has generally high terrain conductivity values than VD mode curve meaning there is a general decrease in weathering with depth along the profile. Points along this profile line may not contain a sufficient quantity of groundwater for public usage shout there be water beneath this profile line. There are few crossover points on this graph but because of the general decrease in the conductivity values for VD mode, station 208 m was selected as VES point because of its nearest to the station 210 m has the highest conductivity value for VD mode. The terrain values from station 150 m to 220 m suggest a weathered zone with the subsurface.

### 5.4.3.3. Sounding curves

VES A214

The results of VES station A214 (Figure 5.20) displayed H – type sounding curve. This curve type indicates a weathering zone in layer 2. Apparent resistivities varied between 289.28 $\Omega$m to 2479.11 $\Omega$m. First layer has a thickness of 2.91 m and apparent resistivity of 756.05 $\Omega$m. Second layer has a thickness of 10.72 m and apparent resistivity value of 289.28 m with the bed rock having resistivity value of 2479.11 $\Omega$m. It is inferred from the model sounding curve that, the second layer is fairly weathered and contain groundwater; hence it is recommended for drilling of borehole.



| N | $\rho$ | h | z |
|---|--------|------|------|
| 1 | 756.05 | 2.91 | 0/0 |
| 2 | 289.28 | 10.72 | 2.91 |
| 3 | 2479.11 | | 13.63 |
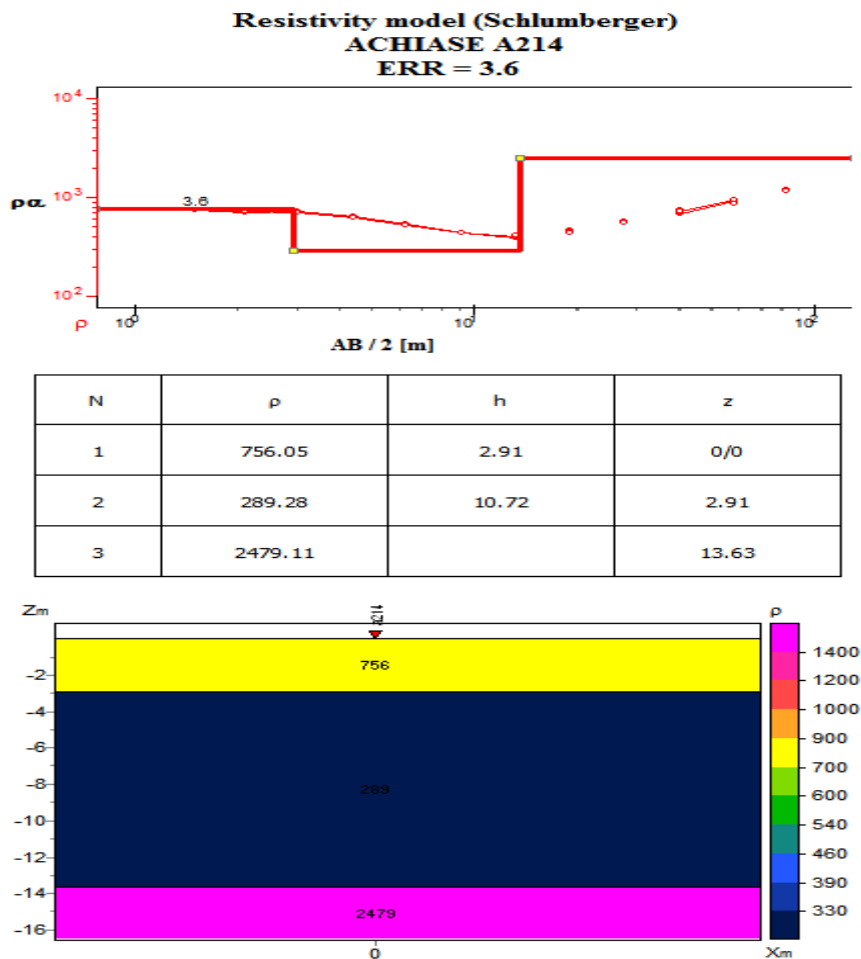


Figure 5.20. VES model curve at station A214 m, Achiase Community

VES B164

Station B164 indicates a three - layered subsurface geological structure and the curve type is A – type. As could be seen from Figures 5.21, the apparent resistivities at this station varies from 59.55 Ωm to 915.42 Ωm. The upper layer which is 1.10 m thick has apparent resistivity value of 59.55 Ωm and it is a characteristic of a weathered formation. It is underlain by a relatively low resistive second layer of thickness and apparent resistivity of 19.65 m and 89.84 Ωm, respectively. The third layer which is also the bedrock has apparent resistivity of 9815.45 Ωm. The aquifer is expected to be intercepted between the first and second layer. It could be possible to locate high quantity of groundwater 1.00 - 20.00 beneath this station.



| N | ρ | h | z |
|---|---|---|---|
| 1 | 59.55 | 1.10 | 0/0 |
| 2 | 89.84 | 19.65 | 1.10 |
| 3 | 9815.42 | | 20.75 |
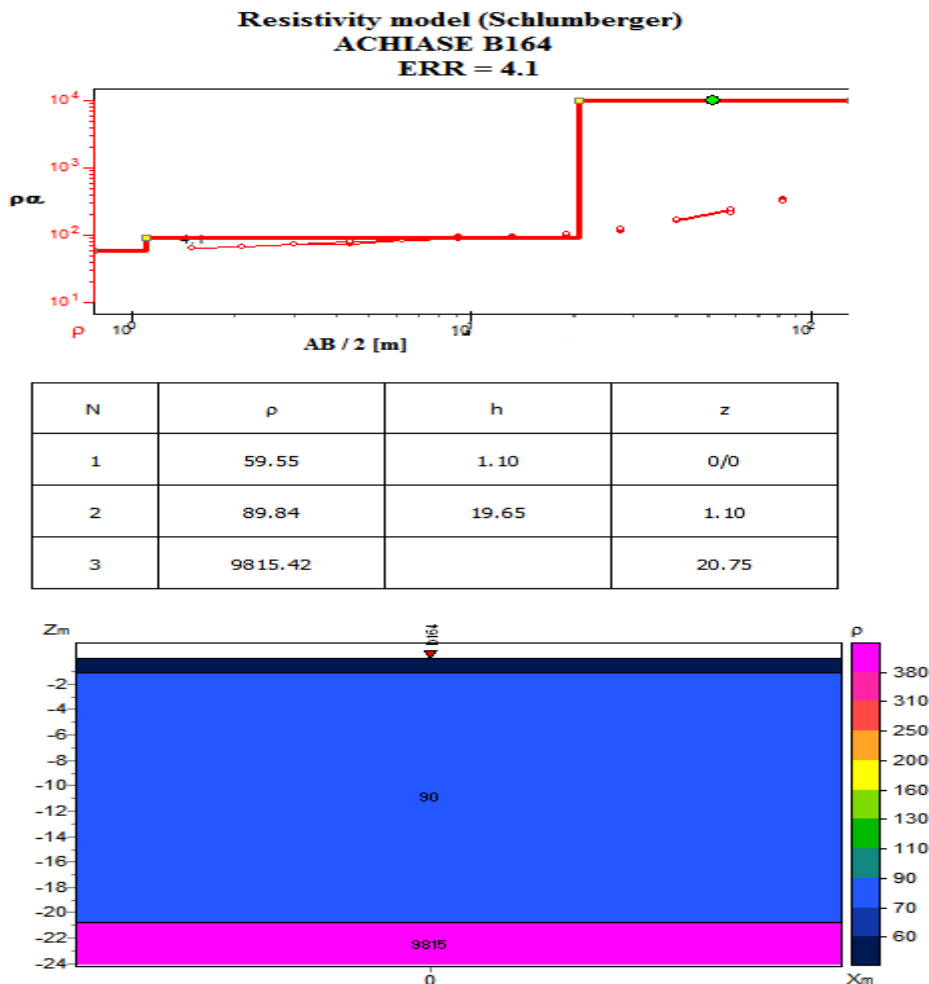
Figure 5.21. VES model curve at station B164 m, Achiase Community

### 5.4.3.4. Discussions of results from Achiase Community

The analysis of all the VES results in this community suggests that the Achiase community is underlain by three geological subsurface structures. The first has resistivity values ranging from 59.55 - 756.05 Ωm and can be intercepted at the mean depth of 2.42 m. The second which has a thickness range of 3.22 - 21.46 m has a mean apparent resistivity value of 166.67 Ωm. This layer is expected to be water-bearing. The third layer which is interpreted to be the bedrock has apparent resisting value ranging from 2479.11 - 43868.702 Ωm.

The contour maps below (Figures 5.22a – 5.22c) show the responds of the apparent resistivity values with depth. The presence of high among of groundwater is shown to start from depth 1.5 m and at 58.0 m at the VES B 164. This VES point might have about 50 m thick aquifer beneath it and that it is ranked the first in this community. The second in roll is the VES point C208, which has high quantity of groundwater showing up between 1.5 m and 40 m deep. The third in rank VES A216 is observed to shows signs of high amount of groundwater from 1.5 m to 27.5 m below the earth surface. At point B58, high quantity of ground water within the labelled B zone show up on the maps between depth 6.3 m and 40 m. VES point A152 shows presence of little amount of groundwater throughout the 83.0 m depth and since this community have enough groundwater, this point is not recommended for drilling but rather wells could be drilled at point within 100 to 200 m from VES 164. The groundwater within the subsurface of Achiase Community is accumulated towards the southern part of the community more that the northern part. This may be because of the Namini and Ntigyina streams take their source from the south and flow towards the north.
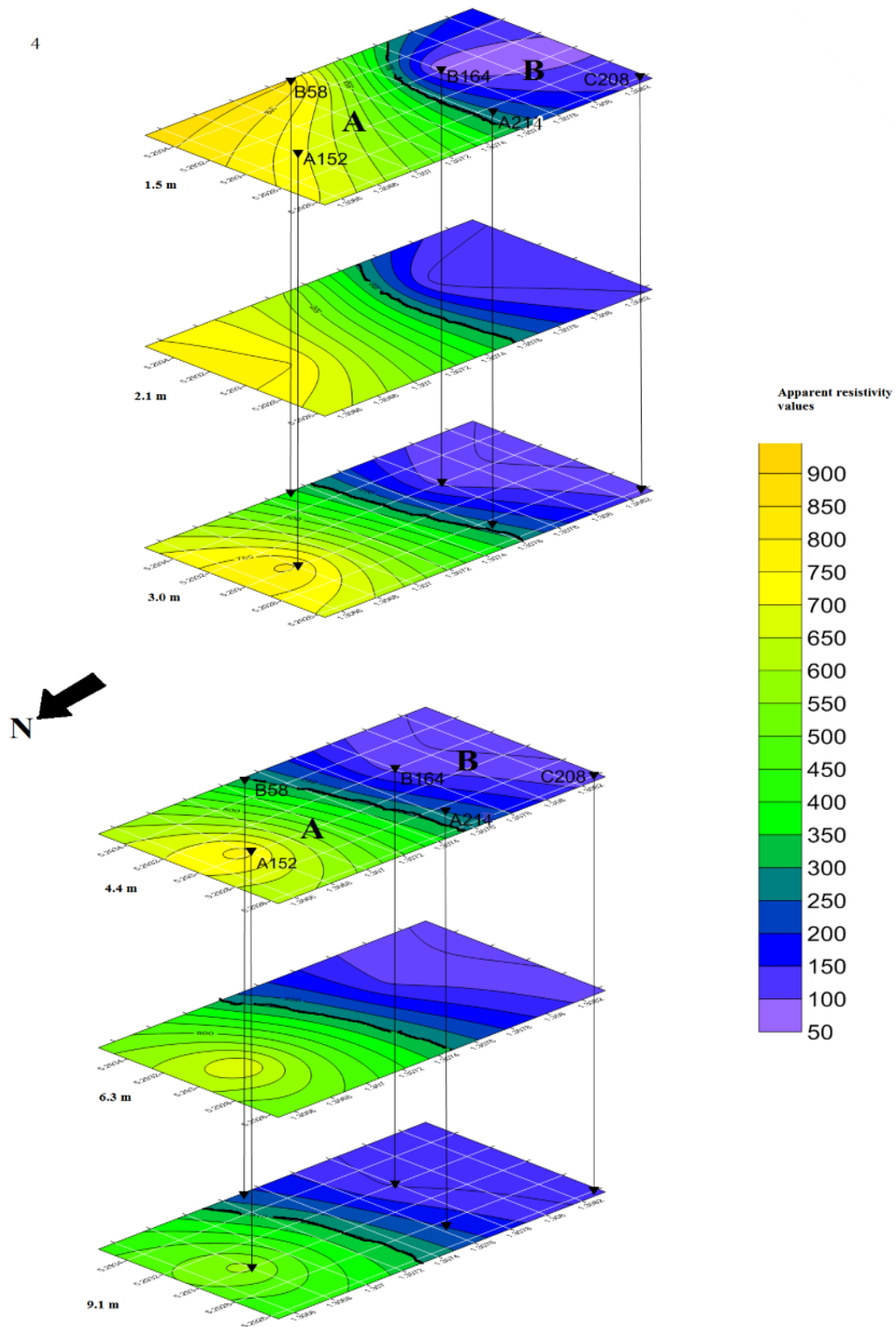
Figure 5.22a. Contour maps showing the apparent resistivity values from depth 1.5-9.1 m beneath the Achiase Community
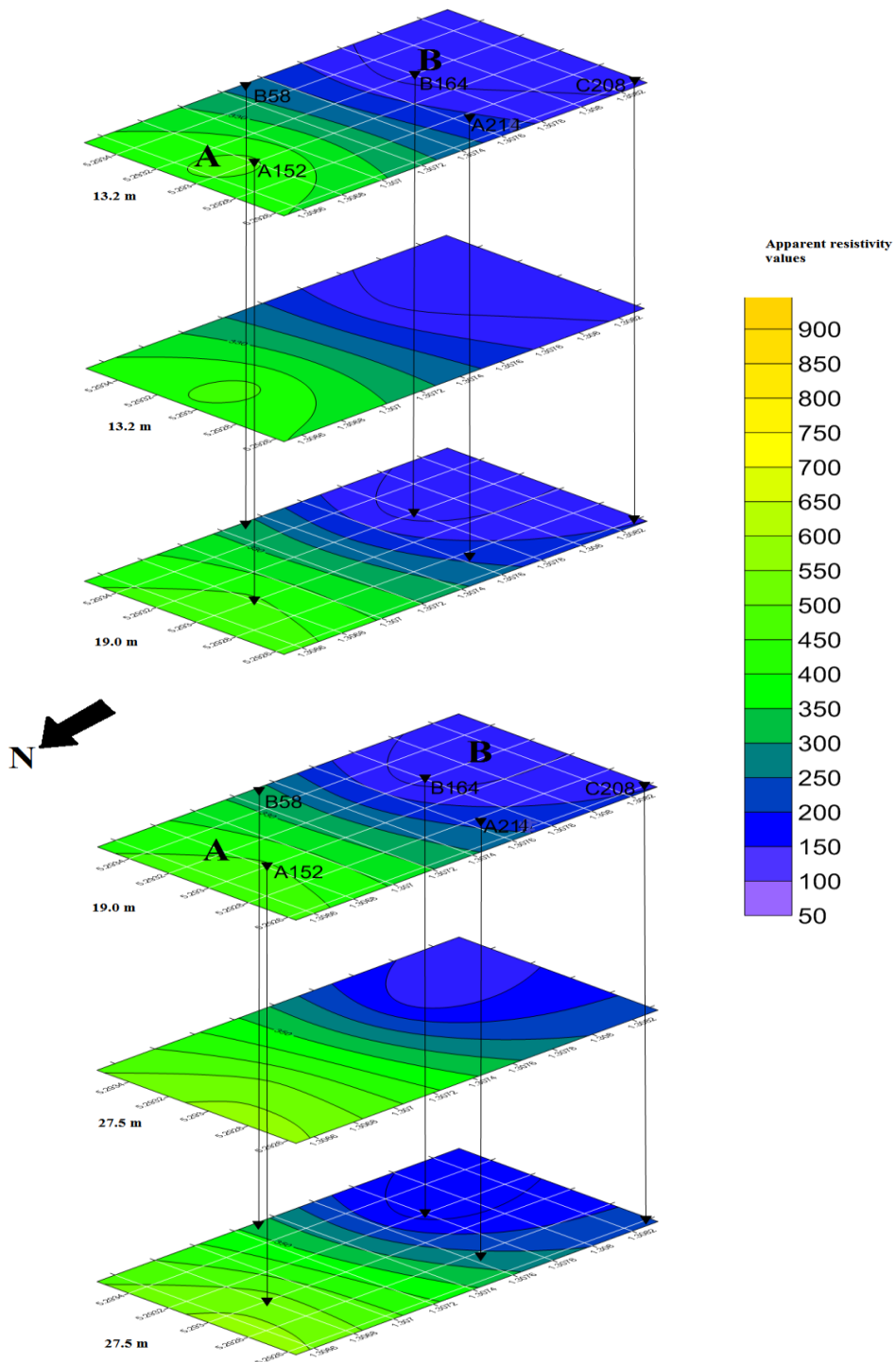
Figure 5.22b. Contour maps showing the apparent resistivity values from depth 13.2 -27.5 m beneath the Achiase Community
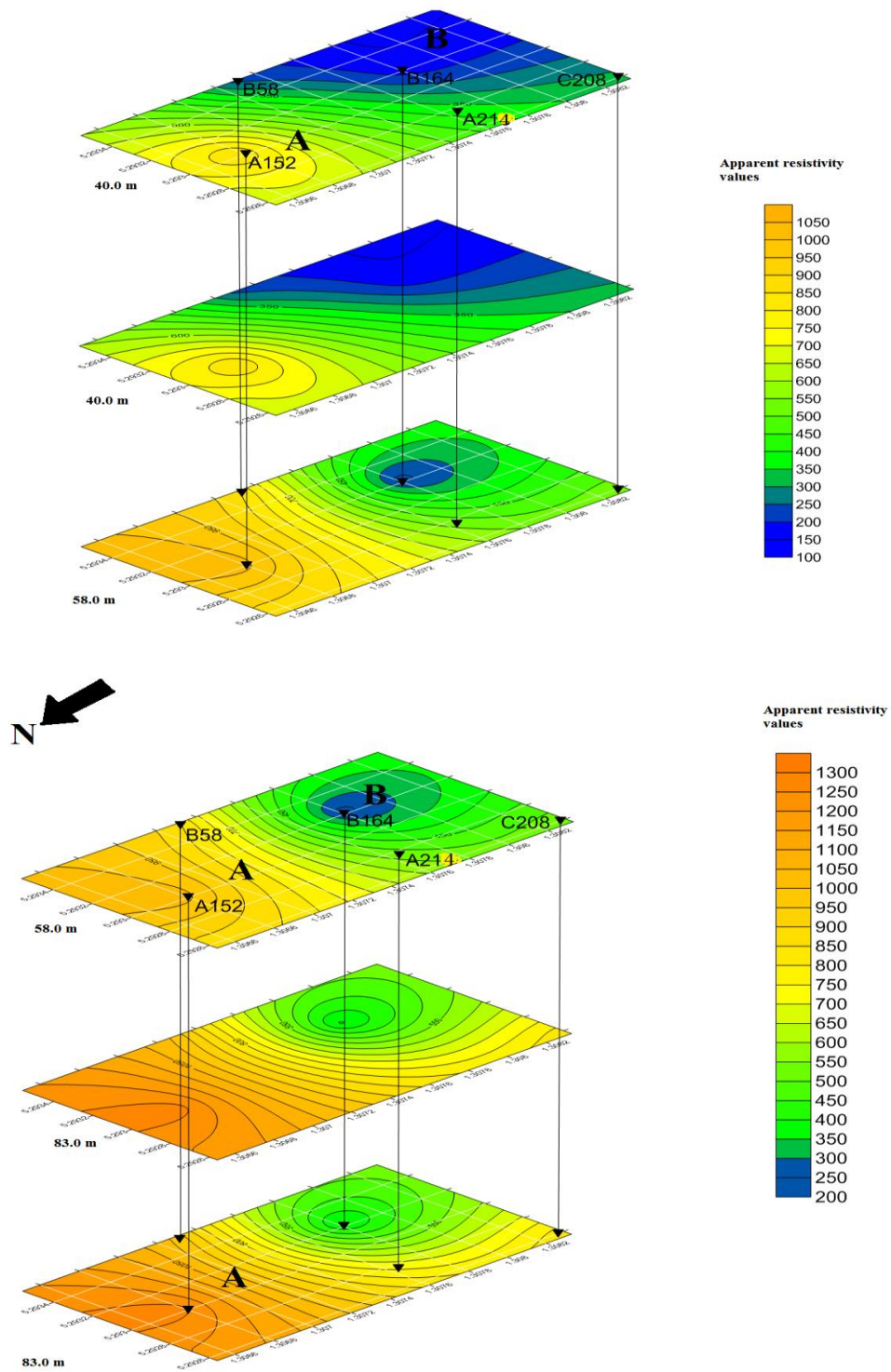
Figure 5.22c. Contour maps showing the apparent resistivity values from 40.0 – 83.0 m beneath the Achiase Community

Table 5.5. Ranked VES points for borehole drilling at Achiase Community

| VES Point | Layer | ρ (Ω–μ) | Depth (m) | Thickness (m) | Rank | Location (GPS) | Remarks |
|---|---|---|---|---|---|---|---|
| B164 | 1 | 59.55 | 1.1 | 1.1 | | | |
| | 2 | 89.84 | 20.75 | 19.65 | 1st | 5.29323N | |
| | 3 | 9815.42 | - | - | | 1.30781W | |
| C208 | 1 | 148.91 | 1.14 | 1.45 | | | |
| | 2 | 33.45 | 4.36 | 3.22 | 2nd | 5.29256N | |
| | 3 | 5721.62 | - | - | | 1.30833W | |
| A214 | 1 | 756.05 | 2.91 | 2.91 | | | |
| | 2 | 289.28 | 13.63 | 10.72 | 3rd | 5.29275N | |
| | 3 | 2479.11 | - | - | | 1.30651W | |
| B58 | 1 | 1232.85 | 0.83 | 0.83 | | 5.29356N | |
| | 2 | 240.06 | 22.29 | 19.65 | 4th | 1.30728W | |
| | 3 | 43868.7 | - | - | | | |
| A152 | 1 | 752 | 5.82 | 5.82 | | | little |
| | 2 | 180.71 | 13.33 | 7.51 | 5th | 5.29303N | amount of water |
| | 3 | 8310.8 | - | - | | 1.30678W | |

### 5.4.4. Beseadze Community

### 5.4.4.1. Introduction

Electromagnetic profiling was conducted along two (2) profiles across the Beseadze community and six VES points investigated (Figure 5.23). Among the 6 VES points investigated 5 VES revealed 3 – layered model and 1 suggest 4 – layered model. The curve types are A, H and KH. There were no available data existing boreholes and hand-dug wells within a 5 km radius of the Beseadze community.

### 5.4.4.2. EM traverses

The traverse was carried out on a profile length of 360 m on a bearing of 160˚ from the True North. The EM readings were taken using 20 m coil spacing at 10 m intervals.

The results of EM profiling as shown in Figure 5.24 displays an erratic movement of both VD mode and HD mode curves along the profile. This suggests complex geological structures. Generally the terrain conductivities within this area are high with the maximum of 11 m mhos/m and the minimum of 7 m mhos/m. The average terrain conductivity of the substance is 9.23 m mhos/m. Three stations were chosen for VES investigation due to their high terrain conductivity for both VD mode and HD mode. There are crossovers of the HD mode and VD mode curve at these chosen points. The points are at Stations A94, A134 and A194.
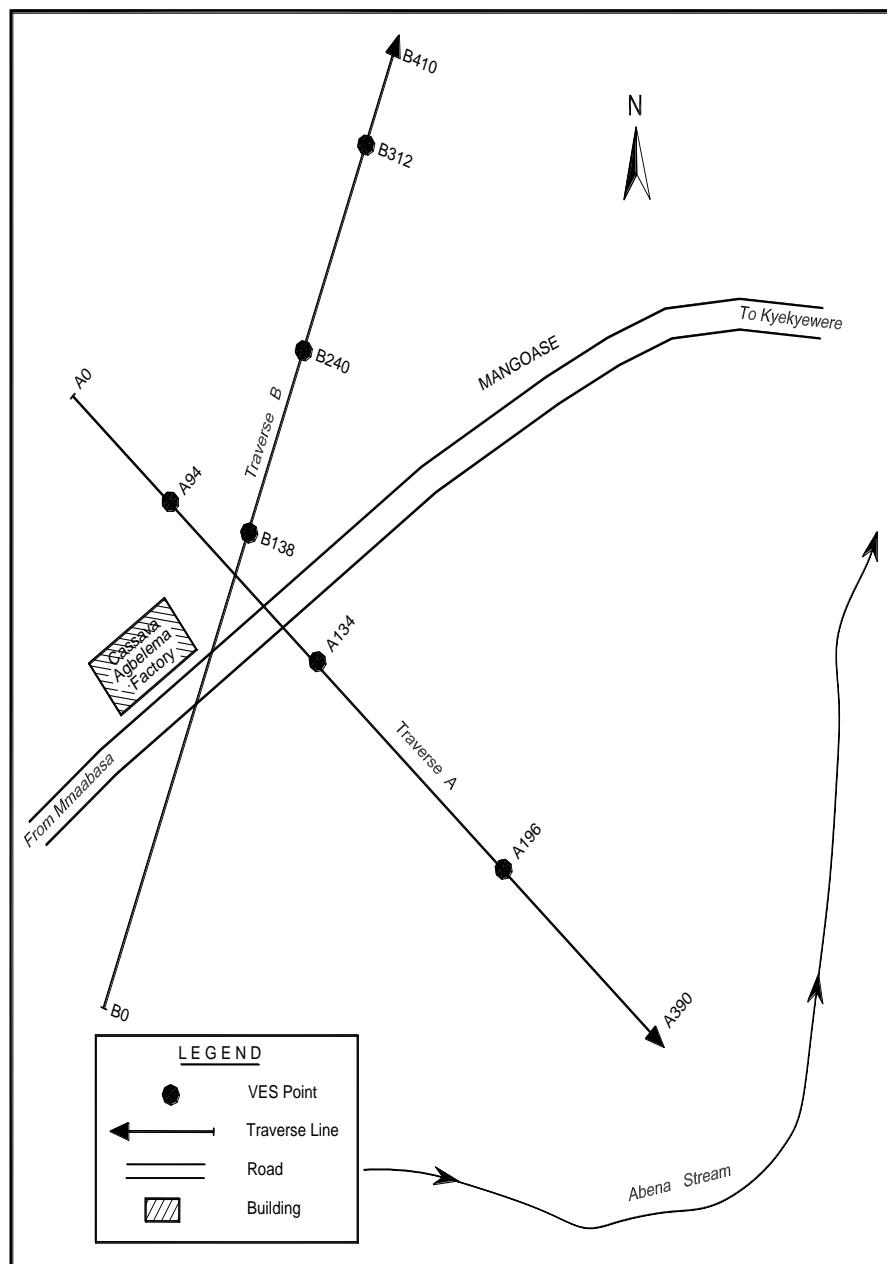


Figure 5.23. Schematic Layout of Beseadze Community (not to scale)
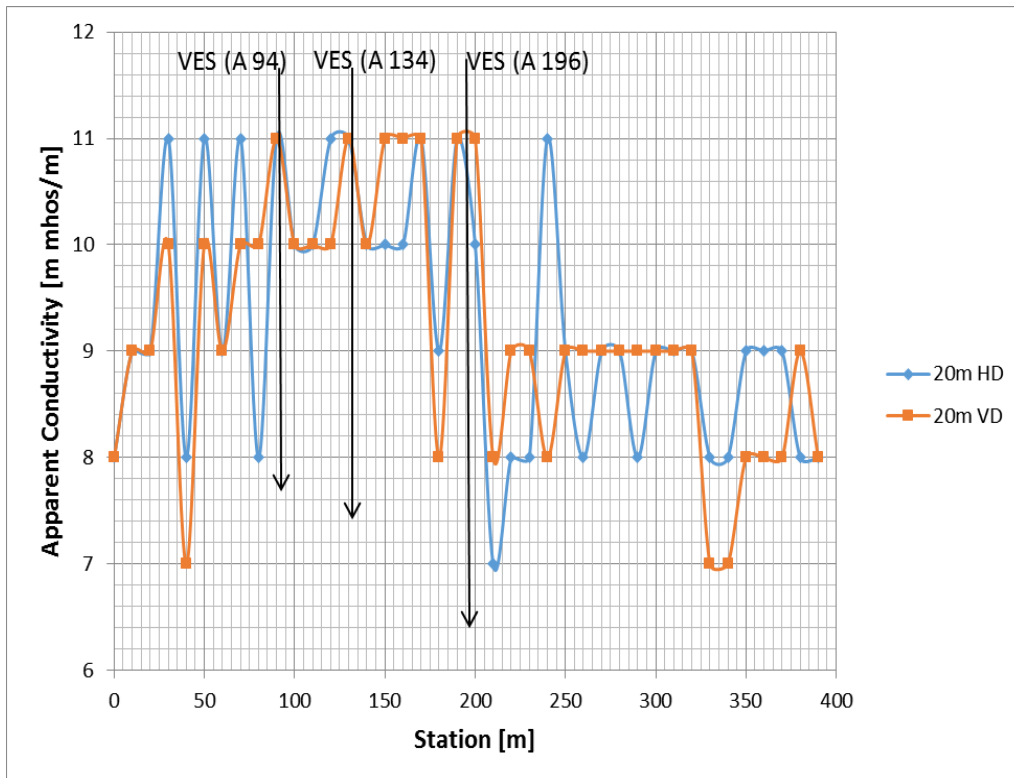
Figure 5.24 EM terrain conductivity measurements along a profile A at Beseadze Community

These points have high probability of fracture within their subsurface. From the Figure 5.30, two zones could be identified; zone of high terrain conductivities which start from Station 25 m to Station 210 m. The second zone which has low terrain conductivities starts from Station 210 m to the end of the profile. The first zone is of interest because high conductivities within the geology of this area may due to fractures and weathered zones which are areas of accumulation of groundwater.

The EM profiling on traverse B was run on bearing of 355° from the True North. The EM readings were carried out along this traverse of length 410 m using 20 m coil spacing and the reading taken at 10 m intervals.

Figure 5.25 below is a graph of the variation of terrain conductivity with distance along profile B at Beseadze community. From the graph, the apparent conductivity values of VD mode are comparatively higher than those of the HD mode along most part of the profile, suggesting an increase in conductivity with depth. The maximum terrain conductivity recorded on this profile is 36 m mhos/m (VD mode) and the minimum is 9 m mhos/m with the average of 12.90 m mhos/m. The three

conductivity peaks belong to the VD mode curve and the highest is between two peaks. The VD mode curve recorded its minimum terrain conductivity from station 170 m to 230 m. Generally curves on this graph are erratic in nature, suggesting a complexity at the subsurface. The peak at station 140 m is believed to have revealed high fracture zone because of its high anomaly. This point and the stations 138 m and 312 m were selected for further investigations.
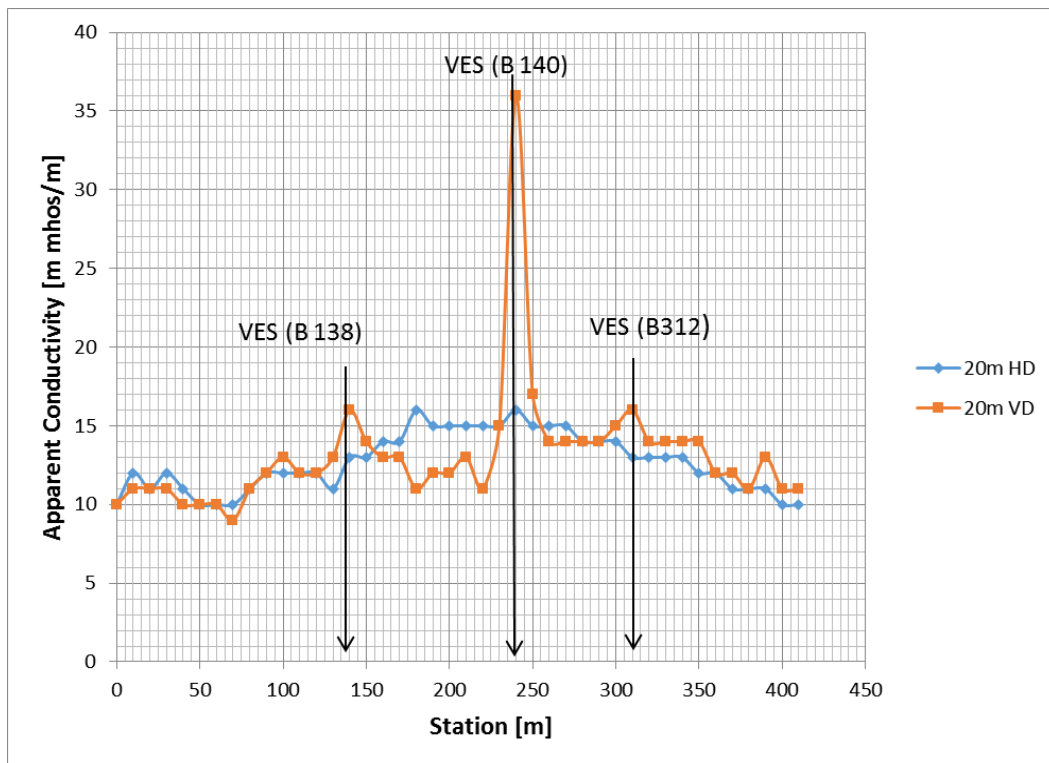


Figure 5.25. EM terrain conductivity measurements along a profile B at Beseadze Community

### 5.4.4.3. Sounding curves

VES A94

Analysis of the VES curve and pseudo section at this station, Figure 5.26 revealed three geological layers at the subsurface. The sounding curve is H – type curve and it displays a weathered zone in layer 2. The top layer is fairly weathered with thickness of 7.42 m and apparent resistivity value of 169.79 $\Omega$m. The second layer which may be heavily fractured or weathered has an apparent resistivity value of 41.96 $\Omega$m and thickness of 11.9 m. The third layer, the bedrock has an apparent resistivity value of 861250.57 $\Omega$m. The great difference between the second layer and the third layer re-enforce the reasoning that the second layer is highly fractured and that may contain

sufficient amount of groundwater for public water supply. This station was recommended for drilling of boreholes.
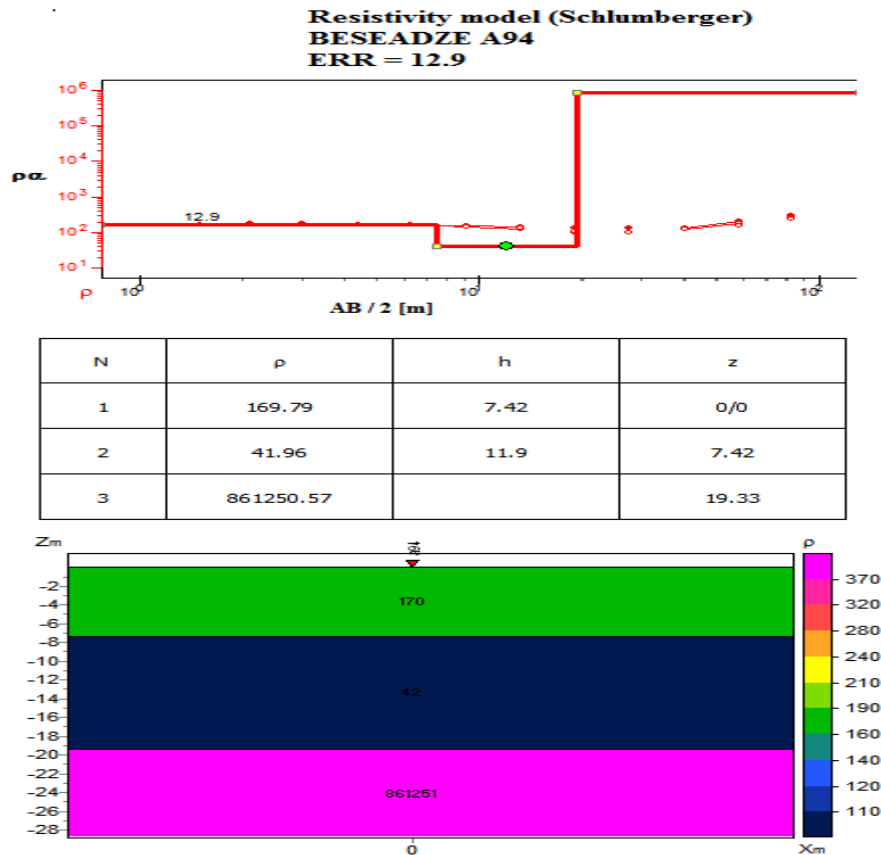


Figure 5. 26. VES model curve at station A94 m, Beseadze Community

VES A134

Station A134 (Figures 5.27) revealed four layers in the subsurface with apparent resistivity values in the range of 508.93 Ωm to 1666.15 Ωm. First layer is 1.28 m and resistivity of 512.51 Ωm. Second layer has thickness of 4.22 m and apparent resistivity of 1633.04 Ωm. Third layer and forth layer have apparent resistivity values of 508.93 Ωm and 1666.15 Ωm respectively. The thickness of the third layer is 18.39 m. The apparent resistivity values of the subsurface at this station start with low resistivity value and finally high resistivity value. There is high probability of locating groundwater reservoir in the third layer and that if there is groundwater presences at this layer it would be of high quantity. This station is recommended for drilling a well.

**Resistivity model (Schlumberger)**
**BESEADZE A134**
**ERR = 12.1**

| N | ρ | h | z |
|---|---|---|---|
| 1 | 512.51 | 1.28 | 0/0 |
| 2 | 1633.04 | 4.22 | 1.28 |
| 3 | 508.93 | 18.39 | 5.50 |
| 4 | 1666.15 | | 23.89 |
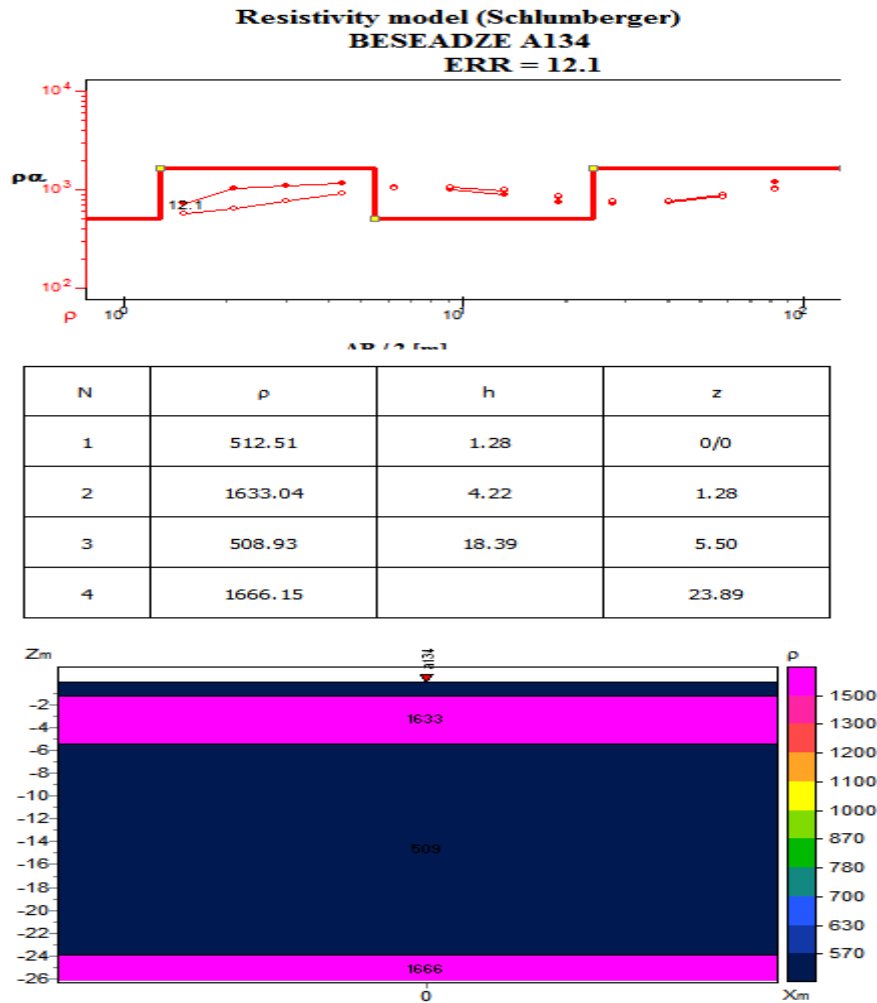
Figure 5.27. VES model curve at station A134 m, Beseasze Community

VES B138

Deduction made from the VES curve and pseudosection at section B138 indicates a three layered subsurface geological structure as shown in Figure 5.28. The sounding curve is A – type curve with the first layer having the minimum resistivity value. The upper layer is 2.26 m thick and has an apparent resistivity of 147.87 Ωm; it is underlain by a second layer (middle layer) of apparent resistivity and thickness of 542.13 Ωm and 17.06 m respectively. Beneath this is the bedrock of apparent resistivity of 58791.04 Ωm. The resistivity and thickness of layers at this station increases with depth. The top layer fairly weathered than the other layers but both the first and the second layer are likely to contain groundwater.
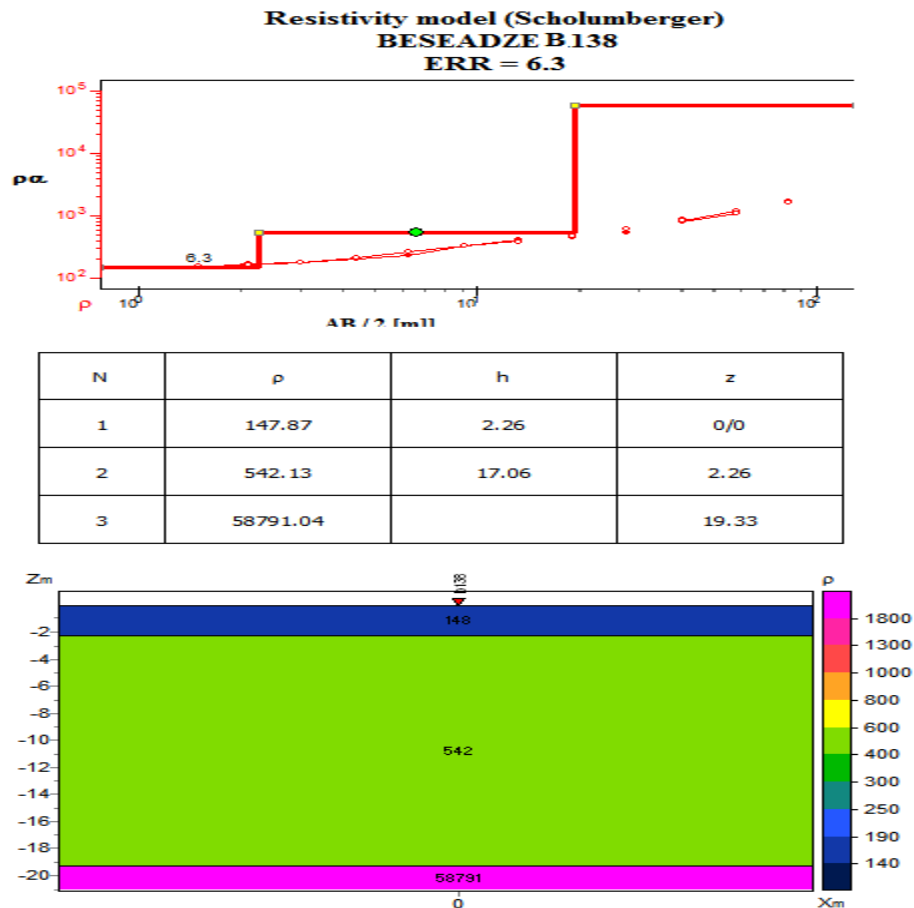
Figure 5.28. VES model curve at station B138 m, Beseadze Community

### 5.4.4.4. Discussions of results from the Bezeadze Community

Analysis of VES curves conducted within this community, suggested that Beseadze community is underlain by three geological structures. The first layer has an apparent resistivity values ranging from 71.93 - 1219.24 Ωm and a mean depth of 4.15 m. The second layer which is expected to be water-bearing has an average apparent resistivity of 573.93 Ωm and thickness ranging from 4.22 - 20.87 m. Third layer has an apparent resistivity values resistivity values ranging between 508.93 - 861250.57 Ωm.

Generally from the surfer models in Figures 5.29a, 5.29b and 5.29c below; the subsurface of Beseadze community is underlain by a good aquifer which stretch from north to south. From one meter depth to about 9.1 m deep, high amount of groundwater is inferred from some of the points investigated. It is also inferred that VES stations A94, B240 and B138 contained a lot of groundwater beneath them. The

highest ranked point is the VES A94 which shows signs of a lot of groundwater from 1.5 − 58.0 m; it is being follow by VES B240 which also has a lot of groundwater shown on the contour map from the depth of 1.5 − 19.0 m. The third ranked VES station is B138. It shows great amount of water beneath it from the depth of 1.5 to about 6.3 m. it may be beyond 6.3 m but less than the 9.1 m depth mark. Three stations where all ranked 4th and these stations are A134, A196 and B312 (Table 5.6 provide a summary of the VES results including a rank-list of the selected points for drilling). These stations contain groundwater but not in high quantities and since there are some points in this community which is mapped to contained greater amount of water than these points, it is advised to drill at point between VES B240 and A94.
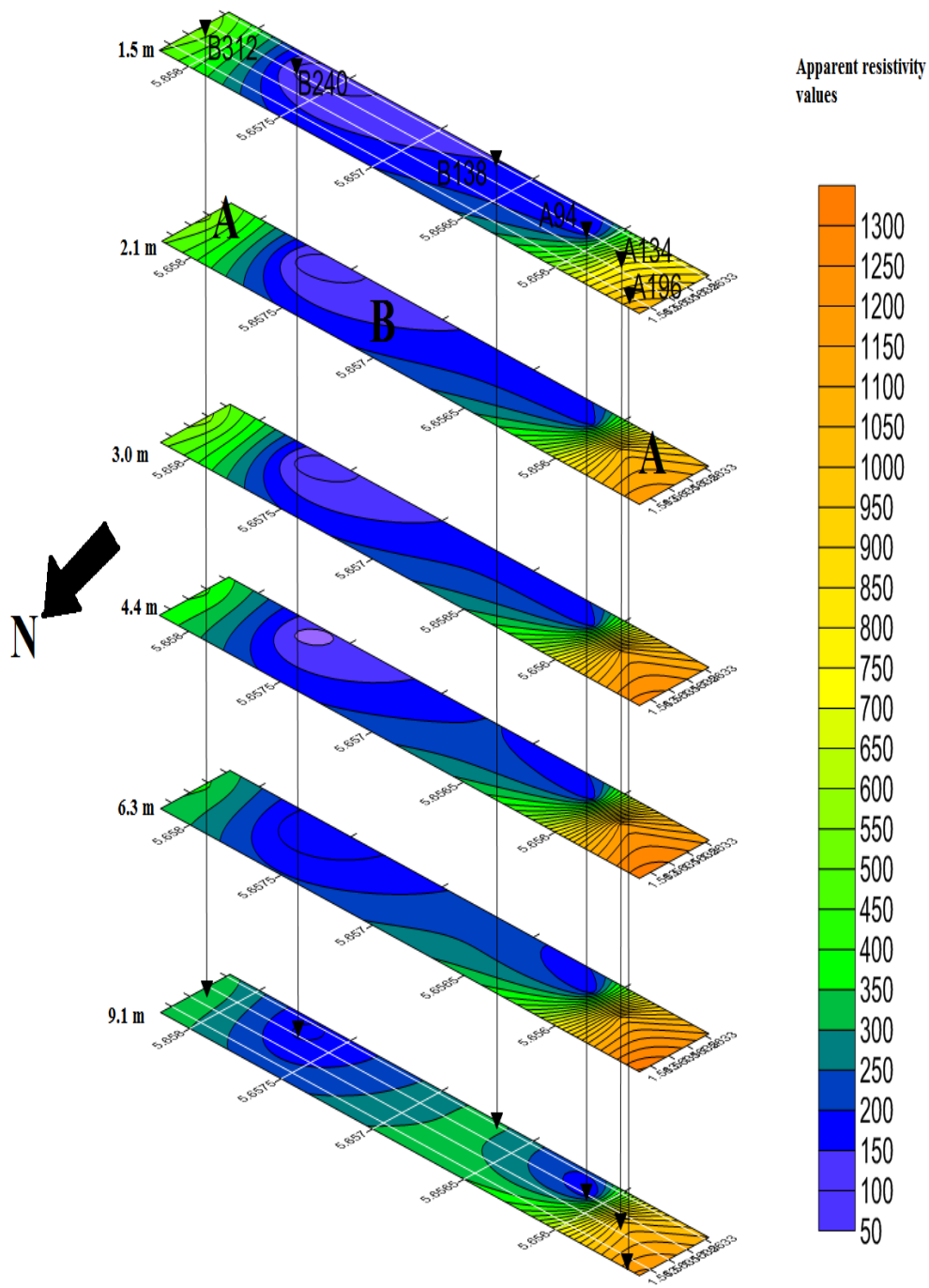
Figure 5.29a. Contour maps showing the apparent resistivity values from depth 1.5-9.1 m beneath the Beseadze Community
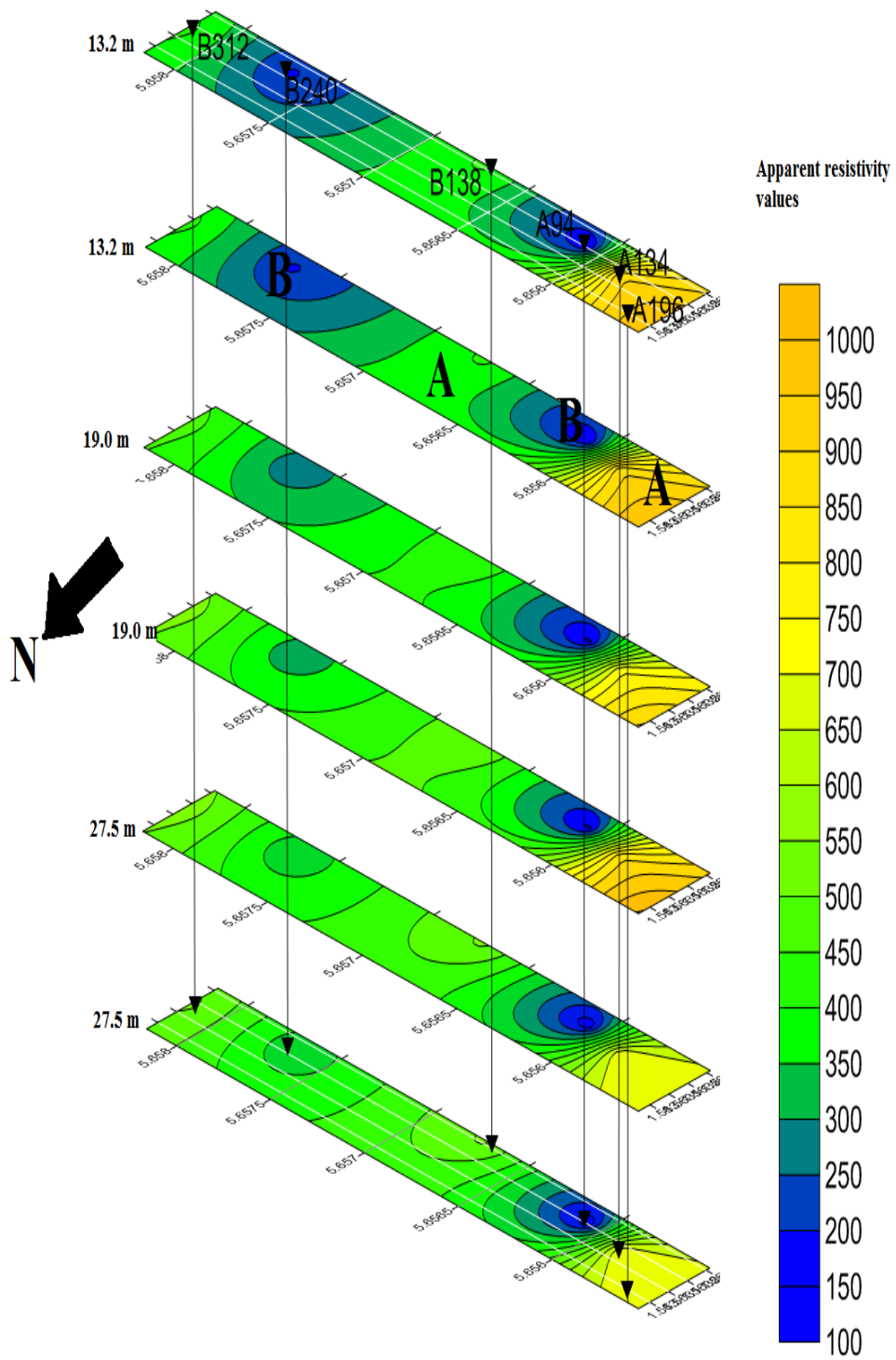
Figure 5.29b. Contour maps showing the apparent resistivity values from depth13.2 – 27.5 m beneath the Beseadze Community
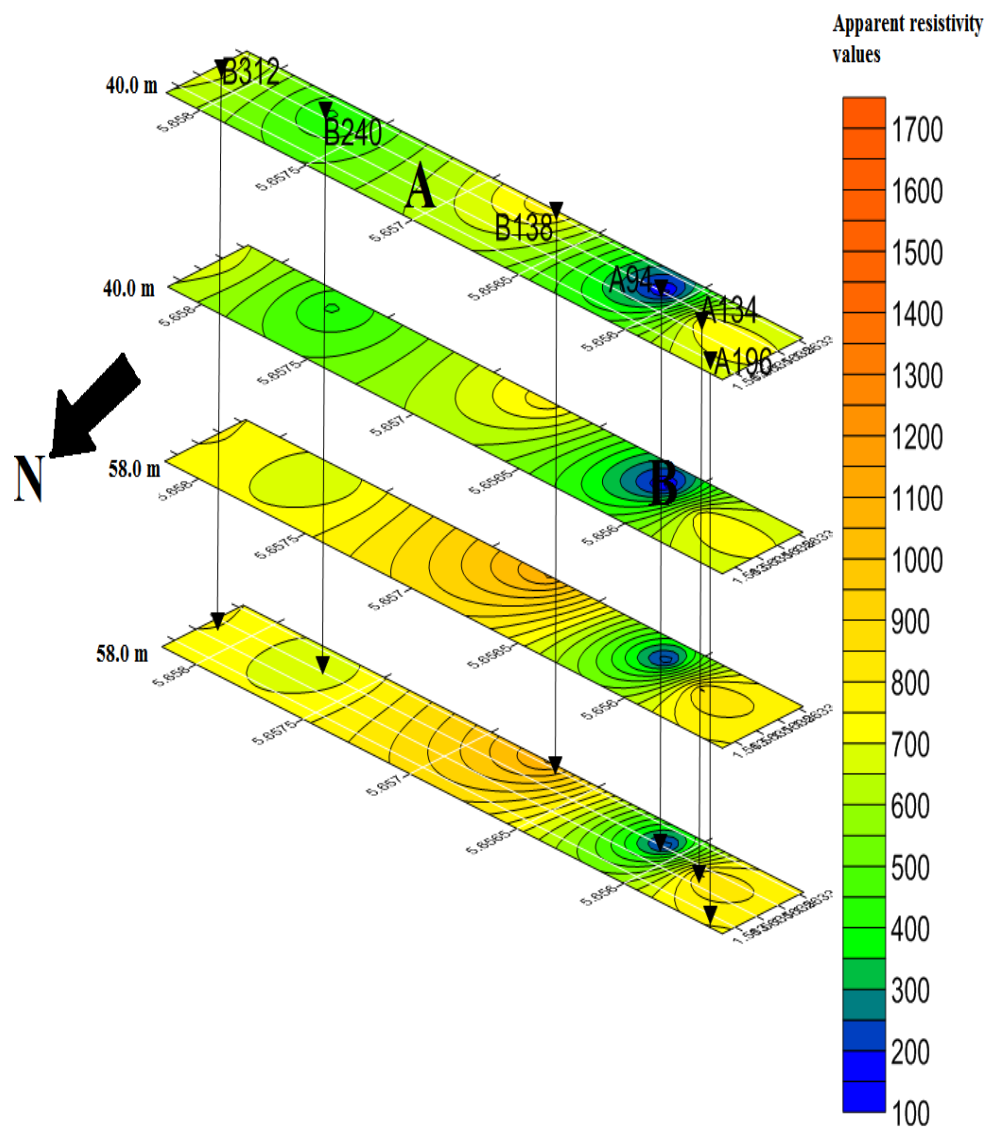
Figure 5.29c. Contour maps showing the apparent resistivity values from depth 40 – 58 m beneath the Beseadze Community

Stations A134, A196 and B312 could still be drilling or hand dug but the fear is that the water that they may produce would not be much and also they may dry up during the dry seasons. By careful observation of the contour maps, it could be realized that the groundwater within this community is located within the central part of the community.

Table 5.6. Ranked VES points for borehole drilling at Beseadze Community

| VES Point | Layer | ρ (Ω−µ) | Depth (m) | Thickness (m) | Rank | Location (GPS) | Remarks |
|---|---|---|---|---|---|---|---|
| | 1 | 169.79 | 7.42 | 7.42 | | 5.65607N | |
| | 2 | 41.96 | 19.33 | 11.9 | | 1.56321W | |
| A94 | 3 | 861250.57 | - | - | 1st | | |
| | 1 | 71.93 | 3.86 | 3.86 | | 5.65768N | |
| | 2 | 522.62 | 14.86 | 11 | | 1.56323W | |
| B240 | 3 | 2790.38 | - | - | 2nd | | |
| | 1 | 609.4 | 2.15 | 2.15 | | 5.65673N | |
| | 2 | 219.24 | 6.5 | 4.35 | | 1.56332W | |
| B138 | 3 | 948.63 | - | - | 3rd | | |
| | 1 | 512.51 | 1.28 | 1.28 | | 5.65586N | |
| | 2 | 1633.04 | 5.5 | 4.22 | | 1.56316W | |
| | 3 | 508.93 | 23.89 | 18.39 | | | |
| A134 | 4 | 1666.15 | - | - | 4th | | |
| | 1 | 1219.24 | 7.94 | 7.94 | | 5.65554N | |
| | 2 | 484.65 | 28.81 | 20.87 | | 1.56294W | |
| A196 | 3 | 1421.67 | - | - | 4th | | |
| | 1 | 147.87 | 2.26 | 2.26 | | 5.65673N | |
| | 2 | 542.13 | 19.33 | 17.06 | | 1.56332W | |
| B138 | 3 | 58791.04 | - | - | 4th | | |

## 5.4.5. Esukese Ekyir Community

## 5.4.5.1. Introduction
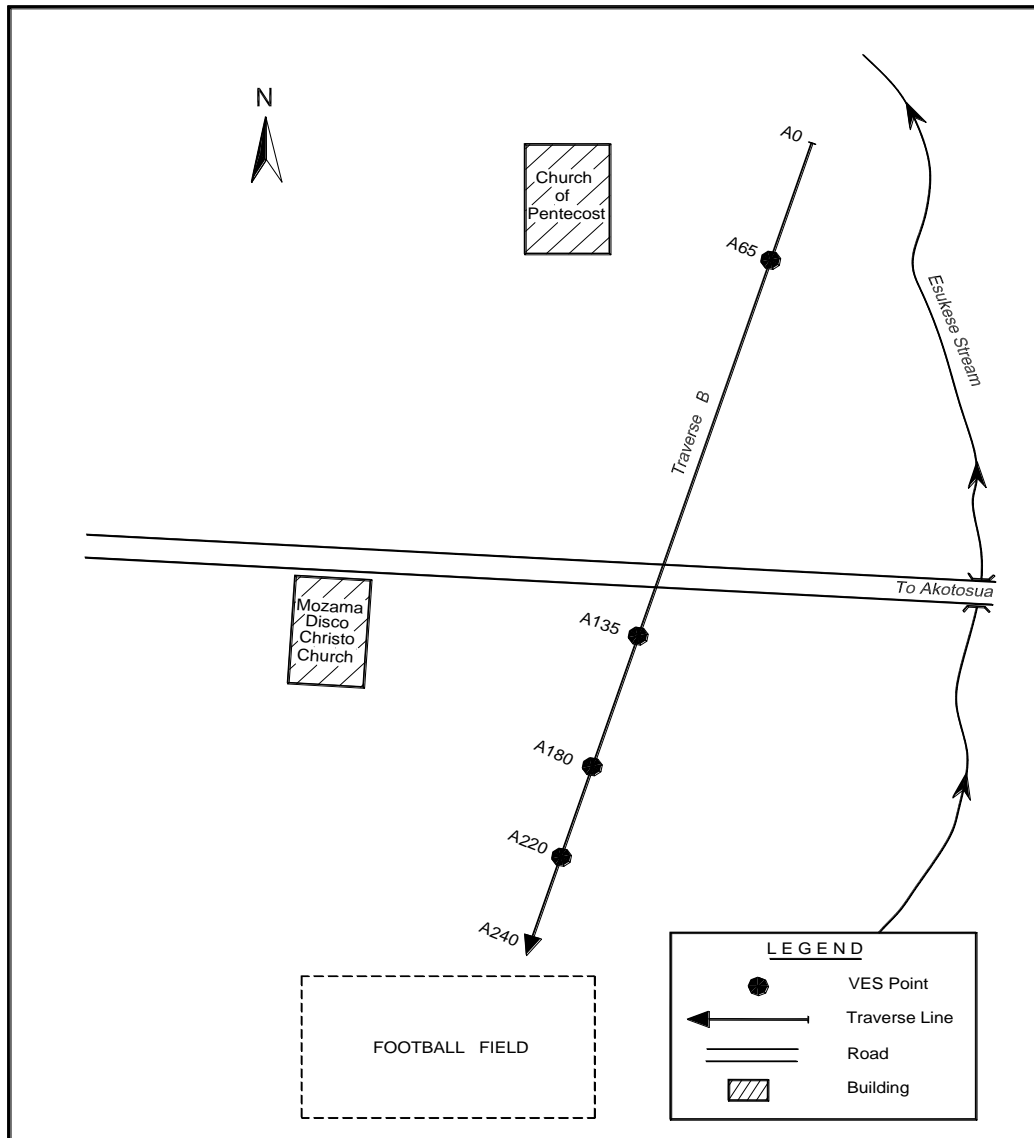


Figure 5.30. Schematic Layout of Esukese Ekyir Community (not to scale)

In this community; one EM traverse was conducted on a profile length of 240 m and on a bearing of 205° from the True North. Four resistivity measurements were taken on four selected points along the EM traverse. 3 out of the 4 VES points investigated within this community suggest a 3 – layered earth model and the remaining 1 suggest a 4 – layered model. The curve types displayed by sounding curves within this

community are A, H and KH. Figure 5.30 is the schematic layout of Esukese Ekyir Community showing the traverse and the VES stations.

### 5.4.5.2. EM traverse

The EM profiling was carried out using 10 m coil spacing and EM readings were taken at 5 m intervals. The terrain conductivity values obtained in this study ranges between 20 and 67 m mhos/m and the average of 17.82 m mhos/m. Four points A65, A135, A180 and A220 as shown in Figure 5.31 below; were selected along the profile for further VES investigations.
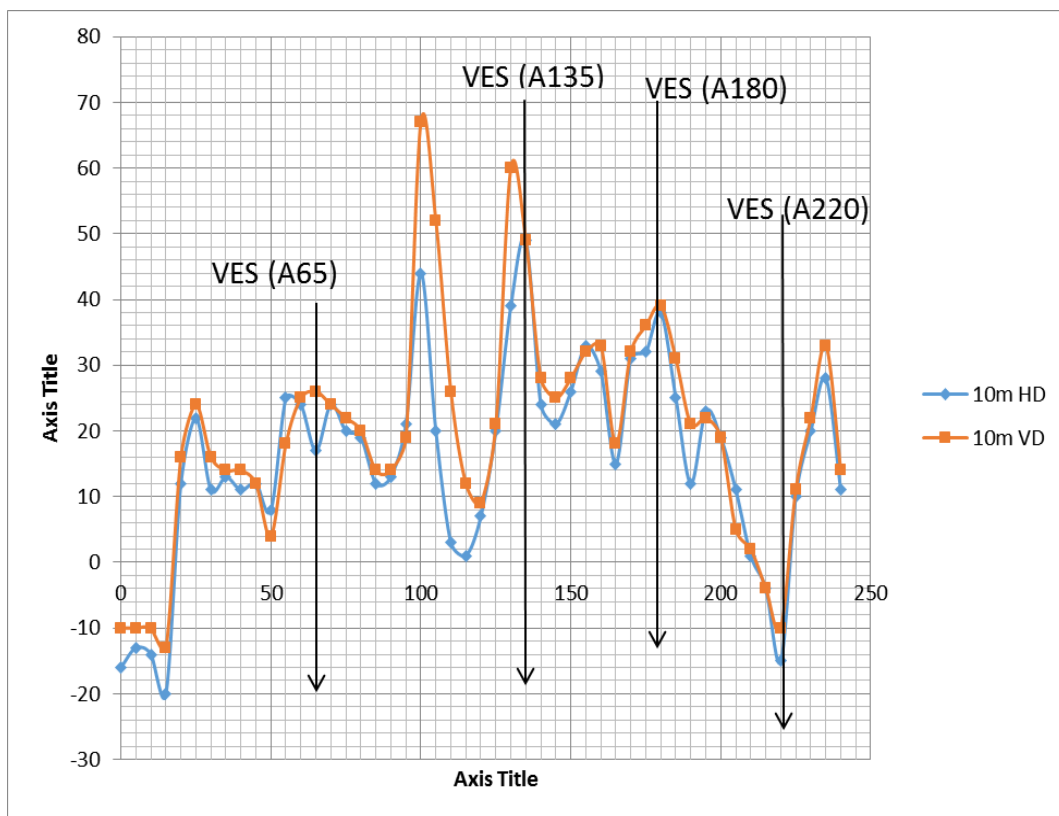


Figure 5.31. EM terrain conductivity measurements along a profile A at Esukese Ekyir Community

Observation of the graph in the Figure 5.31 above shows that both HD mode and VD mode curves are erratic along the profile. The apparent conductivity values for VD mode curve are generally higher than the HD mode suggesting increase in conductivity with depth. The erratic nature of the curves as mention earlier also suggests the subsurface beneath this profile contain a complex geological structure. Generally from station 90 m to station 145 m, both curves recorded their maximum

terrain conductivity values and they recorded their minimum values at stations 15 m and 220 m. Careful analyses of these curves reveal a high possibilities of locating an aquifer with sufficient amount of groundwater at the selected points with point 220 m having the least amount of groundwater.

### 5.4.5.3. Sounding curves

VES A65



**Resistivity model (Schlumberger)**
**ESUKESE EKYIR A65**
**ERR = 9.3**

| N | ρ | h | z |
|---|---|---|---|
| 1 | 79.40 | 2.16 | 0/0 |
| 2 | 201.01 | 5.8 | 2.16 |
| 3 | 82.44 | 4.44 | 7.96 |
| 4 | 15384.97 | | 12.40 |
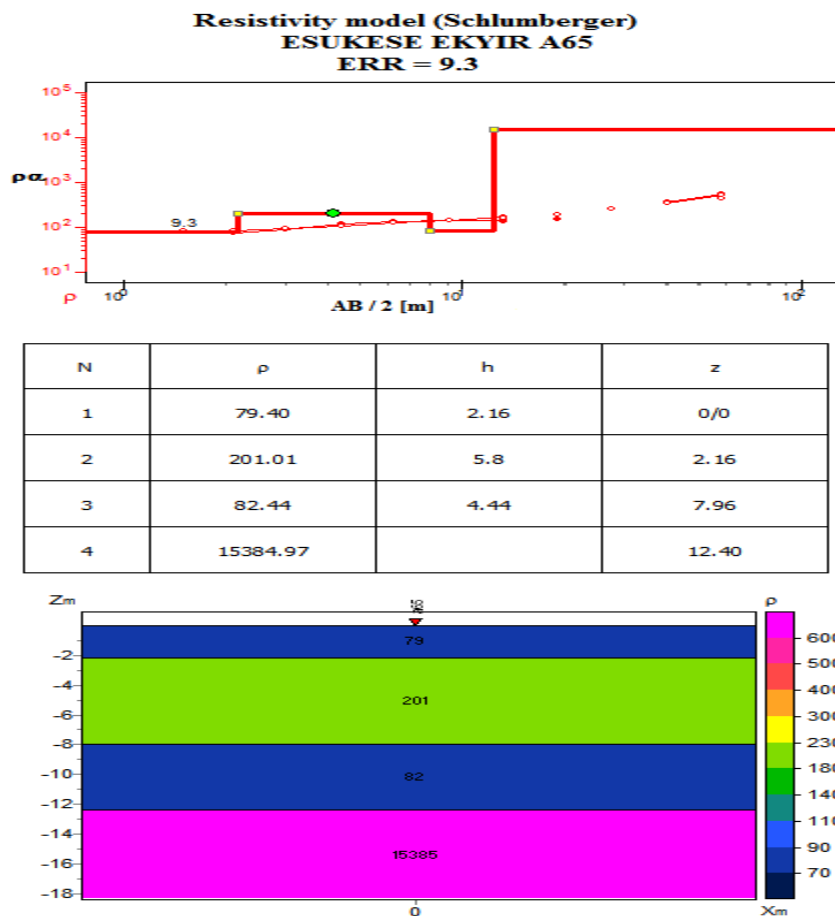
Figure 5.32. VES model curve at station A65 m, Esukese Ekyir Community

Analyses of results from VES A65 reveals that; the point is underlain by four geological structures with apparent resistivity values between 79.40 – 153384.97 Ωm. The sounding curve displays a KH – type curve with the possibility of weathered zones from layer 1 to layer 3. The upper most layer is 2.16 m thick and has an apparent resistivity value of 79.40 Ωm; the second layer is 5.80 m thick and has an apparent resistivity value of 201.01 Ωm. Below this layer is the third layer with the apparent resistivity value of 82.44 Ωm and thickness of 4.44 m. The bedrock

has the resistivity value of 15384.97 Ωm. Figure 5.32 shows the sounding curve and pseudosection of this station. Deduction made from these results indicate that; the first three layers are fractures and contain groundwater within them. Hence this station is recommended for drilling.

VES A135

VES station A135 is underlain by three layered subsurface structures. The curve type is H − type. The apparent resistivity values within these structures range between 58.15 Ωm and 4584.48 Ωm (Figure 5.33). The topsoil has a thickness of 0.81 m and an apparent resistivity of 208.00 Ωm. The thickness of the second layer is 2.24 m. The apparent resistivity value for second layer and third layer are 58.15 Ωm and 4584.48 Ωm respectively. These results suggest that, the second layer is highly fractures compare with the first layer. It is inferred that this station contain a lot of groundwater and hence recommended for construction of well.



| N | ρ | h | z |
|---|---|---|---|
| 1 | 208.00 | 0.81 | 0/0 |
| 2 | 58.15 | 2.24 | 0.81 |
| 3 | 4584.48 | | 3.04 |
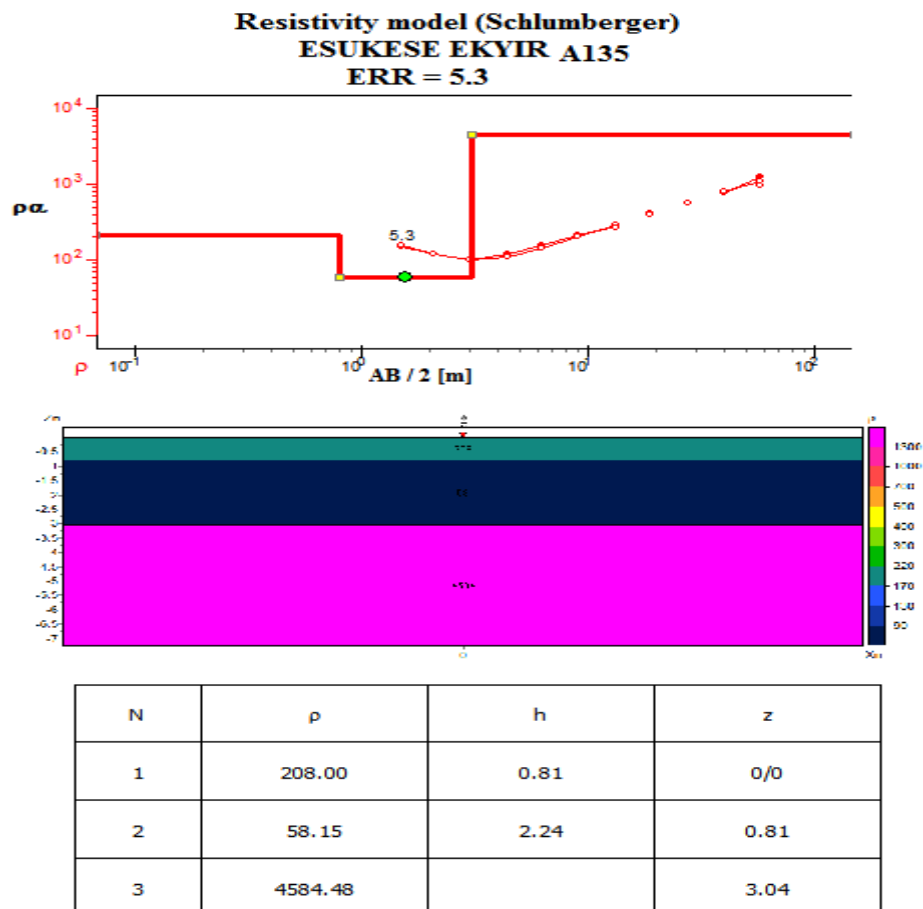
Figure 5.33. VES model curve at station A135 m, Esukese Ekyir Community

VES A220

It is inferred from the results of VES at station A220 that; the subsurface underlain this station is made up of three layered structure. The first layer has the minimum resistivity value and the third layer has the maximum resistivity values. This is A – type curve. The apparent resistivity of the layers range between 58.63 Ωm and 9374 Ωm. As shown in Figure 5.34; the first layer has an apparent resistivity of 58.63 Ωm and a thickness of 1.33m.



| N | ρ | h | z |
|---|---|---|---|
| 1 | 58.63 | 1.33 | 0/0 |
| 2 | 113.43 | 6.76 | 1.33 |
| 3 | 9374 | | 8.09 |
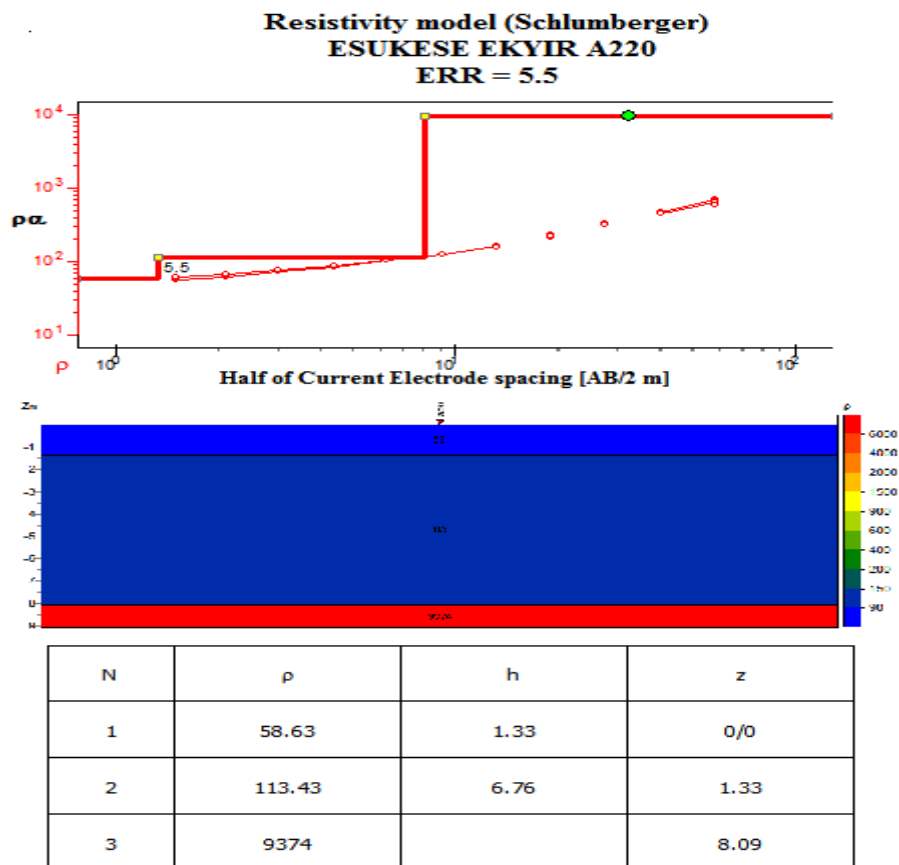
Figure 5.34. VES model curve at station A220 m, Esukese Ekyir Community

The second layer has a thickness of 6.76 m and an apparent resistivity value of 113.43 Ωm. The bedrock has an apparent resistivity of 9374 Ωm. The apparent resistivity values at this station increases with increasing depth. The first two layers have high probability of containing accumulated groundwater resource and hence the point is recommended for drilling or hand dug a borehole.

### 5.4.5.4.  Discussions of results from the Esukese Ekyir Community

Generally the Esukese Ekyir Community is underlain by three layered structure. The first layer has resistivity values between 58.63 Ωm and 208.00 Ωm; and can be intercepted at a mean thickness of 2.22 m. The second layer has thickness range of 2.24 – 10.81 m and a mean apparent resistivity value of 535.52 Ωm while the bedrock has apparent resistivity value range between 82.44 Ωm and 14827 Ωm. From the sounding curves, groundwater may be located within the first two layers.

Contour maps models created from results of VES conducted at four points in the Esukese Ekyir Community revealed high amount of water located within the subsurface of the community. As discussed earlier, the areas on the maps labelled B contain great amount of water and the area labelled A may contain water in small quantity and in community such as Esukese Ekyir where the aquifer is rich in groundwater; any point which falls within the A zone is not recommended for drilling or hand dug of well.

The resistivity measurement in this community was able to penetrate to a maximum depth of 58.0 m. From the Figures 5.35a – 5.35d; it could be noticed that, the groundwater in high
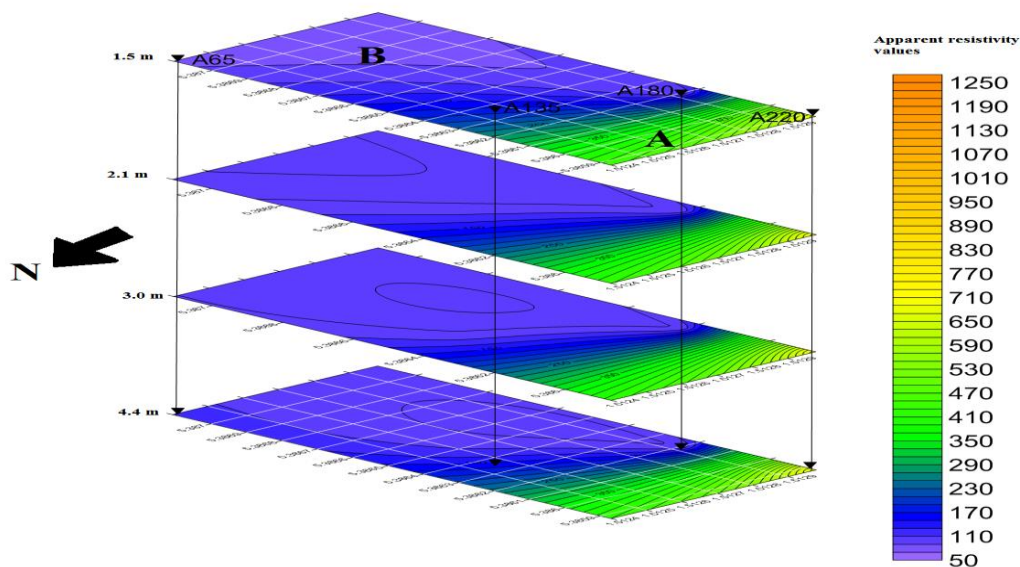


Figure 5.35a. Contour maps showing the apparent resistivity values from depth 1.5 – 4.4 m beneath the Esukese Ekyir Community
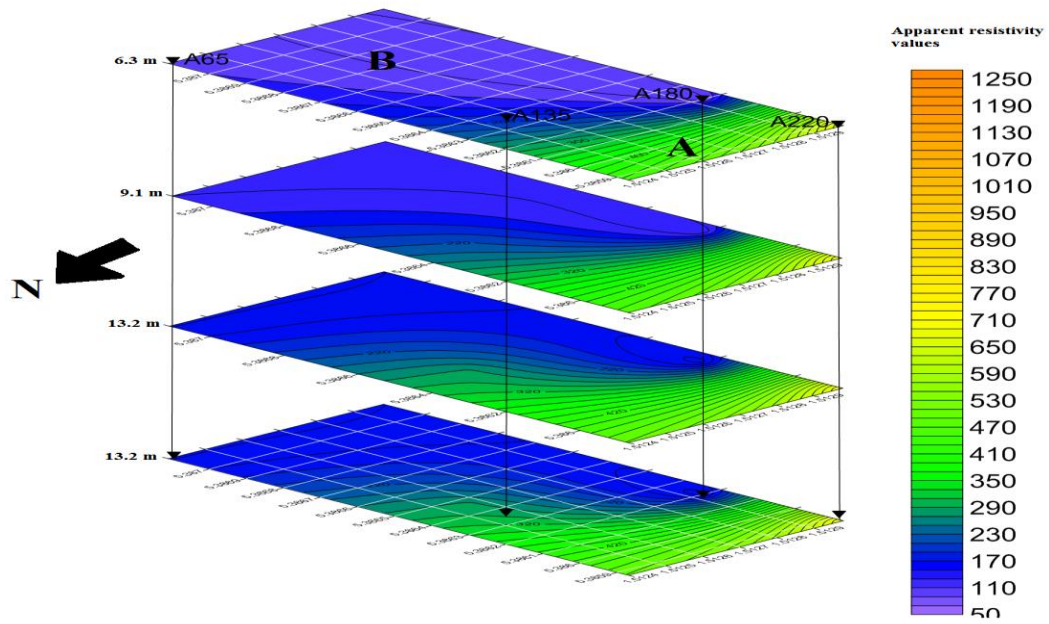
Figure 5.35b. Contour maps showing the apparent resistivity values from depth 6.3 – 13.2 m beneath the Esukese Ekyir Community
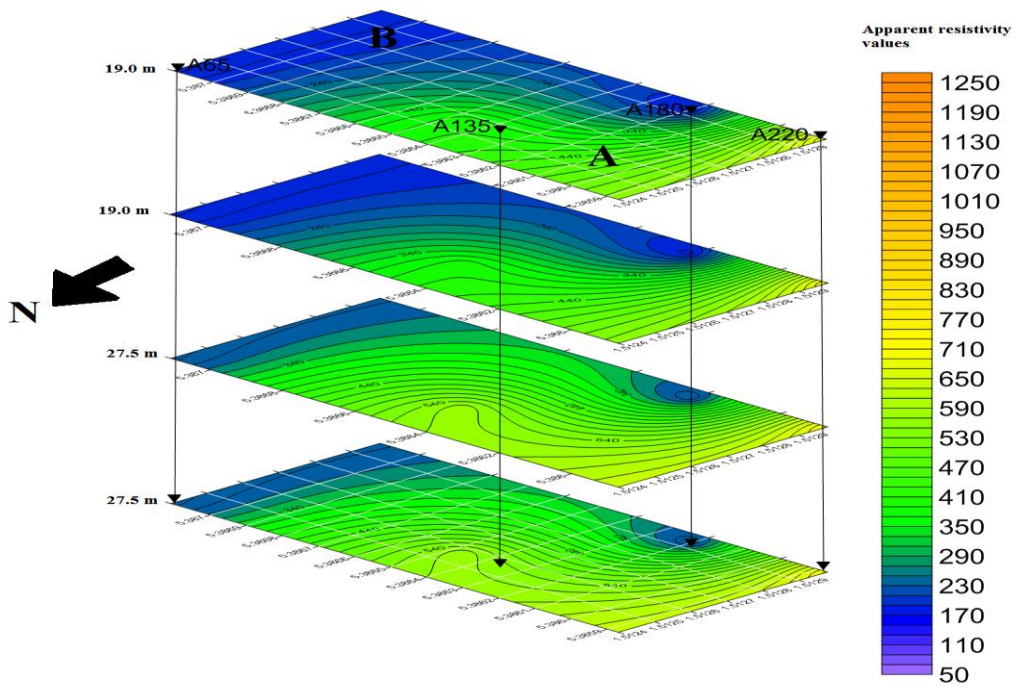


Figure 5.35c. Contour maps showing the apparent resistivity values from depth 19.0 – 27.5 m beneath the Esukese Ekyir Community
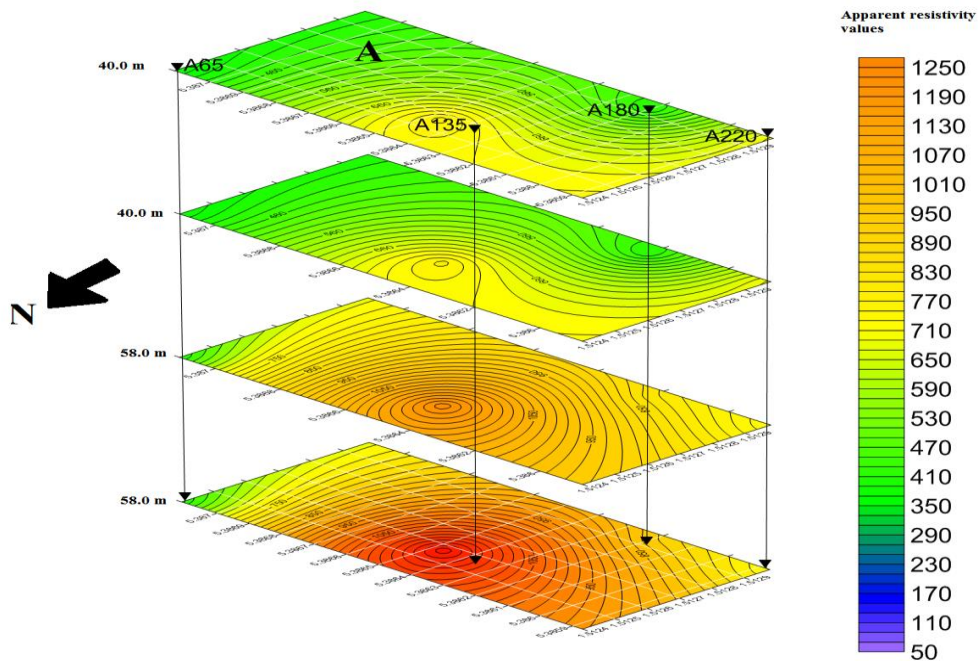
Figure 5.35d. Contour maps showing the apparent resistivity values from depth 40.0 – 58.0 m beneath the Esukese Ekyir Community

Quantity showed up from depth 1.5 m to about depth 27.5 m below the earth surface. It is inferred that, the groundwater might be even before the 1.5 m mark and may go far below the 27.5 m but not up to the 40.0 m mark. Two VES points (A65 and A180) were ranked first, followed by A135 and the lastly A220. Table 5.7 below provide a summary of the VES results including a rank-list of the selected points for drilling or hand dug.

Table 5.7. Ranked VES points hand-dug well development at Esukese Ekyir Community

| VES Point | Layer | ρ (Ω−μ) | Depth (m) | Thickness (m) | Rank | Location (GPS) | Remarks |
|---|---|---|---|---|---|---|---|
| | 1 | 79.4 | 2.16 | 2.16 | | 5.38711N | |
| | 2 | 201.01 | 7.96 | 5.8 | | 1.51240W | |
| | 3 | 82.44 | 12.4 | 4.44 | | | |
| A65 | 4 | 15384.97 | - | - | 1st | | |
| | 1 | 89 | 4.56 | 4.56 | | 5.38620N | |
| | 2 | 248 | 15.36 | 10.81 | | 1.51293W | |
| A180 | 3 | 14827 | - | - | 1st | | |
| | 1 | 208 | 0.81 | 0.81 | | 5.38647N | |
| | 2 | 58.15 | 3.04 | 2.24 | | 1.51257W | |
| A135 | 3 | 4584.48 | - | - | 3rd | | |
| | 1 | 58.63 | 1.33 | 1.33 | | 5.38587N | |
| | 2 | 113.43 | 8.09 | 6.76 | | 1.51298W | |
| A220 | 3 | 9374 | - | - | 4th | | |

The groundwater seems to be in high quantity towards the North Eastern more than the South Western part of the community. This may be due to the flow of the Esukese stream (from which the community had it name) from south to north in the eastern part of the community. The stream may be the main source of recharge for groundwater within this community. If additional boreholes are needed, they could be dug in the north eastern part of the community. Boreholes or wells within this community may yield high amount of water and they may not be likely to dry up during the dry seasons.

### 5.4.6. Kwanyarko Community

### 5.4.6.1. Introduction

In Kwanyarko Community four traverses were created and a total of six stations were survey using the resistivity method of vertical electrical sounding. The results of 5 sounding curves displayed H – type curve and 1 VES result displayed KH – types curve. Figure 5.36 shows the schematic layout of the community. Three EM profiles

were carried out on all the four traverses using 20 m coil separations and the EM readings were taken at 10 m intervals.

Table 5.8. Existing Boreholes within 5 Km radius around Kwanyarko Community ((Mainoo et al. 2007c)

| Community | BH No. | Depth (m) | Yield (m³/h) | SWL (m) | Water Quality | Lithology | Calibration |
|---|---|---|---|---|---|---|---|
| Brofoyeduru | 085/G/77-1 | 23 | 0.42 | 5.67 | N/A | Phyllite / Mica schist | |
| Brofoyeduru | 085/G/77-2 | 47 | 2.4 | 4.31 | N/A | Phyllite / Mica schist | |
| Kyekyewere | 050/D/09-2 | 42 | 0.72 | 8.77 | N/A | Granite / Gneiss | |
| Kyekyewere | 050/D/09-3 | 29 | 5.1 | 10.43 | N/A | Granite / Gneiss | |
| Kyekyewere | 050/D/09-4 | 35 | 1.02 | 8.15 | N/A | Granite / Gneiss | |
| Kyekyewere | 050/D/09-5 | 32 | 3 | 10.17 | N/A | Granite / Gneiss | |
| Kyekyewere | 050/D/09-6 | 39 | 3 | 16.71 | N/A | Schist | |
| Twifo Mampong | 48/I/74-1 | 24 | | 1.34 | N/A | | |
| Twifo Mampong | 48/I/74-2 | 31 | | 2.98 | N/A | | |
| Twifo Mampong | 48/I/74-3 | 37 | | | N/A | | |
| Ntafrewaso | 48/I/35-1 | 37 | | 1.91 | N/A | | |
| Ntafrewaso | 48/I/35-2 | 34 | | 3.04 | N/A | | |
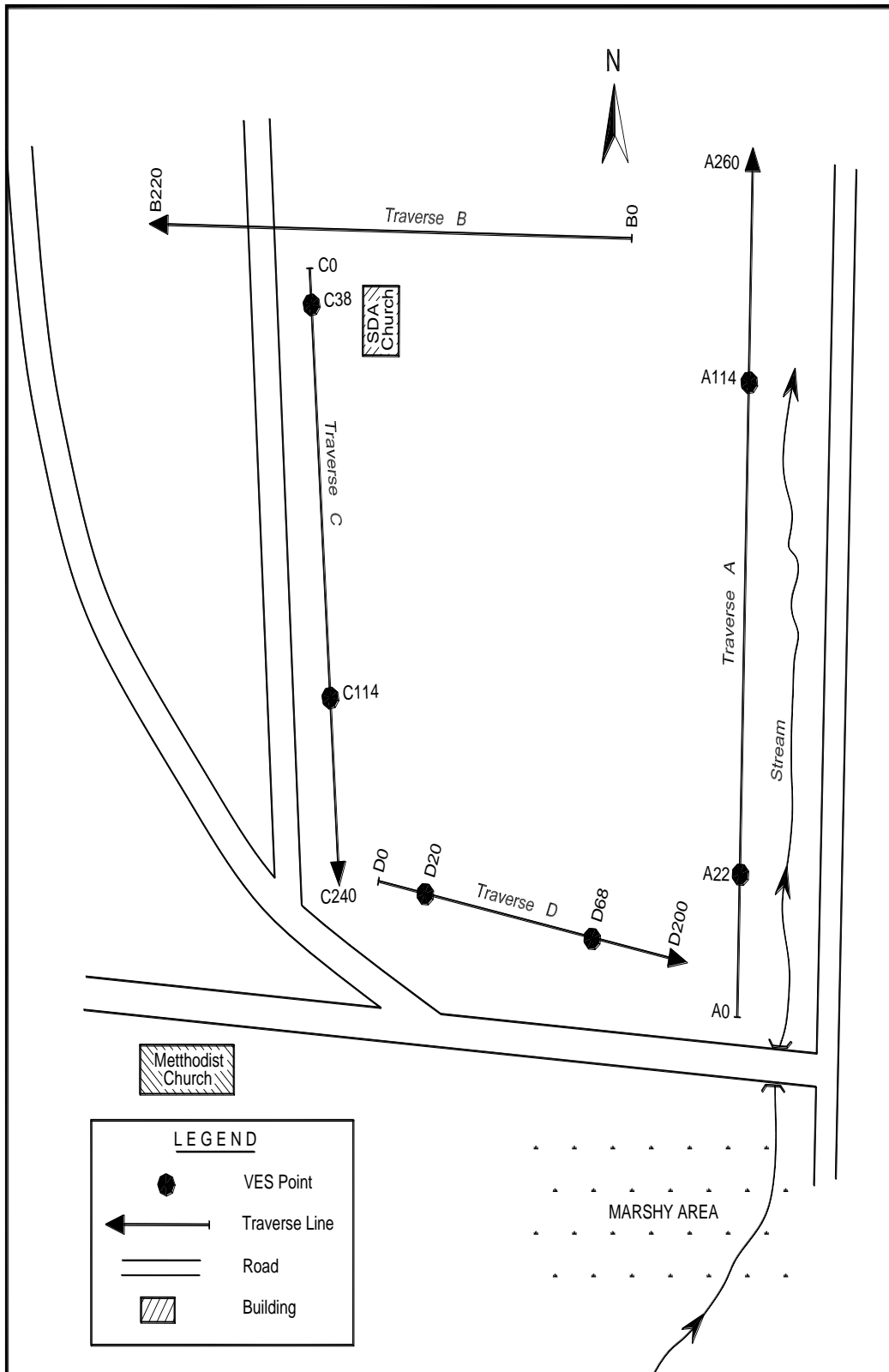
Figure 5.36. Schematic Layout of Kwanyarko Community (not to scale)

Table 5.8 above shows the existing boreholes within the 5 Km radius around Kwanyarko Community. This data was used as guide during the survey and the interpretation of the geophysical results.

### 5.4.6.2.  EM traverses

Traverse A was carried out on a profile length of 260 m on a bearing of 032° from the True North. Figure 5.37 shows the graph of the terrain conductivity curves for HD mode and VD mode. The maximum, minimum and average terrain conductivity values are 20.0, 6.0 and 8.52 m mhos/m, respectively.
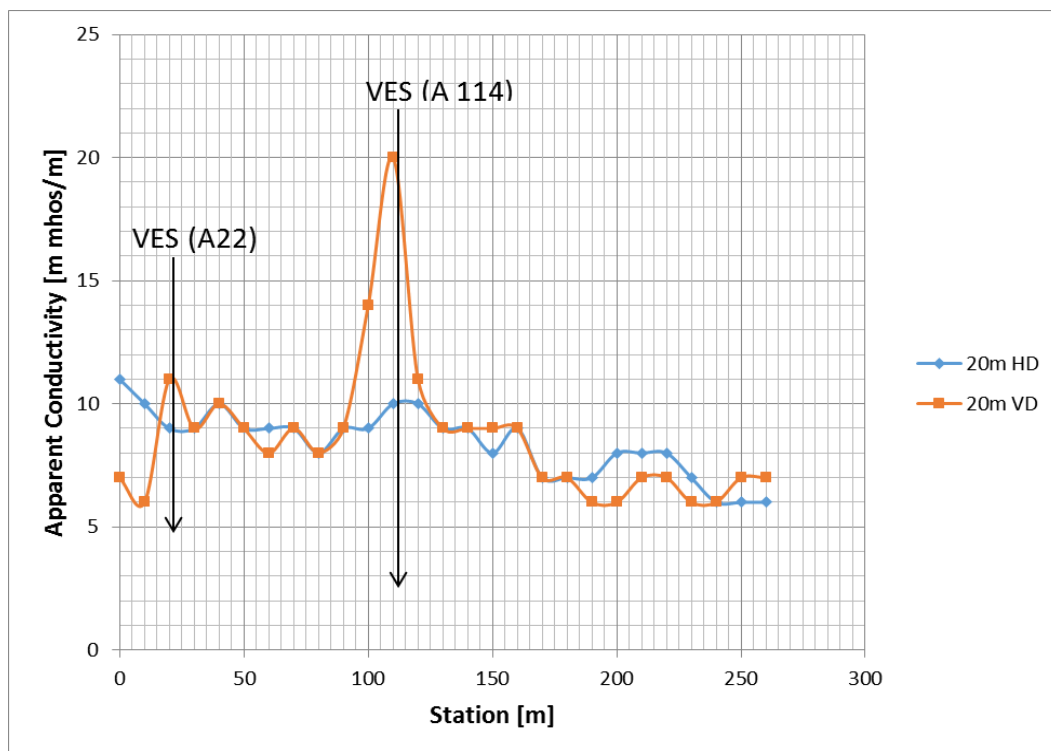


Figure 5.37. EM terrain conductivity measurements along a profile A at Kwanyarko Community

The results for HD mode indicate a decrease in terrain conductivity values from the beginning of the profile at 0 m to 80 m point; from which it increases to its maximum value at point 115 m and then gradually decrease up to the end of the profile. The behaviour of the curves from point 180 m to 240 m suggests a lower terrain conductivity with depth between those two points. There are two peaks for the VD mode curve one at station 20 m and another at 110 m. The positive anomalous behaviour of VD mode curve between points 90 m and 130 m suggest a fracture at

subsurface, which is capable of containing groundwater. Stations 22 and 114 were chosen for further investigation using the resistivity method. There are hopes that these points may contain groundwater.
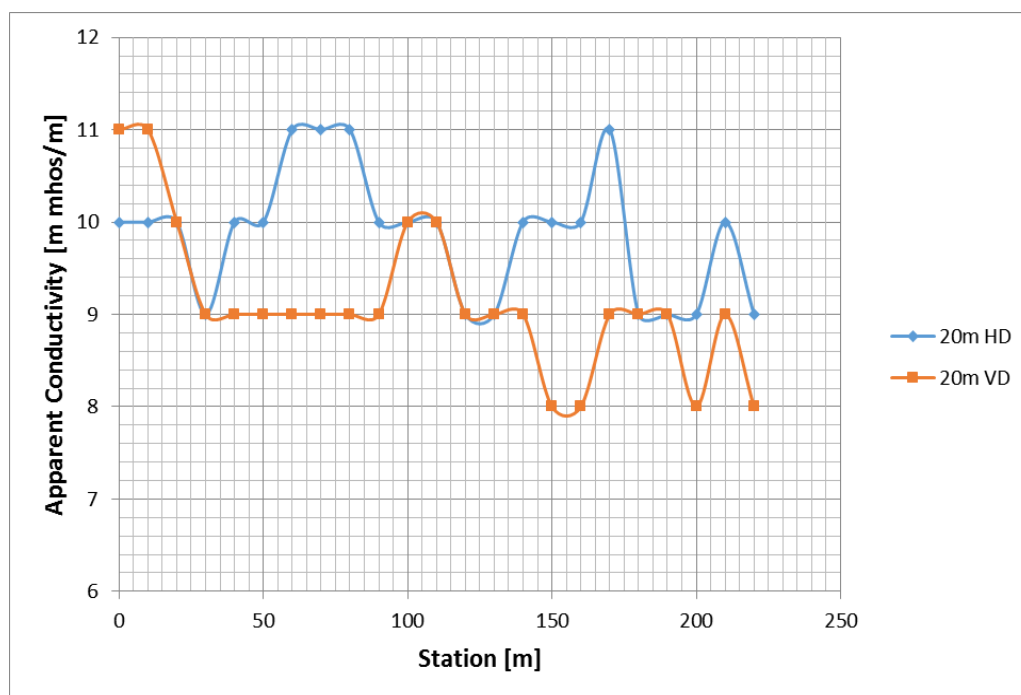


Figure 5.38. EM terrain conductivity measurements along a profile B at Kwanyarko Community

Figure 5.38 above shows the results of terrain conductivity measurements along traverse B which were carried out on profile length of 220 m and on a bearing 034° from the True North.

The behaviour of both HD mode and the VD mode curves are erratically in nature from the beginning to the end of the profile. Generally, throughout the profile the HD mode curve shows higher terrain conductivity values than the VD mode curves. This suggests a decrease in terrain conductivity with depth, meaning geological structure at deeper subsurface have very low conductivity values and hence not capable of containing groundwater.

On the above graph, the only part that the VD mode curves lead the HD mode curves in terms of high conductivity values are between 0 m and 10 m. It could be inferred from the results of this EM traverse that, it would not yield sufficient groundwater for public water supply and hence no VES was conducted on it.

The EM readings on traverse C as in figure 5.39 were taken at 10 m intervals and using 20 m coil spacing on a profile length of 240 m long. The profile was carried out on a bearing of 187° from the True North.

Generally, the both HD and VD modes curves move erratically throughout the profile. It would be observed that the HD mode curves made a sharp increment in terrain conductivity from station 30 m to 80 m. The only place the HD leads the VD in terrain conductivity values are between stations 70 m to 100 m. The maximum value of terrain conductivity (17 m mhos/m) on the graph in the above Figure 5.51 belongs to the VD mode. The behaviour of the VD mode shows a high possibility of fractured zone beneath this profile line and that may contain a sufficient groundwater. Two points C38 and C114 were selected for VES investigation to confirm the presence of groundwater beneath this profile line.
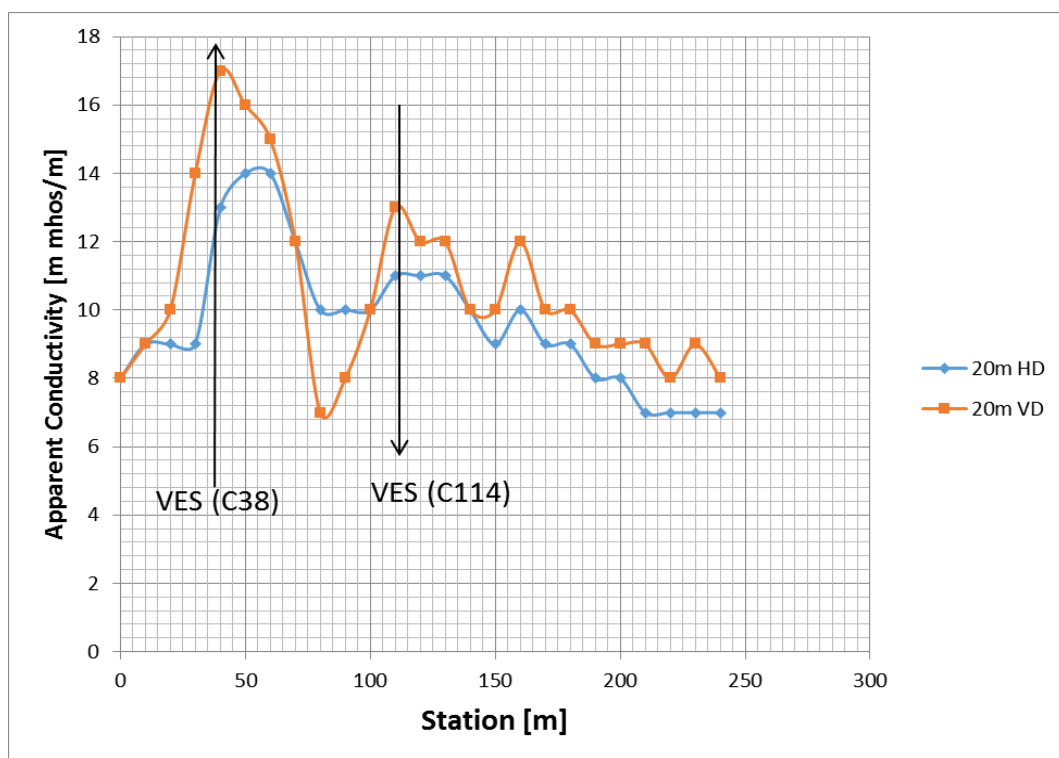
Figure 5.39. EM terrain conductivity measurements along a profile C at Kwanyarko Community

The traverse D is last traverse to be carried out in Kwanyarko Community. It was carried out on a bearing of 148° from the True North and on a profile length of 200 m. The EM readings were taken at 10 m intervals and using a coil spacing 20 m. The average terrain conductivity on graph in Figure 5.40 is 13.26 m mhos/m with the

maximum terrain conductivity of 23 m mhos/m and the minimum of 9 m mhos/m. The VD mode curve has high terrain conductivity values than HD mode; meaning the terrain conductivity at deeper subsurface are conductive and may be as reason of being fractured or weathered.
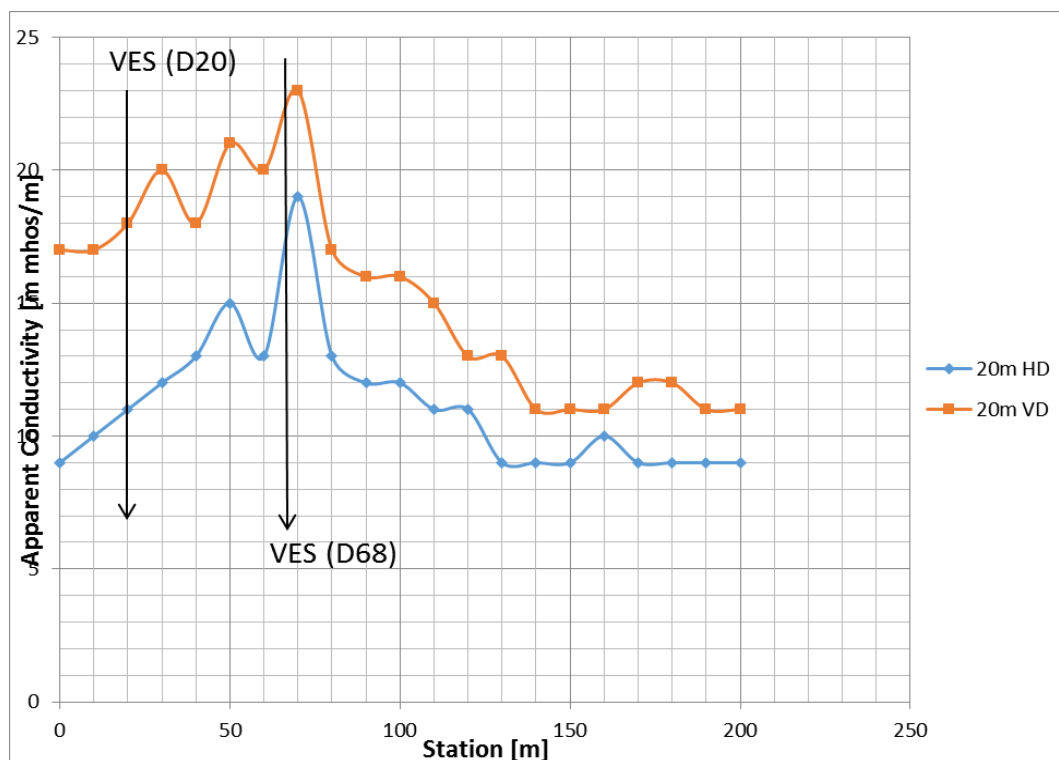


Figure 5.40. EM terrain conductivity measurements along a profile D at Kwanyarko Community

Both curves gradually increase from station 0 m to 70 m and then decrease again gradually to the end of the profile. Both curves have their highest conductivity value at station 70 m. It is deducted from these results that, the subsurface is highly fractured or weathered and the subsurface contain groundwater which would be in high quantities. Points 20 m and 68 m were selected for further investigations using resistivity method.

### 5.4.6.3. Sounding curves

VES C38

A four − layer subsurface structure was revealed at this VES station as shown in Figure 5.41. The curve type is KH − type which indicates a high fractured or wearthered zone in later 3. The modelled curves shows a slight increase in apparent

resistivity of about 512 Ωm in first layer to about 756 Ωm in the second layer. There is a relative increase from the apparent resistivity value of the second layer to about 222 Ωm in the third layer and lastly a drastic rise to about 9644 Ωm in the fourth layer. The thicknesses of the first, second and third layer are 0.90 m 6.90 m and 10.40 m respectively. This has a high probability of containing groundwater but the yield would not be much compare to the VES point on traverse A. It is recommended for drilling or hand dug a borehole.



| N | ρ | h | z |
|---|---|---|---|
| 1 | 512.55 | 0.90 | 0/0 |
| 2 | 756.31 | 6.90 | 0.90 |
| 3 | 222.92 | 10.40 | 7.80 |
| 4 | 9644.30 | | 18.20 |
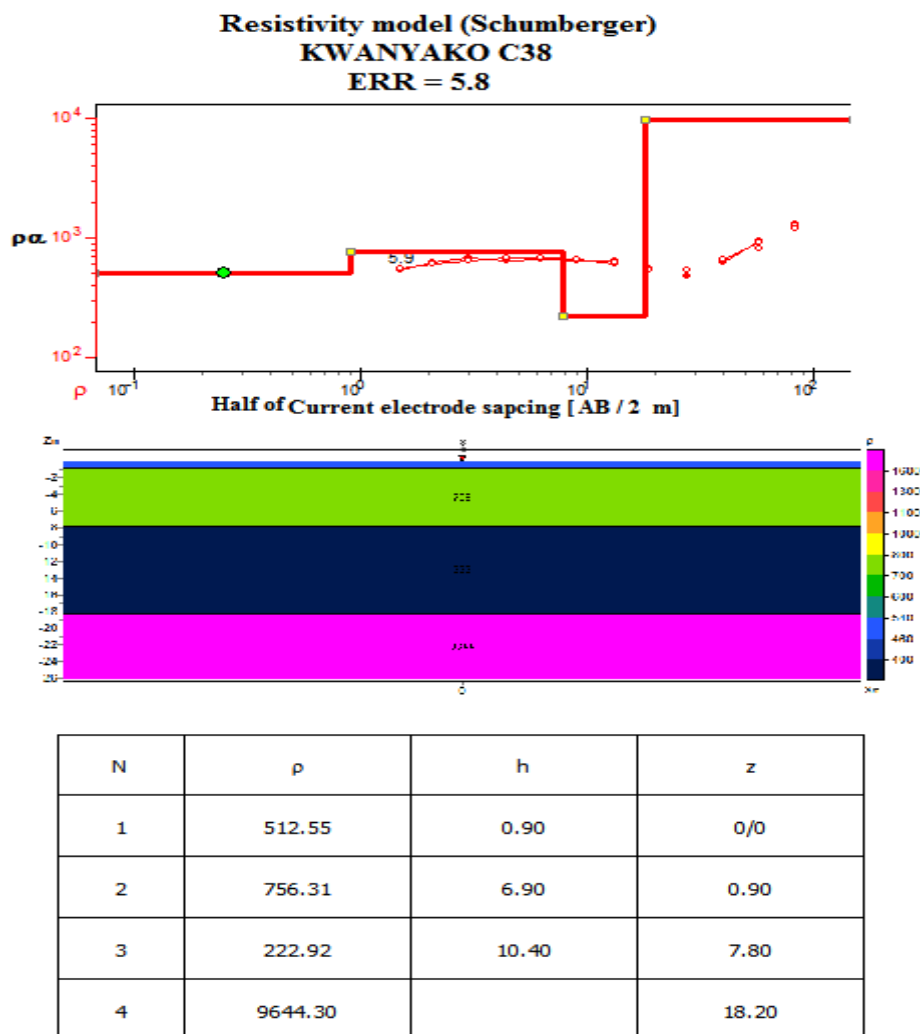
Figure 5.41. VES model curve at station C38 m, Kwanyarko Community

VES D68

VES D68 revealed a three layered subsurface structure (Figure 5.42). The H- type curve is displayed by the sounding curve of the VES D68. It indicates a wearthered or fracture zone in layer 2. The apparent resistivity values range between 167.65 Ωm and 2652.30 Ωm. First and second layers have thicknesses of 1.29 m and 9.71 m

respectively. The apparent resistivity value of the first layer is 715.74 Ωm, this value sharply drop to 167.65 Ωm in the second layer and finally rise drastically to 2652.30 Ωm in third layer. The apparent resistivity values, depths and thicknesses of the layers suggest a fracture or weathering in the second layer and a possibility of obtaining a groundwater at this station. Hence this station was recommended for drilling of borehole.
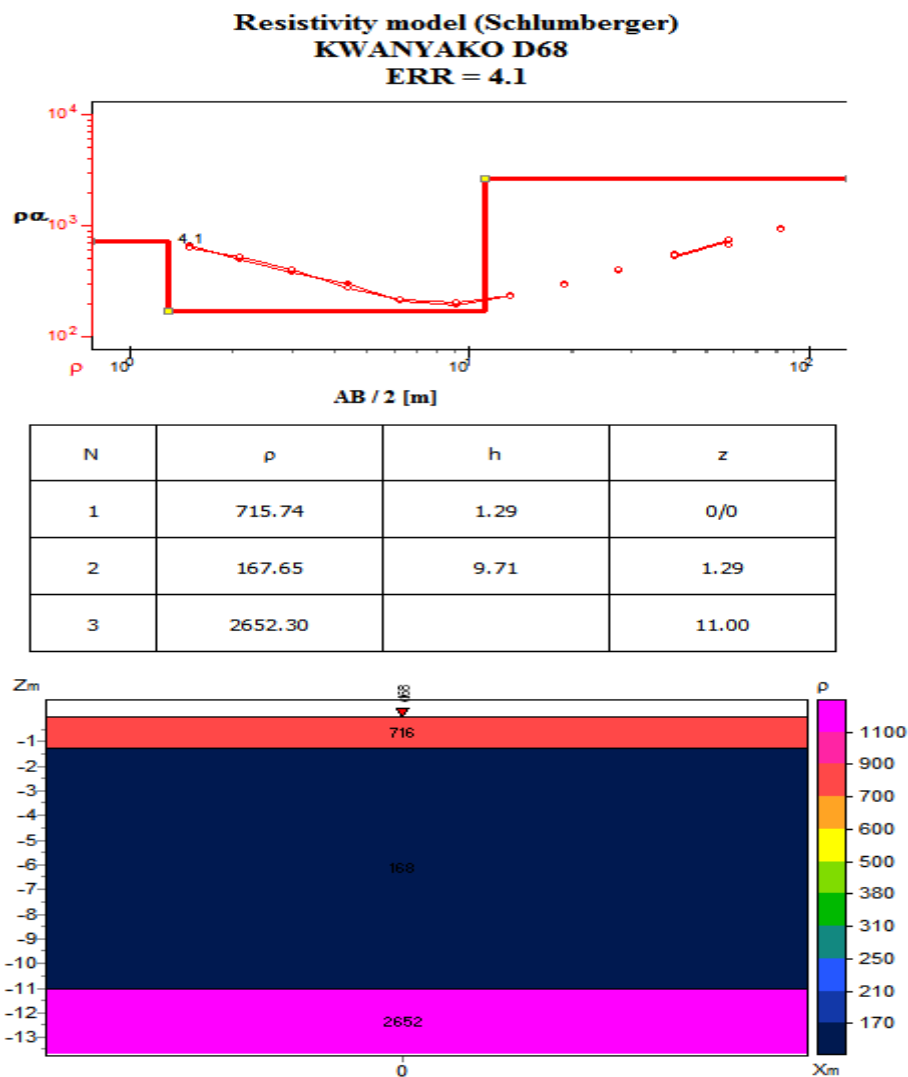


Figure 5.42. VES model curve at station D68 m, Kwanyarko Community

### 5.4.6.4. Discussions of results from the Kwanyako Community

Analyses of the VES curves suggested that the Kwanyako is underlain by three geological substrata. Generally first and third layer have higher resistivity values than second layer. First layer has resistivity value ranging from 363.97 – 1306.28

Ωm, and can be intercepted at a mean depth of 1.91 m. The second layer which is expected to be the water – bearing has a thickness range of 3.50 – 9.74 m and a mean apparent resistivity value of 197.33 Ωm. The third layer has apparent resistivity value ranging from 1434.39 -2715.98 Ωm.

The contour maps displays the resistivity values in slices according to the depth from the earth surface. Areas on the maps in Figures 5.43a – 5.43c where is labelled A means the zone contain very little or no groundwater and the one labelled B indicates areas with a lot of groundwater. Drilling from areas A is risky and that unless in a community like Kwanyako with generally low level of groundwater, it is not recommended for drilling.

Stations were ranked according to the depth beneath it that contain high quantity of water, that is to say, the fraction of a VES station's depths in the B zone. VES point D65 is ranked first, follow by D20, A22 and A114. Point C38 and C114 are ranked fifth. Table 5.9 shows ranked VES points for borehole drilling at Kwanyako Community.

It is noticed that; the groundwater within the subsurface of this community are located in the South Eastern part of the community where the stream flows and near marshy area. Additional boreholes may be drilled around this area.
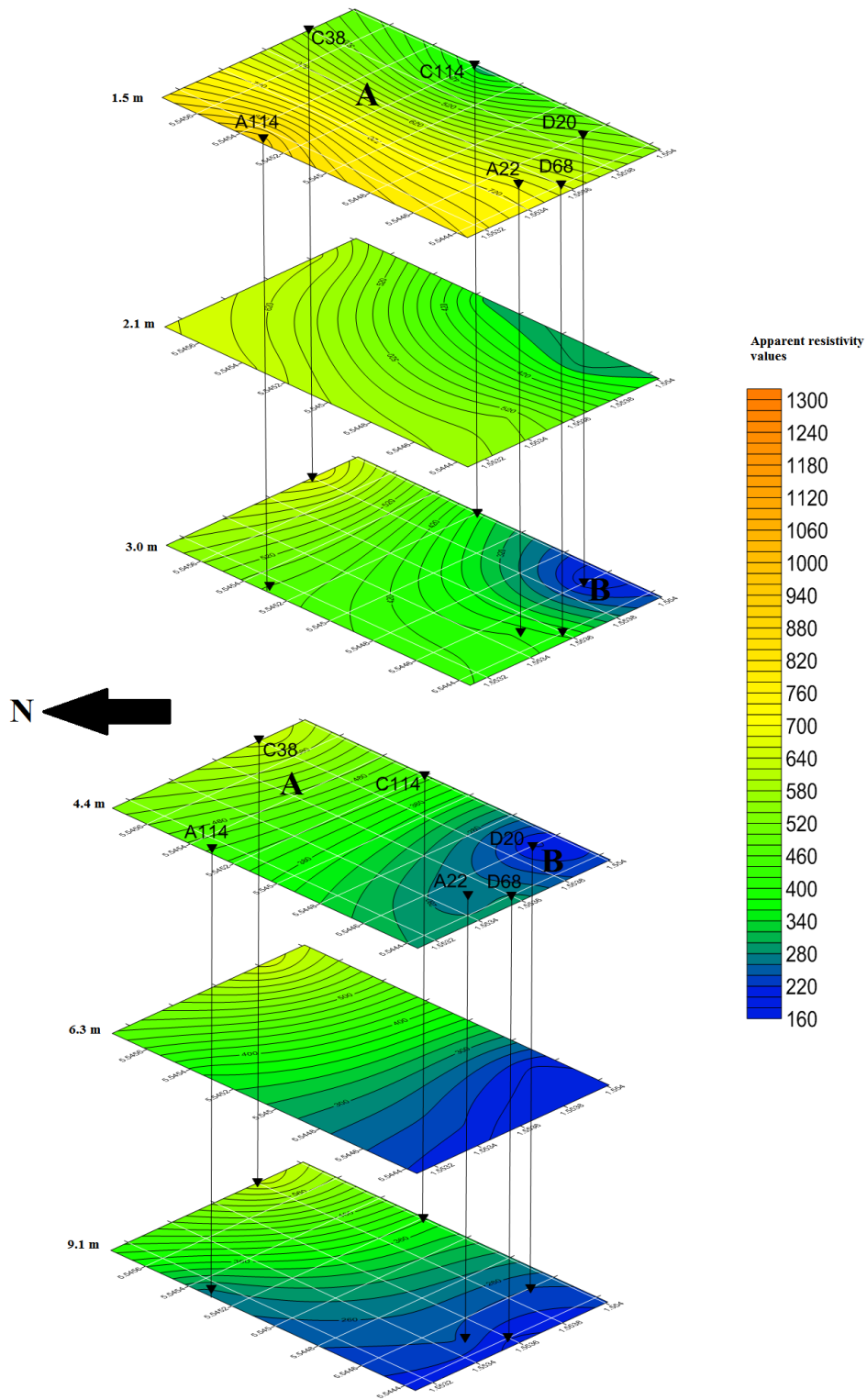
Figure 5.43a. Contour maps showing the apparent resistivity values from depth 1.5 – 9.1 m beneath the Kwanyako Community
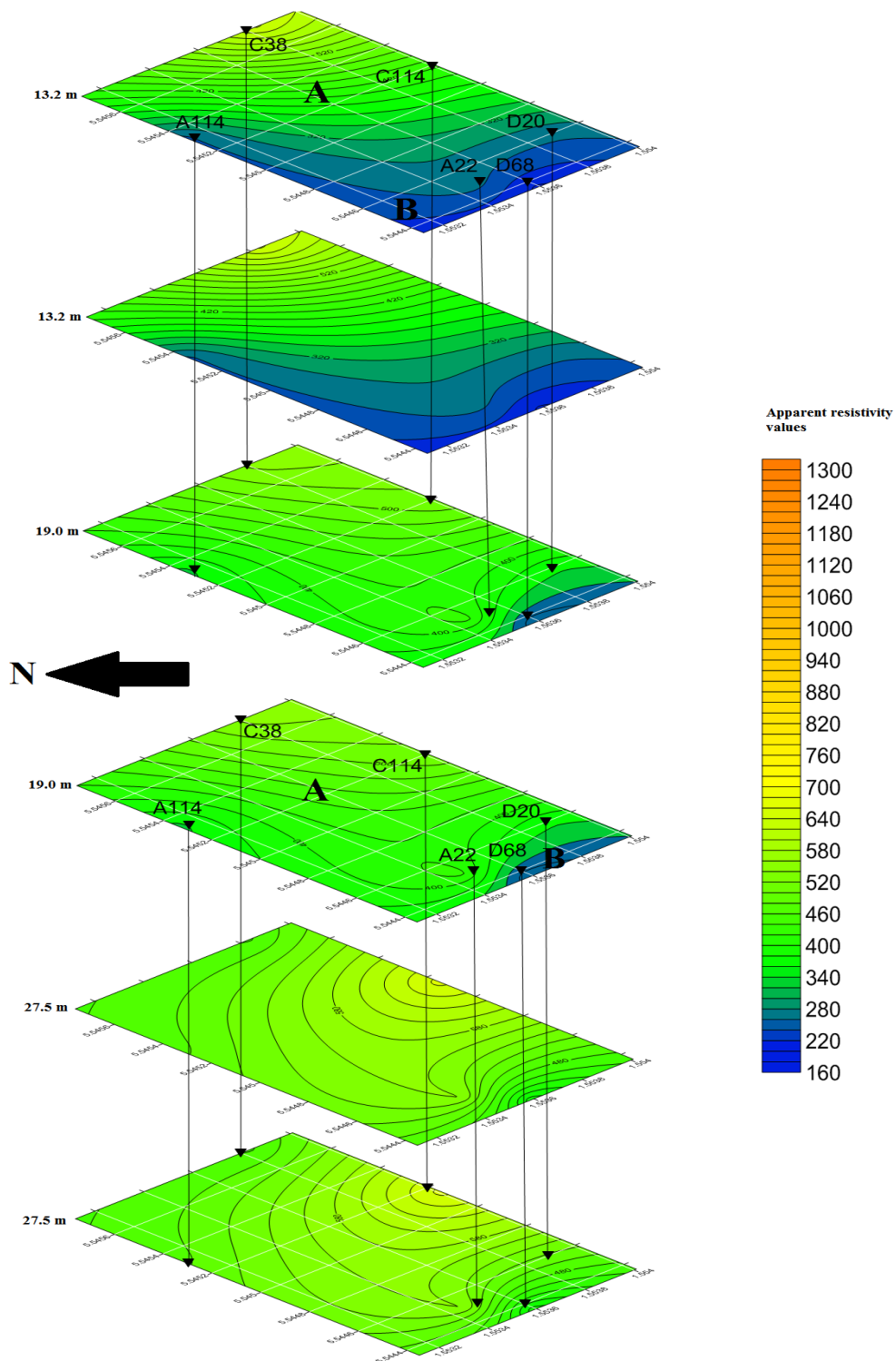
Figure 5.43b. Contour maps showing the apparent resistivity values from depth 13.2 – 27.5 m beneath the Kwanyako Community
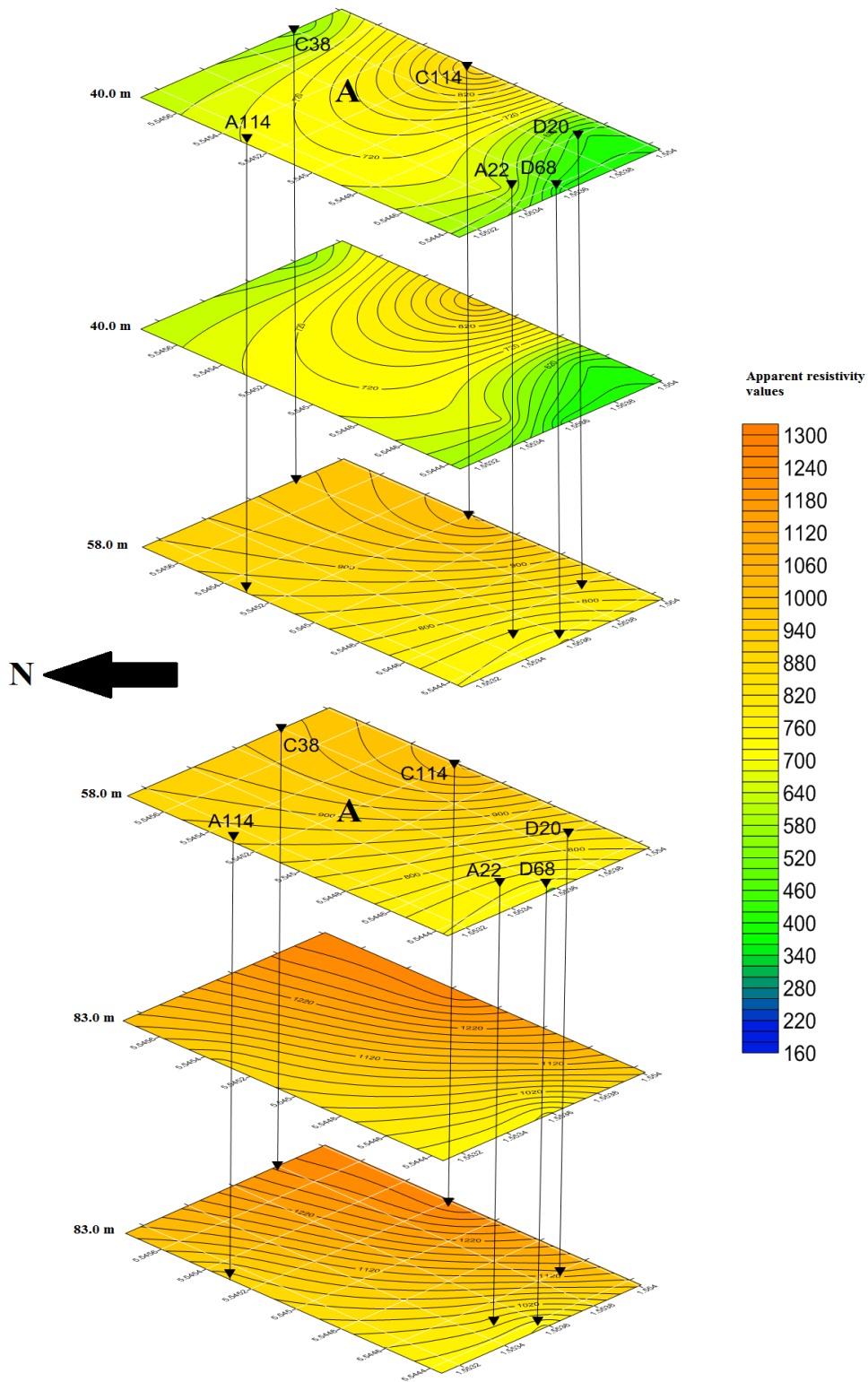
Figure 5.43c. Contour maps showing the apparent resistivity values from depth 40.0 – 83.0 m beneath the Kwanyako Community.

Table 5.9. Ranked VES points for borehole drilling at Kwanyako Community

| VES Point | Layer | ρ (Ω−μ) | Depth (m) | Thickness (m) | Rank | Location (GPS) | Remarks |
|---|---|---|---|---|---|---|---|
| D68 | 1 | 715.74 | 1.29 | 1.29 | | 5.54435N | |
| | 2 | 167.65 | 11.00 | 9.71 | | 1.55359W | |
| | 3 | 2652.30 | - | - | 1st | | |
| D20 | 1 | 1306.28 | 0.52 | 0.56 | | 5.54460N | |
| | 2 | 192.56 | 9.24 | 8.72 | | 1.55392W | |
| | 3 | 2413.44 | - | - | 2nd | | |
| A22 | 1 | 831.41 | 1.15 | 1.15 | | 5.54451N | |
| | 2 | 174.22 | 6.99 | 5.84 | | 1.55346W | |
| | 3 | 1434.39 | - | - | 3rd | | |
| A114 | 1 | 816.84 | 1.68 | 1.68 | | 5.54534N | |
| | 2 | 214.68 | 11.42 | 9.74 | | 1.55312W | |
| | 3 | 2715.98 | - | - | 4th | | |
| C38 | 1 | 512.55 | 0.90 | 0.90 | | 5.54576N | |
| | 2 | 756.31 | 7.80 | 6.90 | | 1.55384W | |
| | 3 | 222.92 | 18.20 | 10.40 | | | |
| | 4 | 9644.30 | - | - | 5th | | |
| C114 | 1 | 363.97 | 5.97 | 5.97 | | 5.54515N | |
| | 2 | 237.55 | 9.47 | 3.5 | | 1.55401W | |
| | 3 | 2300.00 | - | - | 5th | | |

### 5.4.7. Mbaa Mpe Hia No. 2

### 5.4.7.1. Introduction

Electromagnetic profiling was conducted along four profiles across Mbaa Mpe Hia No. 2 Community. Five vertical electrical sounding were carried out on three of the traverse. The VES stations' results revealed 3 – layered and 4 – layered earth model respectively. The traverses and the VES point are shown on schematic layout of the community in Figure 5.44 below. Data on existing boreholes in around 5 Km radius of the Mbaa Mpe Hia No. 2 Community is available during the geophysical survey. The depths of the existing boreholes on the table 5.10 below are within the ranges of 25.0 – 73.0 m. from this information; aquifer is expected within this depth ranges or depth less than the stated above. The data serves as a guide to interpretation of geophysical data.
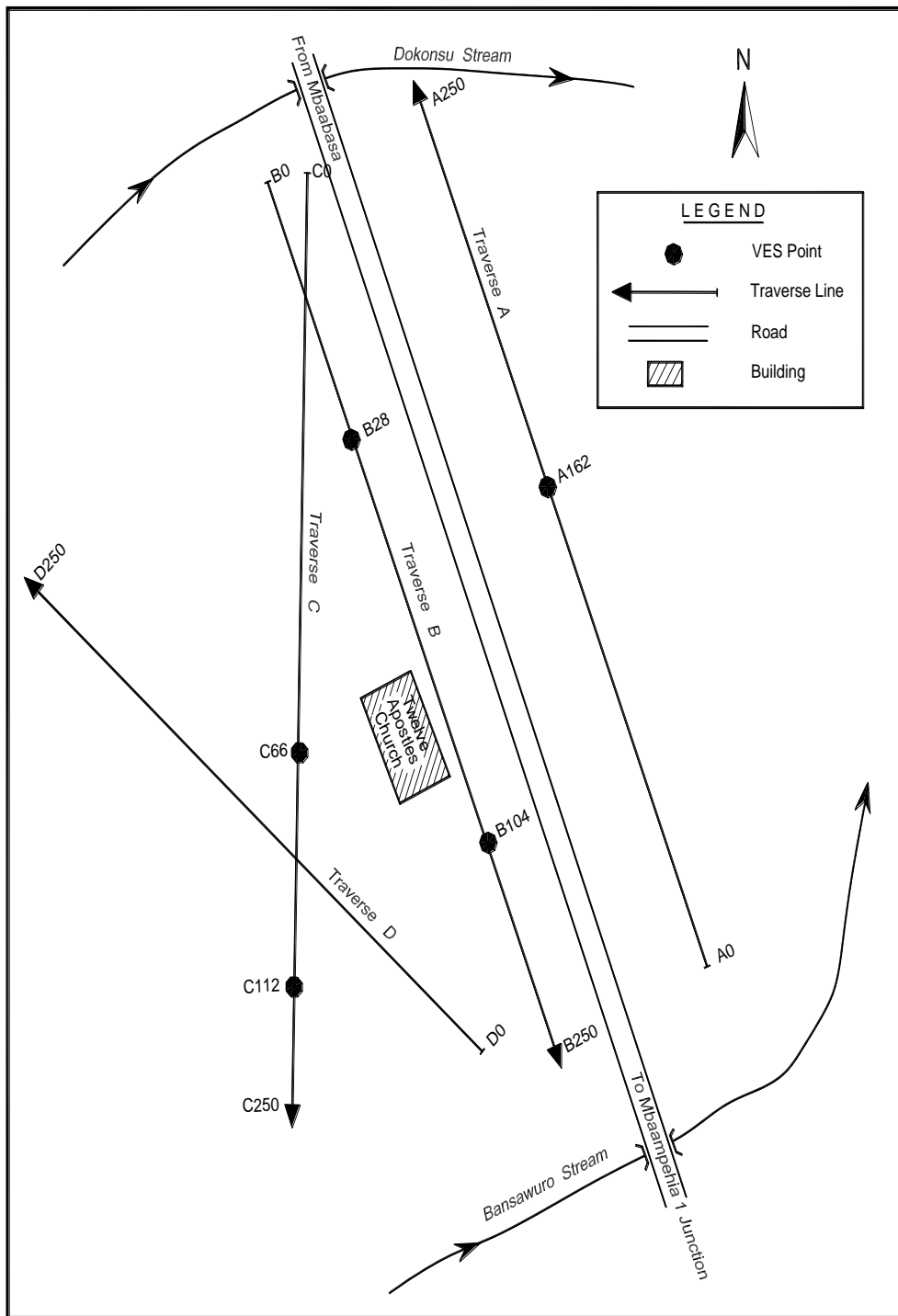
Figure 5.44. Schematic Layout of Mbaa Mpe Hia No.2 Community (not to scale)

Table 5.10. Existing Boreholes within 5Km radius around Study Area (Mainoo et al. 2007d)

| Community | BH No. | Depth (m) | Yield (m³/h) | SWL (m) | Water Quality | Lithology | Calibration |
|---|---|---|---|---|---|---|---|
| NYENASI | 48/E/79-2 | 73 | | | N/A | | |
| TWIFO PRASO | 48/F/74-1 | 27 | | 4.76 | N/A | Schist | |
| TWIFO PRASO | 48/F/74-2 | 28 | | 1.29 | N/A | Schist | |
| TWIFO PRASO | 48/F/74-3 | 31 | | | N/A | Schist | |
| TWIFO PRASO | 48/F/74-4 | 28 | | 7.3 | N/A | Schist | |
| TWIFO PRASO | 48/F/74-5 | 37 | | | N/A | Schist | |
| TWIFO PRASO | 48/F/74-6 | 28 | | 6.84 | N/A | Schist | |
| TWIFO PRASO | 48/F/74-7 | 25 | | 0.95 | N/A | Schist | |

### 5.4.7.2. EM traverses

EM traverse on profile A of length 250 m was run on bearing of 335° from the True North. The EM readings were taken using 20 m coils spacing and at 10 m intervals.

The terrain conductivity values for HD mode curve range between 13 m mhos/m and 9 m mhos/m and those of VD mode range between 13 m mhos/m and 7 m mhos/m. The maximum and minimum terrain conductivity values on the profile are 13 m mhos/m and 7 m mhos/m respectively. The average conductivity value is 10.67 m mhos/m. It is observed from the graph in Figure 5.45 that, HD mode curve started

increasing in apparent conductivity values from 10 m mhos/m at point 0 m to 13 m mhos/m at point 80 m, it maintain this maximum value for about 30 m gap (80 – 110 m). It then falls in an erratical manner. The movements of the VD mode curve are also generally erratic in nature. The VD mode curve increases from an initial value of 8 m mhos/m to 12 m mhos/m, then decreases to 10 m mhos/m and then shoot up to 13 m mhos/m. Between stations 100 m to 140 m the terrain conductivity for the VD mode could be seen to be constant. There was crossover of the two curves at point 162 m. Generally the apparent conductivity values of the VD curves are low compare to HD mode curves, this suggested a general decrease in terrain conductivity values with depth which mean, at deeper subsurface there are less fractures compare to the surface. The erratic nature of both curves also indicates a complex geological subsurface.
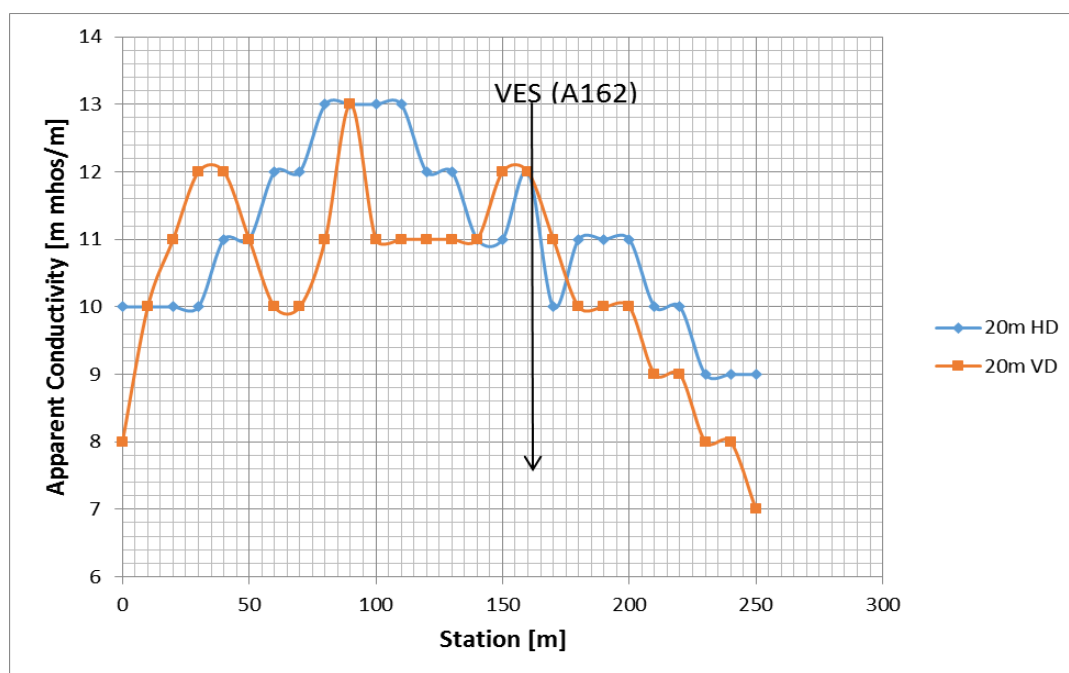


Figure 5.45. EM terrain conductivity measurements along a profile A at Mbaa Mpe Hia No.2 Community

The station 90 m which recorded the highest value of terrain conductivity for VD mode curve should have been considered for VES investigation but it was not considered because of down – stream toilet located beneath it. It is possible that the down – stream toilet is responsible for that high terrain conductivity. For obvious reason, borehole or well could not be constructed there. Only station 162 m was selected for further VES survey with hope of containing groundwater resource.

EM profiling on traverse B readings were taken using 20 m coil separation at 10 intervals. The length of the profile was 250 m and the profile was run on the bearing 165° from the True North.
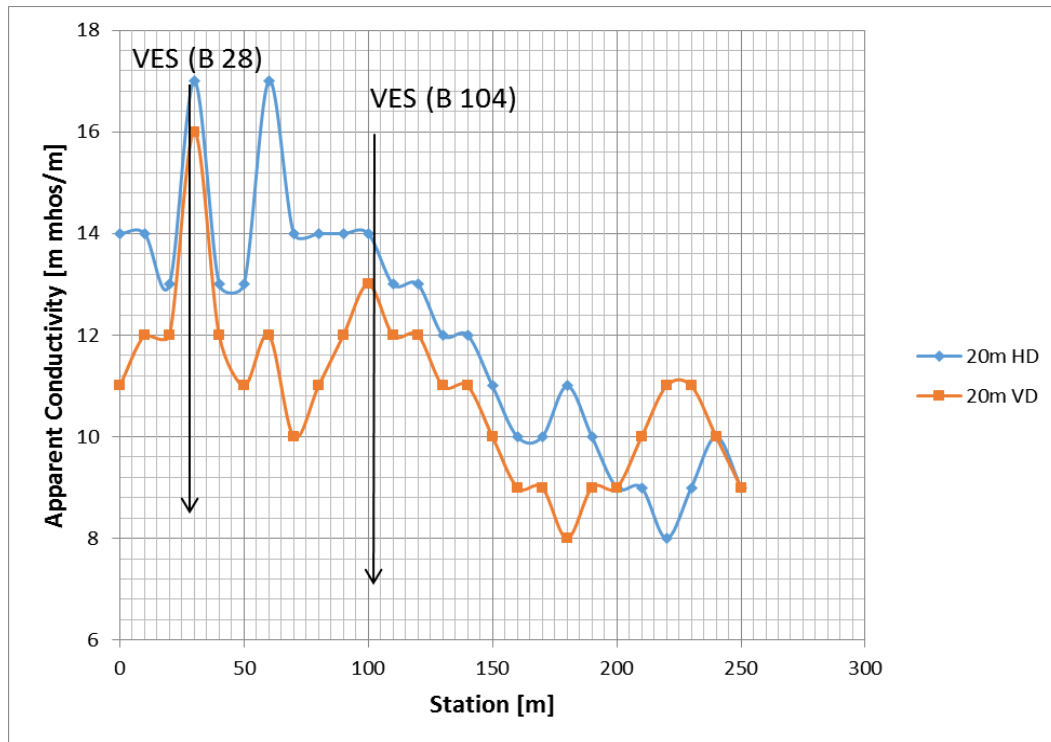


Figure 5.46. EM terrain conductivity measurements along a profile B at Mbaa Mpe Hia No.2 Community

The maximum and minimum apparent conductivity values are 17 m mhos/m and 8 m mhos /m respectively. The average apparent conductivity value is 11.46 m mhos/m. VD mode curve and HD mode curves are both erratic in nature and that suggests a complex subsurface geology. Two points as could be seen in Figure 5.46 were selected for VES investigations. Station 28 m recorded the maximum apparent conductivity value for VD mode and also one of the two highest apparent conductivity values for HD mode. Observing these points surrounding station 28 m, it inferred that, the high positive anomaly at that point is related to deep fractures beyond 30 m depth. Both selected are expected to contain a lot of groundwater.

Traverse C has a profile length of 250 m and was carried out on a bearing of 195° from the True North. Like other traverse carried out in this community, the EM readings were taken using 20 m coil spacing at 10 m intervals.

The apparent conductivity values measured along the profile ranges between 9 – 18 m mhos/m with an average value of 12.73 m mhos/m. From the graph in the Figure 5.47, it is observed that; the curves for both HD mode and VD mode behave erratically. VD mode terrain conductivity values were higher than that of HD mode along most parts of the profile except between stations 0 m and 30 m.

Two VES stations were selected along the profile line. Stations C66 and C112 have high probability of containing groundwater. The characteristics of the two points selected for VES investigation suggest a fracture beneath the subsurface. Generally the behaviour of curves shows that, the subsurface has a complex geological formation.
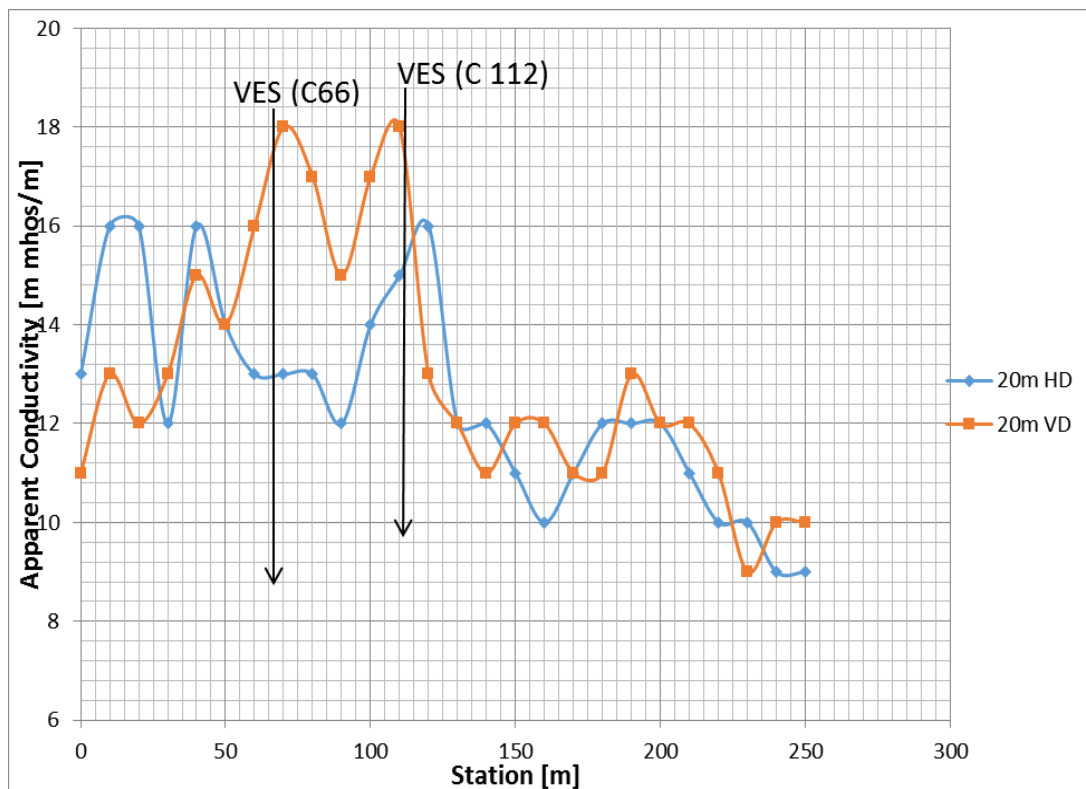


Figure 5.47. EM terrain conductivity measurements along a profile C at Mbaa Mpe Hia No.2 Community

Traverse D is the fourth and the last traverse to be run in Mbaa Mpe Hia No.2 Community for the purpose of this research work. The traverse was run on profile length of 250 m using 20 m coil spacing and at 10 m intervals. The bearing of the profile line is 294° from the True North.
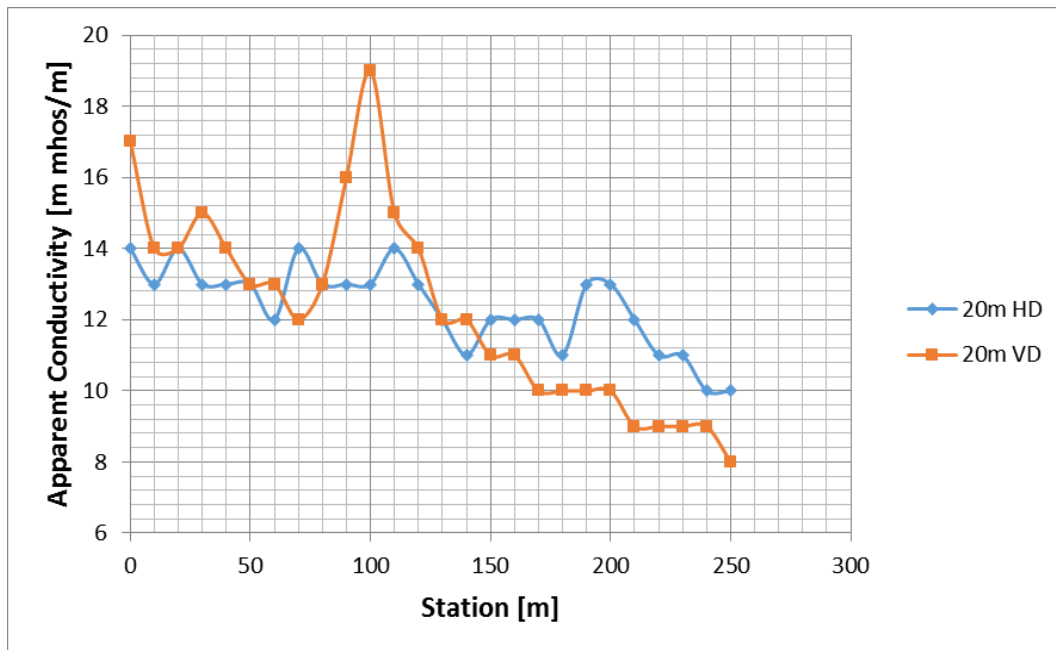
Figure 5.48. EM terrain conductivity measurements along a profile D at Mbaa Mpe Hia No.2 Community

The maximum and the minimum apparent conductivity values are 19 m mhos/m and 8 m mhos/m respectively. The average apparent conductivity value is 12.33 m mhos/m. The higher conductivity values between station 90 m and 110 m are due to roof. The measurement run through roofing of a building and this interfered with the electromagnetic waves produced during measurement. Generally HD mode curves has higher terrain conductivity values than VD mode curve meaning there is very less probability of locating fractures at deeper strata and hence could not contain much water even if there is any. No points on this traverse were recommended for further VES investigations (Figure 5.48).

### 5.4.7.3. Sounding curves

VES B104

This VES B104 was conducted on EM traverse B. It revealed a three – layered subsurface structure, with apparent resistivity range 121.85 – 9347.90 Ωm. Apparent resistivity values of first, second and third layer are 192.54 Ωm, 121.85 Ωm and 9347.90 Ωm respectively. The thicknesses of first and second layer are 1.60 m and 6.77 m respectively (see Figure 5.49). The first layer and the third layer have higher resistivity values and they sandwich the second layer which has a low resistivity value. The characteristics of the curves and the apparent resistivity values suggest

weathering of the first layer and fracture in the second layer. The station is recommended for drilling or hand dug of well for public water supply.



| N | ρ | h | z |
|---|---|---|---|
| 1 | 192.54 | 1.60 | 0/0 |
| 2 | 121.85 | 6.77 | 1.60 |
| 3 | 9347.90 | | 8.37 |
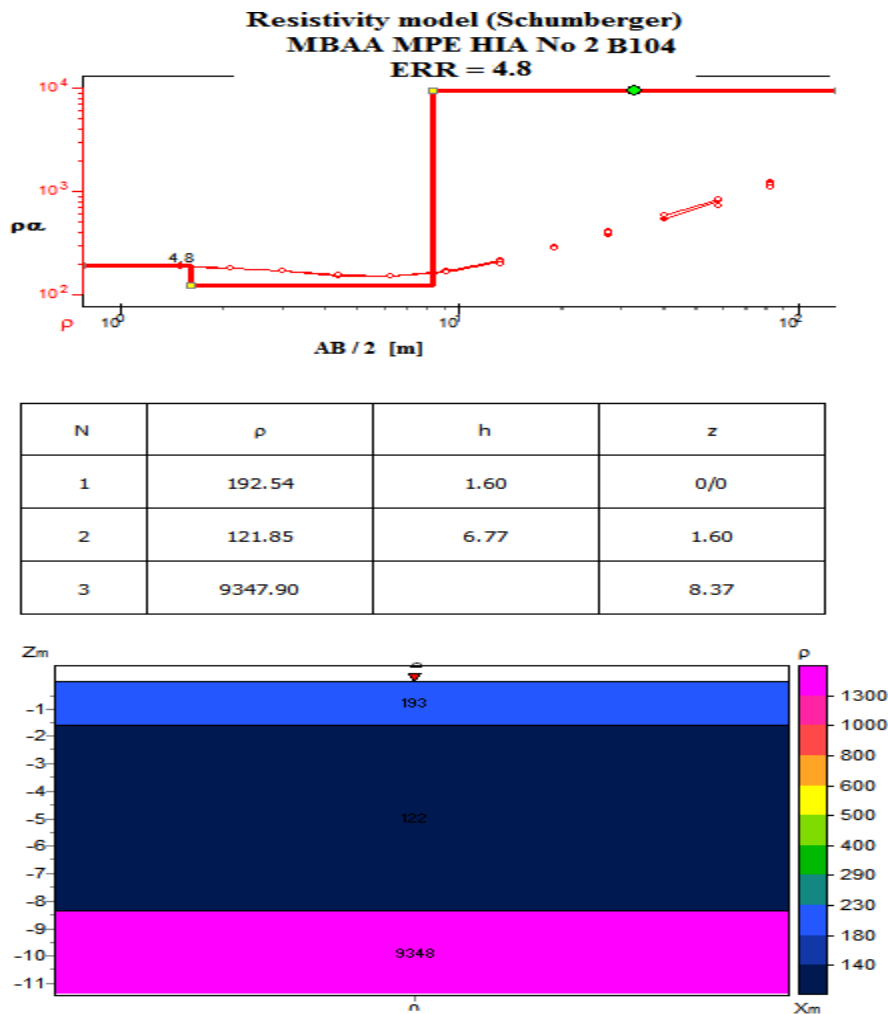


Figure 5.49. VES model curve at station B104 m, Mbaa Mpe Hia No.2 Community

VES C66

The sounding curve indicate QH – type. The geological section at station C66 reveals that the subsurface structure consists of four layers with apparent resistivity values ranging between 120.97 Ωm and 4241.54 Ωm as shown in Figure 5.50. Top layer has a thickness and apparent resistivity value of 0.60 m and 653.70 Ωm, respectively. Second layer has a thickness of 3.50 m and an apparent resistivity value of 233.21 Ωm. Thickness of the third layer is 6.90 m; the apparent resistivity values for third layer and the fourth layer are 120.97 Ωm and 4241.54 Ωm. Analysis of these results reveal that the second layer is probably fairly weathered and underlain by third layer which is most likely highly weathered than the first layer in view of its low apparent

resistivity value. The third layer contains an appreciable quantity of groundwater and hence it is recommended for borehole drilling.
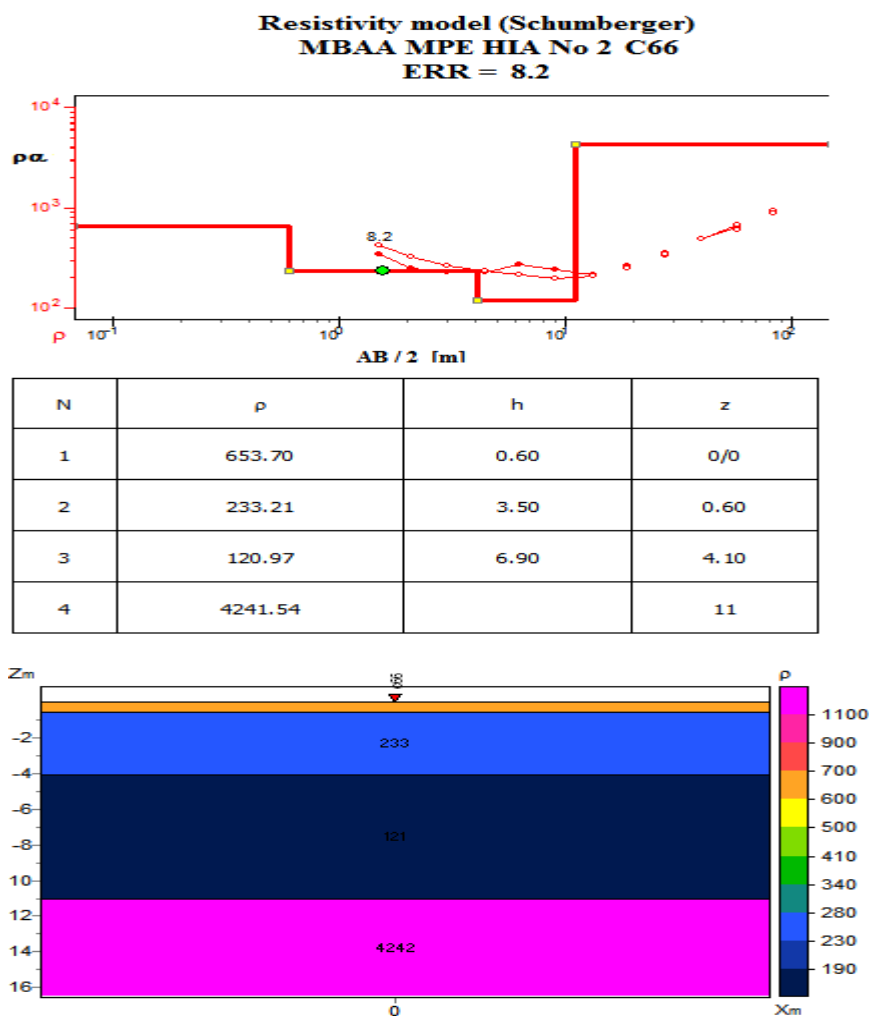


Figure 5.50. VES model curve at station C66 m, Mbaa Mpe Hia No.2 Community

VES C112

The modelled sounding curve at station C112 shows a three layered subsurface structure (see Figure 5.51). First layer has apparent resistivity value of 112.20 Ωm and a thickness of 1.98 m, second layer and third layer have apparent resistivity values of 288.45 Ωm and 5962.44 Ωm respectively. The thickness of the second layer is 33.57 m. The apparent resistivity values for layers one and two indicate a possibility of groundwater within them. Their apparent resistivity values are within the 50 – 2000 Ωm which is the usual ranges of aquifer. The values of apparent resistivity for the first two layers show highly weathered for the first layer and

moderate fracture for the second layer. This station was recommended for drilling borehole.



**Resistivity model (Schumberger)**
**MBAA MPE HIA No 2 C112**
**ERR = 5.6**

| N | ρ | h | z |
|---|---|---|---|
| 1 | 112.20 | 1.98 | 0/0 |
| 2 | 388.45 | 33.57 | 1.98 |
| 3 | 5962.44 | | 35.55 |
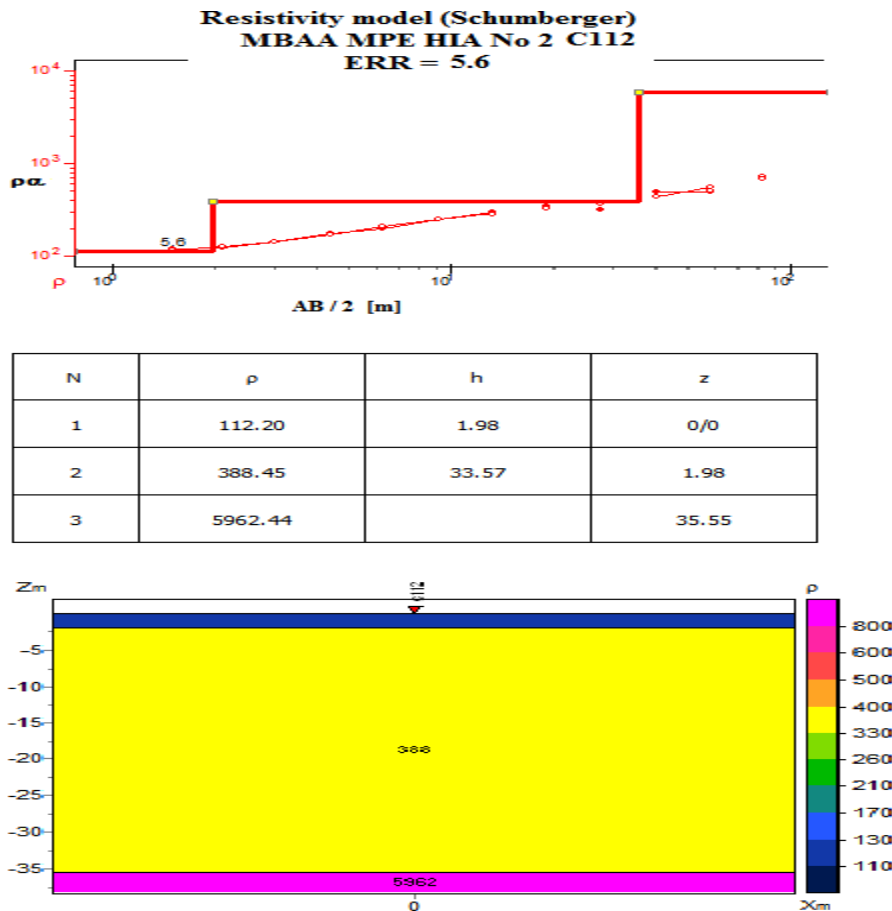
Figure 5.51 VES model curve at station C112 m, Mbaa Mpe Hia No.2 Community

### 5.4.7.4. Discussions of results from the Mbaa Mpe Hia No.2 Community

The analyses of the VES curves suggested that; Mbaa Mpe Hia No.2 Community is generally underlain by three geological layers. First layer has a resistivity value raging 112.2 – 653.70 Ωm and may be intercepted at a mean depth of 1.51 m. Second layer which has a thickness range of 3.10 – 33.57 m has a mean apparent resistivity value of 256.65 Ωm. The third layer has apparent resistivity value ranging 120.97 – 9347.90 Ωm.

The area mapped in this work generally has a lot of groundwater between depths rage of 1.5 – 19.0 m as inferred from the modelled contour maps in Figures 5.52a – 5.52c below.

Generally, all the VES point investigated contain appreciable amount of groundwater. VES B28 is ranked first, followed by VES B104, C66, C112 and A162. The VES A162 may contain the least amount of water among the investigated points and is risk drilling it. Table 5.11 below shows the summary of the VES curves including a rank-list of the selected points for drilling.
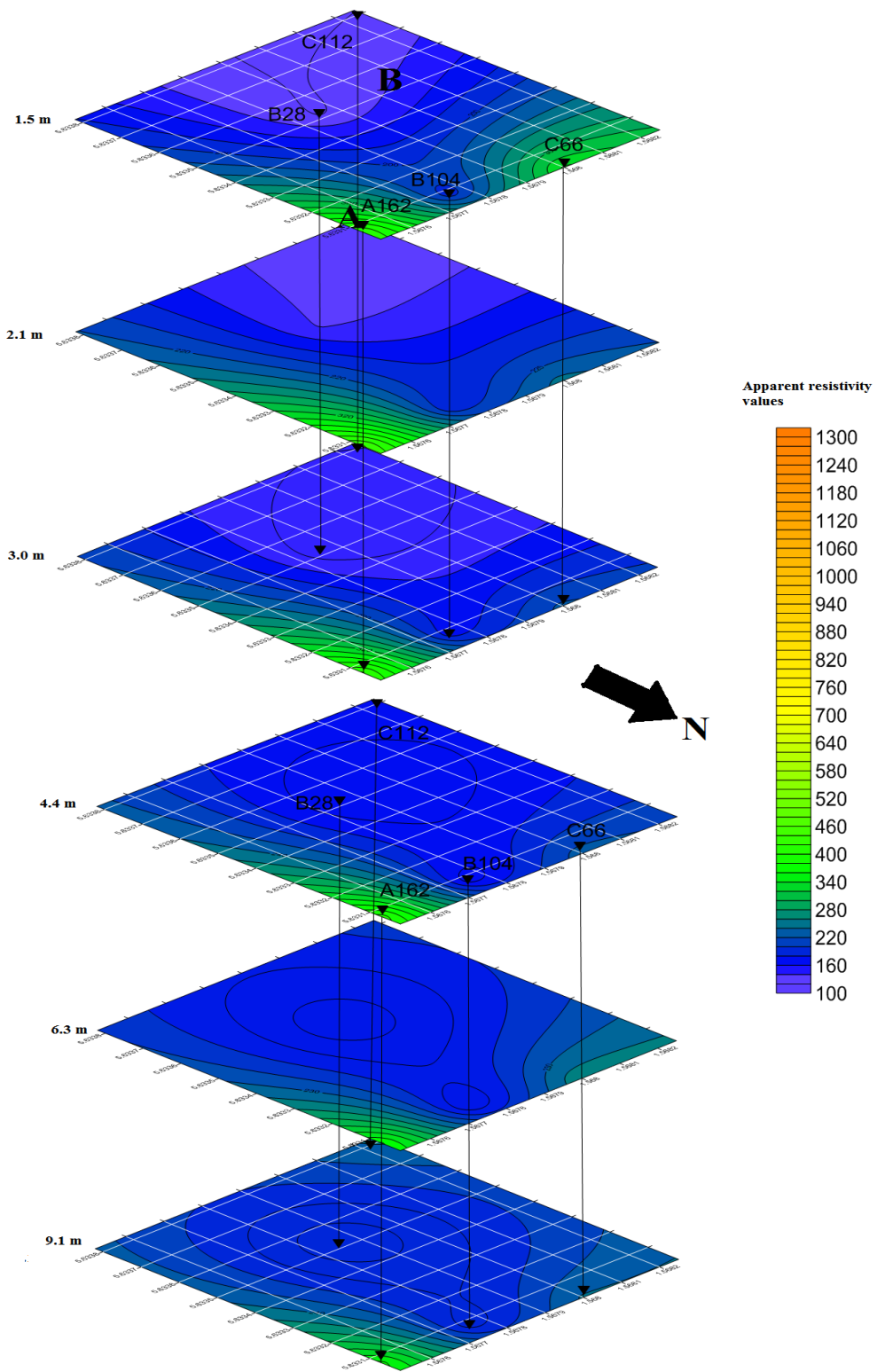
Figure 5.52a. Contour maps showing the apparent resistivity values from depth 1.5 – 9.1 m beneath the Mbaa Mpe Hia No.2 Community
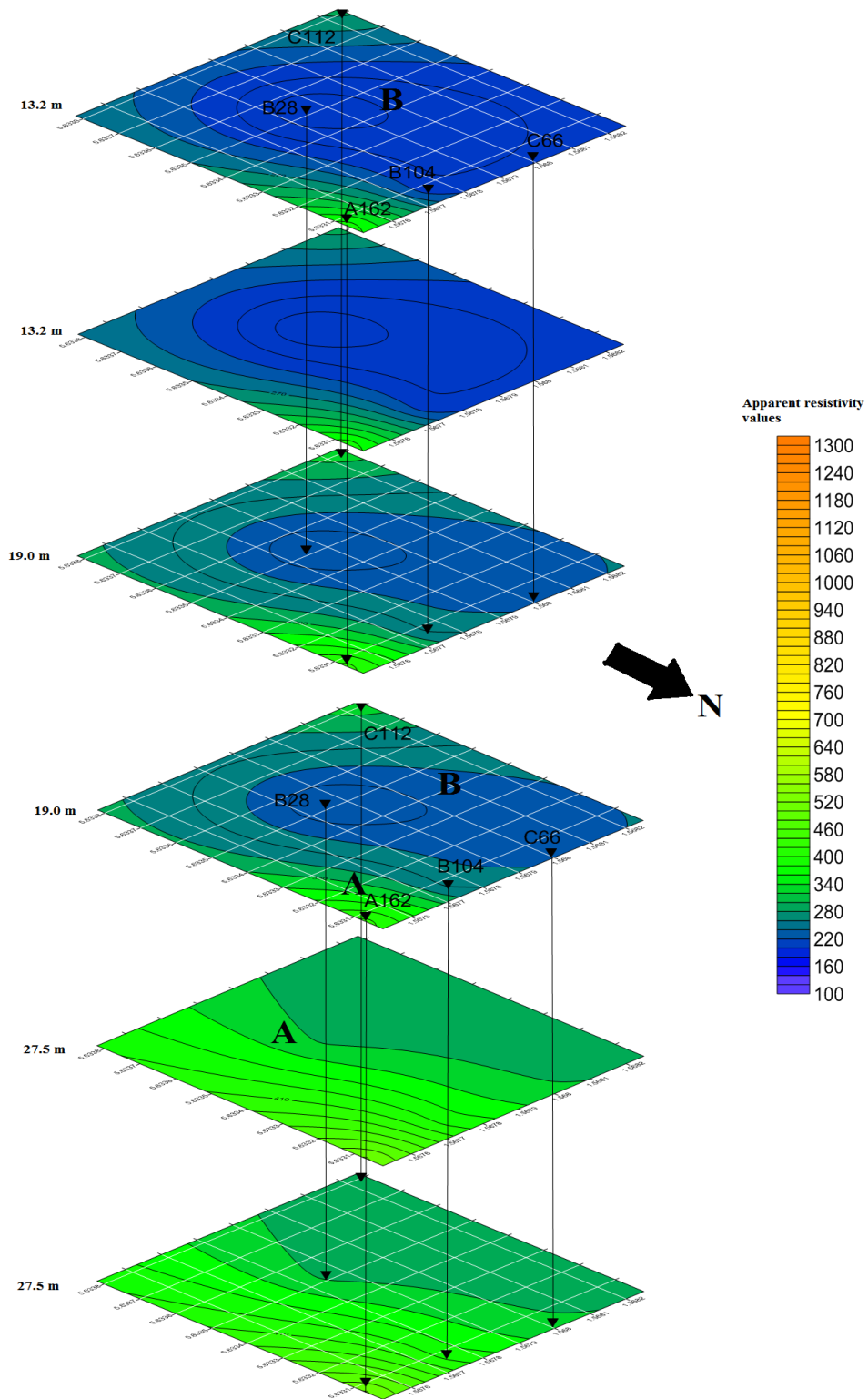
Figure 5.52b. Contour maps showing the apparent resistivity values in the depth range of 13.2 – 27.5 m beneath the Mbaa Mpe Hia No.2 Community
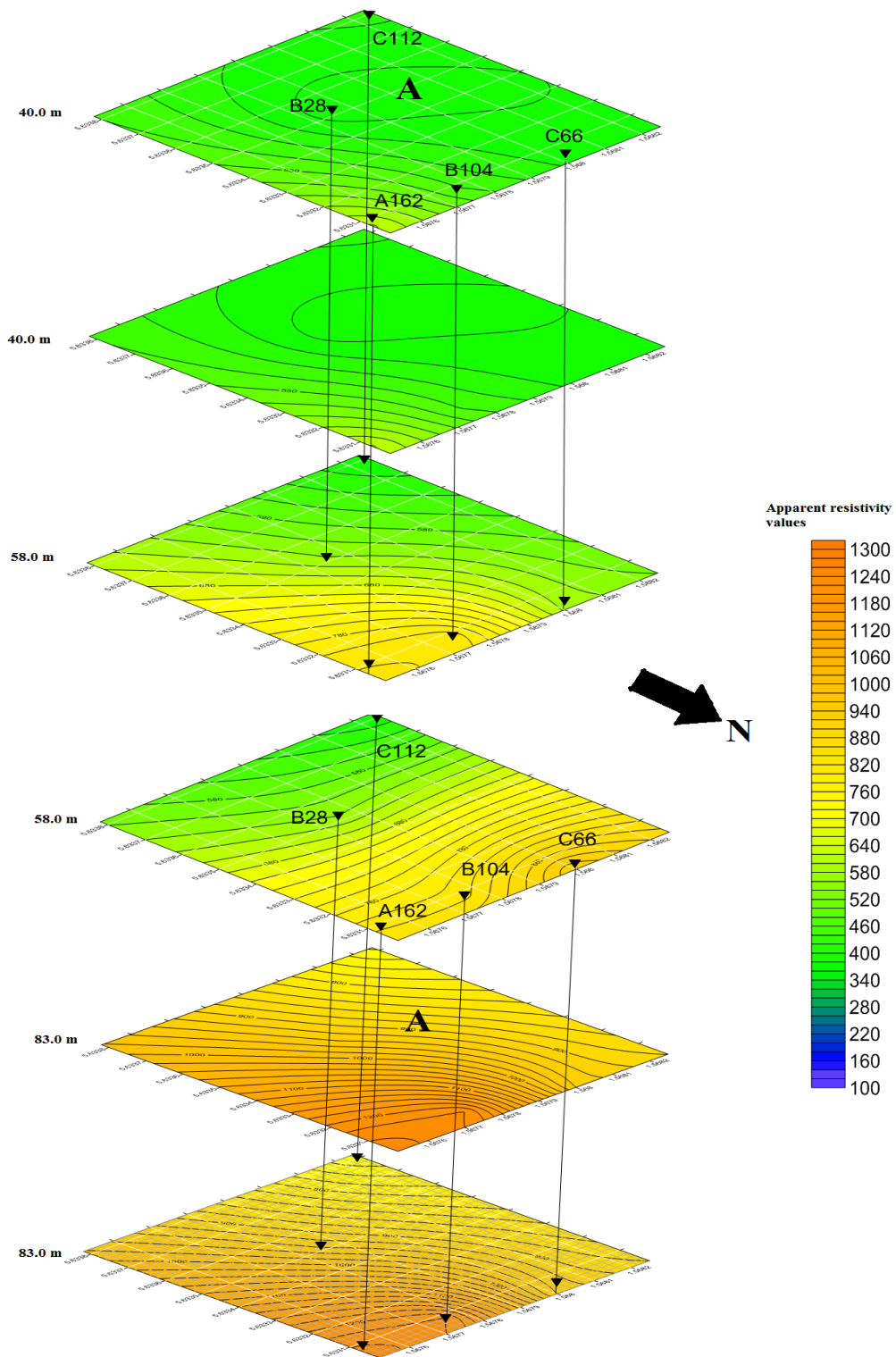
Figure 5.52c. Contour maps showing the apparent resistivity values in the depth range of 40.0 – 83.0 m beneath the Mbaa Mpe Hia No.2 Community.

Table 5.11. Ranked VES points for borehole drilling at Mbaa Mpe Hia No.2 Community

| VES Point | Location (GPS) | Layer | ρ (Ω−μ) | Thickness (m) | Depth (m) | Rank | Remarks |
|-----------|----------------|-------|---------|---------------|-----------|------|---------|
| | 5.63352N | 1 | 122.32 | 1.88 | 1.88 | | |
| | 1.56786W | 2 | 148.35 | 9.10 | 10.98 | | |
| B28 | | 3 | 3573.44 | - | - | 1st | |
| | 5.63308N | 1 | 192.54 | 1.60 | 1.60 | | |
| | 1.56776W | 2 | 121.85 | 6.77 | 8.37 | | |
| B104 | | 3 | 9347.9 | - | - | 2nd | |
| | 5.63302N | 1 | 653.7 | 0.60 | 0.60 | | |
| | 1.56800W | 2 | 233.21 | 3.50 | 4.10 | | |
| | | 3 | 120.97 | 6.90 | 11.00 | | |
| | | 4 | 4241.54 | - | - | | |
| C66 | | | | | | 3rd | |
| | 5.63382N | 1 | 112.2 | 1.98 | 1.98 | | |
| | 1.56825W | 2 | 388.45 | 33.57 | 35.55 | | |
| C112 | | 3 | 5962.44 | - | - | 4th | |
| | 5.63307N | 1 | 438.54 | 1.50 | 1.50 | | |
| | 1.56752W | 2 | 391.37 | 3.10 | 4.60 | | |
| | | 3 | 296.56 | 11.67 | 16.27 | | |
| | | 4 | 4061.89 | - | - | | |
| A162 | | | | | | 5th | |

## 5.4.8. Moseaso Community

## 5.4.8.1. Introduction

Electromagnetic profiling was conducted along four (4) profiles across the Moseaso Community and six resistivity measurements taken. The results of the VES stations suggest 3 − layered and 4 − layered subsurface structures. The four traverse lines on which the electromagnetic readings were taken are shown in Figure 5.53 below. There is existing boreholes and hand-dug wells in 5 Km radius of the study area but there is no information available on hand-dug wells around the study area. Table 5.12 shows information on the existing borehole within 5 Km of radius of the study area. The depths of available well were used as a guide for interpretation of geophysical data. It gives an overview of the depth at which one could expected groundwater, although the exact depth is not expected.
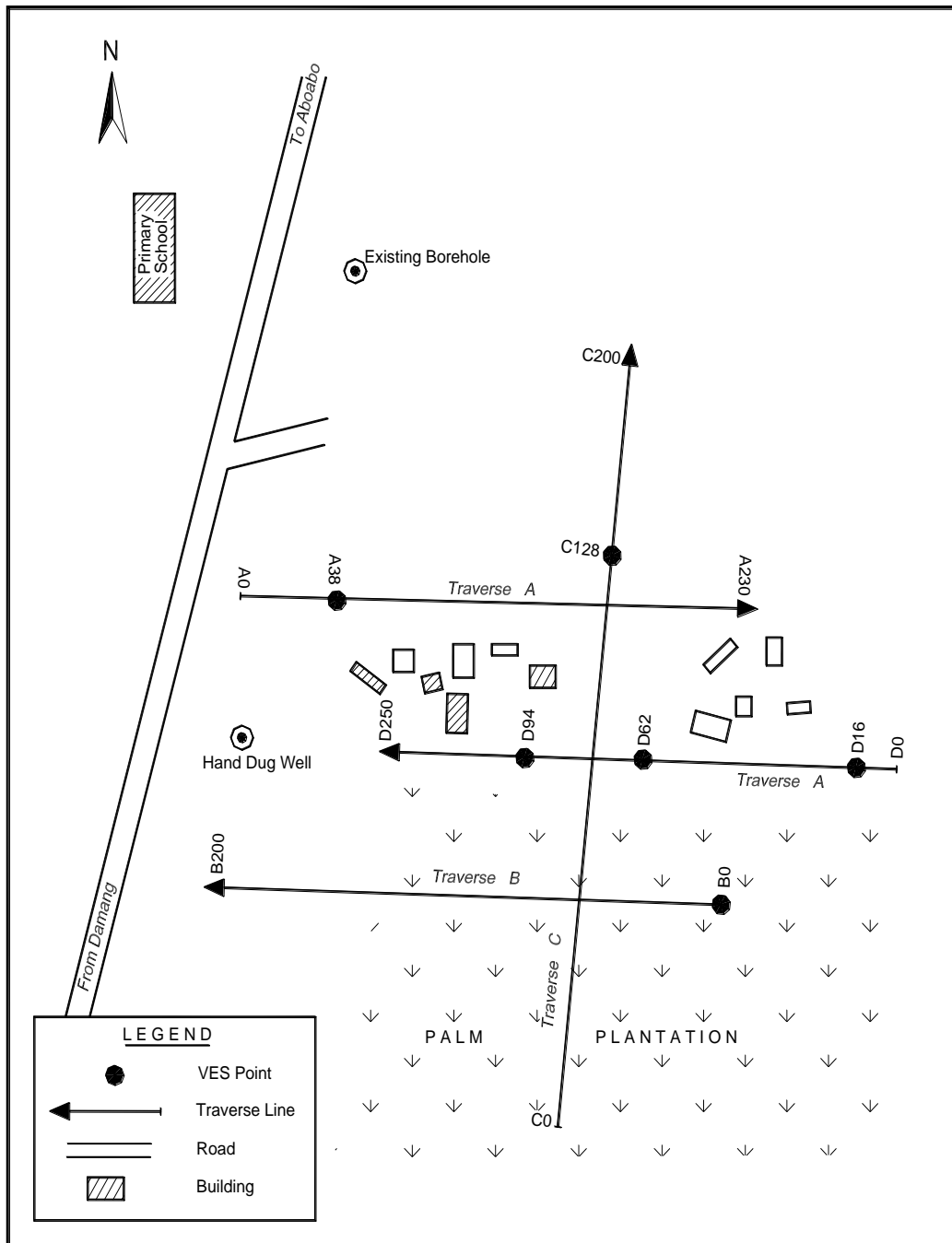
Figure 5.53. Schematic Layout of Moseaso Community (not to scale)

Table 5.12. Existing Boreholes within 5 Km radius around Study Area (Mainoo et al. 2007e)

| Community | BH No. | Depth (m) | Yield (m³/h) | SWL (m) | Water Quality | Lithology | Calibration |
|-----------|--------|-----------|--------------|---------|---------------|-----------|-------------|
| NYENASI | 48/E/79-2 | 73 | | | N/A | | |

### 5.4.8.2. EM traverses

Traverse A was carried out on a profile length of 230 m and on a bearing of 025° from the True North. The EM readings were taken using 20 m coil separation at 10 m interval. The maximum conductivity value is 14 m mhos/m and the minimum conductivity value is also 7 m mhos /m with the average value of 10.62 m mhos/m. The results of the EM profile on this traverse, displays a higher terrain conductivity values for VD mode more than that of HD mode which means that at deeper depth the subsurface is fractured. Stations 40 m and 120 m recorded the highest terrain conductivity values for both VD mode (indicating a possible fracture in the zone) but point 38 was selected for VES investigation and no point near 120 m was selected because twenty meters from the station 120 that is, at station 140 there is a toilet situated there. The toilet is a potential source of groundwater pollution hence the station was avoided. Figure 5.54 shows a graph for the EM profiling on traverse A. Generally, both HD and VD modes curves move erratically throughout the profile, indicating a complex subsurface.
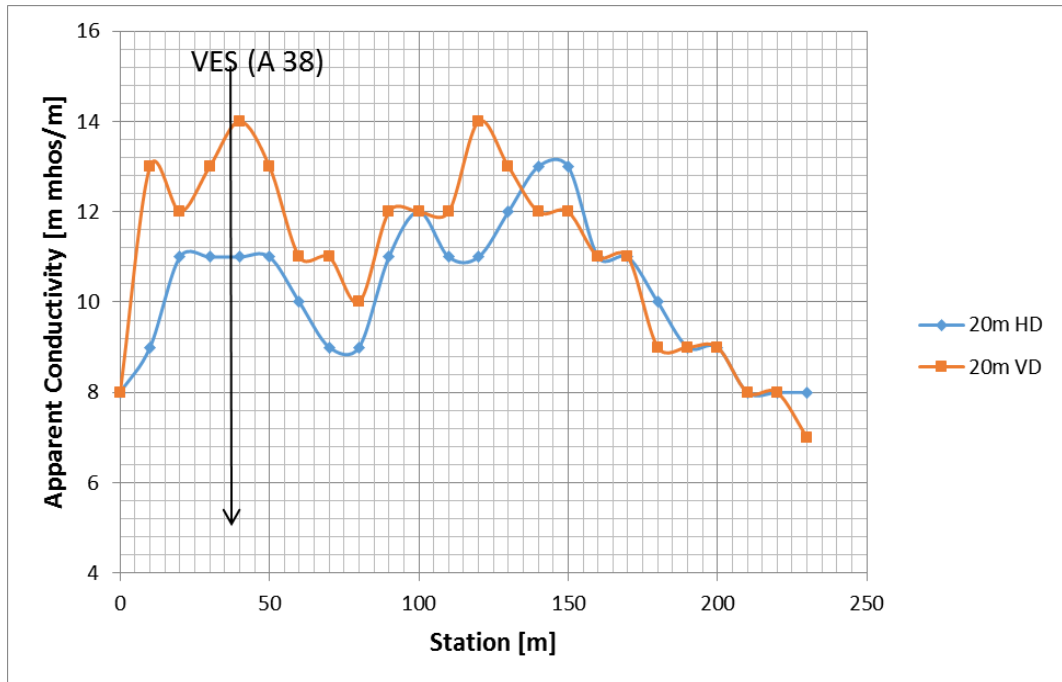
Figure 5.54. EM terrain conductivity measurements along a profile A at Moseaso Community

Traverse B has a total length of 200 m and a bearing 200° from the True North. The EM readings were carried out using 20 m coil separation and at 10 m interval.

The apparent conductivity range on this profile line is between 8 – 13 m mhos/m with an average of 10.21 m mhos/m. From Figure 5.55 below, it could be seen that, generally HD mode curve has a high terrain conductivity values than the VD mode. It means that at deeper depth there are no much fractures and finding groundwater within this zone would be difficult. There is only one peak on the graph for VD mode, at station 0 m. This is also the highest terrain conductivity value for HD mode curve. That point is selected for VES investigation. The point has a capacity of yielding high quantity of groundwater.
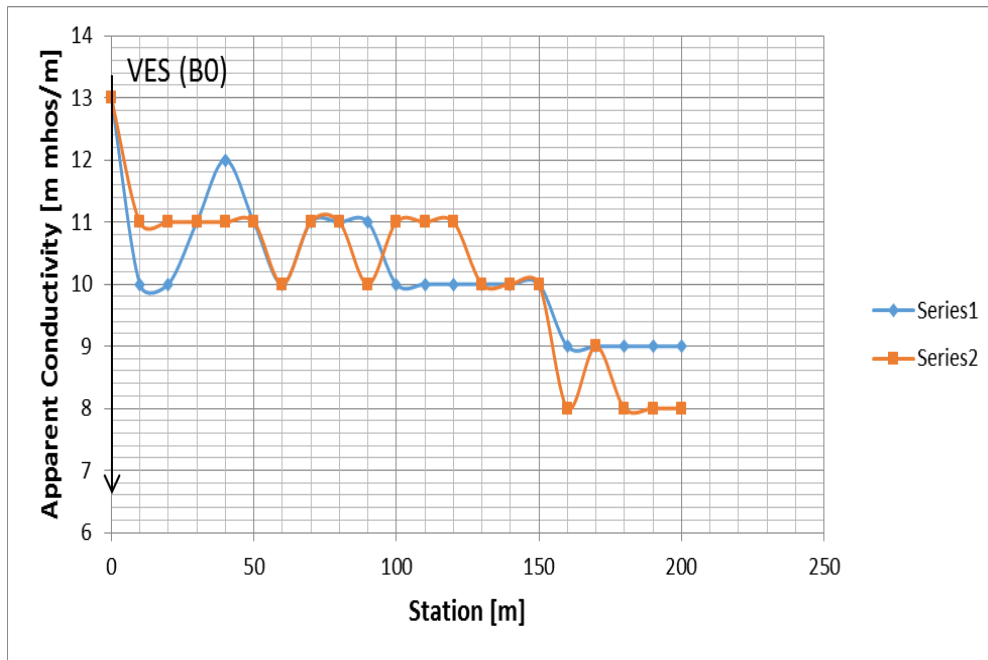
Figure 5.55. EM terrain conductivity measurements along a profile B at Moseaso Community

The traverse C is 200 m long and the EM readings were taken using 20 m coil spacing and 10 m interval. The profile was ran on a bearing 280° from the True North.

The maximum and the minimum terrain conductivity on graph in Figure 5.56 are 14 m mhos/m and 8 m mhos/m respectively. The average apparent conductivity value is 10.64 m mhos/m. The movement of both HD mode and VD mode curves are erratically along the profile, suggesting a complex subsurface. The terrain conductivity of the VD mode is higher than that of HD mode along the profile. There are six crossover points on the graph but they were not selected for VES investigation because of their general low terrain conductivity values. There are two peaks on the graph and prominent one was chosen for further investigation. The chosen point (VES C128) may be fractured at deeper depth due to high terrain conductivity for VD mode.
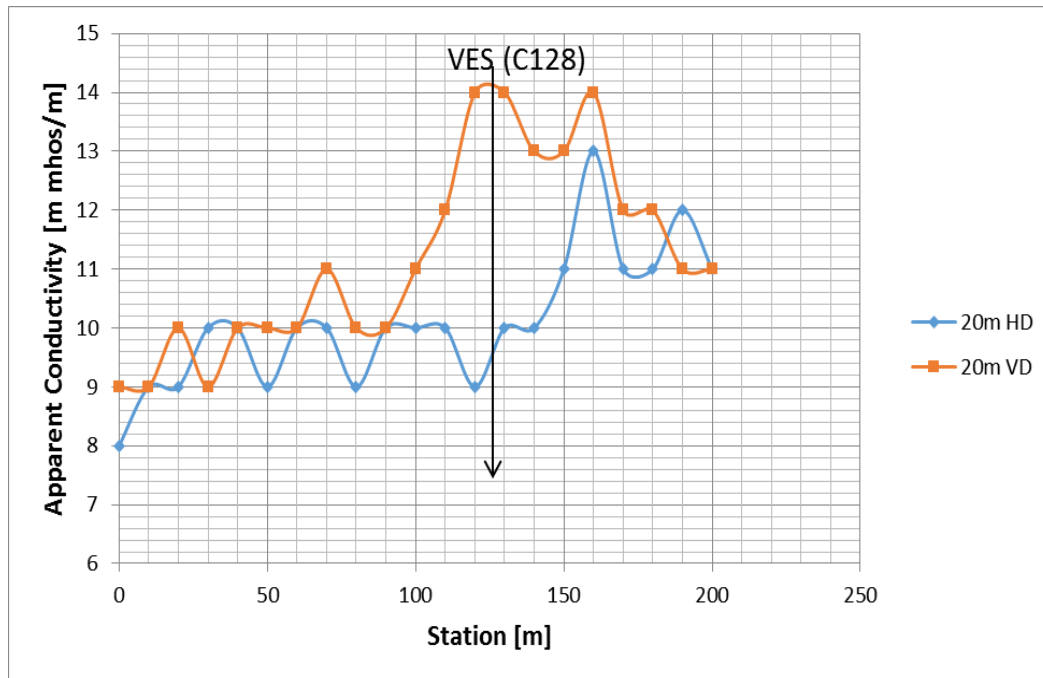
Figure 5.56 EM terrain conductivity measurements along a profile C at Moseaso Community

Traverse D is the last of the four traverse run in Moseaso Community. EM profiling was carried out along this traverse of length 250 m using 20 m coil spacing and EM readings taken at 10 m intervals.

The EM profiling was run on bearing of 177° from the True North. The maximum, minimum and average apparent conductivity values on this traverse are 16, 8 and 10.67 m mhos/m respectively. Among the four profiles, this profile has the highest recorded apparent conductivity value. From Figure 5.57, it is observed that; the curves are erratic in nature and VD mode curve has higher apparent conductivity values along the entire profile with the exception of stations from 200 m to 250 m. There are great differences in the apparent conductivity values between the VD curve and the HD curves. It could be inferred that, the groundwater within this part of the community could be at deeper depths. Three points were selected for further investigation using resistivity method. These points or station are 16 m (a crossover point), 62 m (highest apparent conductivity value) and 94 m. The nature of this graph suggest that, the selected points on this profile would contain more water than other points on other profiles, if this graph is compare with other graphs from this community.
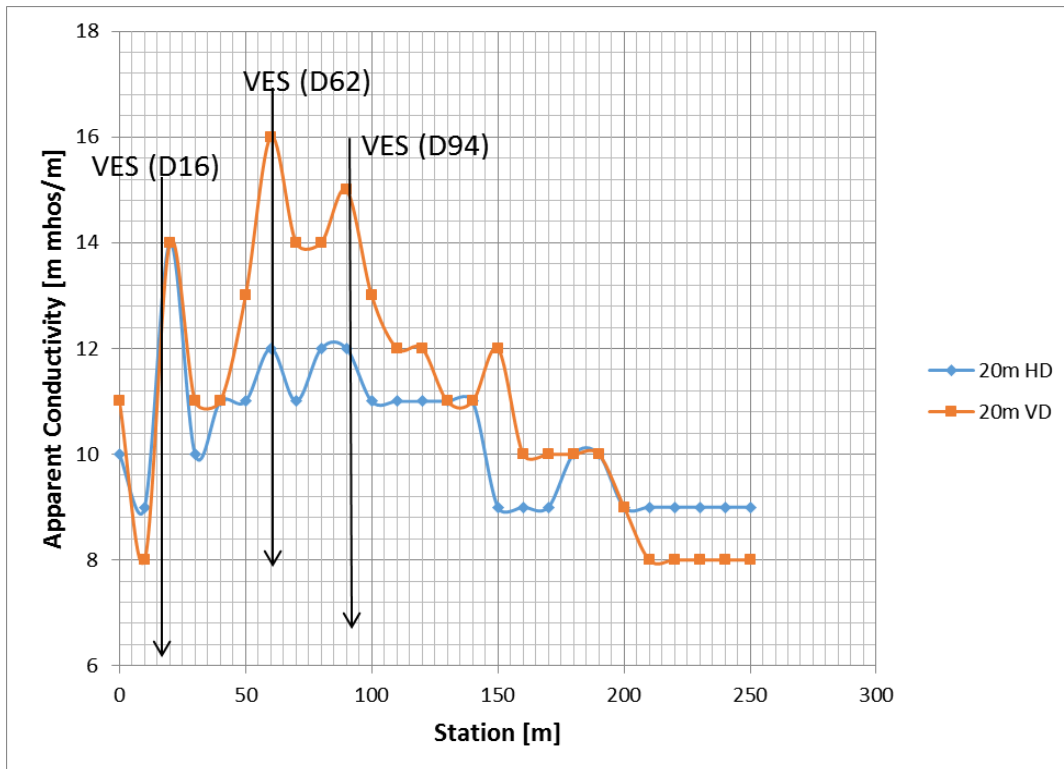
Figure 5.57. EM terrain conductivity measurements along a profile D at Moseaso Community

### 5.4.8.3. Sounding curves

VES A38

The modelled sounding curve of VES at station A38 revealed a four layered subsurface structure (see Figure 5.58). The sounding curve is KH – type which indicated a weathered zone in the third layer. The apparent resistivity values vary between 179.63 Ωm and 1287.38 Ωm. First layer has an apparent resistivity value of 179.63 Ωm and a thickness of 1.66 m; the thicknesses of the second and third layer are 4.80 m and 20.90 m respectively. Second, third and fourth layer have apparent resistivity values of 910.32 Ωm and 199.98 Ωm and 1287.38 Ωm respectively. The apparent resistivity values for first and third layers indicate a possibility of groundwater within them. The apparent resistivity values of those layers also show moderate to high fracture within the layers. This station is recommended for drilling borehole.

**Resistivity model (Schlumberger)**
**MOSEASO A38**
**ERR = 5.3**

| N | ρ | h | z |
|---|---|---|---|
| 1 | 179.63 | 1.66 | 0/0 |
| 2 | 910.32 | 4.80 | 1.66 |
| 3 | 199.98 | 20.90 | 6.46 |
| 4 | 1287.38 | | 27.36 |
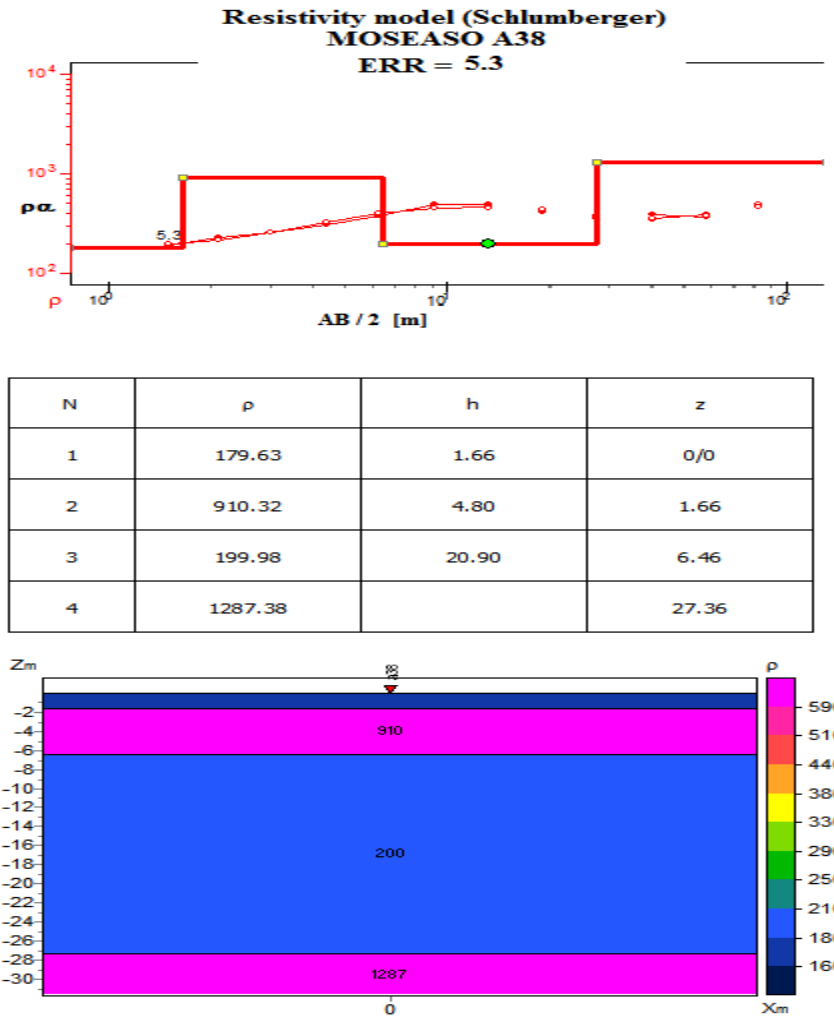
Figure 5.58. VES model curve at station A38 m, Moseaso Community

VES C128 H

The geological section at station C128 reveals that the subsurface structure consists of three layers with apparent resistivity values ranging between 115.21 Ωm and 3901.36 Ωm as shown in Figures 5.59 below. The top layer has a thickness and apparent resistivity value of 10.34 m and 417.77 Ωm respectively. The second layer has a thickness of 12.36 m and an apparent resistivity value of 115.21 Ωm. The third layer has an apparent resistivity value of 3901.36 Ωm. Analysis of these results reveal that the top layer is probably fairly weathered and underlain by second layer which is most likely highly fractured than the first layer in view of its low apparent resistivity value. The second layer contains an appreciable quantity of groundwater and hence it is recommended for borehole drilling.

**Resistivity model (Schlumberger)**
**MOSEASO C128**
**ERR = 6.3**

| N | ρ | h | z |
|---|---|---|---|
| 1 | 417.77 | 10.34 | 0/0 |
| 2 | 115.21 | 12.36 | 10.34 |
| 3 | 3901.36 | | 22.70 |
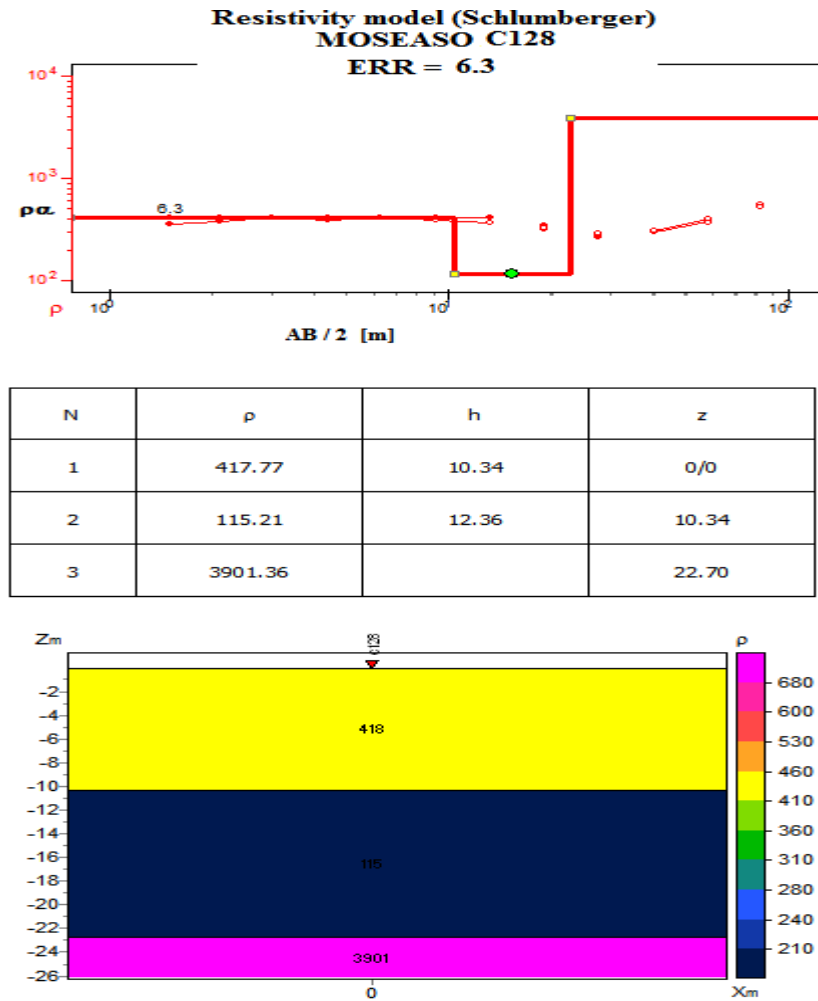
Figure 5.59. VES model curve at station C128 m, Moseaso Community

VES D16

The subsurface geological structure beneath this station is interpreted as four layered (Figure 5.60). The sounding curve displays a QH – type curve with second and third layer having the minimum resistivity values. Top layer has an apparent resistivity value of 1206.62 Ωm and thickness of 2.49 m. Second layer and third layer have apparent resistivity values of 521.33 Ωm and 209.14 Ωm respectively. The thickness of second layer is 7.31 m and that of the third layer is 15.80 m. The fourth modelled layer has apparent resistivity of 1992.83 Ωm. The third layer is sandwiched between two highly resistive formations and the apparent resistivity value of the third layer suggests a possible fracture and / or weathering within the layer.

**Resistivity model (Schlumberger)**
**MOSEASO D16**
**ERR = 5.3**

| N | ρ | h | z |
|---|---|---|---|
| 1 | 1206.62 | 2.49 | 0/0 |
| 2 | 521.33 | 7.31 | 2.49 |
| 3 | 209.14 | 15.80 | 9.80 |
| 4 | 1992.83 | | 25.60 |
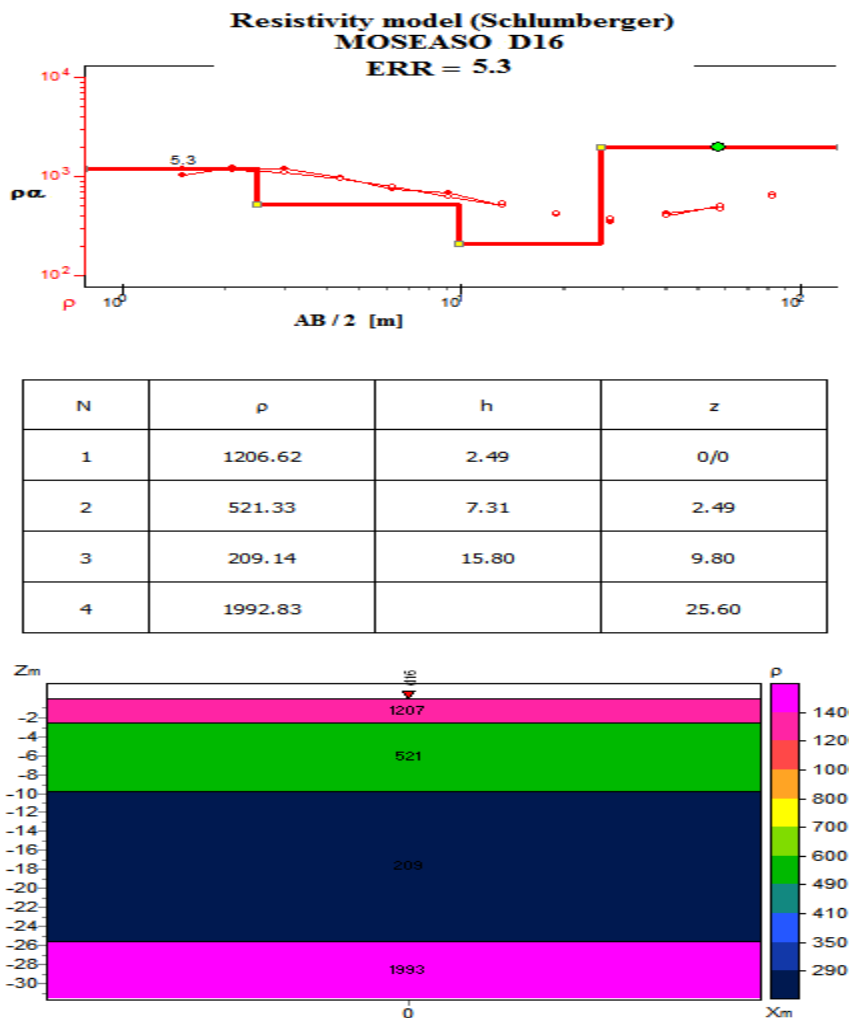
Figure 5.60. VES model curve at station D16 m, Moseaso Community

Fractured zones and weathered zone are major geological features for accumulation of groundwater within this Granite Formation of Ghana. The movement of groundwater within this part of the community would be horizontal one because water could not pass vertically though the top layer. There is a very high probability of locating groundwater beneath this station at deeper depth, around 15 to 20 m deep. This station is recommended for borehole drilling.

### 5.4.8.4. Discussions of results from Moseaso Community

The VES results suggested that Moseaso Community is underlain by four geological substrata. Out of the six VES station investigated, only one station revealed three layered model for the subsurface. Generally the first layer has an apparent resistivity values ranging from 179.63 – 1206.62 Ωm and can be intercepted at a mean depth

2.83 m. The second layer has a thickness range of 2.90 – 12.36 m, and a mean apparent resistivity value of 892.73 Ωm. The third layer which is expected to be water-bearing has a thickness ranging from 12.20 -28.8 m and a mean apparent resistivity value of 794.21 Ωm. The fourth layer has apparent resistivity values ranging between 671.13 Ωm and 2572.31 Ωm.

The contour maps model in Figures 5.60a – 5.60c below, indicate groundwater in high quantity available towards the northern part of the Moseaso Community between depths 1.5 – 83.0 m. The existing borehole (BUI) is situated at a very good location than the place where the VES were conducted.

VES A38 shows sign of high quantity of groundwater from depth 1.5 m to about 3.0 m. The rest of the VES points show signs of high amount of groundwater between depths of 27.5 – 58.0 m. the VES D62 is ranked first, follow by D94, B0, C128, D16 and A38 in descending order (table 5.13). All the VES stations are recommended for drilling or hand-dug. Areas towards the northern part of the community should be target for boreholes in future projects.
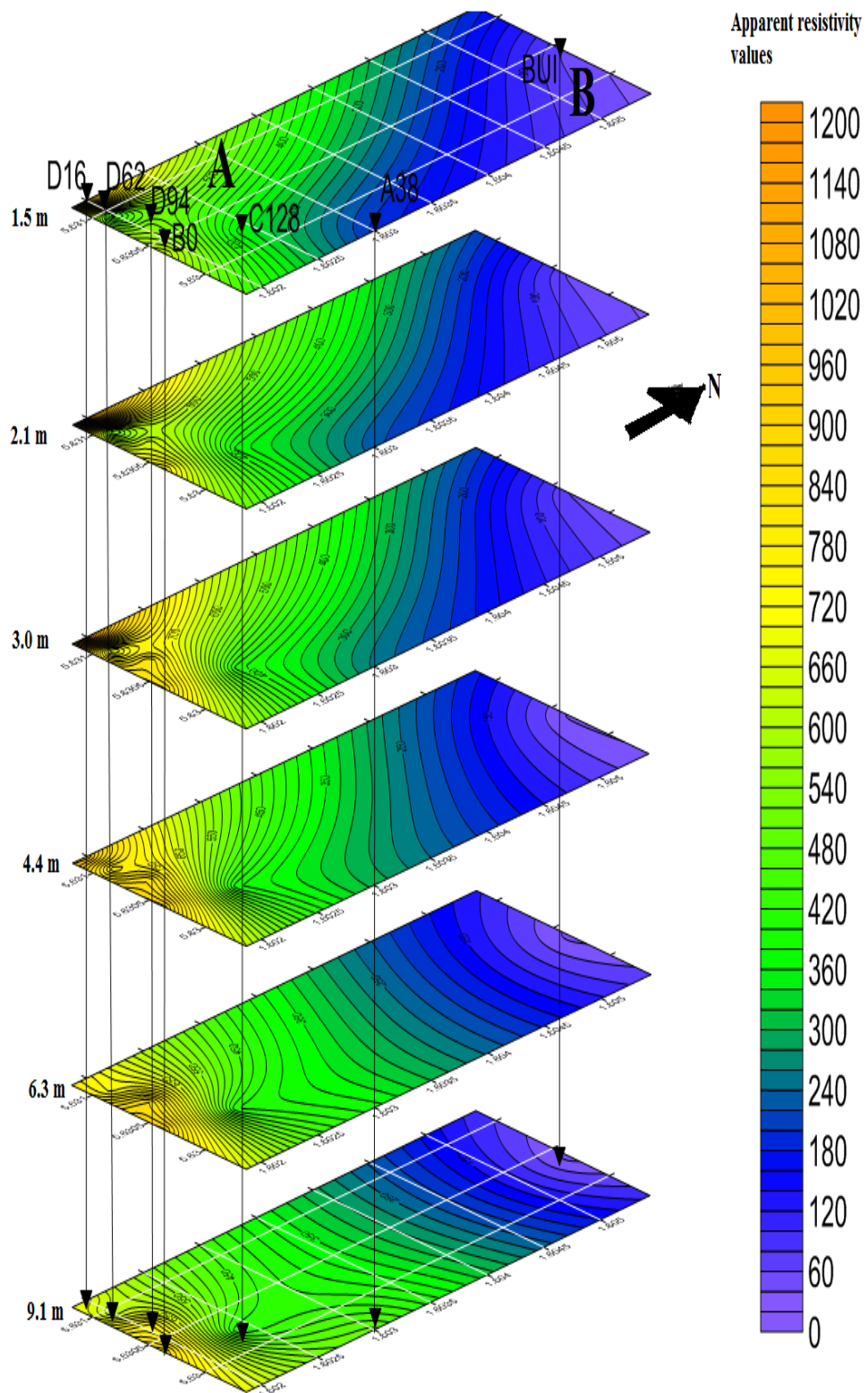
Figure 5.61a. Contour maps showing the apparent resistivity values from depth 1.5 – 9.1 m beneath the Moseaso Community
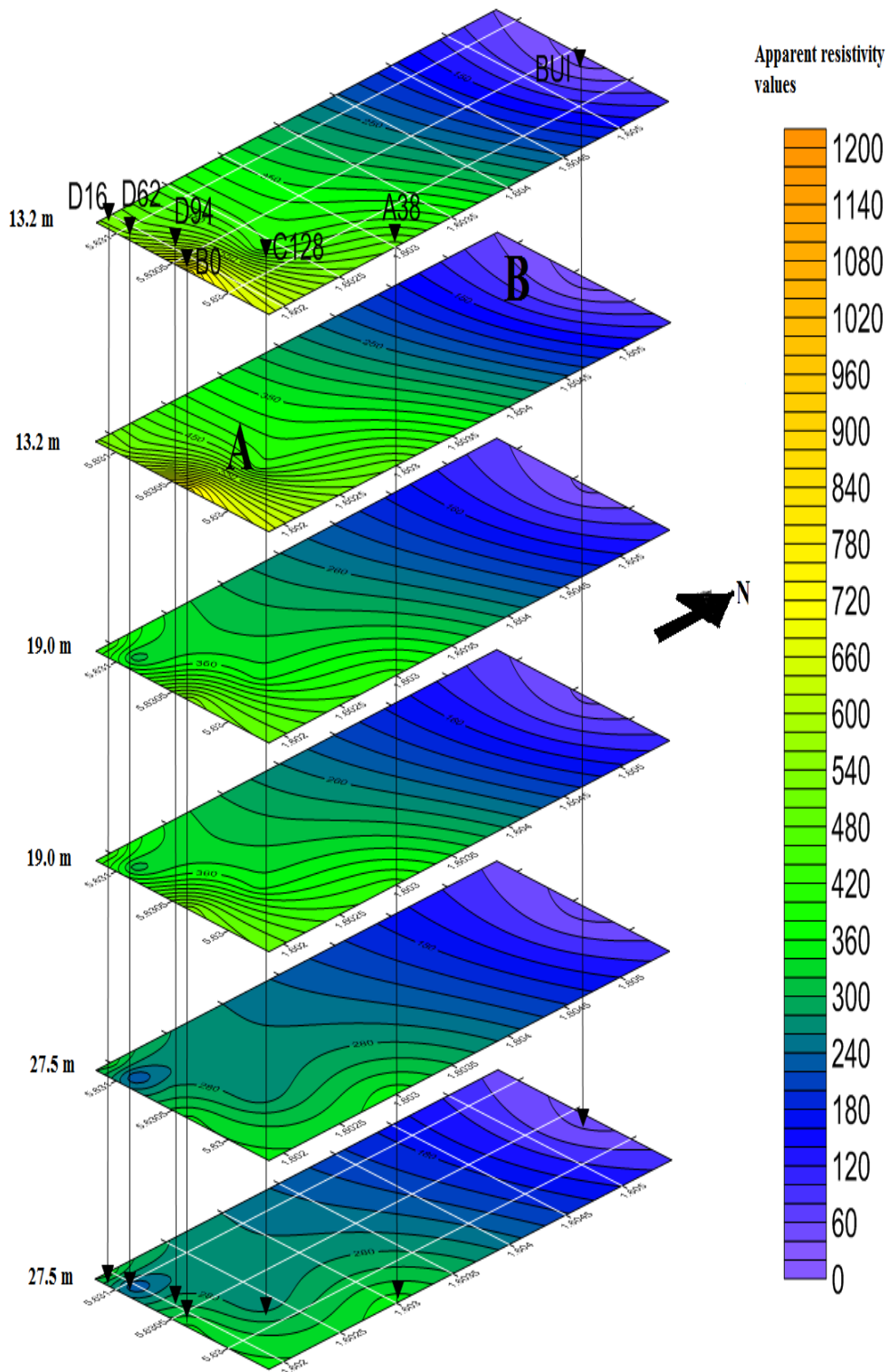
Figure 5.61b. Contour maps showing the apparent resistivity values from depth 13.2 -27.5 m beneath the Moseaso Community
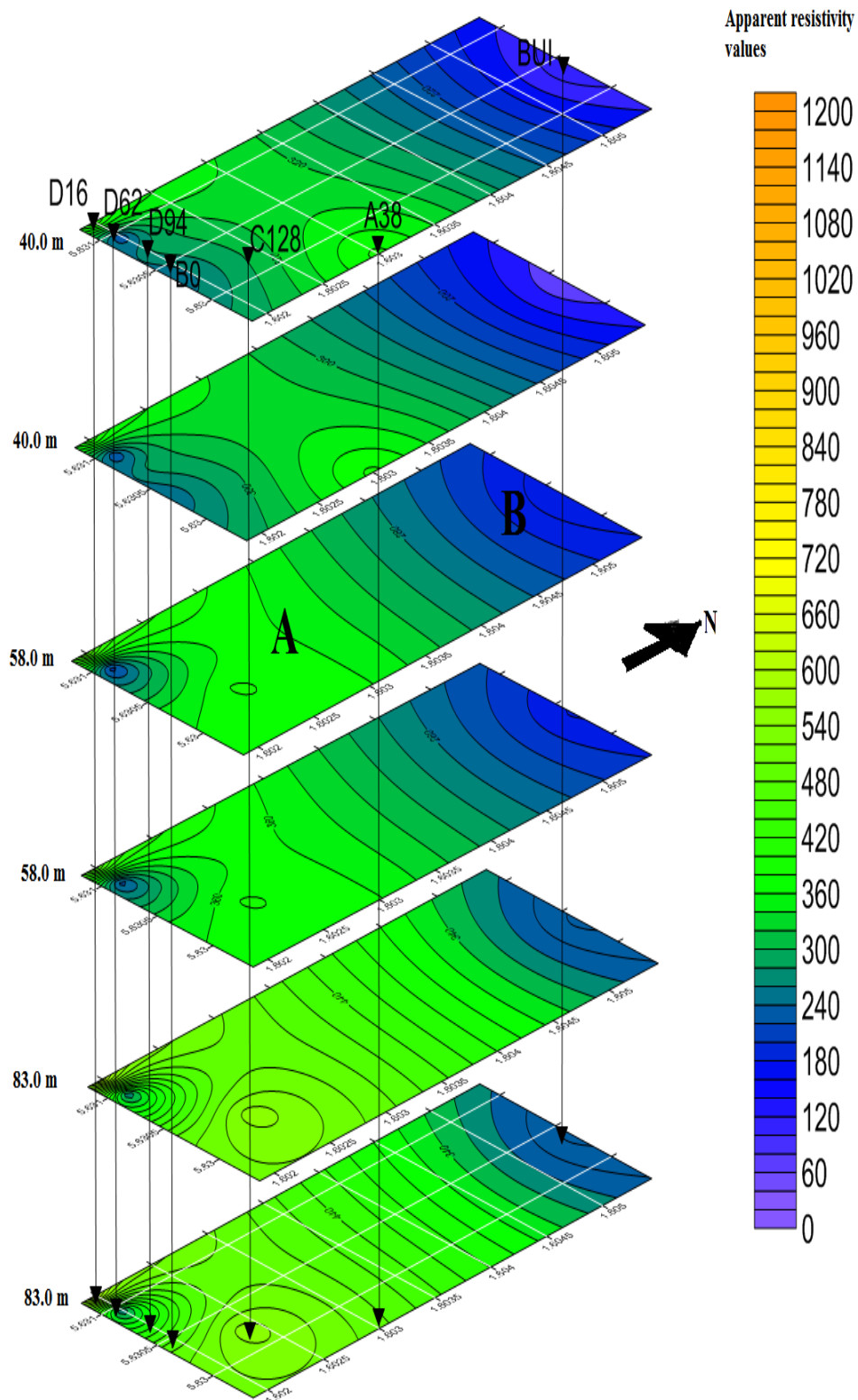
Figure 5.61c. Contour maps showing the apparent resistivity values from depth 40 - 83 m beneath the Moseaso Community

Table 5.13. Ranked VES points for borehole drilling at Moseaso Community

| VES Point | Layer | ρ (Ω−μ) | Depth (m) | Thickness (m) | Rank | Location (GPS) | Remarks |
|---|---|---|---|---|---|---|---|
| | 1 | 283.27 | 0.8 | 0.8 | | 5.63095N | |
| | 2 | 1400.88 | 3.7 | 2.9 | | 1.60199W | |
| | 3 | 154.57 | 31.2 | 27.5 | | | |
| D62 | 4 | 671.13 | - | - | 1st | | |
| | 1 | 399.13 | 0.77 | 0.77 | | 5.63069N | |
| | 2 | 1422.52 | 3.84 | 3.07 | | 1.60206W | |
| | 3 | 216.74 | 32.64 | 28.8 | | | |
| D94 | 4 | 895.42 | - | - | 2nd | | |
| | 1 | 643.81 | 0.95 | 0.95 | | 5.63036N | |
| | 2 | 986.1 | 9.3 | 8 | | 1.60187W | |
| | 3 | 83.51 | 21.5 | 0.35 | | | |
| B0 | 4 | 2572.32 | - | 12.2 | 3rd | | |
| | 1 | 417.77 | 10.34 | 10.34 | | 5.63024N | |
| | 2 | 115.21 | 22.7 | 12.36 | | 1.60238W | |
| C128 | 3 | 3901.36 | - | - | 4th | | |
| | 1 | 1206.62 | 2.49 | 2.49 | | 5.63118N | |
| | 2 | 521.33 | 9.8 | 7.31 | | 1.60200W | |
| | 3 | 209.14 | 25.6 | 15.8 | | | |
| D16 | 4 | 1992.83 | - | - | 5th | | |
| | 1 | 179.63 | 1.66 | 1.66 | | 5.62964N | |
| | 2 | 940.32 | 6.46 | 4.8 | | 1.60300W | |
| | 3 | 199.98 | 27.36 | 20.9 | | | |
| A38 | 4 | 1287.38 | - | - | 6th | | |
| Existing Borehole | 1 | 61.5 | 5.8 | 5.8 | | 5.63035N | |
| | 2 | 34 | 12.7 | 6.9 | | 1.60544W | |
| | 3 | 1568.7 | - | - | | | |

## 5.4.9. Nyamebekyere No. 2

### 5.4.9.1. Introduction

In Nyamebekyere No. 2 Community three traverses were created and a total of five stations were surveyed using the resistivity method of vertical electrical sounding. The sounding curves display 4 curve types and they are A, KH, QH and HA. Figure 5.61 shows the schematic layout of the community. There were no available data on existing boreholes and hand-dug wells within a 5 km radius around the community during the desk studies stage of the project, but it was available during the interpretation of the geophysical survey data. It served as a guide for the interpretation and discussion of geophysical data. Table 5.14 shows the existing boreholes within the 5 Km radius around Kwanyarko Community.
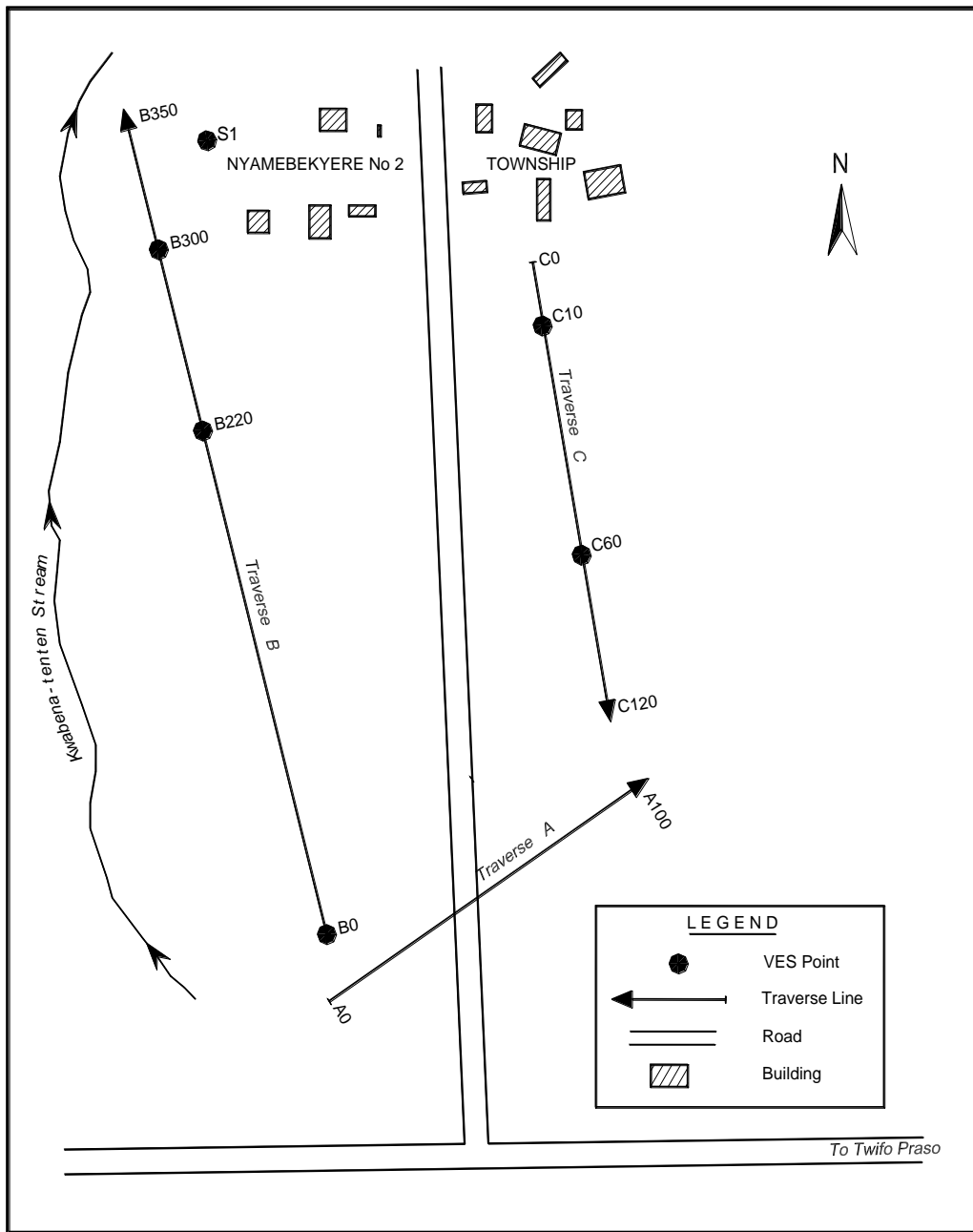
Figure 5.62. Schematic Layout of Nyamebekyere No. 2 Community (not to scale)

Table 5.14. Existing Boreholes within 5 Km radius around Nyamebekyere No.2 Community (Mainoo et al. 2007g)

| Community | BH No. | Depth (m) | Yield (m³/h) | SWL (m) | Water Quality | Lithology | Calibration |
|---|---|---|---|---|---|---|---|
| BREMAN | 085/G/76-1 | 22 | 6 | 5.66 | N/A | Phyllite / Mica schist | |
| BREMAN | 085/G/76-2 | 41 | 4.8 | 4.01 | N/A | Phyllite / Mica schist | |
| WAMASO | 48/B/73-1 | 68 | | | N/A | | |
| WAMASO | 48/B/73-3 | 49 | | | N/A | | |
| NYAMEBEKYERE | 27/H/68-1 | 28 | | 0 | N/A | Quartz Diorite | |
| NYAMEBEKYERE | 27/H/68-2 | 34 | | | N/A | | |
| NYAMEBEKYERE | 27/H/68-3 | 40 | | | N/A | | |
| NYAMEBEKYERE | 27/H/68-4 | 37 | | 2.13 | N/A | Granite | |

### 5.4.9.2.  EM Traverses

Traverse A was carried out on a profile length of 100 m on a bearing of 032° from the True North. The EM reading were taken using 10 m coil spacing and at 5 m intervals. Figure 5.62 shows the graph of the terrain conductivity curves for HD mode and VD mode. The maximum, minimum and average terrain conductivity values are 27.0, 6.0 and 16.17 m mhos/m respectively.

The results of EM profiling show an erratic graph for both HD and VD mode with high terrain conductivity values. There are about seven crossover points which are

potential point for further investigations. Also there are four peaks for the VD mode curves which indicated high conductivity at deeper layers. The behaviour of this graph suggests a ground water at the subsurface.

No VES point was selected on this profile, probably it was carried out to observed the EM responds between the two other traverses in the community or may be because it crosses the main road that linked the community to other community there was a fear that, borehole if drilled on this profile may be filled back to pay way for expansion of the road, and that since there are other places it was better not to consider the traverse A for borehole drilling.
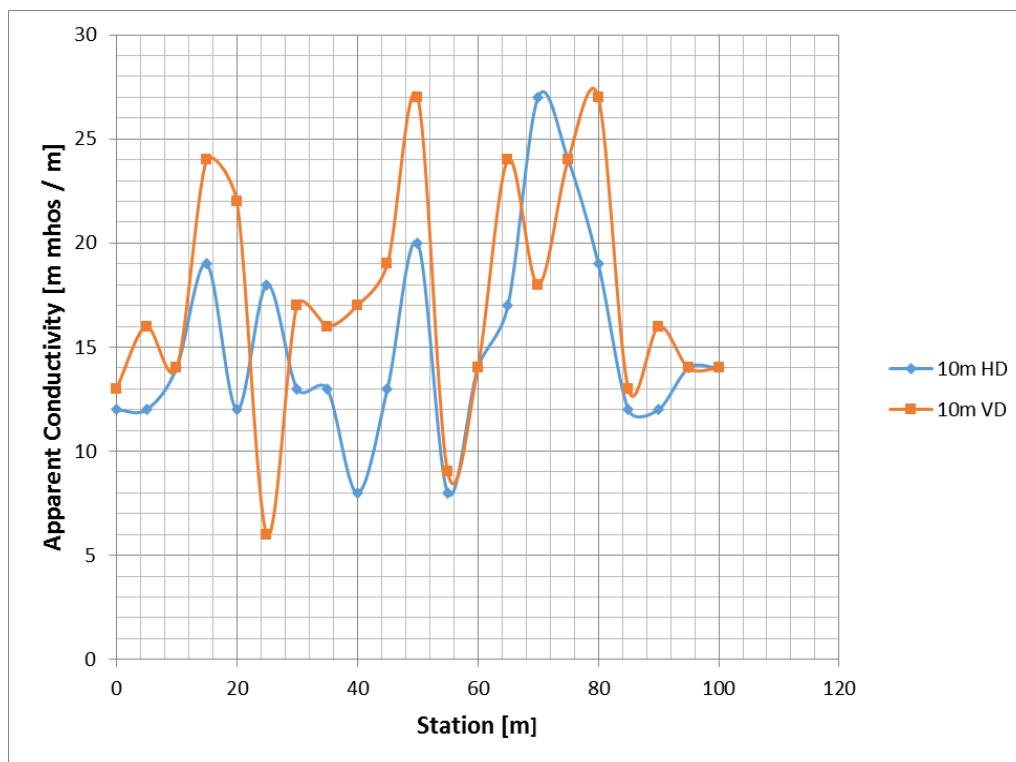


Figure 5.63. EM terrain conductivity measurements along a profile A at Nyamebekyere No. 2 Community

EM traverse B was carried out on a profile length of 350 m; and on a bearing of 275° from the True North. The EM readings were taken using 20 m coil separation and at 10 m intervals.

The apparent conductivity of the community ranges between 3 m mhos/m and 29 m mhos/m with an average value of 14.10 m mhos/m. The erratic nature of the VD and

HD mode curves suggests a complex subsurface geology. Most parts of the profile show higher apparent conductivity values for VD mode than the HD mode from the begging of the profile to end which also suggests a possible fracture at deeper subsurface. There are five outstanding peak on the graph (shown in Figure 5.63) and two were selected for further investigations. The highest peak was not selected probably because of it closeness to stream corridor. It could be inferred by the characteristics these EM survey results that; the subsurface beneath this traverse contain groundwater. The stations that were selected for further investigations are stations 220 m and 300 m.
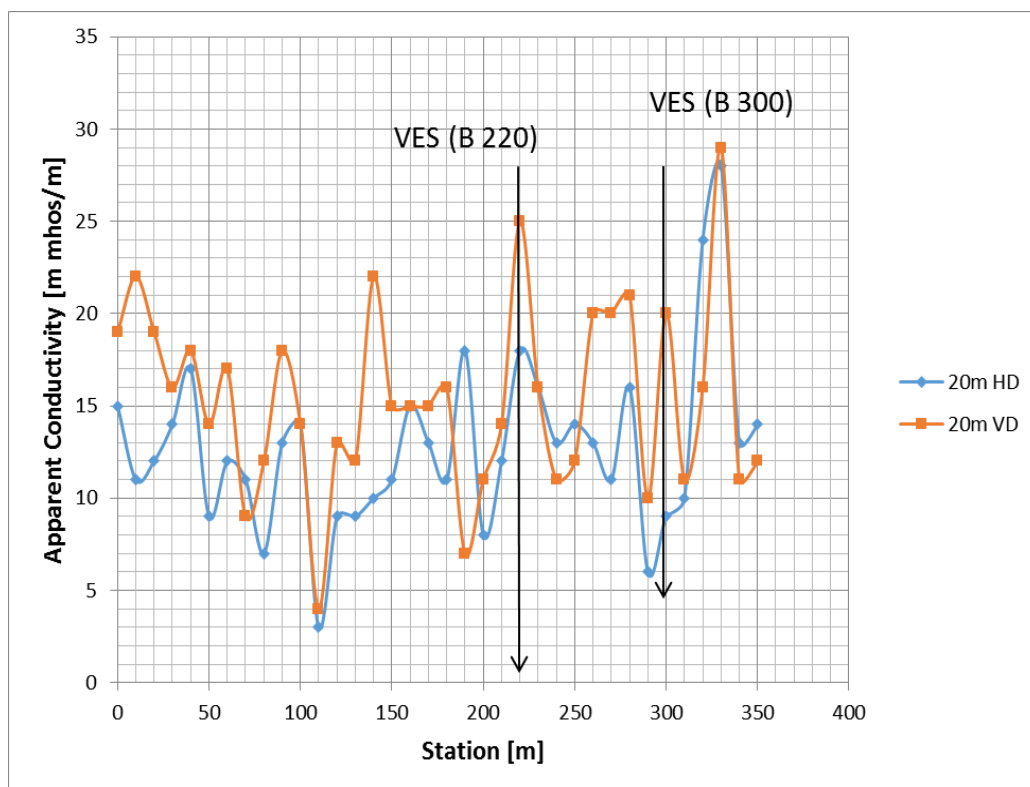


Figure 5.64. EM terrain conductivity measurements along a profile B at Nyamebekyere N0. 2Community

The traverse C was carried out on a profile length of 120 m on a bearing of 135˚ from the True North. The EM readings were taken using 10 m coil spacing at 5 m intervals.

The results of EM profiling as shown in Figure 5.64 displays an erratic movement of both VD mode and HD mode curves along the profile. This suggests the subsurface has complex geological structures. Generally, the apparent conductivities within this

area are high with the maximum of 21 m mhos/m and the minimum of -5 m mhos/m. The average apparent conductivity of the subsurface is 12.78 m mhos/m. Two stations were chosen for VES investigation due to their high terrain conductivity for both VD mode and HD mode. The points are at Stations C10 and C60. These points have high probability of have fracture within their subsurface. From the Figure 5.86, two zones could be identified; zone of high terrain conductivities which starts from Station 0 m to Station 100 m. The second zone which has low terrain conductivity values starts from Station 100 m to the end of the profile. The first zone is of interest because of high conductivities within the geology of this area may be due to fractures and weathered zones which are sites for accumulation of groundwater.
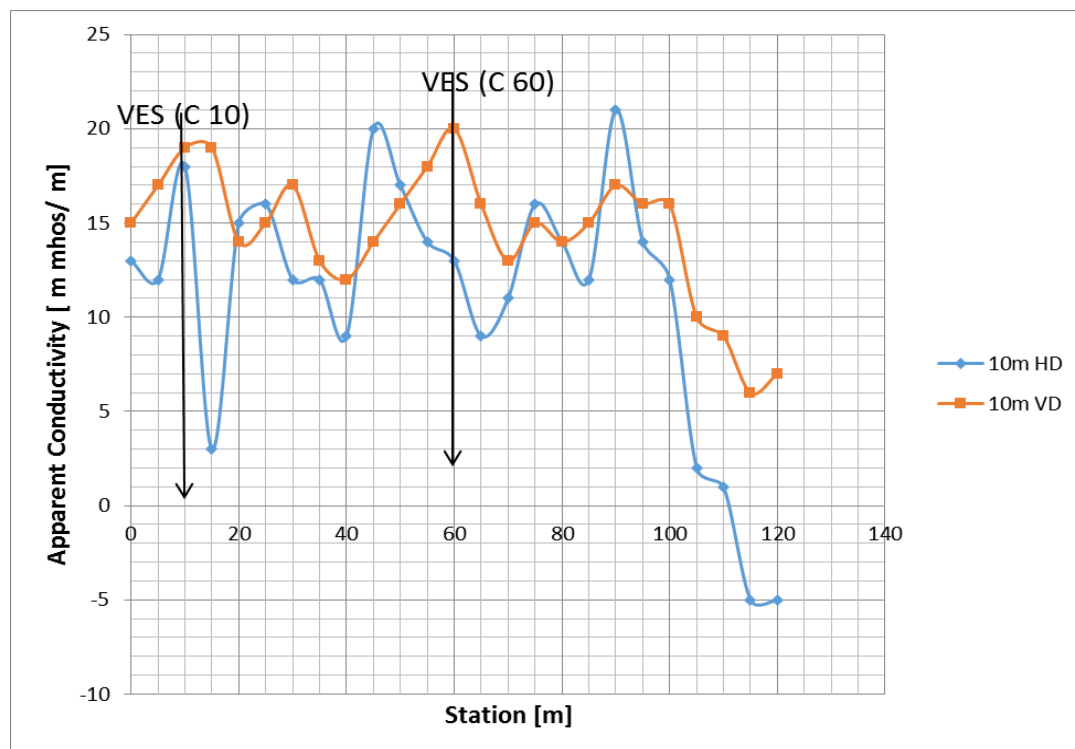


Figure 5.65 EM terrain conductivity measurements along a profile C at Nyamebekyere No. 2 Community.

### 5.4.9.3. Sounding curves

VES B220

The VES modelled curve and pseudosection of the subsurface at station B220 in the Nyamebekyere No. 2 Community depicted four layers as shown in Figures 5.65. The curve indicated a special form of KH curve type where the second layer has the

highest resistivity value. The layers apparent resistivity values varied from 481.88 Ωm to 1996.12 Ωm. First layer's apparent resistivity value is about 907 Ωm with thickness of 0.90 m. Second layer has an apparent resistivity value of 1996.12 Ωm and a thickness of 1.77 m. Third layer has apparent resistivity value of 481.88 Ωm with thickness of 17.36 m. The fourth layer has an apparent resistivity of 915.78 Ωm.
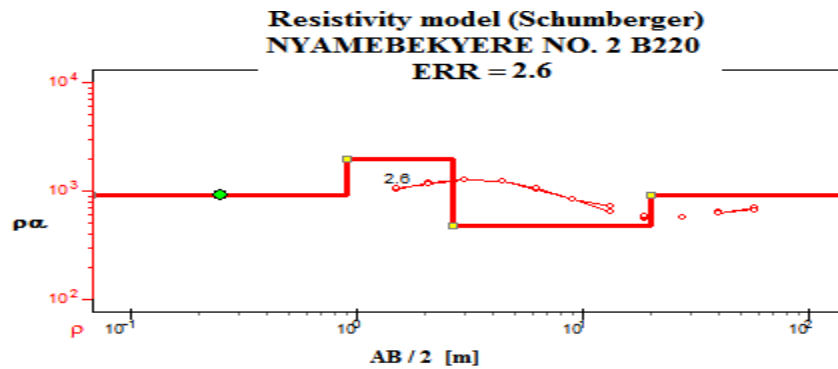


| N | ρ | h | z |
|---|---|---|---|
| 1 | 907.32 | 0.90 | 0/0 |
| 2 | 1996.12 | 1.77 | 0.90 |
| 3 | 481.88 | 17.36 | 2.67 |
| 4 | 915.78 |  | 20.03 |
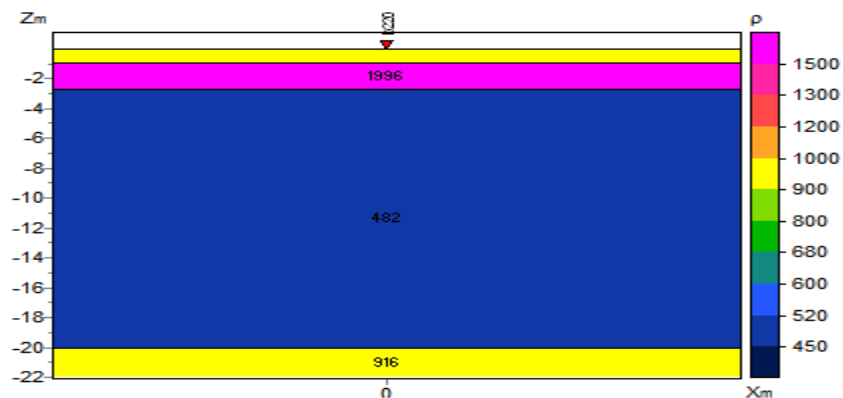
Figure 5.66. VES model curve at station B220 m, Nyamebekyere No. 2 Community

There is a slight decrease of apparent resistivity from the first layer to the second layer and sharp decrease of apparent resistivity value from the second layer to the third layer. An increase in apparent resistivity value was observed from third layer to the fourth layer. The third layer recoded the minimum apparent resistivity value with the largest thickness. These observations show a possible presence of fracture or

weathered zones in the third layer. These are conditions for groundwater accumulation. The third layer and the fourth layer have high probability of containing groundwater and hence VES B220 is recommended for drilling of boreholes.

VES B300 HA
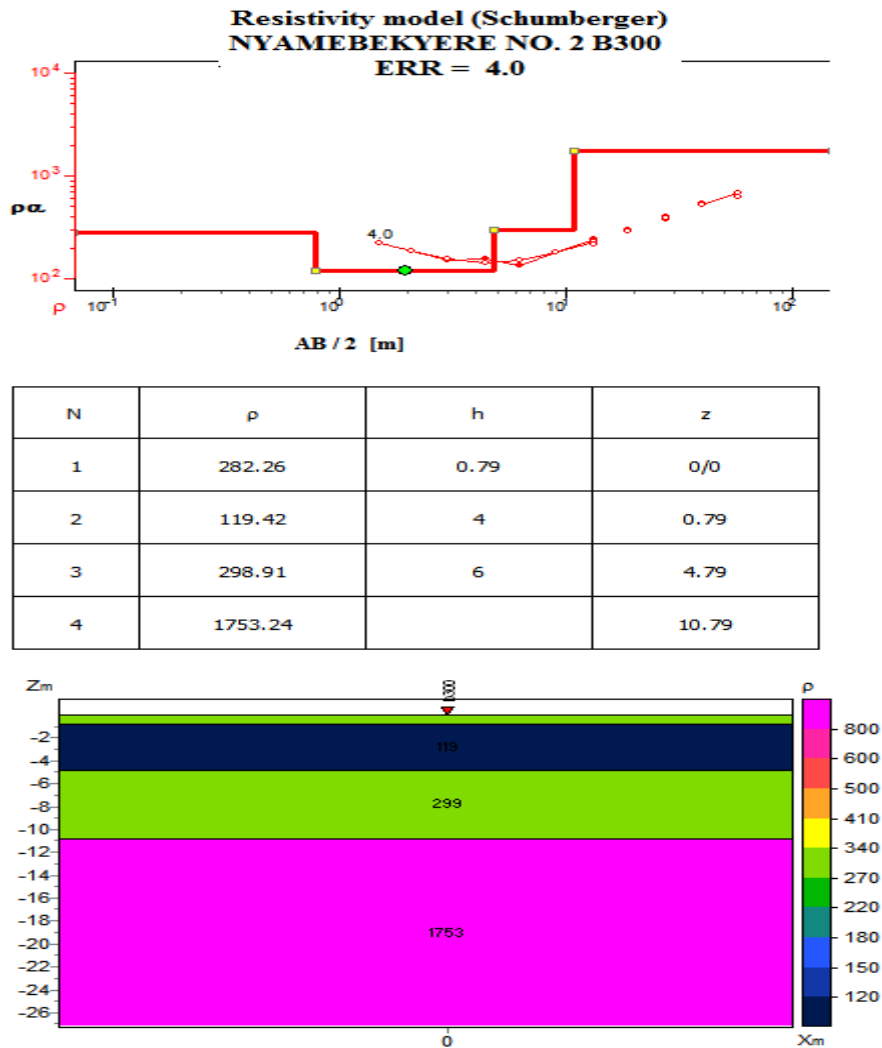


Figure 5.67. VES model curve at station B300 m, Nyamebekyere No. 2 Community

The subsurface structure at station VES B300 is made up of four layers and their apparent resistivity values range between 119.42 Ωm and 1753.24 Ωm. The sounding curve displays HA – type curve with second layer having the minimum resistivity values and hence higly wearthered. The results from both modelled sounding curve and pseudosection (Figures 5.66) indicate that, Topsoil has an apparent resistivity value of 282.26 Ωm and a thickness of 0.79 m. Second layer has apparent resistivity

value of 119.42 Ωm and a thickness of 4.0 m. Third layer has a thickness of 6.0 m with apparent resistivity value of 298.91 Ωm. This layer is underlain by fourth layer of apparent resistivity value 1753.24 Ωm.

There is a slight decrease of the apparent resistivity value from first layer to second layer and an increase from the second layer to third layer. There is a sharp increase of apparent resistivity value from the third layer to the fourth layer indicating likely presence of fracture within the third layer. By considering the apparent resistivity values and the thickness of the layers, it would be observed that, second and third layers would be good zones for groundwater accumulation and hence this station is recommended for drilling of borehole.

VES C10

It is inferred from the results of VES at station C10 that; the subsurface underlain this station is made up of three layered structure. The apparent resistivity values of the layers range between 621.40 Ωm and 1627.76 Ωm, as shown Figures 5.67; First layer has an apparent resistivity of 621.40 Ωm and a thickness of 0.58 m. Second layer has a thickness of 19.97 m and an apparent resistivity value of 694.29 Ωm. The apparent resistivity values of first and second layer are very close to each other with a difference of about 70 Ωm. Third layer which also serves as bedrock has an apparent resistivity of 1627.76 Ωm. The apparent resistivity values at this station increases with increasing depth. The first two layers have high probability of containing accumulated groundwater resource and hence the point is recommended for drilling or hand dug a borehole.
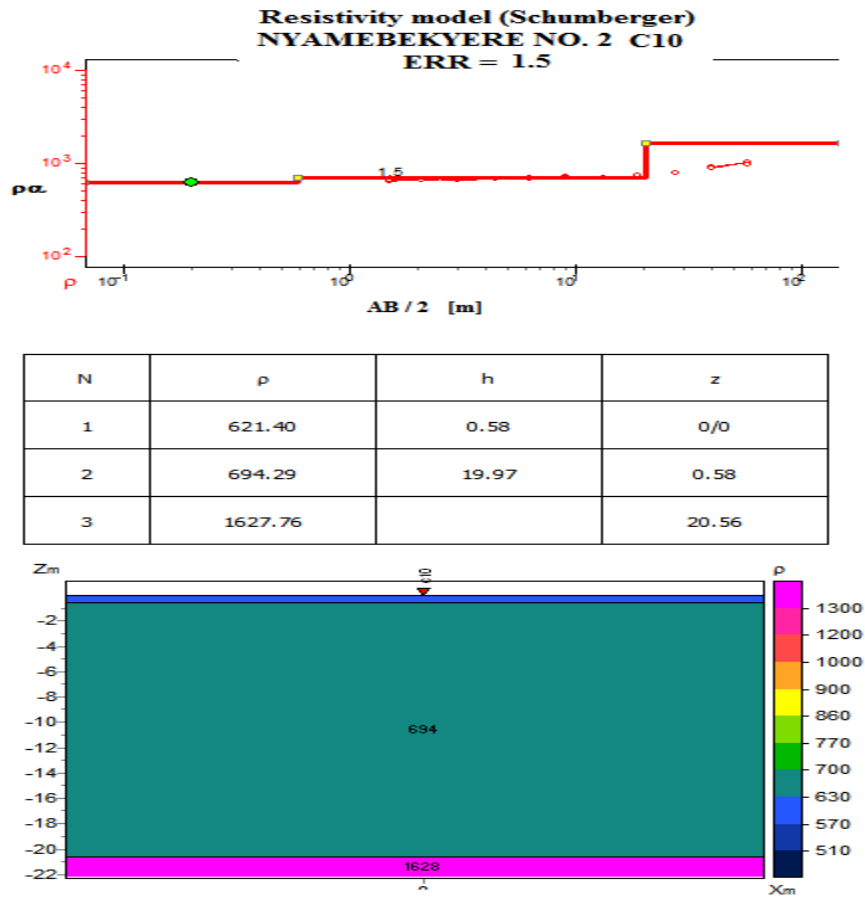
Figure 5.68. VES model curve at station C10 m, Nyamebekyere No. 2 Community

## VES S1

This is the last VES station conducted in this community for the purpose of this project. The point for this VES was chosen not on any of the EM profiles. It was however located near the end of traverse B. The sounding curve is QH – type with the third layer having low resistivity value. The sounding curve and its pseudosection as shown in Figure 5.68 below reveal a four layered subsurface structures beneath this station. First layer, second layer and third layer have apparent resistivity values of 1334.24 $\Omega$m, 755.95 $\Omega$m and 173.65 $\Omega$m respectively. The thicknesses of first, second and third layers are 1.58 m, 3.28 m and 8.55 m respectively. The final layer revealed in this model has an apparent resistivity value of 8689.18 $\Omega$m.

**Resistivity model (Schumberger)**
**NYAMEBEKYERE NO. 2 S1**
**ERR = 3.8**

| N | ρ | h | z |
|---|---|---|---|
| 1 | 1334.24 | 1.58 | 0/0 |
| 2 | 755.95 | 3.28 | 1.58 |
| 3 | 173.65 | 8.55 | 4.85 |
| 4 | 8689.18 | | 13.40 |
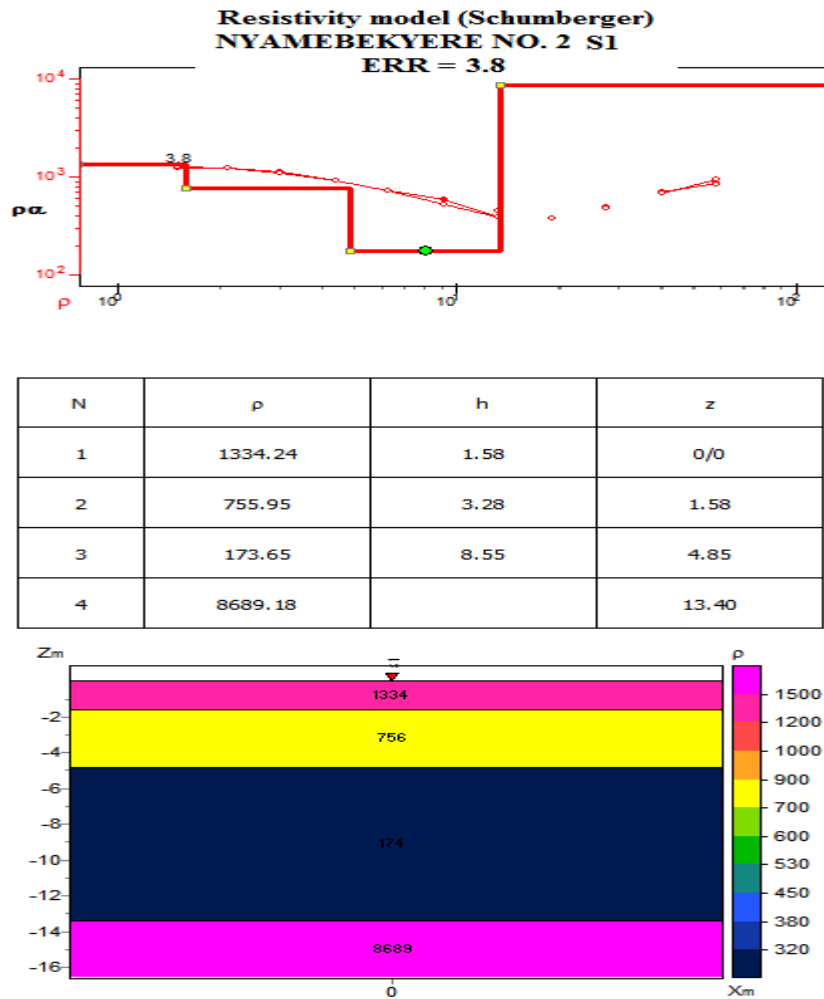
Figure 5.69. VES model curve at station Nyamebekyere No. 2 Community

The third layer beneath this station show a high probability of containing accumulated groundwater which would be sufficient to be drilled for public usage and hence this station is recommended for drilling of borehole.

### 5.4.9.4. Discussions of results from Nyamebekyere No. 2 Community

Generally, the Nyamebekyere No. 2 Community is underlain by four geological layers. Out of the five VES stations investigated in the community only one station (C10) revealed a three – layered geological subsurface structure, the rest indicated a four- layered structure. From the obtained apparent resistivity values of the sounding curves models; the third layer in almost all the VES stations has the minimum resistivity values which is inferred to be due to fractures and is a water – bearing layer.

First layer has apparent resistivity values ranging within 282.26 – 1334.24 Ωm and can be intercepted at a mean depth of 0.91 m. The second layer, which has a thicknesses range of 1.77 – 19.97 m, has a mean apparent resistivity value of 918.95 Ωm. The third layer has thicknesses range of 6.0 – 17.36 m and a mean apparent resistivity value of 332.70 m. The fourth layer has apparent resistivity values ranging from 915.78 – 8689.18 Ωm.

The area mapped within the community generally has a moderate to little quantities of groundwater according to the contour map models use in this project. Most part of the mapped area are in the A zone which indicated that there are little groundwater beneath the area. Drilling boreholes in this zone may not yield groundwater that could be enough for public usage and if water is enough it might stand the dry seasons.

Of the five VES stations investigation, the GPS coordinates of only three stations as shown on the contour maps in Figures 5.69a – 5.69c were available. Because of this reason the ranking of the VES stations largely lies on the sounding curves, unlike in other community were the rankings are made base on the sounding curves model and contour maps model. Table 5.15 provides a summary of the VES results including a rank – list of the selected points for drilling.
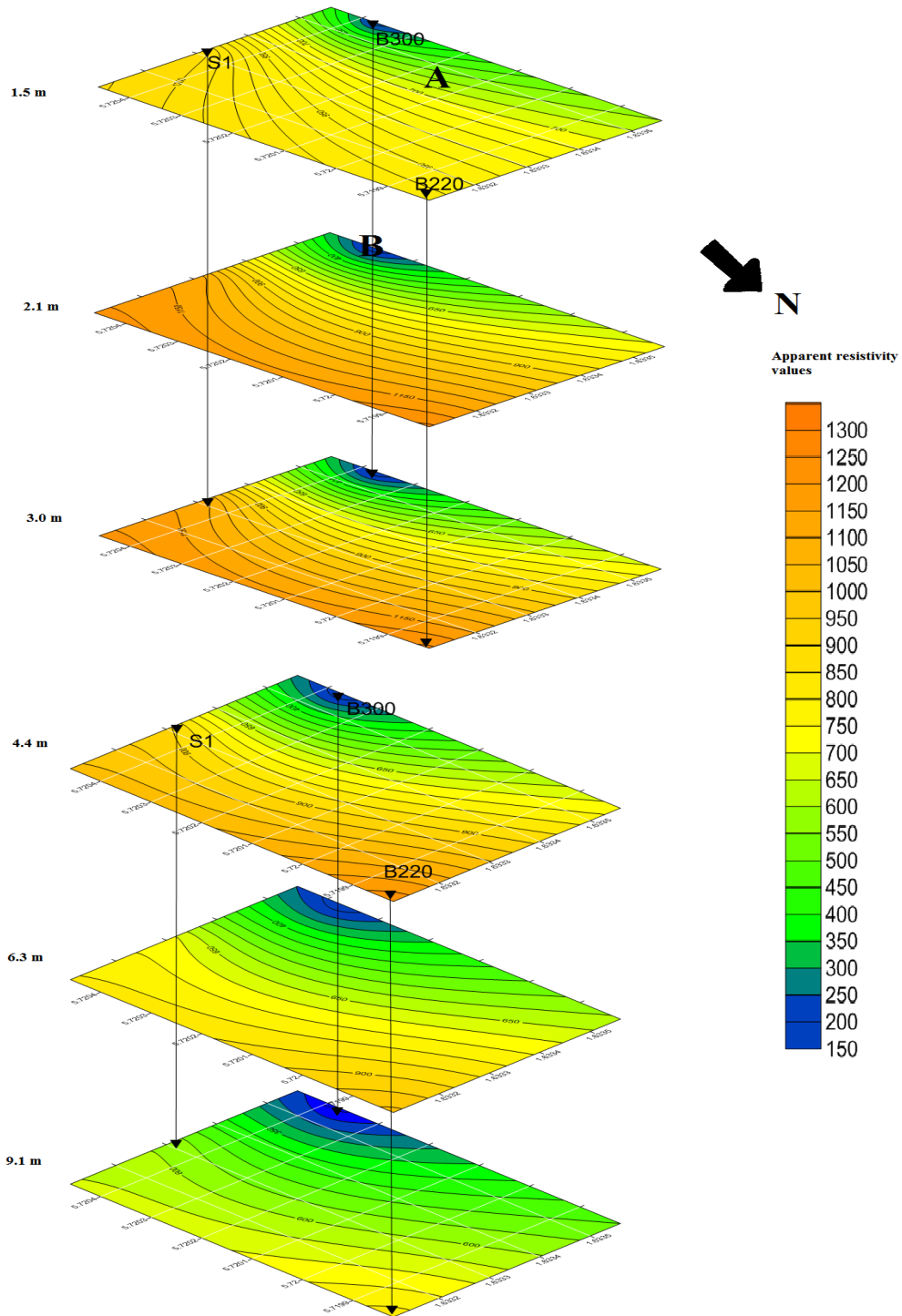
Figure 5.70a. Apparent resistivity contour maps from depth 1.5 to 9.1m at Nyamebekyere No. 2 Community
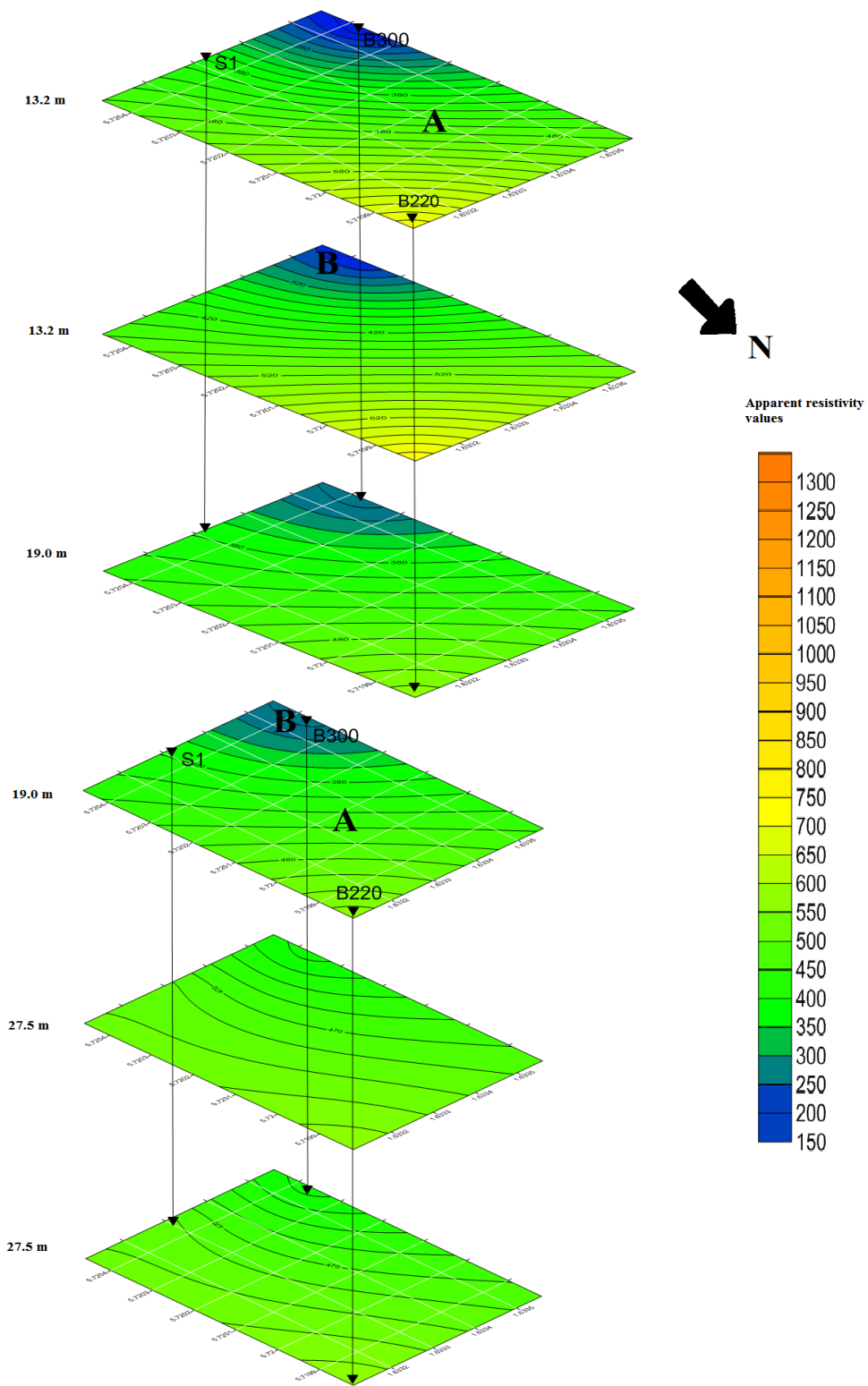
Figure 5.70b. Apparent resistivity contour maps from depth 13.2 to 27.5 m at Nyamebekyere No. 2 Community
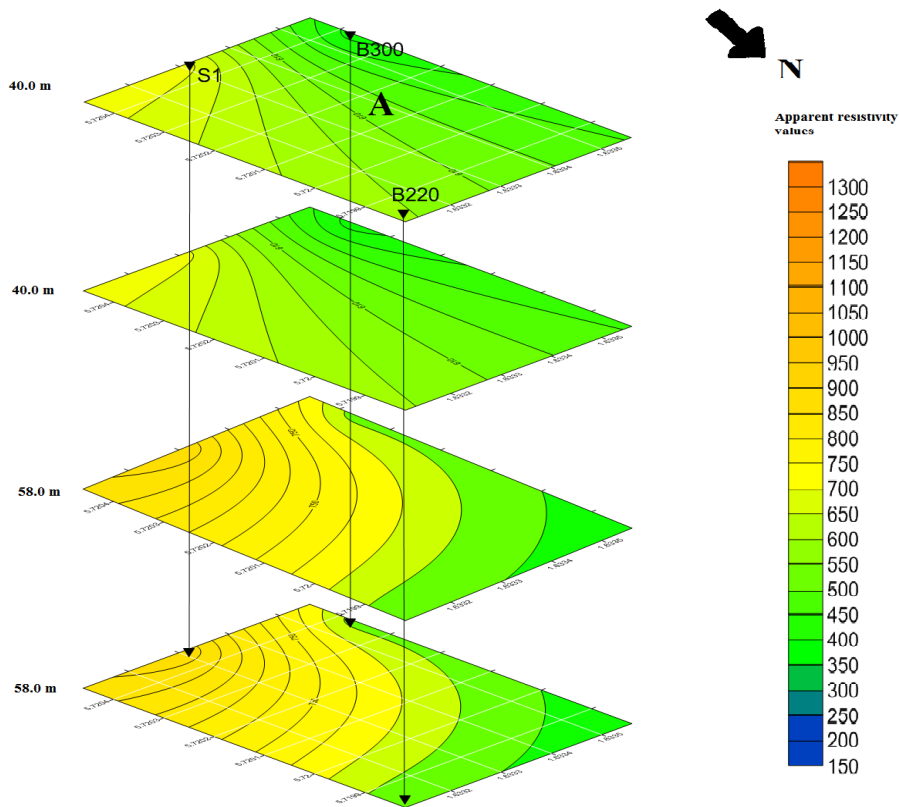
Figure 5.70c. Apparent resistivity contour maps from depth 40 to 58.0 m at Nyamebekyere No. 2 Community

Table 5.15. Ranked VES points for hand-dug well development at Nyamebekyere No. 2 Community

| VES Point | Layer | ρ (Ωm) | Depth (m) | Thickness (m) | Rank | Location (GPS) | Remarks |
|---|---|---|---|---|---|---|---|
| | 1 | 282.26 | 0.79 | 0.79 | | 5.72037N | |
| | 2 | 119.42 | 4.79 | 4.00 | | 1.63356W | |
| | 3 | 298.91 | 10.79 | 6.00 | | | |
| B300 | 4 | 1753.24 | - | - | 1st | | |
| | 1 | 1334 | 1.58 | 1.58 | | 5.72046N | |
| | 2 | 755.95 | 4.85 | 3.28 | | 1.63331W | |
| | 3 | 173.65 | 13.40 | 8.55 | | | |
| S1 | 4 | 8689.18 | - | - | 2nd | | |
| | 1 | 458.08 | 0.69 | 0.69 | | | |
| | 2 | 1028.99 | 4.63 | 3.93 | | | |
| | 3 | 376.36 | 18.43 | 13.80 | | | |
| C60 | 4 | 1854.60 | - | - | 3rd | | |
| | 1 | 907.32 | 0.90 | 0.90 | | 5.71982N | |
| | 2 | 1996.12 | 2.67 | 1.77 | | 1.63311W | |
| | 3 | 481.88 | 20.03 | 17.36 | | | |
| B220 | 4 | 915.78 | - | - | 4th | | |
| | 1 | 621.40 | 0.58 | 0.58 | | | |
| | 2 | 694.29 | 20.56 | 19.97 | | | |
| C10 | 3 | 1627.76 | - | - | 5th | | |

### 5.4.10. Nyame Ye Adom

### 5.4.10.1. Introduction

In Nyameyeadom Community three traverses were carried out and a total of six stations were survey using the resistivity method of vertical electrical sounding. The VES results displayed 3 curve types and they are H, KA and KH. Figure 5.70 shows the schematic layout of the community. The EM profiles were carried out on all the four traverses using 20 m coil separations and the EM readings were taken at 10 m intervals.

Table 5.16 below shows the existing boreholes within the 5 Km radius around Nyame Ye Adom Community. This data was used as guide during the survey and the interpretation of the geophysical results.

Table 5.16. Existing Boreholes within 5 Km radius around Nyame Ye Adom Community (Mainoo et al. 2007f)

| Community | BH No. | Depth (m) | Yield ($m^3/h$) | SWL (m) | Water Quality | Lithology | Calibration |
|---|---|---|---|---|---|---|---|
| KYEKYEWERE | 050/D/09-2 | 42 | 0.72 | 8.77 | N/A | Granite / Gneiss | |
| KYEKYEWERE | 050/D/09-3 | 29 | 5.1 | 10.43 | N/A | Granite / Gneiss | |
| KYEKYEWERE | 050/D/09-4 | 35 | 1.02 | 8.15 | N/A | Granite / Gneiss | |
| KYEKYEWERE | 050/D/09-5 | 32 | 3 | 10.17 | N/A | Granite / Gneiss | |
| KYEKYEWERE | 050/D/09-6 | 39 | 3 | 16.71 | N/A | Schist | |

Figure 5.71. Schematic Layout of Nyameyeadom Community (not to scale)

### 5.4.10.2. EM traverses

Traverse A was carried out on a profile length of 240 m on a bearing of 058° from the True North. Figure 5.71 shows the graph of the apparent conductivity curves for HD mode and VD mode. From the Figure, the maximum, minimum and average terrain conductivity values are 29.0, 10.0 and 14.04 m mhos/m respectively.
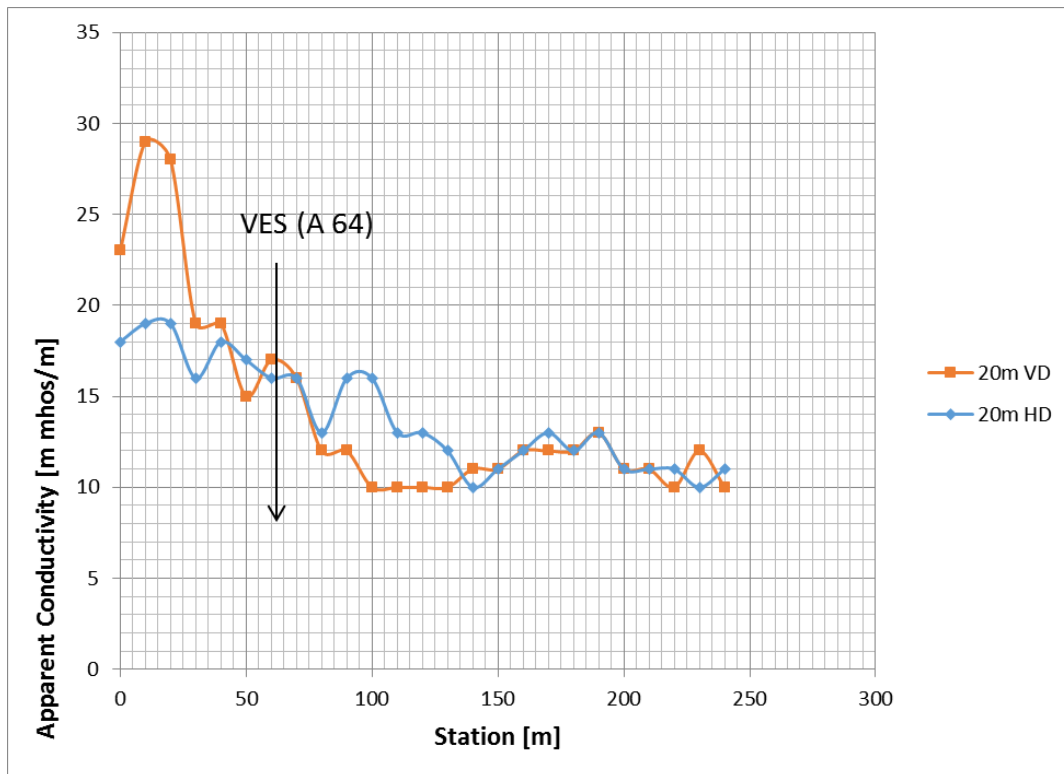


Figure 5.72. EM terrain conductivity measurements along a profile A at Nyameyeadom Community

The high apparent conductivity values from stations 0 m to 30 m are due to roof. Aside that generally the HD mode curve has higher terrain conductivity values than the VD mode curve. On the graph in Figure 5.91, stations 30 − 70 m recorded the higher values for the VD mode. These terrain conductivity values are high and that suggests a possible fracture. One station at 64 m is selected for further VES investigation. The EM interpretation of this point suggests a groundwater at its subsurface.
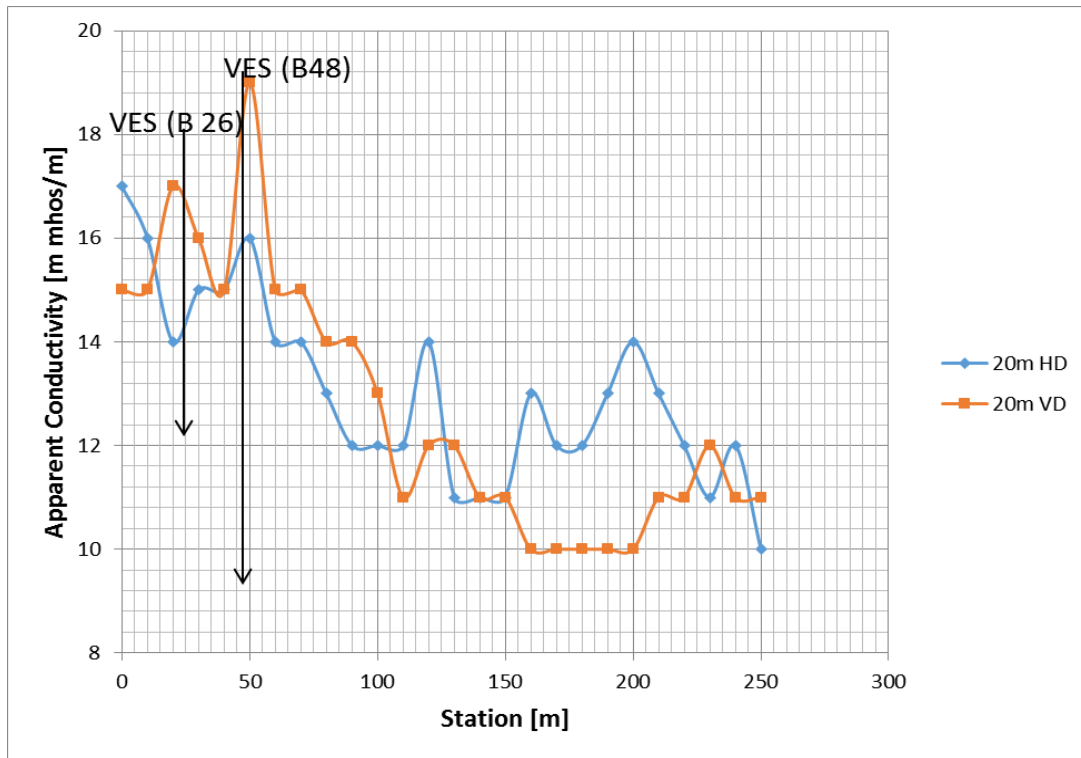
Figure 5.73. EM terrain conductivity measurements along a profile B at Nyameyeadom Community

The profile was on traverse B was carried out on a bearing of 075° from the True North. The EM readings were taken at 10 m intervals using 20 m coil spacing on a profile length of 250 m long. The maximum apparent conductivity value on this profile is 19 m mhos/m, the minimum and average apparent conductivity values are 10 m mhos/m and 12.88 m mhos/m respectively.

Generally, the both HD and VD modes curves move erratically throughout the profile. From Figure 5.72, the VD mode curves made a sharp increment in terrain conductivity from station 40 m to 60 m. It suggests a fracture along the profile. The HD mode curve generally dominate the VD mode in terms of high apparent conductivity values. The areas of interest are point with high terrain conductivity for the VD mode or both VD and HD mode. The behaviour of the curves indicate a fractured zone beneath this profile line between station 10 m to 110 m. Station 26 and 48 were selected for resistivity sounding to confirmed availability of groundwater.

Traverse C was carried out on a bearing of 085° from the True North and on a profile length of 280 m. The EM readings were taken using a coil separation 20 m at 10 m intervals.

The average apparent conductivity on graph in Figure 5.73 below is 14.17 m mhos/m with the maximum terrain conductivity of 20.0 m mhos/m and the minimum of 10.0 m mhos/m. Generally, the HD mode curve has high terrain conductivity values than VD mode. But although the HD mode has higher apparent conductivity values than VD mode, the difference is very small. The apparent conductivity values from station 150 m to 210 m along the profile display a behaviour that suggest a high fracture within the subsurface. That zone recorded the highest apparent conductivity value and two points were selected from this zone for further investigation. The points are C158 and C204. The other point which was also selected is C118 which on a crossover point between the HD and VD mode curves. Both curves are erratic in nature which suggests a complex geological subsurface. From this EM profiling results, it is inferred that those three selected points contain groundwater and that the points would be confirmed by resistivity sounding method.
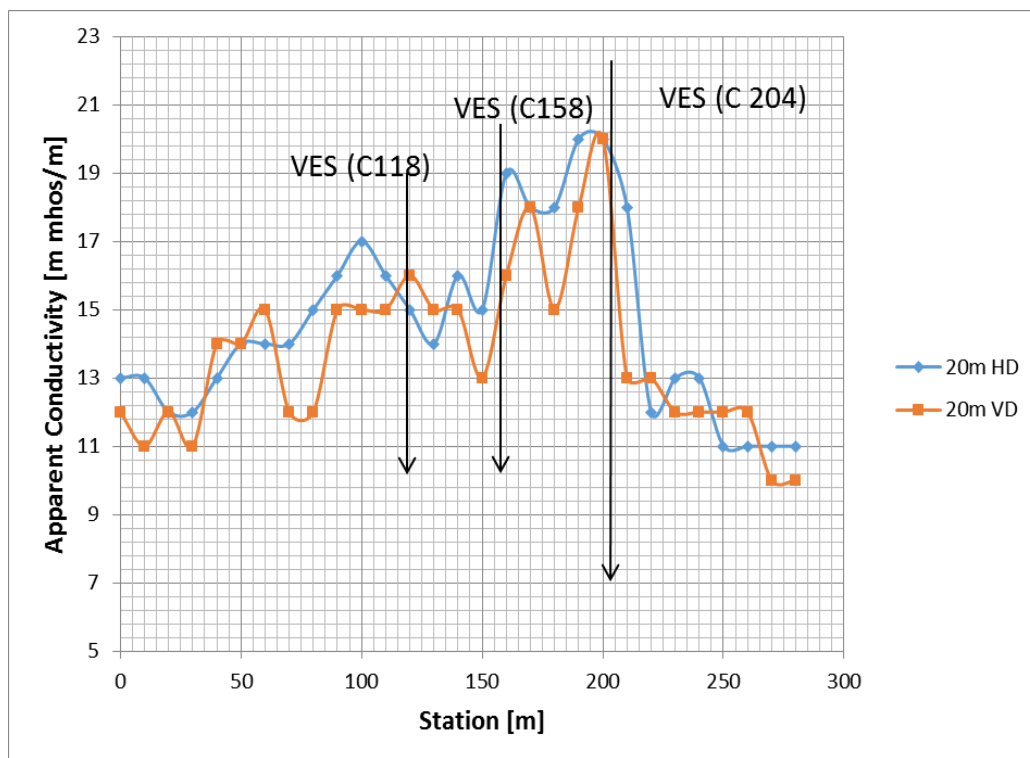


Figure 5.74. EM terrain conductivity measurements along a profile C at Nyameyeadom Community

### 5.4.10.3. Sounding curves

VES A64



**Resistivity model (Schumberger)**
**NYAME YE ADOM A64**
**ERR = 5.8**

| N | ρ | h | z |
|---|---|---|---|
| 1 | 73.28 | 0.79 | 0/0 |
| 2 | 219.40 | 2.30 | 0.79 |
| 3 | 45.20 | 5.10 | 3.09 |
| 4 | 7239.40 | | 8.19 |
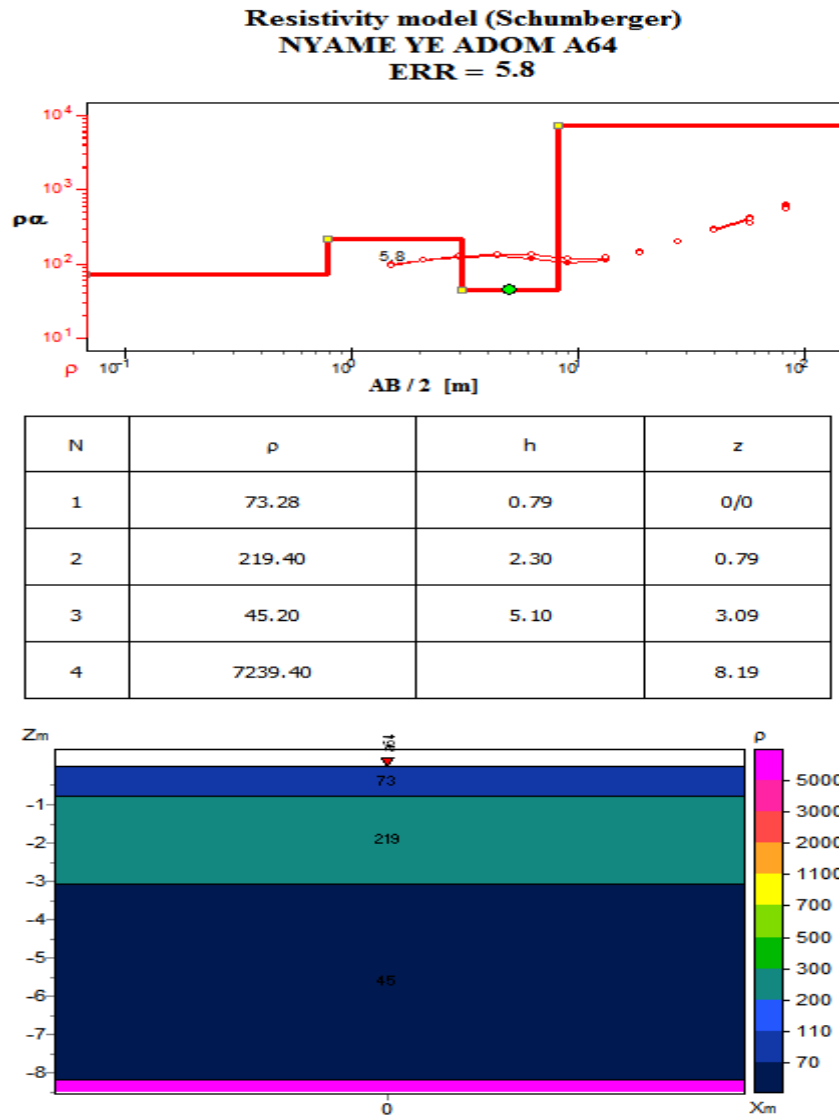
Figure 5.75. VES model curve at station A64 m, Nyameyeadom Community

Analyses of VES results at station A64 as shown in the Figure 5.74 indicates a four -layered model with apparent resistivity values ranging between 45.20 Ωm and 7239.40 Ωm. The curve is KH – type. Top layer has an apparent resistivity value 73.28 Ωm and thickness of 0.79 m, this is followed by second layer of apparent resistivity value of 219.40 Ωm and a thickness of 2.30 m. Third layer has apparent resistivity value of 45.20 Ωm and a thickness of 5.10 m. Fourth layer has apparent resistivity of 7239.40 Ωm. The apparent resistivity values of the first three layers of

this station suggest the presence of weathered zone or fractured zone within the first three layers and that there is groundwater resource beneath this station. Hence this station is recommended for drilling.

VES B48



| N | ρ | h | z |
|---|---|---|---|
| 1 | 516.72 | 0.87 | 0/0 |
| 2 | 76.46 | 7.49 | 0.87 |
| 3 | 3773.48 | | 8.36 |
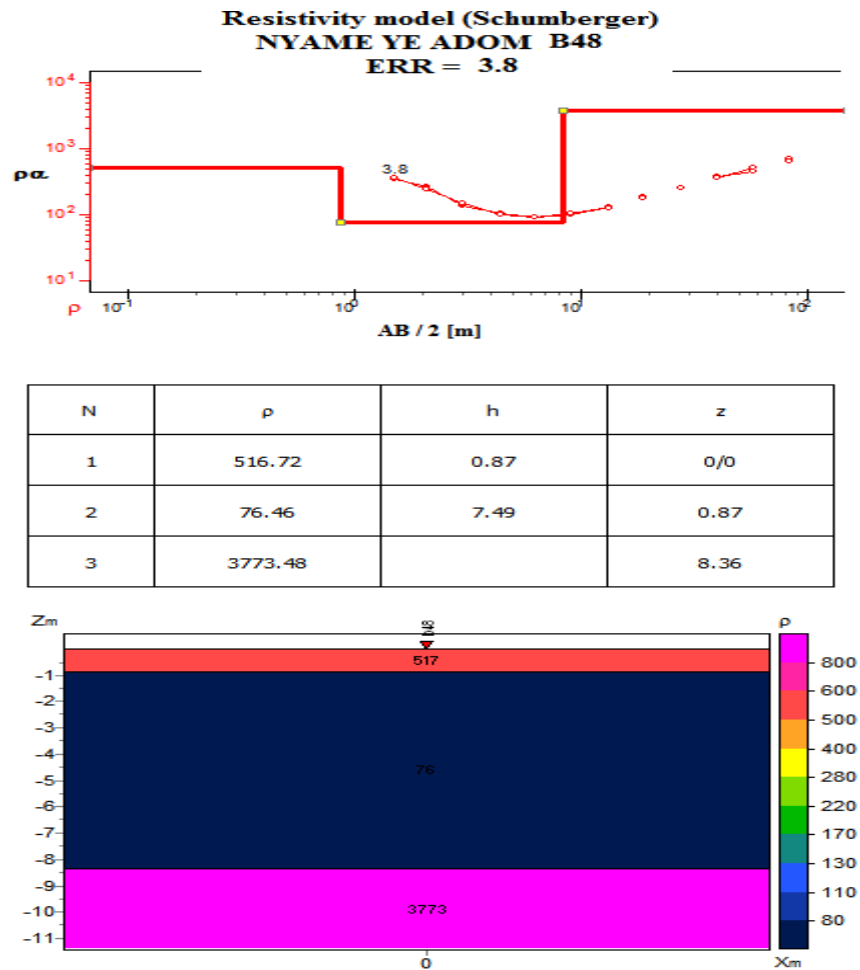
Figure 5.76. VES model curve at station B48 m, Nyameyeadom Community

Results from the VES at station B48 revealed three subsurface structures as shown in Figure 5.75. Apparent resistivity values ranges from 76.46 Ωm to 3773.48 Ωm with first layer having thickness of 0.87 m and apparent resistivity of 516.72 Ωm. Second layer has a thickness of 7.49 m and apparent resistivity value of 76.46 Ωm; and the deepest layer has apparent resistivity of 3773.48 Ωm.

Deductions made from these result is that; the first layer is weathered and second layer highly fractured and contains groundwater. This station is recommended for drilling of borehole.
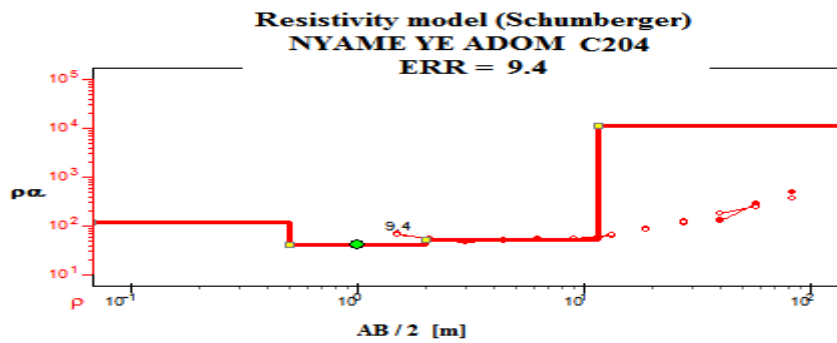
VES C204
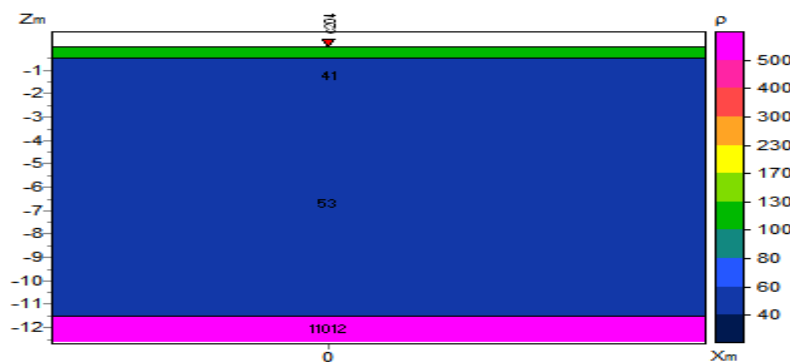


Figure 5.77. VES model curve at station C204 m, Nyameyeadom Community

The VES C204 revealed a four - layered subsurface structure (see Figure 5.76). The apparent resistivity values range between 40.74 Ωm and 11011.90 Ωm. First, second and third layers have thicknesses of 0.50 m, 1.50 m and 9.54 m respectively. The apparent resistivity values for first layer is 119.25 Ωm, this value drops to 40.74 Ωm in second layer, the apparent resistivity slightly increases to 52.72 in third layer and finally rise drastically to 11011.90 Ωm in fourth layer. The apparent resistivity values, depths and thicknesses of the layers suggest a weathering in the first layer

and heavy fracture in second and third layers; and that the first three layers contain groundwater in high quantity. Hence this station was recommended for drilling of borehole.

### 5.4.10.4. Discussions of results from the Nyame Ye Adom Community

Analyses of VES stations conducted within this community suggest that Nyame Ye Adom Community is underlain by three – four geological layers. The first layer has apparent resistivity values ranging from 55.11 - 1184.67 Ωm and a mean depth of 0.98 m. The second layer has thicknesses ranging from 1.50 – 9.03 m and a mean apparent resistivity value of 136.29 Ωm. The third layer also has a mean apparent resistivity value of 51.76 Ωm and thicknesses ranging from 5.10 – 9.54 m. the fourth layer has apparent resistivity values ranging from 3773.48 – 17574.20 Ωm. The second layer and the third layer are expected to be water – bearing layers in this community. The general characteristic of the VES station investigated in this community is that, they mostly have high resistive top layers and last layers, these layers sandwich less resistive layers between them.

The contour maps in Figures 5.77a to 5.77d are the pictorial views of the subsurface in terms of measured apparent resistivity and depths. It is noticed that, the community is underlain by high quantity of groundwater. VES stations C204 and C158 for instance have signs of high quantity of groundwater (area labelled B) showing beneath them from 1.5 m depth to 58.0 m. Table 5.17 shows a summary of the VES results including a rank-list of the selected points for drilling in this community. There is no risk of drilling at any of the pointed investigated in this community and that all would yield high quantity of groundwater.
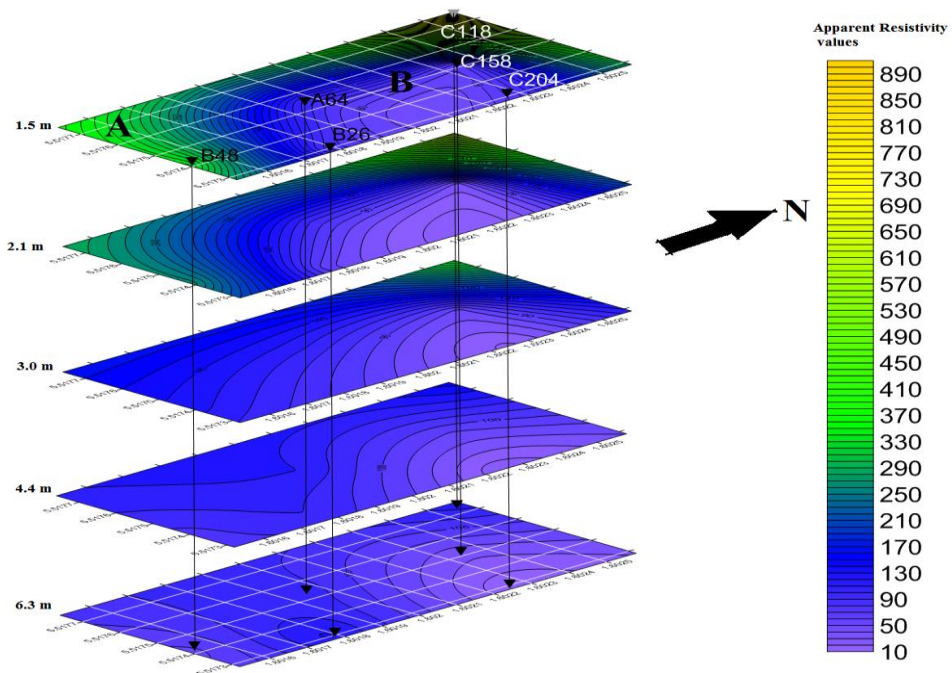
Figure 5.78a. Contour maps showing the apparent resistivity values from depth 1.5 – 6.3 m beneath the Nyameyeadom Community
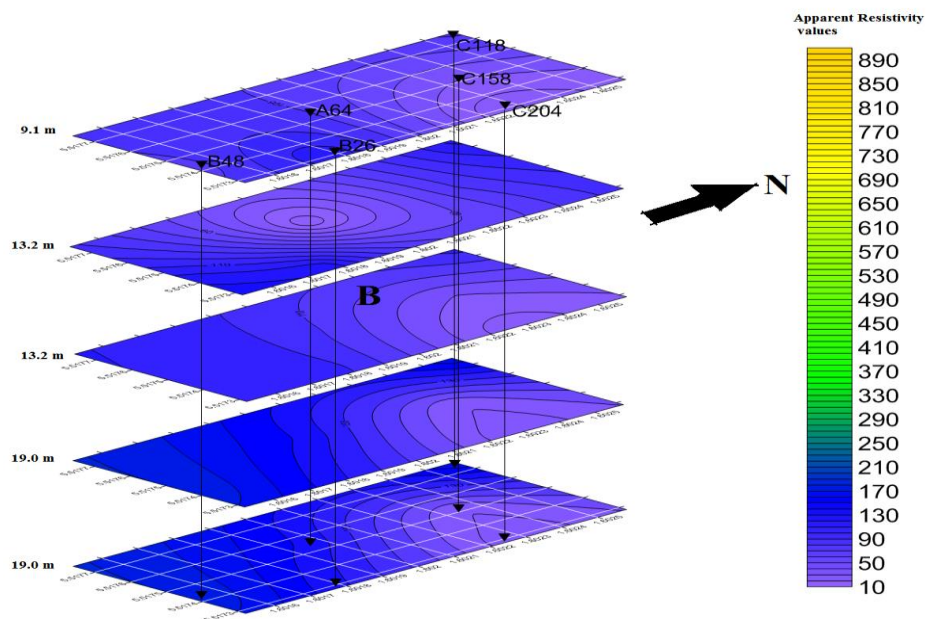


Figure 5.78b. Contour maps showing the apparent resistivity values from depth 9.1 – 19.0 m beneath the Nyameyeadom Community
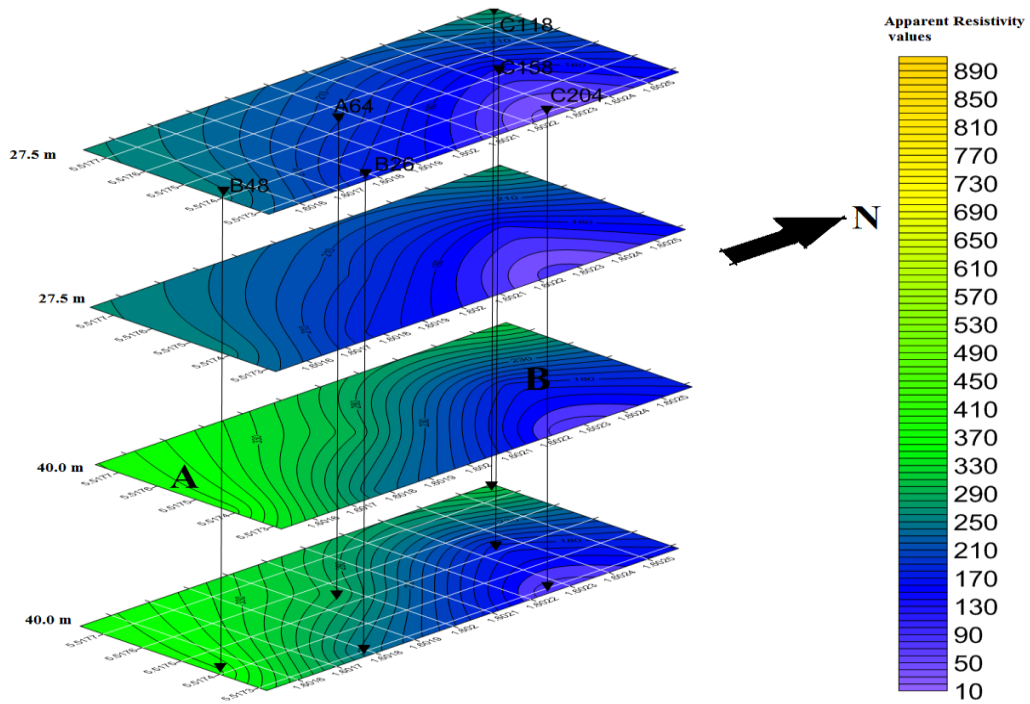
Figure 5.78c. Contour maps showing the apparent resistivity values in the depth range of 27.5 – 40.0 m beneath the Nyameyeadom Community
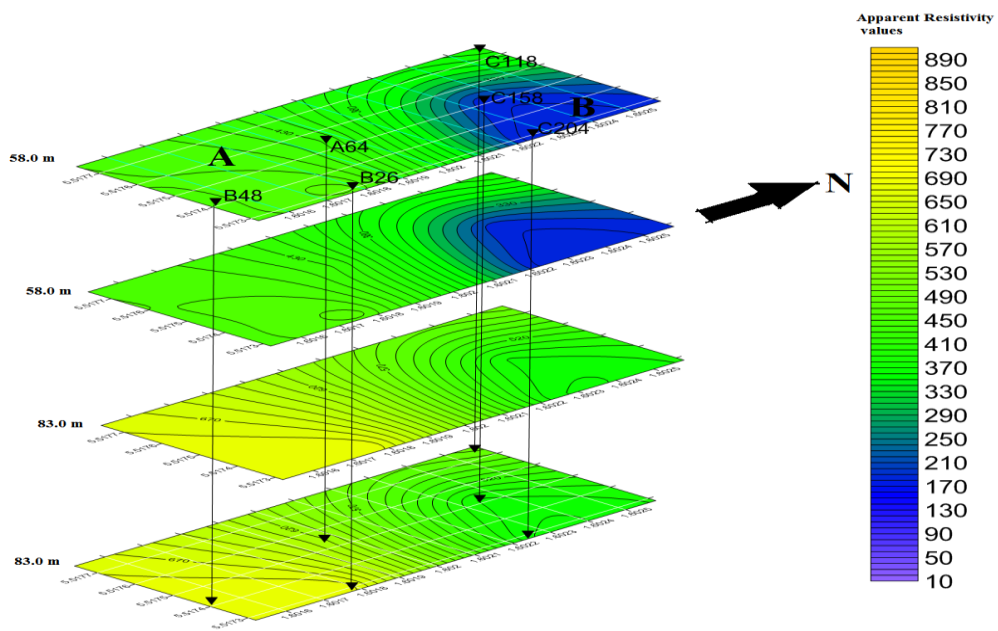


Figure 5.78d. Contour maps showing the apparent resistivity values in the depth range of 58.0 – 83.0 m beneath the Nyameyeadom Community

Table 5.17. Ranked VES points for borehole drilling at Nyameyeadom Community

| VES Point | Layer | ρ (Ω−μ) | Depth (m) | Thickness (m) | Rank | Location (GPS) | Remarks |
|---|---|---|---|---|---|---|---|
| | 1 | 119.25 | 0.50 | 0.50 | | 5.51728N | |
| | 2 | 40.74 | 2.00 | 1.50 | | 1.60225W | |
| | 3 | 52.72 | 11.54 | 9.54 | | | |
| C204 | 4 | 11011.90 | - | - | 1st | | |
| | 1 | 55.11 | 0.90 | 0.90 | | 5.51752N | |
| | 2 | 117.50 | 3.00 | 2.10 | | 1.60235W | |
| | 3 | 40.82 | 9.20 | 6.20 | | | |
| C158 | 4 | 5547.90 | - | - | 2nd | | |
| | 1 | 73.28 | 0.79 | 0.79 | | 5.51755N | |
| | 2 | 219.40 | 3.09 | 2.30 | | 1.60197W | |
| | 3 | 45.20 | 8.19 | 5.10 | | | |
| A64 | 4 | 7239.4 | - | - | 3rd | | |
| | 1 | 78.82 | 1.79 | 1.79 | | 5.51731N | |
| | 2 | 270.6 | 4.39 | 2.6 | | 1.60178W | |
| | 3 | 68.3 | 11.49 | 7.1 | | | |
| B26 | 4 | 17574.2 | - | - | 3rd | | |
| | 1 | 516.72 | 0.87 | 0.87 | | 5.51741N | |
| | 2 | 76.46 | 8.36 | 7.49 | | 1.60152W | |
| B48 | 3 | 3773.48 | - | - | 5th | | |
| | 1 | 1184.67 | 1.04 | 1.04 | | 5.51776N | |
| | 2 | 93.04 | 10.07 | 9.03 | | 1.60258W | |
| C118 | 3 | 1543.85 | - | - | 6th | | |

## 5.5. Summary

Total of 29 electromagnetic profiles were carried out throughout the 10 communities considered in this work. Profile lengths of traverses range between 410 m and 100 m. The apparent or terrain conductivity values also range between 67 m mhos/m and -20 m mhos/m. The EM readings on 13.79% of the traverse line were taking using 10 m coil spacing and at 5 m intervals. The remaining 86.21% of the traverse line 20 m and 10 m interval was used in taken the EM readings. Table 5.18 shows the summary of the EM profiles.

Generally, the graphs of EM responds in most communities show erratic movements for both HD and VD mode respectively. The erratic nature of the graphs is associated with the complexity of the subsurface. The Microsoft Excel is very good in displaying the EM curves.

Table 5.18. Summary of Electromagnetic Profiles

| Community | No. of EM traverses | Maximum apparent conductivity value (m mhos/m) & its traverse line | Minimum apparent conductivity value (m mhos/m) & its traverse line | Length of traverse lines (m) | | Coil spacing | |
|---|---|---|---|---|---|---|---|
| | | | | Longest | Shortest | 10 m | 20 m |
| Ablaso | 1 | 39 | 3 | 200 | - | ALL | - |
| Aboso | 4 | 16, D | 3, C | 330, B | 240, D & A | - | ALL |
| Achiase | 3 | 20, B | 8, A & C | 350, C | 250, A & B | - | ALL |
| Beseadze | 2 | 36, B | 7, A | 410, B | 390, A | - | ALL |
| Esukese Ekyir | 1 | 67 | -20 | 240 | - | ALL | - |
| Kwanyarko | 4 | 23, D | 6, A | 260, A | 200, D | - | ALL |
| Mbaa Mpe Hia No. 2 | 4 | 19, D | 7, A | 250 | - | - | ALL |
| Moseaso | 4 | 16, D | 7, A | 250, D | 200, B &C | - | ALL |
| Nyamebekyere | 3 | 29, B | ; C | 350, B | 100, A | A & C | B |
| Nyameyeadom | 3 | 29, A | 10; A ,B &C | 280, D | 240, A | - | ALL |

Total of 52 vertical electrical soundings surveys were conducted throughout the 10 communities. The sounding curves revealed 3 – layers (51.9% occurrence), 4 – layers (44.2%) and 5 – layers (3.8%) earth models respectively. In most communities the $2^{nd}$ and or $3^{rd}$ layer(s) are expected to be the water – bearing layer(s).

Only two curves types were displayed by the 3 layered sounding curves; the type H ($\rho_1 > \rho_2 < \rho_3$) which was the dominant and then type A curve ($\rho_1 < \rho_2 < \rho_3$). For the 3 layered geological subsurface, the sounding curves types were KH, QH and HA. The 5 layered curves types were QHA and HKH. The dominant curve types in the study area are the H – Type and KH – Type which Okafor & Mamah (2012) cited Omosuyi (2010) saying; these curves types (H and KH) are often associated with groundwater possibilities. Worthington (1977) in (Okafor & Mamah 2012) state that, field curves or sounding curves often mirror image geo – electrically nature of the successive lithology sequence in an area and hence can be used as qualitative to assess the groundwater prospected of an area. Table 5.19 shows the summary of the vertical electrical sounding surveys.

The other VES model is the contour map model; it revealed help in showing the behaviour of the weathered zones beneath the subsurface of the communities. Some of the communities like Esukese Ekyir, Mbaa Mpe Hia No. 2 and Nyameyeadom are shown to be underlain by a possibly great amount of groundwater while others like Aboso, Kwanyarko and Nyamebekyere have possible less amount groundwater per the parameters used in this modelling.

Table 5.19. Summary of VES surveys

| Community | No. of VES Stations | No. of layers | | | Sounding Curve Type(s) | Expected Water-bearing layer(s) |
|---|---|---|---|---|---|---|
| | | 3 - layers | 4 - layers | 5 - layers | | |
| Ablaso | 3 | - | A20, A65 | A80 | QH & QHA | 3rd & 4th |
| Aboso | 6 | C182, A84 | S1, B74 & B314 | D88 | KH, HKH, H & A | 2nd & 3rd |
| Achiase | 5 | ALL | - | - | A & H | 2nd |
| Beseadze | 6 | 5 | A134 | - | KH, A & H | 1st & 2nd |
| Esukese Ekyir | 4 | 3 | A65 | - | KH, A & H | 2nd |
| Kwanyarko | 6 | 5 | C38 | - | KH & H | 1st & 2nd |
| Mbaa Mpe Hia No. 2 | 5 | 3 | C66 & A162 | - | QH, A & H | 3rd |
| Moseaso | 6 | C128 | 5 | - | KH, QH & H | 3rd |
| Nyamebekyere | 5 | C10 | 4 | - | KH, QH, HA & A | 2nd & 3rd |
| Nyameyeadom | 6 | B48, C118 | 4 | - | KH, HA & H | |

The contour maps successfully modelled the subsurface in depth ranges. It allows good observations of subsurface and it helps in determining possible level of groundwater beneath the surface. It also assist in determining the extent to which a borehole would be drilled. What makes this model useful is that, depending on the groundwater history of a site obtained from available wells and boreholes, the parameters of the contour maps could be modified to suit the project purpose. The contour map model and the sounding curve model help in making a right drilling decision.

# CHAPTER 6. CONCLUSION AND RECOMMENDATIONS

Integrated geophysical methods were used to explore zones of high groundwater potentials and suitable sites for borehole drilling and / or hand dug were recommended in ten communities within the Twifo − Hemang Lower Denkyira District of the Central Region of Ghana. The study sought to eliminate the waste of precious time, resources and labour that is use in drilling and / or hand dug unproductive boreholes and wells. It also sought to maximise the effective use of the resistivity data in groundwater exploration.

Electromagnetic Profiling was conducted and the data were qualitatively interpreted. The results of the electromagnetic method were used to selected points for the VES investigations. The VES data were interpreted both qualitatively by curve type system and quantitatively by one − dimensional sounding curve model and contour map model.

It was found out that; all zones that show high conductivity on the EM curves also show relative low resistivity when investigated using VES method. This re-enforces the basic physics relation between resistivity and conductivity. And this also gave us confidence that these data and their analyses and interpretations can be rely on in making drilling decisions. The VES results suggested that; the study area is dominated by the H and KH types of sounding curves and also indicated that the subsurface of the study area are underlain by 3 − 5 geological layers. The water − bearing layer is inferred to be within layers 2 to 4.

The major contribution of this work is the idea of using depth of investigation together with the measured resistivity values and GPS positions of the VES stations to model the subsurface using stacked contour map model. Alhough the ploting and the editing of the maps are not easy work, the final effects of the models pay off. It

helps in identification of zones, thicknesses and depths of groundwater accumulation beneath the study area.

It is recommended that;

1. Test borehole should be drilled or dug-well should be carried out at the point ranked $1^{st}$.

2. Should the test borehole or dug-well at the first ranked VES point fail to give water of desired yield or quality, the consultant should be contacted for advice before attempting digging the second ($2^{nd}$) ranked point.

3. Where groundwater of appreciable yield and good water quality is obtained the borehole or well should be developed into production borehole / hand-dug well.

4. Water quality analysis should be conducted on the well water to determine its portability.

5. The well / borehole should be well constructed to avoid infiltration of potential groundwater pollutants around the well.

# REFERENCES

A. Awomeso, J., *Groundwater Hydrology I*, Abeokuta. Available at: http://unaab.edu.ng/attachments/466_HYDROLOGY 303 LECTURE NOTES final.pdf.

Adomako, D., 1996. *The use of EM34-3 Electromagnetic Terrain Conductivity and Geo-Electrical Methods in Hydrogeological Investigations*. Kwame Nkrumah University of Science and Technology, Kumasi,. Available at: URI:

Afoh, E., 2000. *Groundwater exploration in the Fanteakwa District of the Eastern Region of Ghana using the dipole-dipole method*. Kwame Nkrumah University of Science and Technology, Kumasi,.

Andorful, D., 2013. *GROUNDWATER EXPLORATION IN ADANSI NORTH DISTRICT OF GHANA USING RESISTIVITY METHOD*. Kwame Nkrumah University of Science and Technology, Kumasi,.

Anechana, R., 2013. *GROUNDWATER POTENTIAL ASSESSMENT OF KINTAMPO NORTH MUNICIPALITY OF GHANA, USING THE ELECTROMAGNETIC METHOD AND VERTICAL ELECTRICAL SOUNDING BY*. Kwame Nkrumah University of Science and Technology, Kumasi.

Anon, 20 Skin Effect. Available at: ecee.colorado.edu/~ecen3400/Chapter 20 - The Skin Effect.pdf.

Anon, 1997. Applied Geophysics for Groundwater Studies. , (1976). Available at: http://www.st-andrews.ac.uk/~crb/web/GWATER1.pdf.

Anon, 2011. DC Terrameter ABEM SAS1000. *Geophysics Research Center, Prince of Songkla University*. Available at: http://www.geophysics.sci.psu.ac.th/knowtype.php?L=EN.

Anon, Electronic configurations. *hckgeo*. Available at: https://www.google.com.tr/search?q=electrode+configuration&es_sm=93&source=lnms&tbm=isch&sa=X&ei=Yt6FVImaL4r7ywOQ4oCIDw&ved=0CAgQ_AUoAQ&biw=1366&bih=643#facrc=_&imgdii=n82-e4HFDlKvIM:;U_-dJI2l326dEM;n82-e4HFDlKvIM:&imgrc=n82-e4HFDlKvIM%3A;ThCae8-9mSyD-M;http%3A%2F%2Fdc302.4shared.com%2Fdoc%2Fz5-PiW72%2Fpreview_html_3de82ce4.gif;http%3A%2F%2Fdc302.4shared.com%2Fdoc%2Fz5-PiW72%2Fpreview.html;337;334 [Accessed December 2, 2014b].

Anon, Factors Influencing Electrical Conductivity, Environmental Geophysics. *U.S. Environmental Protection Agency*. Available at: http://www.epa.gov/esd/cmb/GeophysicsWebsite/pages/reference/properties/Electrical_Conductivity_and_Resistivity/Factors_Influencing_Electrical_Conductivity.htm.

Anon, 2014a. File:Central Ghana districts.png. *Wikimedia Commons*. Available at: http://commons.wikimedia.org/wiki/File:Central_Ghana_districts.png.

Anon, Geological Formation in Ghana. Available at: https://www.google.com.tr/search?q=geological+map+of+Ghana&es_sm=93&t

bm=isch&tbo=u&source=univ&sa=X&ei=nnaqVLfRJcKAU_7Lg6AL&ved=0
CBwQsAQ&biw=1366&bih=643#facrc=_&imgdii=_&imgrc=SR5XpHTSGN5
ztM%3A;gESEKLo_H7Og4M;http%3A%2F%2F131.220.109.2%2Fgeonetwor
k%2Fsrv%2Fru%2Fresources.get%3Fid%3D2542%26fname%3DGVP_soil-
geology_geology_ghana_2010_pol_s.png%26access%3Dpublic;http%3A%2F
%2F131.220.109.2%2Fgeonetwork%2Fsrv%2Fru%2Fgoogle.kml%3Fuuid%3D
aaa9ea09-cc51-4612-8609-c18e476c7be9%26layers%3DGVP%3AGVP_soil-g.

Anon, *Geology 228/378 Environmental Geophysics Lecture 10*, Available at: www.engr.uconn.edu/~lanbo/G228378Lect0510EM1.pdf.

Anon, Geophysics and Groundwater: a primer. *Water Well Journal*, XXV(7).

Anon, 2013. Gray Location Map of Twifo Denkyira Heman. *www. maphill*. Available at: http://www.maphill.com/ghana/central/twifo-denkyira-heman/location-maps/gray-map/.

Anon, Groundwater Storage. *co. portage .wi.us*, p.1. Available at: http://www.co.portage.wi.us/groundwater/undrstnd/aquifer.htm.

Anon, Inorganic Chemicals in Ground Water. *ENV 302 - Lectures*. Available at: http://jan.ucc.nau.edu/~doetqp-p/courses/env302/lec35/LEC35.html [Accessed January 25, 2015h].

Anon, 1999. *Intruction Manual for Terrameter SAS 4000 / SAS 1000*, Sundbyberg, Sweden: ABEM. Available at: http://www.abem.se/files/upload/manual_terrameter.pdf.

Anon, OCCURRENCE OF GROUNDWATER. In p. 79. Available at: http://www.hwe.org.ps/Education/Birzeit/GroundwaterEngineering/Chapter 1-Occurrence of groundwater.pdf.

Anon, Propagation of Waves. *Introduction to Naval Weapons Engineering*. Available at: http://www.fas.org/man/dod-101/navy/docs/es310/propagat/Propagat.htm.

Anon, 2014b. *Terrameter SAS – VES system description*, Sundbyberg, Sweden. Available at: http://www.abem.se/support/downloads/brochure/terrameter-sas-ves-system-layout.

Anon, 2014c. *THE COMPOSITE BUDGET OF THE TWIFO HEMANG LOWER DENKYIRA DISTRICT ASSEMBLY FOR THE 2014 FISCAL YEAR*, Cape Coast. Available at: http://www.mofep.gov.gh/sites/default/files/budget/2014/CR/Hemang_Lower_Denkyira.pdf.

Apaydin, A., 2011. Groundwater legislation in Turkey: problems of conception and application. *Water International*, 36(3), pp.314–327. Available at: http://www.tandfonline.com/doi/abs/10.1080/02508060.2011.586750 [Accessed October 12, 2014].

Ariyo S, O., Adeyemi G, O. & Oyebamiji A, O., 2009. Electromagnetic Vlf Survey for Groundwater Development in a Contact Terrain ; a Case. *Journal of Applied Sciences Research*, 5(9), pp.1239–1246. Available at: http://www.aensiweb.com/old/jasr/jasr/2009/1239-1246.pdf.

Asare, V.S. & Menyeh, A., 2013. Geo-Electrical Investigation of Groundwater Resources and Aquifer Characteristics in Some Small Communities in The Gushiegu and Karaga Districts of Northern Ghana. *International Journal of Sceince and Technology Research*, 2(3), pp.25–35. Available at: www.ijstr.org.

Ashvin Kumar, M., 2011. *EXPLORATION OF GROUND WATER USING ELECTRICAL RESISTIVITY METHOD*. National Institute of Technology Rourkela.

Babu, H.V.R., Rao, N.K. & Kumar, V.V., 1991. Short Note Bedrock topography from magnetic anomalies-An aid for groundwater exploration In hard-rock terrains. *Geophysics*, 56(7), pp.1051–1054. Available at: http://library.seg.org/doi/pdf/10.1190/1.1443113.

Bartram, J. & Richard, B. eds., 1996. WATER QUALITY. In *Water Quality Monitoring - A Practical Guide to the Design and Implementation of Freshwater Quality Studies and Monitoring Programmes*. UNEP/WHO. Available at: http://www.who.int/water_sanitation_health/resourcesquality/wqmchap2.pdf.

Bernard, J., 2003. *SHORT NOTE ON THE PRINCIPLES OF GEOPHYSICAL METHODS FOR GROUNDWATER INVESTIGATIONS DEFINITION OF MAIN HYDROGEOLOGICAL PARAMETERS ELECTRICAL METHODS FOR GROUNDWATER*,

Bernard, J. & Legchenko, a., 2003. Groundwater exploration with the Magnetic Resonance Sounding method. *ASEG Extended Abstracts*, 2003(2), p.1. Available at: http://www.publish.csiro.au/?paper=ASEG2003ab013 [Accessed November 15, 2014].

Bosu, john K., 2004. *Groundwater exploration in the granitic basement in the Assin District of the Central Region using the electrical resistivity method*. Kwame Nkrumah University of Science and Technology, Kumasi. Available at: http://hdl.handle.net/123456789/1872.

C.Ralph, H., 1982. *Basic Ground-Water Hydrology: U.S. Geological Survey Water - Supply Papper 2220* Revised., Virginia: North Carolina Dept. of Natural Resource and Community Develpment.

Carl A., B. & Stewart H., F., 1943. DEVELOPMENTS IN THE APPLICATION OF GEOPHYSICS TO GROUNDWATER PROBLEMS. In *Fourth Annual Water Conference, Engineers Society of Western Pennsylvania*. Urbana, Illinois: State Geological Survey. Available at: https://www.ideals.illinois.edu/bitstream/handle/2142/45009/developmentsinap108bays.pdf?sequence=2.

Chilton, J. & P. Seiler, K., Groundwater occurrence and hydrogeological environments. In *Groundwater occurence and hydrological environments*. pp. 1–24.

Crain, E.R. (Ross), Crain ' s Petrophysical Handbook - RESISTIVITY CONCEPTS - . *Spec2000.net*, p.1. Available at: http://www.spec2000.net/06-resistivityohm.htm.

Dobecki, T.L., 1985. Geotechnical and groundwater geophysics. *Geophysics*, 50(12), pp.2621–2636.

Dramani, B.F., 2013. *BASELINE STUDY INTO GROUNDWATER RESOURCES IN THE RIVER TAIN SUB-BASIN OF THE BLACK VOLTA Baseline study into groundwater resources in the River Tain basin of the Black Volta*. Kwame Nkrumah University of Science and Technology, Kumasi,.

Enrique A, N. et al., 2013. Determinación de perfiles de humedad en suelos homogéneos a través de un método geoeléctrico. *Ciencia del suelo*, 31(02). Available at: http://www.scielo.org.ar/scielo.php?pid=S1850-20672013000200013&script=sci_arttext.

Ewusi, A., 2006. *Groundwater Exploration and Management using Geophysics : Northern Region of Ghana.* Brandengurg Technical University of Cottbus.

Fitterman, D. V & Stewartj, M.T., 1986. Transient electromagnetic sounding for groundwater. *Geophysics*, 51(4), pp.995–1005.

GEM, 1990. Very Low Frequency Electromagnetics. *GEM Systems*, pp.4–6. Available at: http://www.gemsys.ca/products/very-low-frequency-electromagnetics/.

Gyamera, E.A. & Kuma, J.S., 2014. Hydrogeological studies on soils developed over granitic deposits. , 2, pp.29–40.

Gyau-Boakye, P. & Dapaah-Siakwan, S., 2000. Groundwater as source of Rural Water supply in Ghana. *Jounal of Applied Science anf Technology*, 5(1 & 2), pp.77–86.

H. Loke, M., 2001. *Tutorial : 2-D and 3-D electrical imaging surveys*, Available at: http://web.gps.caltech.edu/classes/ge111/Docs/DCResistivity_Notes.pdf.

Kearey, P., Brooks, M. & Hill, I., 2002. *An Introduction to Geophysical Exploration* 3rd ed., Iowa: Blackwell Science Ltd. Available at: http://eu.wiley.com/WileyCDA/WileyTitle/productCd-0632049294.html [Accessed November 10, 2014].

Kesse, G.O., 1985. *The mineral and rock resources of Ghana*, Rotterdam, Netherlands: A. A. Balkema.

Löfgren, M., Electrical methods - formation factor and electromigration experiments at HYRL. Available at: http://kyt2014.vtt.fi/md_workshop_13092012/lofgren.pdf.

M. Reynolds, J., 1997. *An Introduction to Applied and Environmental Geophysics* First., West Sussex, England: John Wiley & Sons Ltd.

Mainoo, P.A. et al., 2007a. *Hydrogeological Investigations to Select Borehole Drilling Sites at Aboso Community in the Twifo-Hemang Lower Denkyira District of Central Region of Ghana.*, Accra, Ghana.

Mainoo, P.A. et al., 2007b. *Hydrogeological Investigations to Select Borehole Drilling Sites at Achiase Community in the Twifo-Hemang Lower Denkyira District of Central Region of Ghana.*, Accra, Ghana.

Mainoo, P.A. et al., 2007c. *Hydrogeological Investigations to Select Borehole Drilling Sites at Kwanyako Community in the Twifo-Hemang Lower Denkyira District of Central Region of Ghana.*, Accra, Ghana.

Mainoo, P.A. et al., 2007d. *Hydrogeological Investigations to Select Borehole Drilling Sites at Mbaa Mpe Hia No.2 Community in the Twifo-Hemang Lower Denkyira District of Central Region of Ghana*, Accra, Ghana.

Mainoo, P.A. et al., 2007e. *Hydrogeological Investigations to Select Borehole Drilling Sites at Moseaso Community in the Twifo-Hemang Lower Denkyira District of Central Region of Ghana.*, Accra, Ghana.

Mainoo, P.A. et al., 2007f. *Hydrogeological Investigations to Select Borehole Drilling Sites at Nyameyeadom Community in the Twifo-Hemang Lower Denkyira District of Central Region of Ghana.*, Accra, Ghana.

Mainoo, P.A. et al., 2007g. *Hydrogeological Investigations to Select Hand Dug Well Development Sites at Nyamebekyere No. 2 Community in the Twifo-Hemang Lower Denkyira District of Central Region of Ghana.*, Accra, Ghana.

McNeill, J., 1980. *Electromagnetic Terrain Conductivity measurement at Low induction Number*, Ontario, Canada. Available at: http://www.geonics.com/pdfs/technicalnotes/tn6.pdf.

Menyeh, A., Noye, R.M. & Danuor, S.K., 2005. Prospecting for Groundwater using the Electromagnetic Method in the Voltaian Sedimentary Basin in the Northern Region of Ghana - A Case Study of the Gushiegu - Karaga District. *Journal of Science and Technology*, 25(2), pp.53–65.

Methods, E., *Geology 228 Applied Geophysics*,

Nascimento Da Silva, C.C. et al., 2004. Resistivity and ground-penetrating radar images of fractures in a crystalline aquifer: A case study in Caiçara farm - NE Brazil. *Journal of Applied Geophysics*, 56(4), pp.295–307. Available at: http://linkinghub.elsevier.com/retrieve/pii/S0926985104000588 [Accessed September 21, 2014].

Nils, P. & Lennart, W., 2005. *Tools for Groundwater Prospecting and Geophysical Prospecting for Water in Ocotal , Nicaragua*. Luleå University of Technology.

Nkhoma, M., AQUIFERS – THE WATER BEARERS. *waterincrisis.com*, p.6. Available at: http://www.waterincrisis.com/pages/aquifers_mn1/aquifers.html.

O. Omosuyi, G., 2010. Geoelectric Assessment of Groundwater Prospect and Vulnerability of Overburden Aquifers at Idanre, Southwestern Nigeria. *Ozean Journal of Applied Sciences*, 3(1), pp.19 – 28.

Obuobie, E. & Barry, B., 2010. *Groundwater in sub-Saharan Africa : Implications for food security and livelihoods.*, Accra, Ghana.

Okafor, P. & Mamah, L., 2012. Integration of Geophysical Techniques for Groundwater Potential Investigation in Katsina - Ala, Benue State, Nigeria. *The Practical Journal of Science and Technology*, 13(2), pp.463–474. Available at: http://www.akamaiuniversity.us/PJST.htm.

Oxforddictionary, Definition of groundwater in : *Oxford dictionary*. Available at: http://www.oxforddictionaries.com/definition/english/groundwater.

R. Worthington, P., 1977. Geophysical Investigations of Groundwater Resources in the Kalahari Basin. *Geophysics*, 42(4), pp.838 – 849.

Reinhard, K. ed., 2006. *Groundwater Geophysics: A TOOL FOR HYDROGEOLOGY*, Heidelberg, Germany: Springer.

Reynolds, J.M., 1997. *An Introduction to Applied and Environmental Geophysics*,

Robinson S., E. & Çoruh, C., 1988. *Basic Exploration Geophysics*, Singapore: John Wiley & Sons Ltd.

S. Badrinarayanan, T., *Ground water exploration- an introduction.*, Tamilnadu.

Sharma, P. V., 1997. *Environmental and Engineering Geophysics*, Cambridge University Press. Available at: http://books.google.com/books?hl=en&lr=&id=ic-sOMgM-rEC&pgis=1 [Accessed November 28, 2014].

Somiah, J., 2013. *Application of Electromagnetic and Electrical Resistivity Methods in Investigating Groundwater Resources of The Sunyani Municipality in The Brong-Ahafo Region of Ghana*. Kwame Nkrumah University of Science and technology, Kumasi.

Telford, W.M., Geldart, L.P. & Sheriff, R.E., 1990. *Telford - Applied Geophysics*, Available at: http://books.google.com/books?id=oRP5fZYjhXMC&pgis=1.

Tsikudo Kwasi, B., 2009. *GEOPHYSICAL INVESTIGATION FOR GROUNDWATER IN THE GUSHIEGU-KARAGA AND ZABZUGU-TATALE DISTRICTS OF THE NORTHERN REGION OF GHANA USING THE ELECTROMAGNETIC METHOD*. Kwame Nkrumah Universty of Science and Technology, Kumasi.

Wikipedia, 2015. Granite. *Wikipedia*. Available at: http://en.wikipedia.org/wiki/Granite [Accessed January 16, 2015].

Wikipedia, 2014. Granodiorite. *Wikipedia*. Available at: http://en.wikipedia.org/wiki/Granodiorite [Accessed January 16, 2015].

Wikipedia, 2009. Water. *Wikipedia*, (November), p.21. Available at: http://en.wikipedia.or/wiki/Water.

Wikipedia, Water cycle. *Wikipedia*, p.8. Available at: http://en.wikipedia.org/wiki/Water_cycle Water.

Xia, J., Weis, T. V. & Miller, R.D., 2001. Findings from Electromagnetic Surveys Surrounding a Hog Confinement Facility in Western Kansas Over a Two Year Period. *Kansas Geological Survey, Open-file Report 2001-7*. Available at: http://www.kgs.ku.edu/Geophysics/OFR/2001/07/.

Zhu, Z. et al., 2009. Ground Penetrating Radar Exploration for Ground Water and Contamination. , pp.1316–1320.

Zohdy, A.. A.R., Eaton, G.P. & Mabey, D.R., 1990. APPLICATION OF SURFACE GEOPHYSICS TO GROUND-WATER INVESTIGATIONS. In *Techniques of Water-Resources Investigations of the United States Geological Survey*. Denver: USGS Publications, p. 116. Available at: http://pubs.usgs.gov/twri/twri2-d1/pdf/TWRI_2-D1.pdf.

# RESUME

Hafiz MOHAMMED NAZIFI was born and raised in Kumasi, Ghana. He attended his nursery and primary school at Wataniyya Islamic School, Kumasi. He had his Junior High School education in Kings International School, Kumasi from 2000 to 2003. He wrote Basic Education Certificate Examination in 2003 and had a 06 grade certificate (The highest grade at the Time). He then continued with senior high school education in T. I. Ahmadiyya Senior Secondary School, Kumasi where he read General Science from 2003 to 2006. In May, 2006 he wrote the West African Senior School Examination and successful passed all of the subjects he took. From June, 2006 to August, 2007 he worked as a sales personnel at Trice Cutter Enterprise in Kumasi. In August, 2007 he had admission to read a 4 - year Physics programme at the Kwame Nkrumah University of Science and Technology, Kumasi. He graduated from this university in June, 2011 with Bachelor of Science (PHYSICS) Second Class Honours. During his 4 years he won two financial grants from the University and the Students Representative Council (SRC) in 2008 and 2010 respectively. He was appointed to serve the Department of Physics in a position of Teaching and Research assistance for 2011/2012 academic year as part of his Ghana national service. In October, 2012, he won a postgraduate scholarship of the Turkish Government to study Masters of Science Geophysics Engineering at Sakarya University, Sakarya. He studied and successfully passed C1 certificated examination of Turkish Language. In 2015, he won Erasmus Grant to do a 3 month internship in Kutec AG Salt Technologies, Sondershausen – Germany.